2019

ERalpha isoforms modulate the tumorigenicity of 24R,25(OH)2D3 in estrogen-responsive cancer

Anjali Verma
Virginia Commonwealth University

VCU Biomedical Engineering
College of Engineering

ERα isoforms modulate the tumorigenicity of 24R,25(OH)$_2$D$_3$ in estrogen-responsive cancer

A thesis submitted in partial fulfillment of the requirements for the degree of Doctor of Philosophy at Virginia Commonwealth University

by

ANJALI VERMA

B.Sc. Biomedical Engineering, Case Western Reserve University 2013

April 2019

Acknowledgments

I would first like to thank my advisors, Dr. Zvi Schwartz, and Dr. Barbara Boyan. When I first joined the Boyan-Schwartz laboratory as a research technician, I had no intention of pursuing graduate school anytime in the near future. They were quick to encourage me to take my love of science and problem solving and apply them towards a Ph.D. Their optimism, critical insight, and rigorous work ethic have served as an inspiration to those of us who have the good fortune to be mentored by them. Thank you.

I would also like to thank Dr. D. Joshua Cohen, who facilitated all the animal work in this thesis; his clinical expertise and leadership in our laboratory have become indispensable. My mentor, committee member, and collaborator Dr. Jennifer Koblinski has shared her expertise in mouse models and graciously given me advice on careers in cancer research. Dr. Daniel Conway's expertise in cell signaling and Dr. Hu Yang's wealth of experience in drug delivery and encouragement to look at the therapeutic potential of 24R,25(OH)$_2$D$_3$ have been invaluable.

Dr. Thomas Carey at the University of Michigan created and provided the laryngeal cancer cell lines used in many chapters of this thesis. Dr. Nofrat Schwartz provided her expertise in otolaryngology, laryngeal cancer, and rapid signaling mechanisms.

Many administrators and staff members supported me in my work. Lori Floyd-Miller's support and encouragement were essential in navigating the red-tape maze that every doctoral candidate has to negotiate. Caroline Bivens provided much of the artwork for this thesis. Julie Farnsworth and Dr. XinYan Pei at the Flow Cytometry Shared Resource Core taught me about cell sorting and FACS analysis. Pamela Grizzard at the VCU Tissue and Data Acquisition Core helped me to acquire clinical samples of laryngeal

carcinoma and matched laryngeal tissue. Dr. Bin Hu at the VCU Massey Cancer Mouse Models Shared Resource was helpful with animal studies and imaging. Vita Kraskauskiene at the Histology Shared Resource lent her histological expertise while Madhavi Puchapalli helped and advised on working with hard-to-transfect cell lines. Frances White gave her expertise with cryosectioning and histology. I would also like to thank the Biomedical Engineering Ph.D. program at VCU for their support: Dr. Jennifer Wayne and Dr. Christopher Lemmon, my program chairs, Dr. Henry Donahue, our department chair, and Pam Mason.

The Boyan-Schwartz Lab is a uniquely supportive and competitive environment. Chandana Muktipaty and Vaidehi Patel, my undergraduate mentees, have been critical to the success of this thesis. Smita Singh and Thomas W. Jacob's endless patience, support, and cell culture expertise are much appreciated. Sharon Hyzy's encouragement and expertise in cell biology were wonderful assets. Dr. Michael McClure's expertise in muscle cell signaling was helpful. I would also like to thank my fellow graduate students who have acted in turn as co-conspirators, collaborators, and mentors. Particularly Dr. Alice Cheng, Dr. Shirae Leslie, and soon to be Drs. Kayla Scott, Niels Asmussen, Ethan Lotz, Michael Berger, Jingyao Deng, Lucas Olson, and Cydney Dennis—thank you!

Lastly, I would like to thank my family and friends who have supported me throughout this journey. My parents, Dr. Niraj Verma and Dr. Namita Verma have given me endless patience, encouragement, advice, and taught me the importance of education and resilience. And my sister, Priya, who often reminds me that there is life outside the academy.

Services and products in support of this research project were generated by the Virginia Commonwealth University Cancer Mouse Models Core Laboratory, the VCU Massey Cancer Center Tissue and Data Acquisition and Analysis Core, and the VCU Microscopy Shared Resource, supported, in part, with funding from NIH-NCI Cancer Center Support Grant P30 CA016059.

Table of Contents

List of Tables

List of Figures

List of Symbols and Abbreviations

1α,25(OH)$_2$D$_3$	1α,25-dihydroxyvitamin D$_3$
24R,25(OH)$_2$D$_3$	24R,25-dihydroxyvitamin D$_3$
24S,25(OH)$_2$D$_3$	24S,25-dihydroxyvitamin D$_3$
25(OH)D$_3$	25-hydroxyvitamin D$_3$
2BP	2-bromopalmitate
AA	African American
AF1	Transcriptional activation domain 1
AF2	Transcriptional activation domain 2
ANOVA	Analysis of variance
AR	Androgen receptor
BAX	B cell lymphoma protein 2-associated X protein
BCL2	B cell lymphoma protein 2
BME	Basement membrane extract
CA	Caucasian American
CD-FBS	Charcoal-dextran stripped fetal bovine serum
CXCL12	C-X-C- motif chemokine 12
CXCR4	Chemokine receptor type 4
DAG	Diacylglycerol production
DPBS	Distilled phosphate buffered saline
E$_2$	17β-estradiol
ECM	Extracellular matrix
EdU	5-ethynyl-2'-deoxyuridine
EGF	Epidermal-like growth factor
ELISA	Enzyme-linked immunosorbent assay

ER	Estrogen receptor
ER-	ER negative
ER+	ER positive
ERBB2	Erythroblastic oncogene B
Erk	Extracellular signal-regulated kinases
ERs	Estrogen receptors
ERα36	Estrogen receptor α 36
ERα66	Estrogen receptor α 66
ERα66-	ERα66 negative
ERα66+	ERα66 positive
ERβ	Estrogen receptor β
FBS	Fetal bovine serum
FGF	Fibroblast growth factor
GAPDH	Glyceralde-3-phosphate dehydrogenase
GFP	Green fluorescent protein
GPER1 a.k.a. GPR30	G-protein coupled estrogen receptor
H&E	Hematoxylin and eosin
HG DMEM	High-glucose Dulbecco's minimum essential medium
I3K	Phosphor-inositol-3-kinase
IGF-1	Insulin-like growth factor
IP_2	Inositol triphosphate
IRB	Institutional review board
KD	Knockdown
LPA	Lysophosphatidic acid
LSCC	Laryngeal squamous cell carcinoma

MAPK	Mitogen-activated protein kinase
MBC	Methyl β-cyclodextrin
M-CSF	Macrophage colony stimulating factor
MEM	Minimum essential growth media
MMP1	Matrix metalloproteinase 1
MMPs	Matrix metalloproteinases
NP-40	Nonidet p40
NSG	NOD.Cg-Prkdc^{scid}Il2rg^{tm1Wjl}/SzJ
OC	Osteoclast
OCGM	Osteoclast precursor growth medium
OCPs	Osteoclast precursors
OCT	Optimal cutting temperature compound
OPG	Osteoprotegerin
ORF	Open-reading-frame
OS	Overall survival
OV	Overexpressed
RPMI	Roswell Park Memorial Institute 1640 media
PBS	Phosphate buffered saline
PGE_2	Prostaglandin E_2
PKB/Akt	Protein kinase B
PKC	Protein kinase C
PLA_2	Phospholipase A_2
PLC	Phospholipase C
PLD	Phospholipase D
PR	Progesterone receptor

PTH	Parathyroid hormone
RANK	Nuclear factor kappa-B
RANKL	RANK ligand a.k.a. Nuclear factor kappa-B ligand
RFP	Red fluorescent protein
RIPA	Radioimmunoprecipitation assay
SNAI1	Snail family transcriptional repressor
TCGA	Total Cancer Genome Atlas
TDAAC	Tissue and Data Acquisition and Analysis Core
TdT	Terminal deoxynucleotidyl transferase
TNBC	Triple-negative breast cancer
UCSC	University of California Santa Cruz
VCU	Virginia commonwealth university
VDR	Vitamin D receptor
VDRE	Vitamin D response element
VEGF	Vascular endothelial growth factor

Abstract

Over 200,000 cases of breast cancer are diagnosed every year. Nearly 20% of these patients supplement their diets with some form of vitamin D. This high frequency of vitamin D supplement use may be due in part to research suggesting that cancer patients with higher serum vitamin D$_3$ levels have better prognoses than patients with low serum vitamin D$_3$. However, double-blind clinical trials on the efficacy of vitamin D$_3$ supplementation in breast cancer have been inconclusive. A recent meta-analysis showed evidence of reduced cancer recurrence in patients taking vitamin D$_3$ supplements who had 'estrogen receptor positive' (ERα66+) breast cancer, but not those who had estrogen receptor negative' (ERα66-) breast cancer.

Once ingested, vitamin D$_3$ is metabolized in the liver into the circulating pre-hormone 25(OH)D$_3$, which is then further metabolized into 1α,25(OH)$_2$D$_3$ and 24R,25(OH)$_2$D$_3$. 24R,25(OH)$_2$D$_3$ has been shown to activate a number of membrane signaling pathways, some of which overlap with 17β-estradiol (E$_2$) signaling through ERα36, a membrane isoform of ERα66. The ***central hypothesis*** of this thesis was that 24R,25(OH)$_2$D$_3$ is tumorigenic in certain cancers and that this tumorigenicity is mediated in part by ERα isoforms.

E$_2$ signaling through ERα36 has been described in the ERα66-, ERα36+ breast cancer cell line HCC38[1]. ***Specific aim 1*** determined whether E$_2$ signaling through ERα36 was tumorigenic other cancers with different ERα profiles. ***Specific aim 2*** determined how 24R,25(OH)$_2$D$_3$ affected tumorigenicity in breast cancer using the common breast cancer cell line MCF7 (ERα66+, ERα36+) as a model. ***Specific aim 3*** investigated the role of ERα isoforms in 24R,25(OH)$_2$D$_3$ signaling in breast cancer cell lines by comparing

the tumorigenic effects of 24R,25(OH)$_2$D$_3$ in MCF7 cells (ERα66+, ERα36+) and HCC38 cells (ERα66-, ERα36+). To determine whether ERα66 regulates the effects of 24R,25(OH)$_2$D$_3$, ERα66 was expressed in two ERα66- cell lines. The effect of 24R,25(OH)$_2$D$_3$ on apoptosis was assessed in wild-type and ERα-expressing cell lines.

Chapter 1.

Introduction

Nearly 1 in 8 women will be diagnosed with breast cancer in her lifetime[2]. Approximately 20% of these women will supplement their diets with some form of vitamin D[3,4]. This high frequency of vitamin D_3 supplement use may be due in part to reports that suggest that cancer patients with higher serum 25-hydroxyvitamin D_3 (25(OH)D_3) levels have better prognoses and increased survival rates than patients with low 25(OH)D_3[5]. However, double-blind clinical trials and some pre-clinical studies investigating the efficacy of vitamin D_3 supplementation on cancer patient outcomes have been inconclusive, and recent large-scale studies do not show any correlation between vitamin D_3 supplement use and cancer incidence[6,7]. One reason for this may be that most double-blind clinical trials do not account for the heterogeneous nature of breast cancer in their analyses. A recent meta-analysis of vitamin D_3 serum levels in breast cancer patients showed that elevated serum vitamin D_3 is associated with a reduced risk of tumor recurrence in patients with 'estrogen receptor positive' (ER+) disease, but did not show a similar association between vitamin D_3 status and cancer recurrence in patients with 'estrogen receptor negative' (ER-) tumors[8] (Figure 1.1). This suggests that estrogen receptor status may be a factor in the efficacy of vitamin D supplementation in cancer.

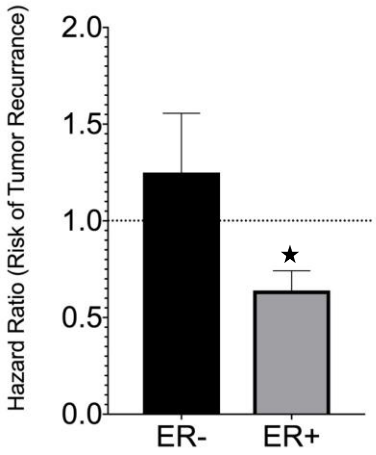

Figure 1.1 Effect of vitamin D supplementation on breast cancer recurrence in ER- and ER+ breast cancer.[7]

*indicates significance against a no-treatment control (-- line, hazard ratio of 1).

Breast cancer is a multifaceted, heterogeneous disease with numerous molecular subtypes that

influence disease severity. These molecular subtypes can be demarcated by the expression of hormone receptors, such as the estrogen receptor. Estrogen receptor status is a discrete identification paradigm that allows clinicians to divide patients into meaningful groups for personalized treatment regimens. Patients with ER+ tumors generally have better outcomes than patients with ER- tumors[9]. This is in part because ER+ breast cancer responds favorably to treatment with anti-estrogen drugs[10]. However, the mechanisms governing the more aggressive pathology of ER- tumors compared to their less aggressive ER+ counterparts have not been fully elucidated.

One reason for this may lie in the intrinsically misleading histological classifications assigned to 'ER+' and 'ER-' tumors. In actuality, ER+ and ER- tumor classification denote the intra-tumoral expression of **only one** estrogen receptor – the transcriptionally active steroid hormone receptor ERα66. Both ER+ and ER- tumors express many other estrogen receptors, such as the membrane receptor ERα36, an isoform of ERα66; estrogen receptor β (ERβ), another transcriptionally active ER[11]; and G-protein coupled receptor 30 (GPR30), a membrane estrogen receptor[12].

Another reason for different serum vitamin D$_3$ levels in ER+ vs. ER- patients may be because serum vitamin D$_3$ is actually a measure of 25(OH)D$_3$, which is in itself a precursor to the active steroid hormone metabolites 1α,25(OH)$_2$D$_3$ and 24R,25(OH)$_2$D$_3$. Once ingested, vitamin D$_3$ is metabolized in the liver into the circulating pre-hormone 25(OH)D$_3$, which is then further metabolized into 1α,25(OH)$_2$D$_3$ and 24R,25(OH)$_2$D$_3$[13]. Research has shown that 1α,25(OH)$_2$D$_3$ has anti-tumorigenic effects in certain cancers, including both ER+ and ER- breast cancer[14]. However, little has been done to study the effects of 24R,25(OH)$_2$D$_3$ on cancer tumorigenicity.

The effect of 24R,25(OH)$_2$D$_3$ on ER+ vs. ER- breast cancer tumorigenicity is particularly interesting because 24R,25(OH)$_2$D$_3$ has been shown to activate a number of membrane signaling pathways, some of which overlap with 17β-estradiol (E$_2$) signaling through the membrane receptor ERα36. In chondrocytes, 24R,25(OH)$_2$D$_3$ has been shown to rapidly increase the activity of phospholipase-D2 (PLD2)[15] and subsequently activate protein kinase C (PKC)[16]. Studies with 24S,25(OH)$_2$D$_3$, the enantiomer of 24R,25(OH)$_2$D$_3$, have shown that this rapid pathway is unique to the 24R,25(OH)$_2$D$_3$ metabolite [17]. Downstream of PKC, 24R,25(OH)$_2$D$_3$ promotes p53 ubiquitination and subsequent degradation, reduces the ratio of B cell lymphoma protein 2-associated X protein to B cell lymphoma protein 2 (BAX/BCL2), inhibits cytochrome C translocation, and blocks caspase-3 cleavage to prevent apoptosis[18].

The receptor that mediates the actions of 24R,25(OH)$_2$D$_3$ has not yet been definitively identified. However, three candidate receptors have been suggested: a membrane isoform of the vitamin D receptor (mVDR), which binds 24R,25(OH)$_2$D$_3$ and can be isolated from tibial chick fracture calluses[19,20]; catalase-1, an enzyme isolated from chick intestine cell membranes which binds 24R,25(OH)$_2$D$_3$[21]; and family 57 b2 (FAM47B2), a transmembrane protein in articular cartilage cells which synthesizes ceramide sphingolipids in cartilage and binds 24,25(OH)$_2$D$_3$ with a higher affinity than 1,25(OH)$_2$D$_3$[22]. All three of these receptors candidates are associated with membrane-signaling complexes. This, coupled with the 24R,25(OH)$_2$D$_3$ pathway, suggests that 24R,25(OH)$_2$D$_3$ is modulated by a membrane-associated protein signaling complex[23].

Many estrogen receptors act through membrane-associated pathways. GPR30, for example, is a G-protein coupled receptor (GPCR) estrogen receptor which signals

through the epidermal growth factor receptor (EGFR) to activate the phosphoinositol-3-kinase (PI3K) pathway. Downstream of PI3K, GPR30 signaling prevents apoptosis and enhances metastasis [24]. Similarly, ERβ has been described as a potent estrogen receptor with a high affinity for 17β-estradiol (E_2). However, ERβ has primarily been described as a classical genomic nuclear receptor[25] rather than a membrane receptor. It does have some extra-nuclear activity[26], but this extra-nuclear activity has been most well-described in the mitochondria and cytoplasm or in conjunction with other estrogen receptors such as GPR30 at the membrane[12].

The membrane isoform of ERα (ERα36), on the other hand, has been shown to signal at the membrane through the second messengers PKC and PLD. Our lab has shown that in both ER+ and ER- cancers, rapid E_2 signaling through ERα36 activates PKC, which subsequently activates PLD. This is a similar pathway to that described by 24R,25(OH)$_2$D$_3$ in chondrocytes. However, as stated above, 24R,25(OH)$_2$D$_3$ activates PLD, then PKC; while the E_2-ERα36 signaling cascade activates PKC before PLD. The similarity in these two pathways suggests crosstalk between the 24R,25(OH)$_2$D$_3$ pathway and E_2-ERα36 pathway may be partially regulating the effects of 24R,25(OH)$_2$D$_3$ on ER+ and ER- breast cancer.

It is important to note that while our work has shown that the rapid effects of E_2 on PKC at the membrane are the result of ERα36 signaling, other labs have shown that ERα46 and ERα66, the nuclear and cytosolic classic isoforms of ERα, can be trafficked to the membrane via palmitoylation. Once at the membrane, signaling by E_2-ERα66 may mimic E_2-ERα36 signaling. Therefore, it is necessary to investigate both the ERα36 and ERα66 isoforms for the possibility of crosstalk between 24R,25(OH)$_2$D$_3$, and membrane-

ERα signaling. The parallel mechanisms and potential crosstalk between the signaling mechanisms of 24R,25(OH)$_2$D$_3$ and ERα36 led us to investigate the role of 24R,25(OH)$_2$D$_3$ in breast cancer.

Our lab has shown that in both ER+ and ER- breast cancer, E$_2$ binds to ERα36 and activates PKC-PLD mediated signaling pathways at the membrane that act downstream to prevent apoptosis and promote proliferation[27]. In chondrocytes, 24R,25(OH)$_2$D$_3$ binds to a membrane receptor to initiate a similar signaling cascade that prevents apoptosis[18]. The ***overall goal*** of this thesis was to determine the effect of 24R,25(OH)$_2$D$_3$ on tumorigenicity in breast cancer, and to determine whether those effects were modulated by ERα isoforms.

E$_2$ signaling through ERα36 has been described in the ERα66-, ERα36+ breast cancer cell line HCC38[1]. ***Specific aim 1*** determined whether E$_2$ signaling through ERα36 was tumorigenic in other cancers that have different ERα profiles. The tumorigenicity of E$_2$ was assessed in two laryngeal squamous cell carcinoma (LSCC) cell lines with different ERα isoform expression. Cancer stage and metastasis was correlated with ERα isoform expression in primary LSCC tumor samples and matched normal controls to assess correlations between ERα isoform expression and tumor aggression.

Specific aim 2 determined how 24R,25(OH)$_2$D$_3$ affected tumorigenicity in breast cancer using the common breast cancer cell line MCF7 (ERα66+, ERα36+) as a model. The tumorigenicity of 24R,25(OH)$_2$D$_3$ was assessed *in vitro* by examining DNA synthesis and markers for apoptosis, epithelial-to-mesenchymal transition and metastasis, and *in vivo* in a xenograft mammary fat pad murine tumor model. The mechanism of 24R,25(OH)$_2$D$_3$ signaling in MCF7 (ERα66+, ERα36+) was identified using chemical and

antibody inhibitors. ***Specific aim 3*** investigated the role of ERα isoforms in 24R,25(OH)$_2$D$_3$ signaling in breast cancer cell lines by comparing the tumorigenic effects of 24R,25(OH)$_2$D$_3$ in two breast cancer cells: MCF7 (ERα66+, ERα36+) and HCC38 (ERα66-, ERα36+). Tumorigenicity was assessed *in vivo* and *in vitro*, and the mechanism of 24R,25(OH)$_2$D$_3$ signaling in HCC38 (ERα66-, ERα36+) was elucidated using chemical and antibody inhibitors and enzyme activity assays. To determine which isoform of ERα regulates the effects of 24R,25(OH)$_2$D$_3$ on apoptosis ERα66 was overexpressed in HCC38 (ERα66-, ERα36+). To investigate whether ERα66 was only tumorigenic in breast cancer cell lines, ERα was overexpressed in an unrelated cell line, C2C12 (ERα66-, ERα36+). The effect of 24R,25(OH)$_2$D$_3$ on apoptosis was assessed in wild-type and ERα-overexpressed cell lines. The ***central hypothesis*** of these aims was that 24R,25(OH)$_2$D$_3$ is tumorigenic in certain cancers and that this tumorigenicity is mediated in part by ERα isoforms.

Specific Aim 1: Determine the estrogen receptor profile and estrogen responsiveness in laryngeal cancer and clinical outcomes.

There is growing evidence that laryngeal squamous cell carcinomas (LSCC) are responsive to sex hormones, specifically 17β-estradiol (E$_2$), despite the controversy regarding the presence and characterization of E$_2$ receptors (ER). Determination of sex hormone responsiveness impacts the prognosis of LSCC patients and the treatment modalities implemented by their clinicians. Discovery of membrane-associated steroid hormone receptors and rapid membrane signaling opened the possibility that cancers previously labeled ‘non-hormone dependent,’ and ‘ER negative’ might be susceptible to

the effects of E_2 via these membrane receptors. The ***objective*** of this aim was to show that the expression of different membrane ERs in LSCC is not uniform, which may result in differential and antagonistic responses to E_2. This aim ***hypothesized*** that E_2 signaling through ERα36 was tumorigenic, and that primary LSCC aggression was proportional to ERα36 and inversely proportional to ERα66 expression.

ERα isoform expression was characterized in LSCC cell lines and primary clinical samples. Tumorigenicity of E_2 in LSCC was assessed by examining the effects of E_2 on proliferation and apoptosis *in vitro* and tumor burden in a mouse xenograft model *in vivo*. A possible E_2 signaling mechanism was determined by using chemical signaling inhibitors and an ERα36-blocking antibody. Associations between ERα expression and LSCC aggression were confirmed using data from the Total Cancer Genome Atlas.

Specific Aim 2: Determine if 24R,25-Dihydroxyvitamin D$_3$ regulates breast cancer cells *in vitro* and *in vivo.*

Epidemiological studies indicate that high serum 25-hydroxyvitamin D_3 [25(OH)D_3] is associated with improved prognosis and survival in some breast cancer patients. Pre-clinical studies attributed this to the anti-tumorigenic properties of its steroid hormone metabolite 1α,25(OH)$_2$D$_3$. However, 1α,25(OH)$_2$D$_3$ is highly calcemic and thus has a narrow therapeutic window. Here we investigate the effects of another steroid hormone metabolites of 25(OH)$_2$D$_3$, 24R,25(OH)$_2$D$_3$, as an alternative non-calcemic vitamin D_3 supplement. The ***objective*** of this aim was to assess the effect of 24R,25(OH)$_2$D$_3$, a steroid hormone metabolite of vitamin D_3, on tumorigenic markers in the MCF7 (ERα66+, ERα36+), an ERα66+, ERα36+ breast cancer cell line. We ***hypothesized*** that

24R,25(OH)$_2$D$_3$ would be anti-tumorigenic in MCF7 and that a rapid membrane-associated mechanism would stimulate this effect.

NOD-SCID-IL2γR null female mice with MCF7 xenografts in the mammary fat pad were treated with 24R,25(OH)$_2$D$_3$ and changes in tumor burden and metastases were assessed *in vivo*. Breast cancer cell lines were treated *in vitro* with 24R,25(OH)$_2$D$_3$ to determine its effects on proliferation, apoptosis, migration, and metastatic markers. A possible 24R,25(OH)$_2$D$_3$ signaling mechanism was determined by using chemical signaling inhibitors and an ERα36-blocking antibody to determine the dependence of ERα isoforms on 24R,25(OH)$_2$D$_3$ signaling.

Specific Aim 3: Determine if 24R,25(OH)$_2$D$_3$ differentially regulates tumorigenicity in estrogen receptor α dependent manner.

Our lab has identified an understudied metabolite of vitamin D$_3$, 24R,25(OH)$_2$D$_3$, which has anti-tumorigenic effects in the ERα66+, ERα36- breast cancer cell line MCF7. However, preliminary evidence suggests that ERα66 and ERα36 may modulate the anti-tumorigenic effects of 24R,25(OH)$_2$D$_3$. The objective of this aim was to evaluate the effect of 24R,25(OH)$_2$D$_3$ in the breast cancer cell line HCC38 (ERα66-, ERα36+) and determine the role of ERα66 and ERα36 on 24R,25(OH)$_2$D$_3$ tumorigenicity. We hypothesized that 24R,25(OH)$_2$D$_3$ would be pro-tumorigenic in HCC38 and that this effect would be modulated by ERα66.

NOD-SCID-IL2γR null female mice with HCC38 xenografts in the mammary fat pad were treated with 24R,25(OH)$_2$D$_3$ and changes in tumor burden were assessed *in vivo*. Breast cancer cell lines were treated *in vitro* with 24R,25(OH)$_2$D$_3$ to determine its effects

on proliferation, apoptosis, migration, and metastatic markers. A possible 24R,25(OH)$_2$D$_3$ signaling mechanism was determined by enzymatic activity assays and by using chemical signaling inhibitors and an ERα36-blocking antibody to determine the dependence of ERα isoforms on 24R,25(OH)$_2$D$_3$ signaling. To determine which isoform of ERα regulates the effects of 24R,25(OH)$_2$D$_3$ on apoptosis ERα66 was overexpressed in the ERα66-negative HCC38. To investigate whether ERα66 was only tumorigenic in breast cancer cell lines ERα was also overexpressed in an unrelated cell line, C2C12. The effect of 24R,25(OH)$_2$D$_3$ on apoptosis was assessed in wild-type and ERα-overexpressed cell lines.

Chapter 2.

Background and Literature Review

Steroid hormones mediate a wide variety of vital developmental and physiological functions in different organs, such as the reproductive system, bone, brain, and fat differentiation and metabolism. When steroid hormones are deficient or abnormal, they have deleterious effects such as promoting the development and progression of hormone-responsive cancers[28]. Traditionally, steroid hormones signal by binding to receptors in the cytosol followed by either homodimerization or heterodimerization to form a complex, which is then translocated to the nucleus. In the nucleus, the complex functions as a transcription factor by binding to either specific response elements or to transcription initiation complexes on the DNA to either activating or repressing transcription[29].

This process occurs in a matter of hours to days[30,31]. In contrast, it is now well-accepted that most steroid hormones induce a non-nuclear rapid signaling response that occurs in seconds to minutes, which is not delayed by inhibition of transcription or translation[31–35]. The signaling response is a result of steroid hormones binding to specific extra-nuclear receptors, which mainly reside in the cell membrane, particularly the caveolae. When activated, these receptors trigger signaling cascades that involve kinases, phospholipases, calcium flux, and other secondary messengers[36,37].

Nature of steroid-hormone membrane receptors

Rapid signaling is mediated through receptors that reside in the cell membrane. Many of these receptors act as G protein-coupled receptors upon ligation, leading to

signaling cascades that regulate existing protein function and downstream gene expression [34,38]. The nature of these receptors is a matter of controversy. Some have advocated that they are the traditional receptors residing in the cell membrane, particularly concerning receptors for estrogen, progesterone, androgen, and glucocorticoids, and the vitamin D receptor[39–42]. Others have suggested that they are truncated isoforms of traditional nuclear membrane receptors[43]. For example, the well-described membrane estrogen receptor ERα36 is a truncated isoform of the canonical estrogen receptor ERα66. However, others have identified novel orphan receptors that also mediate rapid membrane signaling[44–47].

Classical nuclear receptor trafficking

Nuclear receptors for sex hormones have been found in the plasma membranes of hormone-responsive cancers where they activate rapid signaling pathways that enhance cancer cell survival and proliferation [27,48]. It is thought that the classical receptors exert their effects through transactivation of the epidermal-like growth factor (EGF) or insulin-like growth factor-1 (IGF-1) tyrosine kinase receptors to stimulate kinase cascades. Another theory suggests that classical receptors signal through collaboration with G-protein coupled receptors[47,49,50].

Trafficking of the classical receptors to the plasma membrane occurs through palmitoylation,[35,51] which involves the attachment of palmitic acid to an internal cysteine residue. Palmitoylation promotes the association of the receptor with caveolin-1, a transporter protein, to caveolae rafts in the plasma membrane[52]. Palmitoylation occurs in a nine amino acid motif, which includes the cysteine palmitoylation site. This

palmitoylation motif is highly conserved in estrogen receptor (ER) isoforms α and β, progesterone receptor (PR) and androgen receptor (AR)[35,40]. Once the receptor is associated with the caveolae, it may interact with many signaling proteins associated with the caveolae rafts and activate various Gα and Gβ/γ proteins within seconds[53,54].

Estrogen Receptor α and its isoforms

In the last ten years, several isoforms of ERα have come to light [43]. The most widely studied of these alternative receptors are ERα46 and ERα36, a membrane-bound variant of the classical ERα, ERα66. Both ERα46 and ERα36 arise from alternative splicing of the ESR1 gene [42], with ERα36 including a novel exon of the gene, exon 9 [42]. ERα36 has been identified in many breast cancer cell lines that were previously characterized as ERα negative [1], such as HCC38 and MDA-MB-231 [55]. In breast cancer, the presence of ERα36 has been associated with increased aggression and metastasis *in vitro*, *in vivo*, and *in situ* [56,57]. In one study, a continuum of ERα66/ERα36 positive/negative cell line-derived xenografts was examined *in vivo*. ERα66+, ERα36- tumors found to be the least aggressive, ERα66+, ERα36+ slightly more aggressive, ERα66-, ERα36- second-most aggressive, and ERα66-, ERα36+ tumors the most aggressive of all four phenotypes. This suggests that the relative levels of ERα66 and ERα36 within a tumor are more important modulators of breast cancer aggression than the presence of each receptor individually. However, it should be noted that this study did not examine levels of ERα46, which could have further modulated tumor aggression. ERα46 has been found in some breast cancer cell lines, but little is known about its function as an estrogen receptor independent of ERα66 and ERα36 [27,58].

In a sampling of breast cancer cells, MCF7, which is widely regarded as a less-aggressive breast cancer cell line [59], was found to have high levels of ERα66+, low levels of ERα46, and moderate levels of ERα36 (Figure 2.1). HCC38, a moderately aggressive breast cancer cell line [1], had no ERα66, moderate levels of ERα46, and moderate levels of ERα36 (Figure 2.1). MDA-MB-231, an aggressively metastatic breast cancer cell line [60], had no ERα66, high levels of ERα46, and moderate levels of ERα36 (Figure 2.1). It is not clear which of these isoforms or what combination of isoforms determines the relative levels of aggression or metastatic potential of each cell line; however, it is crucial to take the expression of each of the ERα isoforms into account when classifying them as 'ER positive' or 'ER negative.'

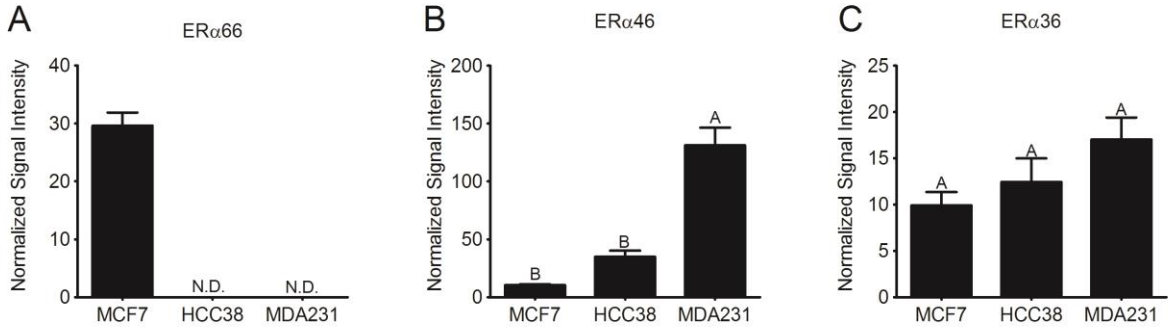

Figure 2.1 Western blot data of ERα isoforms in breast cancer cells.

[**A**] ERα66, [**B**] ERα46, and [**C**] ERα36 normalized to GAPDH and expressed as mean normalized signal intensity ± standard error in MCF7, HCC38, and MDA-MB-231 breast cancer cell lines[61].

Estrogen and estrogen receptors in laryngeal cancer

Although the importance of estrogen and estrogen receptor signaling has been well-established in breast cancer, estrogen signaling is also important in other hormonally responsive cancers. The larynx is a secondary sex organ that undergoes trophic changes in response to hormonal shifts during puberty, the role of steroid hormones and steroid hormone receptors in laryngeal squamous cell carcinoma (LSCC) has been understudied. Researchers first began to describe functional estrogen receptors (ERs) in LSCC cell lines over three decades ago[62,63]. These studies led to a small clinical trial on the use of tamoxifen, a potent anti-estrogen, in the treatment of LSCC[64,65]. However, the trial failed within six months because there was no observed clinical response or reduction in tumor size. This largely ended investigations into ER and the use of anti-estrogens in the treatment of LSCC.

ERα36 is present in both ERα66 positive (ERα66+) and ERα66 negative (ERα66-) LSCC samples[66–68]. However, unlike breast cancer[27], ERα36 expression in LSCC is highly variable. This suggests that crosstalk between rapid and genomic signaling pathways mediated by multiple ERs may control the estrogen response in LSCC. This section highlights some of the rapid estrogen signaling pathways previously described in LSCC and suggests that clinical decisions regarding prognosis and treatment of LSCC may be informed by the ERα profiles of individual LSCC patients.

Previous studies by our laboratory show that loss of nuclear ER staining, but not membrane ER staining (as measured by immunohistochemistry) is associated with reduced patient prognoses and increased lymph node metastases in LSCC[66]. This is similar to trends observed in ER- breast cancer[66,67,69]. A loss of estrogen receptor β

expression (ERβ) has been associated with increased aggression in LSCC[70]. Changes in the non-traditional transmembrane ER G-protein coupled estrogen receptor (GPER1) and ERα36 have also been associated with malignancies observed in histology of human vocal fold tissue[71] and *in vitro* experiments on human LSCC cells[66,67].

Estrogen receptor signaling

Classical estrogen signaling is mediated by the nuclear receptors ERα and ERβ. E_2 binding to these receptors in the cytoplasm leads to hetero-or homo-dimerized ERs and the translocation of the E_2-ER ligand-receptor complex to the nucleus. Here it acts as a transcription factor for genes associated with proliferation, cell survival, metastasis, invasion, migration, and others[68,72]. Simultaneously, membrane-associated E_2-ER binding triggers many rapid signal transduction pathways, such as phosphoinositol-3-kinase (PI3K) / protein kinase B (PKB, also known as Akt), extracellular signal-regulated kinases (ERK), and mitogen-activated protein kinase (MAPK)[68,73]. Both the canonical and rapid signaling pathways induced by E_2-ER binding stimulate pro-tumorigenic phenotypes. In this way E_2 is a potent mitogen and EMT stimulus, promoting invasion and metastasis in prostate, ovarian, breast, uterine, and LSCC cells[67,74–79].

E_2-ER interactions encompass a complex network of canonical and rapid responses. In addition to stimulating a number of mitogenic and cell survival pathways in LSCC as described below, E_2 also stimulates the transcription of its own receptors. Canonically, the ESR1 gene, which encodes ERα, has both distal and proximal promoter regions. The E_2-ER complex directly stimulates the transcription of ESR1 by binding to one or more of these promoters in certain cell types[80,81] and indirectly stimulates them by

binding to other receptors that can enhance ER transcription downstream (such as EGFR)[82,83]. Treatment with dose-dependent E_2 increased gene expression of ERα36 and ERα66 (Figure 2.2).

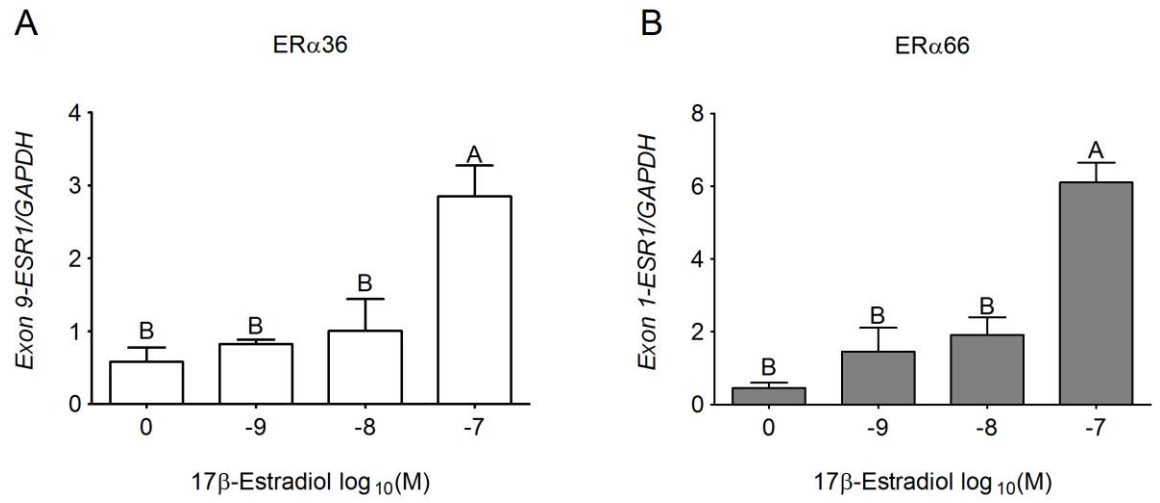

Figure 2.2 E2 upregulates the expression of ERα36 and ERα66 in UM-SCC-12, a laryngeal cancer cell line.

Effects of E2 on gene expression of [**A**] ERα36 and [**B**] ERα66 in estrogen receptor positive UM-SCC-12 laryngeal cancer cells[84].

Rapid Estrogen Signaling

Estrogen, like other steroid hormones, initiates some non-nuclear rapid signaling pathways that initiate a number of mitogenic, anti-apoptotic, invasive, and metastases-promoting signaling mechanisms.[30,85]. Many of these pathways involve phospholipases, kinases and other secondary messengers such as phospholipase D (PLD) and protein kinase C (PKC)[68]. These may result in altered mRNA transcripts downstream, but these non-genomic pathways are still distinct from classical signaling in that they do not directly involve the activation or suppression of DNA response elements by the E$_2$-ER complex.

One commonly studied membrane-associated estrogen receptor is ERα36. ERα36 lacks the transcriptional activation domains AF1 and AF2, which implies that ERα36 is incapable of directly stimulating transcription by binding to gene promoter sites. This lack of transcriptional activity distinguishes the actions of ERα36 from the transcriptionally active canonical receptor ERα66. ERα36 does, however, retain the DNA binding, ligand binding, and partial dimerization zones of the canonical protein[42,86]. Thus ERα36 may act as a co-factor to dimerize with other, possibly transcriptionally active, ERs. ERα36 also has a unique function mediated by 27 amino acids transcribed from the novel exon 9 of the ESR1 gene[35]. Although the specific function of these 27 amino acids has not been fully described, research suggests that they are involved in the membrane-associated signaling actions of ERα36. Breast cancer cells transfected with ERα36 lacking exon 9 are unable to trigger the rapid membrane-associated signaling described for wild-type ERα36, suggesting a unique function for ERα36 independent from its role as a truncated dimerizing ERα66 variant[55].

ERα36 is highly expressed in many breast cancer tumors that were previously diagnosed as ER negative[55,87]. In these tumors, E_2 signaling through ERα36 stimulates some tumorigenic and cell cycle disrupting pathways[1]. Evidence of E_2 signaling in ERα66-,ERα36+ cells has called into question traditional pathological classifications that describe ERα66 negative breast cancers as 'estrogen non-responsive.' Furthermore, in addition to promoting E_2 signaling, unlike the traditional ERα66, high expression of ERα36 is associated with unfavorable clinical prognosis, suggesting that ERα36 might have value as a prognostic biomarker[88].

Similar trends have been observed in LSCC, with ERα36-expressing cancers expressing more markers of clinical aggression than their ERα66 positive counterparts[67]. Some studies have shown that E_2 increases proliferation in LSCC cells through both genomic[89–91] and non-genomic mechanisms[64]. Our lab and others have shown that E_2 stimulation of ERα36 triggers PKC activation[66,67]. This mechanism is also present in breast cancer cells[1,67]. *In vitro* activation of ERα36 by E_2 in HEp-2 and UM-SCC-12 cells inhibits apoptosis and enhances proliferation, and activates PLD and PKC (Figure 2.3)[66,67]. Further investigation into the mechanism of membrane E_2 signaling has revealed that the pro-proliferative and anti-apoptotic mechanisms of E_2 are dependent upon PLD and PKC activation[67]. However, the specific receptors which control E_2 signaling in laryngeal cancer have not been identified (Figure 2.3).

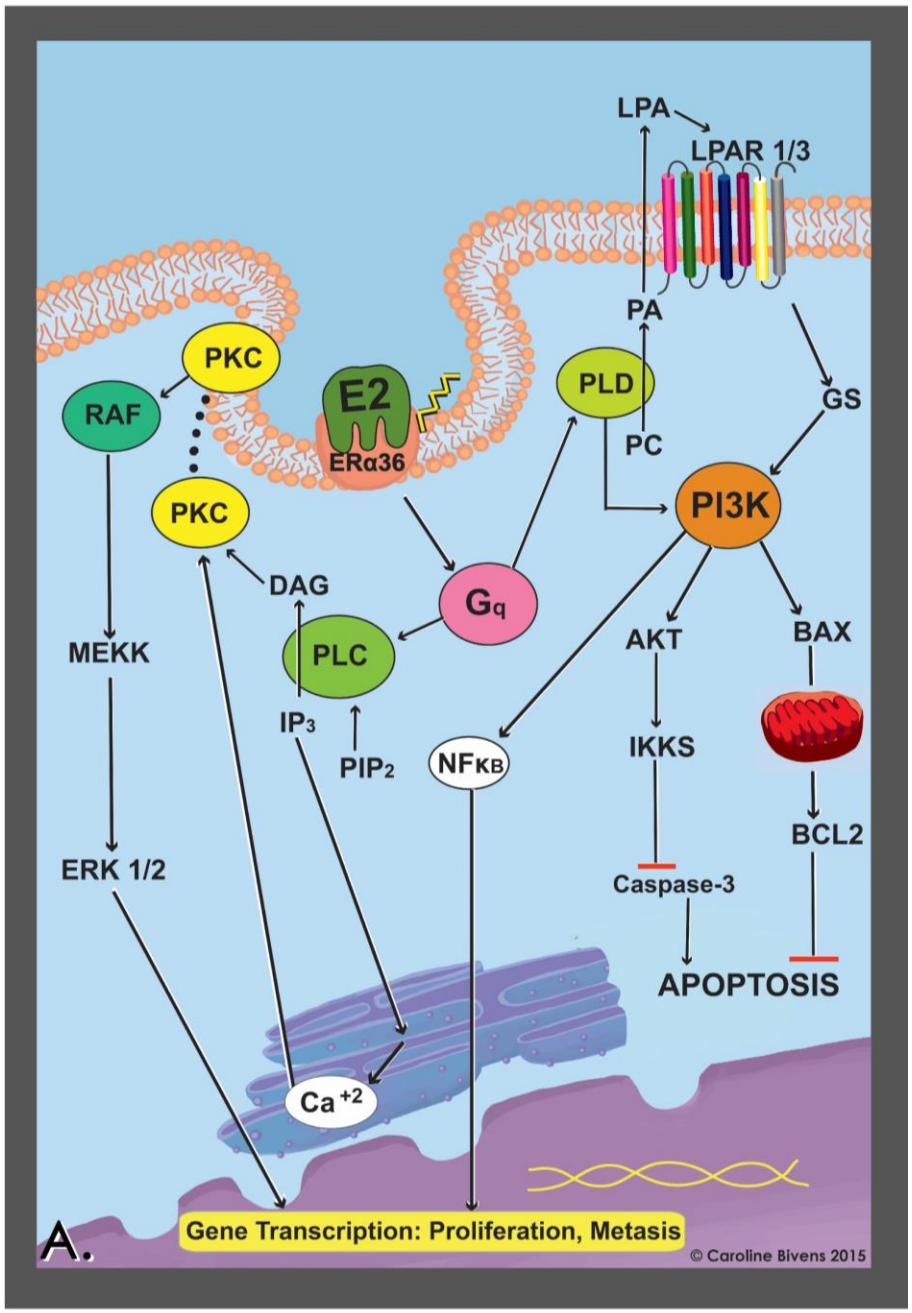

Figure 2.3 Mechanism of E2 signaling through ERα36.

E2 activates ERα36 in the caveolae and leads to Gq-mediated phospholipase D and PLC pathways. PLD activates PI3K-mediated anti-apoptotic pathways, and PLC activates PKC-ERK pathways, leading to proliferation and metastasis[68].

24R,25(OH)$_2$D$_3$ signaling

A similar parallel mechanism has been demonstrated in 24R,25(OH)$_2$D$_3$ signaling in chondrocytes [18,92,93], which has been shown to inhibit apoptosis through an as yet unidentified membrane receptor. Once ingested, vitamin D$_3$ – the most bioavailable form of vitamin D – is hydroxylated in the liver into 25(OH)D$_3$, the circulating form of vitamin D$_3$ commonly measured as 'serum vitamin D' [13]. 25(OH)D$_3$ is then further hydroxylated in the kidneys to become the steroid hormones 1,25(OH)$_2$D$_3$ or 24,25(OH)$_2$D$_3$ [13]. 1α,25(OH)$_2$D$_3$ has been widely studied because of its role in regulated calcium homeostasis in concert with parathyroid hormone (PTH) [94]. 1α,25(OH)$_2$D$_3$ is also an essential hormone for bone health because of its role in sequestering calcium within the bones to maintain bone mineralization and strength. 24R,25(OH)$_2$D$_3$ is not as well studied, partially because it is often regarded as a 'waste product' that cycles with 1α,25(OH)$_2$D$_3$ to regulate the production of the latter hormone. However, studies by our lab and others have demonstrated a role for 24R,25-(OH)$_2$D$_3$ in growth plate development and fracture callus healing, where 24R,25-(OH)$_2$D$_3$ has an anti-apoptotic effect and is an essential regulator of chondrocyte sensitivity to 1α,25(OH)$_2$D$_3$.

24R,25(OH)$_2$D$_3$ plays a key role in fracture healing and chondrocyte differentiation via a membrane-mediated PLD dependent pathway [93,95]. Unlike 1α,25(OH)$_2$D$_3$, which helps regulate calcium mineralization of the lower parts of the growth plate, 24R,25(OH)$_2$D$_3$ is essential for cell cycle regulation in earlier stages of the growth plate, particularly in the progression of pre-proliferative chondrocytes to proliferative chondrocytes [96]. Recent studies have suggested that 24R,25(OH)$_2$D$_3$ or the 24-hydroxylase that produces it, CYP24A1, may modulate cell proliferation and apoptosis in cancer cells [97–99]. This effect

may be a direct result of the activities of either the hormone or enzyme; or may be the result of modulation of the effects of 1α,25(OH)$_2$D$_3$. 24,25(OH)$_2$D$_3$ has been shown to regulate the production of the 1-hydroxylase enzyme CYP27B1, which converts 25(OH)D$_3$ to 1,25(OH)$_2$D$_3$ [100]. In a similar manner, 24R,25(OH)$_2$D$_3$ promotes chondrocyte sensitivity to 1α,25(OH)$_2$D$_3$ [93], encouraging a positive feedback loop where each hormone regulates the production of the other, resulting in 1α,25(OH)$_2$D$_3$ and 24R,25(OH)$_2$D$_3$ cycling within the body [101,102].

As described above, 24R,25(OH)$_2$D$_3$ has been shown to signal through an as-yet unidentified receptor to stimulate PLD and subsequent anti-apoptosis response in chondrocytes. The identity of this receptor has been a matter of debate for decades. Larsson et al., while studying the lysosomal membranes of chick intestinal cells, reported that catalase-1 specifically binds 24R,25(OH)$_2$D$_3$ [21], suggesting a rapid peroxidase-involved signal transduction pathway for 24,25(OH)$_2$D$_3$. A number of papers from the lab of Dr. Anthony Norman have reported evidence for a membrane-bound receptor for 24R,25(OH)$_2$D$_3$ in chick fracture healing callus that may be involved in rapid or genomic signal transduction [19,20]. Crystallographic studies of the classical vitamin D receptor (VDR) suggest that conformational changes in the receptor may accommodate the transient binding of 24R,25(OH)$_2$D$_3$ to the ligand-binding pocket of VDR[54]. Recently, another 24R,25(OH)$_2$D$_3$ receptor, FAM57B2, was identified by Martineau et al., which may be essential to the 24R,25(OH)$_2$D$_3$ response in fracture callus repair[22]. Numerous studies in rat growth plate chondrocytes have characterized a specific membrane-associated signal transduction pathway that mediates both classical genomic and rapid responses of

24R,25(OH)$_2$D$_3$, strongly suggesting the presence of a membrane receptor or signaling complex that regulates the actions of 24R,25(OH)$_2$D$_3$ [17,23,93,103].

While a consensus receptor for 24R,25(OH)$_2$D$_3$ remains elusive, membrane signaling by 24R,25(OH)$_2$D$_3$ has been described. In costochondral resting zone chondrocytes, 24R,25(OH)$_2$D$_3$ binds to an as yet unidentified membrane-bound receptor and inhibits phospholipase A$_2$ activity (PLA$_2$) [104]. The resulting signaling pathway alters fatty acid turnover and subsequently inhibits the release of arachidonic acid and prostaglandin E$_2$ (PGE$_2$) production [23,103,105]. This inhibition of arachidonic acid turnover alters membrane fluidity and calcium flux within the cell, modulating signal transduction downstream and stimulating PKC activity [23,103,106,107]. The effect of 24R,25(OH)$_2$D$_3$ is stereospecific; 24S,25(OH)$_2$D$_3$ does not activate this pathway, providing further evidence that the response to the hormone is receptor mediated.

24R,25(OH)$_2$D$_3$ binding to the membrane receptor also stimulates PLD, which increases diacylglycerol production (DAG), to in turn activate PKCα [15,16,18]. This increase in PKCα has been observed in whole cell lysate and cell membrane fractions, while 24R,25(OH)$_2$D$_3$ has been shown to increase PKCζ in resting zone matrix vesicles [23,108].

Although 24,25(OH)$_2$D$_3$ stimulation of PLD2 activates DAG to stimulate PKC, this subsequent activation of PKC does not coincide with the translocation of PKC to the plasma membrane [16]. This suggests that 24R,25(OH)$_2$D$_3$ stimulation of PKC activity via PLD may not be a direct result of 24R,25(OH)$_2$D$_3$ binding to a membrane receptor and is instead a result of downstream signaling by other secondary messengers. Furthermore, although resting zone cells have active phospholipase C (PLC) isoforms – namely PLCβ1 and PLCβ3 – neither PLC is activated by 24R,25(OH)$_2$D$_3$, and inhibition of PLC does not

affect 24R,25(OH)$_2$D$_3$ stimulation of PKC [15,17]. Together with the inhibition of PLA$_2$ and stimulation of DAG act to enhance PKC activity to stimulate the phosphorylation of multiple proteins in multiple anti-apoptotic downstream pathways, including MAPK and ERK, which are also stimulated by 17β-estradiol through both genomic and non-genomic pathways [36,47,83,109,110] (Figure 2.4).

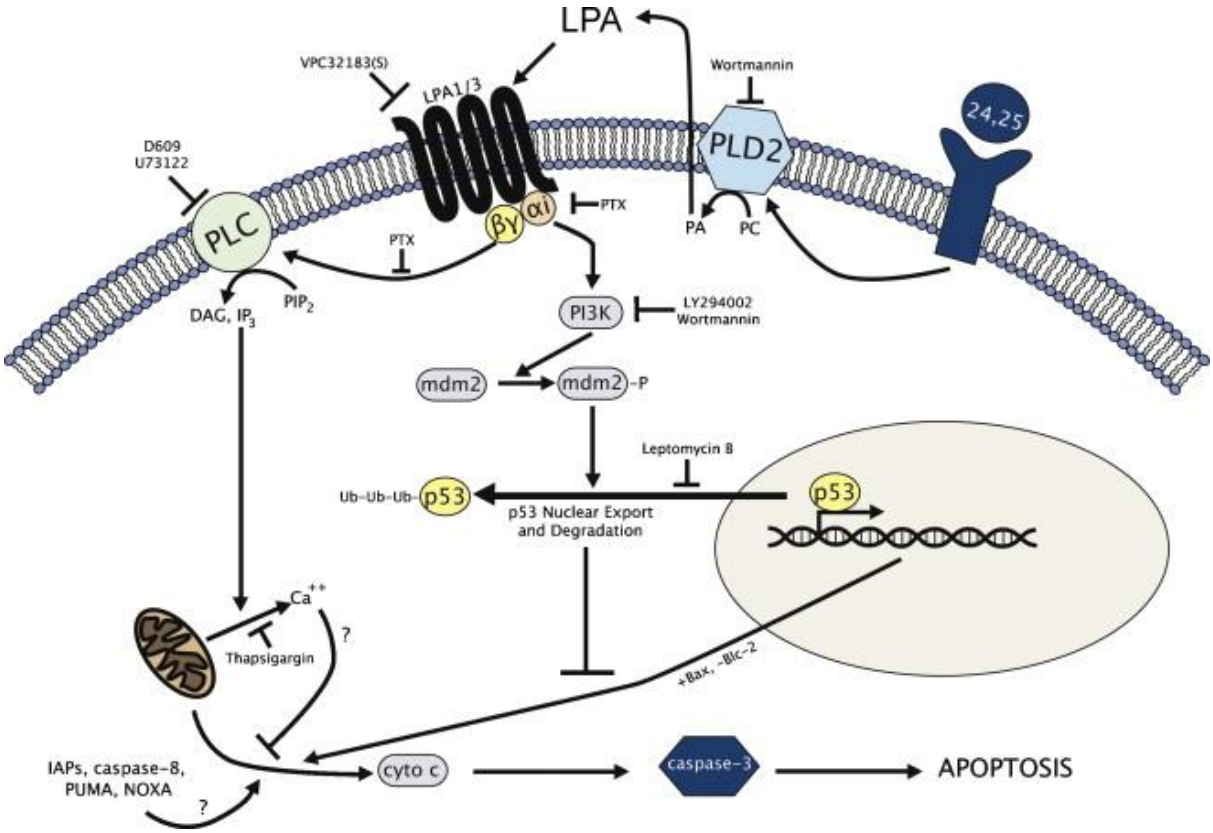

Figure 2.4 24R,25 signaling through PLD.

24R,25(OH)$_2$D$_3$ binds to an unidentified membrane receptor to stimulate PLD2 in resting zone chondrocytes. Activation of PLD2 stimulates lysophosphatidic acid (LPA), which stimulates PLC and PI3K. Downstream of PI3K, 24R,25(OH)$_2$D$_3$ inhibits p53 ubiquitination in chondrocytes, preventing apoptosis.

Vitamin D3 supplementation in cancer.

Preclinical studies and meta-analyses have suggested that 1,25(OH)$_2$D$_3$ and 25(OH)D$_3$ may have potential as a preventive therapy for breast cancer. Despite this, clinical studies investigating vitamin D supplementation on breast cancer prognosis have been largely inconclusive [8,111–113]. Oral vitamin D3 has been shown to increase cell turnover, autophagy, and reduce tumor growth in the mammary glands of normal mice [14,114], and intravenous 1α,25(OH)$_2$D$_3$ has been shown to reduce tumor growth in ER-positive breast cancer xenografts [14]. *In vitro*, 1α,25(OH)$_2$D$_3$ has been shown to reduce angiogenic, metastatic, and apoptotic markers in ER-positive breast cancer cells, but not in normal cultured human mammary epithelial cells [115–118]. This could be a function specific to the interactions of 1α,25(OH)$_2$D$_3$ with the VDR, which regulates 1α,25(OH)$_2$D$_3$'s genomic actions by dimerizing with the retinoic acid receptor to form a transcription complex [119]. Dimerized VDR bound to 1α,25(OH)$_2$D$_3$ has been shown to suppress transcription of the ESR1 gene [120], which could inhibit the feed-forward loop of estrogen-ERα signaling [121]. Alternatively, 1α,25(OH)$_2$D$_3$'s anti-tumorigenicity could be a function of its non-genomic actions, as its analogs 1,24,25-trihydroxyvitamin D3 and 1,25,26-trihydroxyvitamin D3, which are incapable of binding to VDR, have also been shown to inhibit the growth of breast cancer cells *in vitro* [122].

Studies examining the use of 1α,25(OH)$_2$D$_3$ as a safe, easy to deliver supplement against breast cancer tumorigenicity have been promising; however, there is a risk of hypercalcemia with excess 1α,25(OH)$_2$D$_3$. Hypercalcemia is a common co-morbidity of cancer, with up to 30% of all cancer patients suffering severe hypercalcemia [123]. It is the leading cause of hospitalization in cancer patients, and who have breast cancer are

particularly susceptible [124]. Excess 1α,25(OH)$_2$D$_3$ is a documented cause of hypercalcemia [125], and blood serum levels of free 1α,25(OH)$_2$D$_3$ as low as 200pmol/L (with ~85 pmol/L approximating normal 1α,25(OH)$_2$D$_3$ levels) can be toxic [126]. Many *in vitro* studies only observe the anti-tumorigenic effects of 1α,25(OH)$_2$D$_3$ when treating with 1-100 nmol/L, well above the toxicity threshold for this compound [127–129].

The search for non-calcemic analogs of vitamin D3 that can approximate 1α,25(OH)$_2$D$_3$'s anti-tumorigenic effects has led researchers to look at modifications of 1α,25(OH)$_2$D$_3$ that do not bind to VDR and thus do not have the same hypercalcemic effects. Some of these studies have been successful, but the majority are not approved for the treatment of cancer [130].

Although connections between improved breast cancer prognoses and high vitamin D serum levels have been well-established, there is no consensus on the efficacy of vitamin D supplementation in the treatment of breast cancer. Studies examining breast cancer prognosis and vitamin D serum levels could be improved by considering the breast cancer molecular subtypes, particularly the ER status, of the patients involved. 24R,25(OH)$_2$D$_3$, an understudied vitamin D3 metabolite, may have potential as a non-calcemic vitamin D3 metabolite with tumor modulating properties. Further research is needed to understand the connections between ER status and the anti-tumorigenicity of vitamin D supplements, and the parallels between membrane mediated estrogen signaling through ERα36 and 24R,25(OH)$_2$D$_3$ may provide insight into this connection.

Chapter 3.

Estradiol Receptor Profile and Estrogen Responsiveness in Laryngeal Cancer and Clinical Outcomes

[Chapter 3 is published as: Schwartz N, Verma A, Muktipaty C, Bivens C, Schwartz Z, Boyan BD. Estradiol receptor profile and estrogen responsiveness in laryngeal cancer and clinical outcomes. Steroids. 2019; 142(2):34-42]

Introduction

Laryngeal cancer, despite arising from a secondary sex organ and having a clear gender disposition, is not uniformly accepted as sex hormone-dependent. The determination of sex hormone responsiveness, specifically to 17β-estradiol (E_2), impacts the prognosis of the patients and the treatment modalities that are implemented in these types of cancers. E_2 plays a key role in the pathogenesis of hormone-responsive cancers, the most well studied being breast cancer and prostate cancer [46,131], by enhancing cell proliferation, survivability, and metastasis [76,132,133]. Due to its effects on cancer progression and behavior, the presence of E_2 receptors (ER) has long been the most important molecular marker used in the diagnosis and as a predictor of prognosis in breast cancer dictating treatment.

Classically, E_2 mediates its effects through interaction with its nuclear receptors, ERα and ERβ. These receptors act as transcription factors by binding to specific response elements, or transcription initiation complexes, on the DNA to either activate or repress transcription in a process that occurs in a matter of hours to days [29,134]. Steroid hormones also initiate non-nuclear, non-genomic rapid signaling within seconds to minutes that

occurs independently of transcription or translation [30,85]. This results from steroid binding to specific extra-nuclear receptors associated with the cell membrane, leading to the activation of signaling cascades that involve kinases, phospholipases, calcium flux and other second messengers, and may result in altered mRNA levels [34,35]. Recent studies indicate that motifs within ER exons encode sequences associated with palmitoylation, thereby linking the receptor to the membrane[35].

One of the key candidates for the membrane mediated action of E_2 is a novel ERα splice variant with a molecular mass of approximately 36 kDa, which has been named ERα36. ERα36 differs from ERα66, the classic nuclear ER receptor, by lacking both transcriptional activation domains (AF1 and AF2) (exons 7 and 8) but retaining the DNA-binding domain and partial dimerization and ligand-binding domains of the nuclear receptor. This suggests that although it may still bind to DNA, ERα36 may not directly activate transcription. Rather, it may affect transcriptional function as a co-factor due to its ability to dimerize with other ERs and bind to DNA[42,86]. In addition, ERα36 contains a novel exon 9, which encodes 27 amino acids of unknown function[35]. Breast cancer cells transfected with ER36 lacking exon 9, lack the ability to trigger rapid activation of membrane associated signaling[55], suggesting that this may be an important key to its role in E_2 responsiveness.

ERα36 is gaining special interest particularly in regards to its role in mediating E_2 responsiveness in traditionally diagnosed ER negative tumors[55,87], and its role in modulating anti-estrogen resistance in ER positive tumors[1], which have otherwise been clinically regarded as hormone-unresponsive. Inclusion of this receptor in screens of ER negative breast cancers showed that high levels of ERα36 expression were correlated

with an unfavorable clinical prognosis independent of nuclear ER status[88]. Thus ERα36 has been suggested as an important novel marker for breast cancer clinical characterization, suggesting it may serve a valuable function for laryngeal cancers as well.

ERα36 has the ability to mediate the effects of E_2 independently of nuclear ERα, as demonstrated in ERα66 null cells and in studies using antibodies against the nuclear and membrane isoforms of ERα [109]. The receptor has been shown to initiate divergent pathways from the plasma membrane that re-converge downstream to affect cancer cell survivability. E_2 binding to ERα36 affects proliferation through the activation of G-proteins, which in turn lead to the activation of phospholipase C (PLC). PLC activation leads to the production of diacylglycerol (DAG) and inositol trisphosphate (IP_3), which subsequently trigger calcium signaling and protein kinase C (PKC) activation. Together, calcium signaling and PKC activation culminate in downstream activation of mitogen-activated protein kinase (MAPK) [1] to increase DNA synthesis and gene transcription. At the same time, E_2 activation of ERα36 reduces apoptosis by blocking effects of common chemotherapeutics, such as Taxol [66], by activating phospholipase D (PLD) at the membrane, leading to activation of lysophosphatidic acid (LPA) signaling and phosphoinositol-3 kinase (PI3K). This in turn attenuates the caspase cascade that promotes apoptosis [27,55]. This mechanism of E_2's action was also shown in laryngeal cancer cells [66].

As laryngeal cancer is not perceived to be a sex hormone-responsive cancer, most studies do not examine tumor responses or tumorigenesis regulation by steroid hormones in laryngeal cancer. Little can be concluded from the sparse data available on the relation

of E_2 with laryngeal cancer. Even the presence of classical cytosolic ERs in laryngeal cancer is controversial. Several studies have argued that laryngeal cancer does not possess any functional ER [135], or rather implied that the presence of the receptors originates from stromal or mesenchymal tissues in the larynx and not from the epithelial component, which constitutes the origin of laryngeal cancer [136]. Other studies affirm the presence of classical nuclear ERs in laryngeal cancer [137,138] and even correlate the presence and number of the receptors with local metastasis status [139]. Despite this lack of agreement, there is growing evidence that laryngeal cancer cells display E_2 responsiveness, as E_2 was found to increase the proliferation of laryngeal cancer cells [89–91] via a non-genomic mechanism [64]. Furthermore, 4'hydroxytamoxifen has been demonstrated to inhibit the growth of laryngeal cancer, in part, due to its anti-estrogen effect [63,140]; and this effect is eliminated with the addition of E_2[63,64,137].

Previously, we have shown that Hep2 laryngeal carcinoma epithelial cells express both ERα66 and ERα36. ERα36 was found to reside in the plasma membrane, and stimulation of ERα36 by E_2 stimulated PKC activation via a mechanism comparable to that shown in breast cancer cells [1]. In vitro, E_2 activation of ERα36 was shown to cause a PLD-dependent increase in PKC activity, followed by an upregulation of angiogenic and metastatic factors. ERα36 signaling enhanced both proliferation and the anti-apoptotic effect of E_2 against chemotherapeutics, indicating a role in tumorigenesis. Furthermore, it was demonstrated both *in vitro* and *in vivo* that E_2 enhanced vascular endothelial growth factor (VEGF) and fibroblast growth factor (FGF) expression. An association has been suggested between high levels of ERα36 and VEGF and a more aggressive tumor phenotype, as evidenced by the correlation to lymph node metastasis[66].

These findings advocate a role for E_2 in the tumorigenesis of laryngeal cancer and raise the option of heterogeneity of expression of ERs and responsiveness in the tumor cells that warrants further exploration. In the present study we studied two laryngeal cancer lines with different ERα expression to examine the signaling pathways activated by E_2 in an attempt to clarify the importance of profiling laryngeal cancer E_2 responsiveness and the clinical implications ER profiling might have for the treatment of laryngeal cancer.

Materials and Methods

Cell Culture

UM-SCC-11A and UM-SCC-12 cells were obtained from the Carey Laboratory at the University of Michigan (Ann Arbor, MI) and cultured in high-glucose Dulbecco's minimum essential medium (HG DMEM) lacking phenol red (Invitrogen, Carlsbad, CA), supplemented with 10% fetal bovine serum (FBS) (ThermoFisher, Waltham, MA, USA), 2mM L-glutamine, and 100U/100U penicillin-streptomycin (ThermoFisher).

Presence of ER Isoforms

ERα expression in laryngeal cancer cells was identified using sequence-specific primers, designed in our lab previously[16], to identify traditional ERα66 and the spliced variant ERα36. A commercial primer was used to identify ESR2 (ERβ) (Qiagen, Hilden, Germany). UM-SCC-12 and UM-SCC-11A cells were plated in 24-well plates at 20,000 cells/cm^2 (n=6 per variable) and cultured to confluence. RNA was extracted with TRIzol and used to synthesize cDNA libraries (Thermo Fisher Scientific, High Capacity cDNA Reverse Transcription kit). Levels of RNA expression were quantified using gene-specific

primers (Table 3.1). RNA expression for ERα46/66 was done with primers that amplified exon 1 of the ESR1 gene, and primers for ERα36 amplified exon 9 of the ESR1 gene. Data were verified with a commercial primer from Qiagen, which amplified exon 3/4 of ESR1. Expression of ERβ was assessed with a commercial primer from Qiagen, which amplified exon 5/6 of ESR2. All gene expression was quantified using a whole-cell standard and normalized to GAPDH.

Gene	Forward Primar	Reverse Primer
ERα46/66	TGCGTCGCCTCTAACCTCG	TCCCAGATGCTTTGGTGTGG
ERα36	TCCTCGTGTCTAAAGCCTCTG	AAAATGTCCCCACGTCCACA
GAPDH	CTATAAATTGAGCCCGCAGCC	TGGCGACGCAAAAGAAGATG

Table 3.1 Human primers used in real-time PCR analysis.

Western blots were used to identify and quantify ER protein in the laryngeal cell lines. Cells were plated at 10,000 cells/cm^2 in T-75 flasks (Corning) and cultured to confluence. Monolayers were washed twice with 1X PBS and ERα66, ERα46, ERα36, and ERβ were assessed using a western blot assay with GAPDH protein as the loading control. UM-SCC-12, UM-SCC-11A, and MCF7 cells were lysed in 200µL radioimmunoprecipitation assay buffer (RIPA) and resolved on 4-20% Tris-glycine extended gels using gel electrophoresis. Proteins were transferred from the gel onto a PVDF membrane using the Bio-rad Mini Trans-Blot® Electrophoretic Transfer Cell. Membranes were blocked and probed with primary and secondary antibodies according

to the LI-COR Western Blot Protocol. Membranes were then imaged on the Odyssey®CLx Infrared Imaging System from LI-COR.

Response to 17β-Estradiol

17β-Estradiol (#BML-DM200-0050) was purchased from Sigma Aldrich (Farmingdale, NY) and reconstituted to 1mM stock solutions in absolute ethanol. Stock solutions were diluted in warm complete media to final treatment concentrations. For all experiments except DNA synthesis, cells were treated at confluence. Media were aspirated and cell layers were treated with media containing 0 (vehicle), 10^{-9}M, 10^{-8}M, or 10^{-7}M E_2 for 9 minutes at 37^0C, 5%CO_2, 100% humidity. Media were then removed by aspiration and cells were harvested (PKC, PLD assays) or incubated with fresh complete media for 24 hours (p53 and VEGF protein expression).

Specific inhibition of membrane associated factors involved in ERα36 signaling was used to examine whether the effects of E_2 were mediated via these mechanisms. PLD was inhibited by wortmannin (VWR, Radnor, PA, #80055-508) [15,141,142]. Caveolae were disrupted using methyl β-cyclodextrin, which depletes the membranes of cholesterol (Millipore-Sigma, St. Louis, MO, #C4555-10G) [1]. Estrogen receptors were inhibited using a neutralizing antibody to ERα36 (Chi Scientific, Maynard, MA) [1]. Confluent cultures were pre-treated with media containing different concentrations of the inhibitor as indicated below. After 30 minutes, the media were replaced with fresh media containing either 0, 10^{-8}, or 10^{-7} M E_2 for 9 minutes. These media were removed by aspiration and cells were harvested immediately for analysis of PKC and PLD activity. Alternatively, fresh media were added to the cultures for 24 hours and protein expression for p53 and VEGF determined by duo-set ELISA as described below.

DNA Synthesis

Cells were cultured to 70% confluence; then serum-starved in phenol-red free HG DMEM supplemented with 1% charcoal-dextran filtered FBS and 100U/100U penicillin-streptomycin. After 48 hours in starvation media, cells were treated with 17β-estradiol or inhibitors (see above) and incubated with fresh complete media for 20 hours. At that time, cells were pulsed with 10µL of a 1:100 dilution of 5-ethynyl-2'-deoxyuridine (EdU) and incubated for an additional 4 hours. Cells were then harvested and assayed for EdU incorporation according to manufacturer's instructions (ThermoFisher Scientific).

DNA Fragmentation

Apoptosis was examined by assessing cells for DNA fragmentation by colorimetric terminal deoxynucleotidyl transferase (TdT)-mediated dUTP nick end labeling (Trevigen, TiterTAC™ *in situ* microplate TUNEL assay). After E2 treatment, cells were incubated with fresh media for 24 hours and fixed with formaldehyde containing 3.7% sucrose before being processed for TUNEL staining following manufacturer's instructions. Final absorbance was detected at 450 nm using a microplate spectrophotometer.

PKC Specific Activity

Cells were cultured to confluence in 24-well plates and treated with E2 as above; media were removed by aspiration and cells were washed twice with 2mL/well of 1X PBS. Cells were lysed in 200µL of PKC lysis buffer as per manufacturer's instructions and assayed for PKC activity using the PKC Activity Kit from (AbCam, Cambridge, UK). Cell lysates were assessed for total protein content using the Pierce BCA 660 reagent kit (VWR) and PKC activity was normalized to total protein.

PLD Specific Activity

Cells were cultured to confluence in 24-well plates and treated with E2 as above; media were removed by aspiration and cells were washed twice with 2mL/well of 1X PBS. Cells were lysed in PLD lysis buffer as per manufacturer's instructions and assayed for PLD activity using the PLD Activity Kit from Thermo Fisher Scientific. Cell lysates were assessed for total protein content using the Pierce BCA 660 reagent kit and PLD activity was normalized to total protein.

Total p53 Levels

P53 is a tumor suppressor gene that induces apoptosis [143]. Total p53 levels were measured 24 hours post-treatment using a sandwich ELISA (Human Total p53 DuoSet® IC, R&D Systems, Minneapolis, MN). Cells were plated in 24-well plates, treated with E2 for 9 minutes as described above, and incubated for 24 hours. After 24 hours, cells were lysed in 200µL of 1X PBS, 1mM EDTA, 0.5% Triton™ X-100 [144]. Lysates were centrifuged at 10,000*g* for 15 minutes and the supernatant was collected and assayed for total protein content (ThermoFisher, Pierce 660 nm Protein Assay) and total p53 content following manufacturer's instructions. Data are presented as a ratio of picograms of total p53 to total protein content.

Statistical Analysis

Data are presented as mean ± standard error of six independent cultures per treatment group. Outliers were removed with Grubbs' test using a P-value of 0.05. Data with one independent variable were analyzed by analysis of variance (ANOVA) with Tukey's post-test to determine significance between groups. Groups that do not share a letter are considered significant with p-values < 0.05. Experiments with two independent

variables (DNA synthesis, total p53 content, PKC, and PLD assays) were analyzed with one-way ANOVA as described above and two-way ANOVA with Bonferroni's modification of Student's t-test post-tests between all group means using Graphpad Prism 7. P-values <0.05 were considered significant and were marked with $*$ denoting significance between 0 vs. E$_2$ treatments for a given x-axis group.

Results

Western blots of UM-SCC-12 and UM-SCC011A cells showed that different laryngeal carcinoma cell lines express different sex hormone receptors (Figure 3.1A). As expected, the breast cancer MCF7 cell line possessed ERα66, ERα46, ERα36, and ERβ, confirming the gel system was working. UM-SCC-12 cells expressed mRNA for ERα66 whereas none was found in the UM-SCC-11A cells (Figure 3.1B). Both laryngeal cancer cell lines expressed mRNA for ERα36 (Figure 3.1C), but only UM-SCC-11A cells expressed mRNA for ERα (Figure 3.1C).

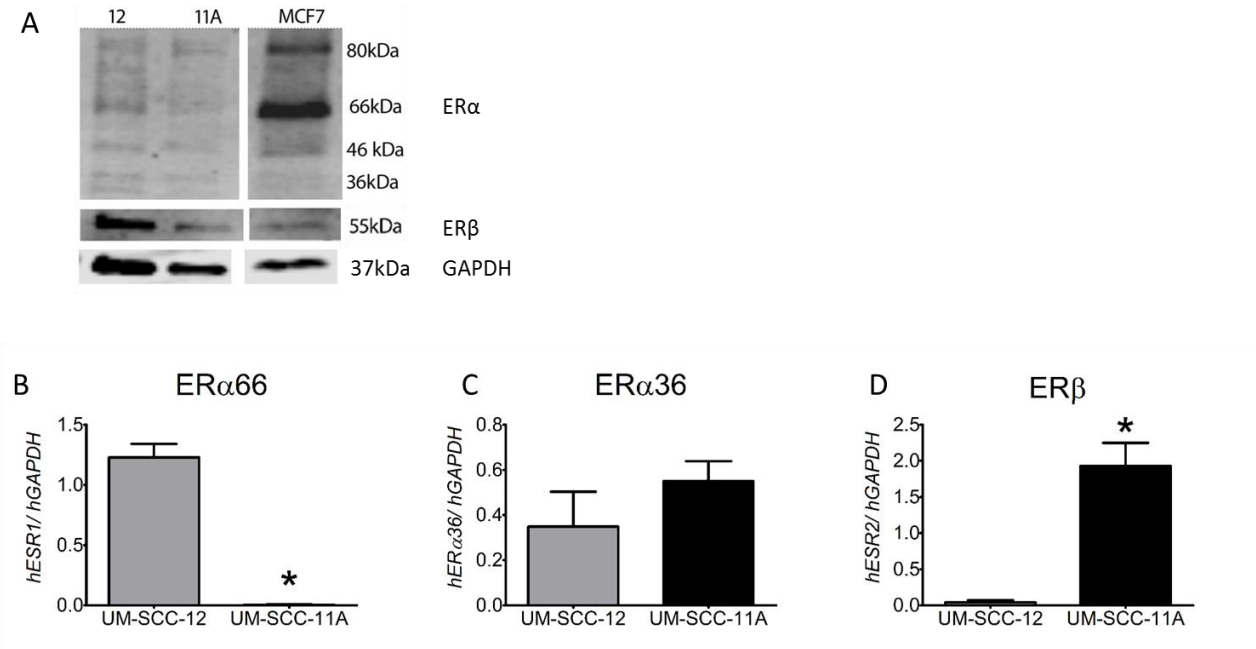

Figure 3.1 Estrogen receptor expression in whole cell lysates of UM-SCC-12 and UM-SCC-11A cells.

[**A**] ERα66, ERα36, and ERβ protein were identified via western blot using MCF7 breast cancer cells as controls. mRNA expression of [**B**] exon 1 of ESR1 (ERα66), [**C**] exon 9 of ESR1 (ERα36), and [**D**] ESR2 (ERβ) was measured by real-time qPCR.

E_2 regulated proliferation in the two cell lines in a differential manner. E_2 caused a slight decrease in DNA synthesis in UM-SCC-11A cells, which was significant at 10^{-7}M (Figure 3.2A). In contrast, E_2 increased DNA synthesis in UM-SCC-12 cells, which was significant at 10^{-8}M and 10^{-7}M (Figure 3.2B). Antibodies to ERα36 had no effect on cell proliferation in untreated UM-SCC-11A cells, but slightly increased proliferation in UM-SCC-11A cells treated with E_2 (Figure 3.2C). In contrast, antibodies to ERα36 did not affect the stimulatory effect of E_2 on cell proliferation in the UM-SCC-12 cells (Figure 3.2D). In UM-SCC-11A cells, inhibition of PLD with wortmannin alone did not affect proliferation. However, treatment with 0.1 and 1 M wortmannin in combination with 10^{-7}M E_2 reduced DNA synthesis as compared to matched-dose wortmannin treatment alone (Figure 3.2E). Similarly, wortmannin alone did not affect DNA synthesis, but it prevented an E_2-dependent increase in DNA synthesis in UM-SCC-12 cells (Figure 3.2F).

Apoptosis was regulated by E_2 in a cell line-specific manner. E_2 did not have a significant effect on DNA fragmentation measured via TUNEL assay in the UM-SCC-11A cells (Figure 3.3A). In contrast, E_2 caused a dose-dependent inhibition in TUNEL in the UM-SCC-12 cells (Figure 3.3B). E_2 did not affect total p53 in the UM-SCC-11A cells (Figure 3.3C) but reduced significantly p53 content of UM-SCC-12 cells (Figure 3.3D). Depletion of membrane cholesterol with methyl β-cyclodextrin reduced p53 levels to the same extent as 10^{-7}M E_2 in UM-SCC-12 cells but did not further reduce the inhibitory effect of the hormone (Figure 3.4).

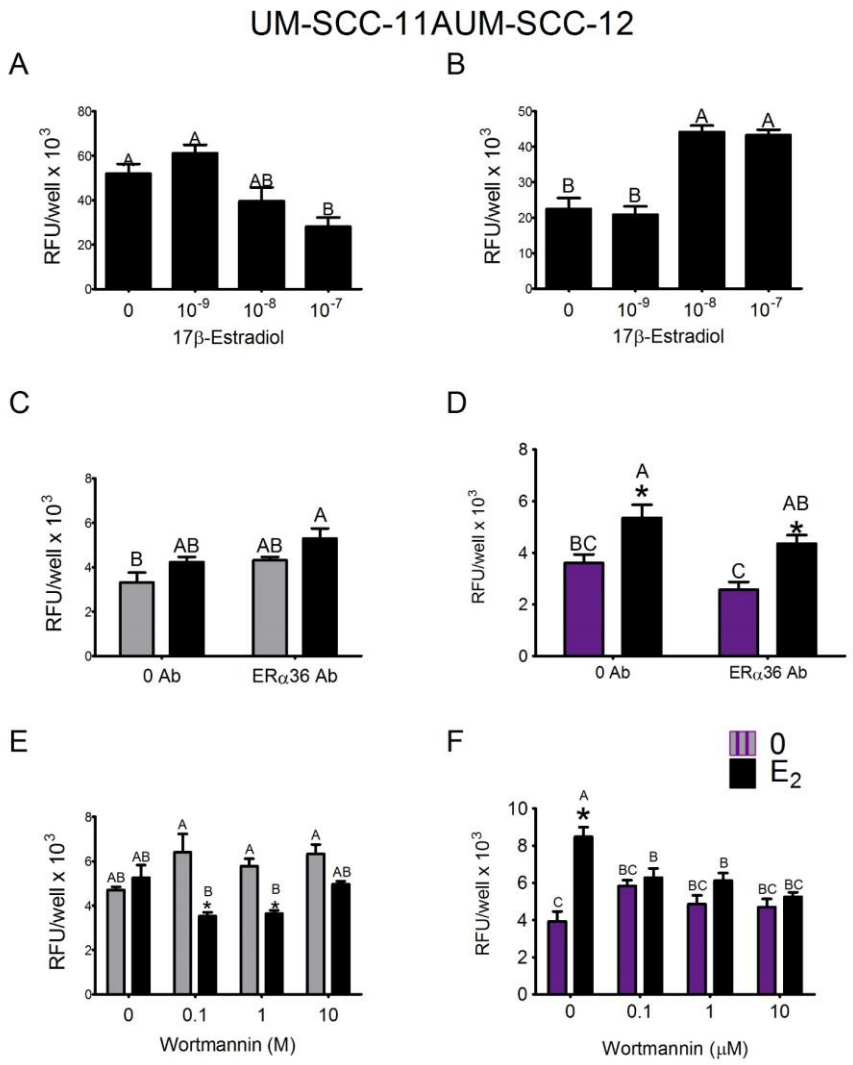

Figure 3.2 UM-SCC-12 and UM-SCC-11A cells were serum-starved and treated with E2 for 9 minutes.

Media were changed, and 24 hours later: [**A, B**] DNA synthesis was measured using a ClickiT EdU Microplate assay. [**C**, **D**] A second set of cultures was pre-treated with media or an antibody to ERα36 and then treated with vehicle or 10^{-7}M E_2 for 9 minutes. Media were changed and 24 hours later, DNA synthesis was measured. [**E**, **F**] A third set of cultures was pre-treated with wortmannin and then treated with vehicle or 10^{-7}M E_2 for 9 minutes before media were changed and DNA synthesis was measured 24 hours later.

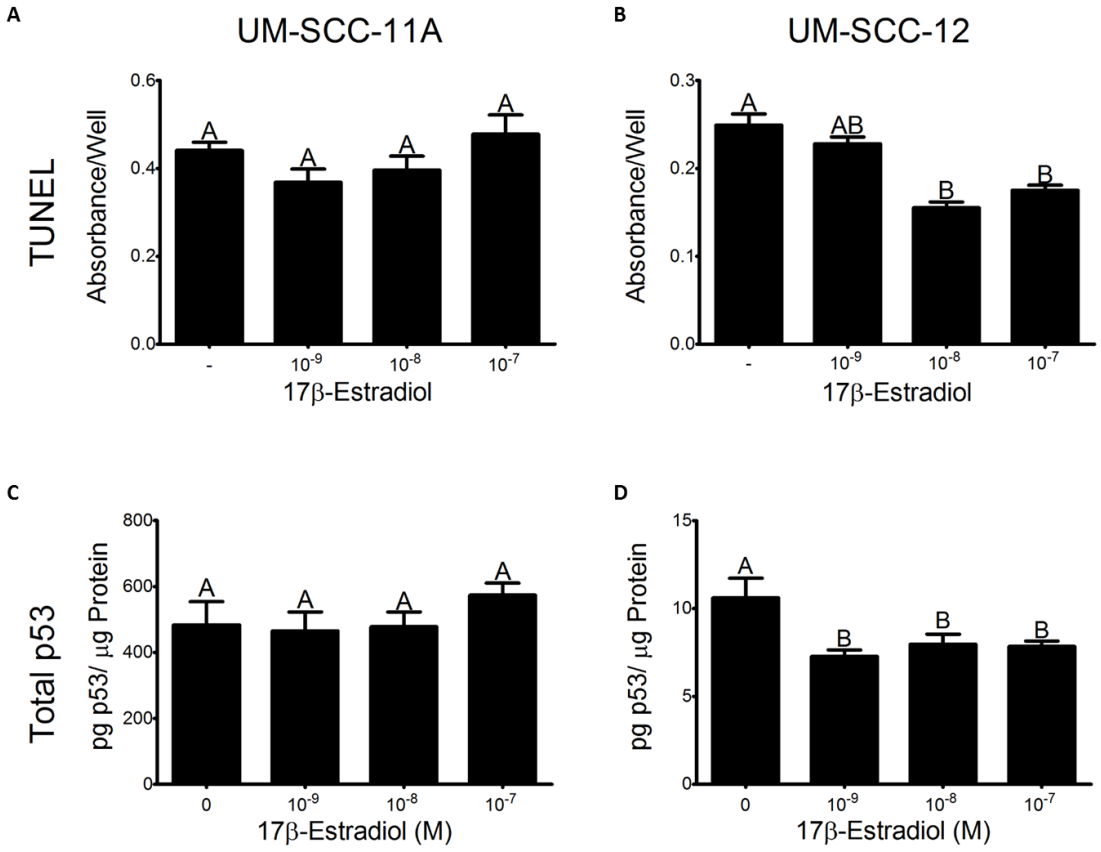

Figure 3.3 UM-SCC-12 and UM-SCC-11A cells were treated with E2 for 9 minutes.

[**A, B**] Media were changed, and 24 hours later, DNA fragments were measured in cultures using TUNEL staining. [**C**, **D**] A second set of cultures was treated identically and total intracellular p53 content was quantified with a sandwich ELISA assay.

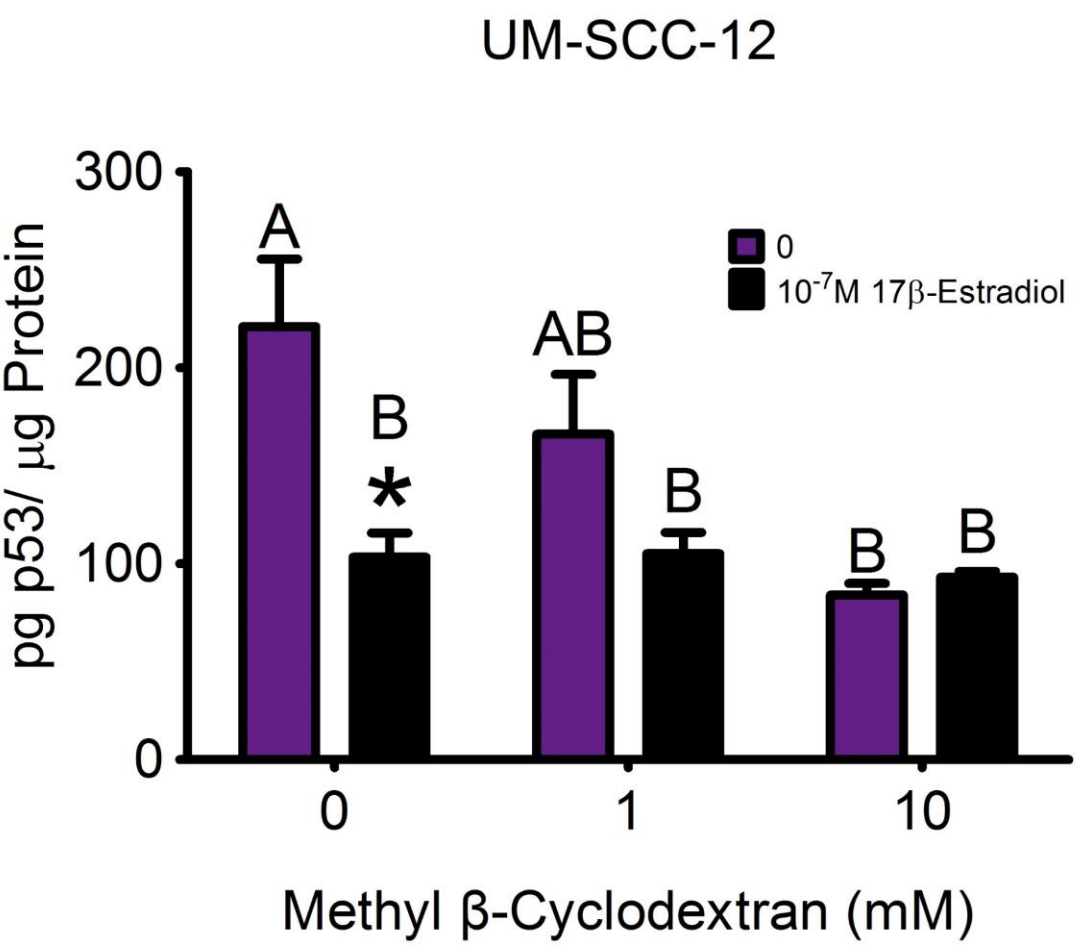

Figure 3.4 UM-SCC-12 cells were treated with methyl-β-cyclodextrin for 30 minutes, then treated with 10-8M E2 for 9 minutes. Media were changed, and 24 hours later total intracellular p53 content was quantified with a sandwich ELISA assay.

PKC activity in the UM-SCC-12 cells was regulated by a membrane-associated mechanism. E_2 caused a dose-dependent increase in PKC specific activity (Figure 3.5A). This stimulatory effect of E_2 required intact caveolae. Depletion of plasma membrane cholesterol prevented the E_2-dependent increase in enzyme activity (Figure 3.5B) in a biphasic manner, with the maximum effect at 0.1mM methyl-β-cyclodextrin (MBC). 1mM MBC slightly reduced basal PKC activity, but 1mM MBC and 10^{-7}M E_2 together slightly increased PKC activity (Figure 3.5B). A neutralizing antibody specific to ERα36 increased PKC activity, but the addition of 10^{-7}M E_2 to cultures treated with the ERα36 antibody did not further increase PKC activity, suggesting that the effects of E_2 in UM-SCC-12 cells are at least partially elicited through the activation of membrane ERα36 (Figure 3.5C).

E_2 caused a biphasic increase in PLD specific activity in the UM-SCC-12 cells that was significant at 10^{-8}M (In the present study, we observed that the expression of ERs in laryngeal cancer cell lines is not uniform, which might explain the controversies in the literature regarding the presence and nature of the ER in laryngeal cancer. UM-SCC-11A expressed ERα36 and ERβ with no apparent ERα66, while UM-SCC-12 expressed both ERα66 and ERα36 with minimal ERβ. This diversity in ER expression translates to a disparate response to E2. E2 had a detrimental effect in UM-SCC-12 cells, enhancing proliferation and reducing apoptosis. UM-SCC-11 cells were much less responsive to E2, inhibiting DNA synthesis at high concentrations, although not affecting the apoptotic rate. **UM-SCC-11A cells expressed high levels of ERβ, which might offer an explanation for the protective effect conferred by E2. ERβ has been postulated to be a dominant-negative regulator of ERα modulating transcriptional responses to estrogens. The ratio of ERα vs. ERβ within a cell may determine the cell sensitivity**

to E2 and its biological responses26. This protective effect of ERβ has been observed in breast cancer cells in which the expression of ERβ was found to inhibit proliferation and cell invasion146, and in colorectal cancer in which the decrease of expression of ERβ was hypothesized to have a role in tumorigenesis147 and might demonstrate the same effect in laryngeal cancer cells.

Figure 3.5 E2 stimulates PKC activity in UM-SCC-12 cell layer lysates.

[**A**] UM-SCC-12 cells were treated with E_2 for 9 minutes. [**B**] A second set of cultures was treated with methyl-β-cyclodextrin for 30 minutes, then treated with 10^{-8}M E2 for 9 minutes. [**C**] A third set of cultures was treated with a neutralizing antibody to ERα36 for 30 minutes, then treated with 10^{-8}M E_2 for 9 minutes. For all cultures, media were aspirated and monolayers were washed twice with 1X PBS. PKC activity in cell layer lysates was measured using a commercial kit and normalized to total protein content and reaction incubation time.

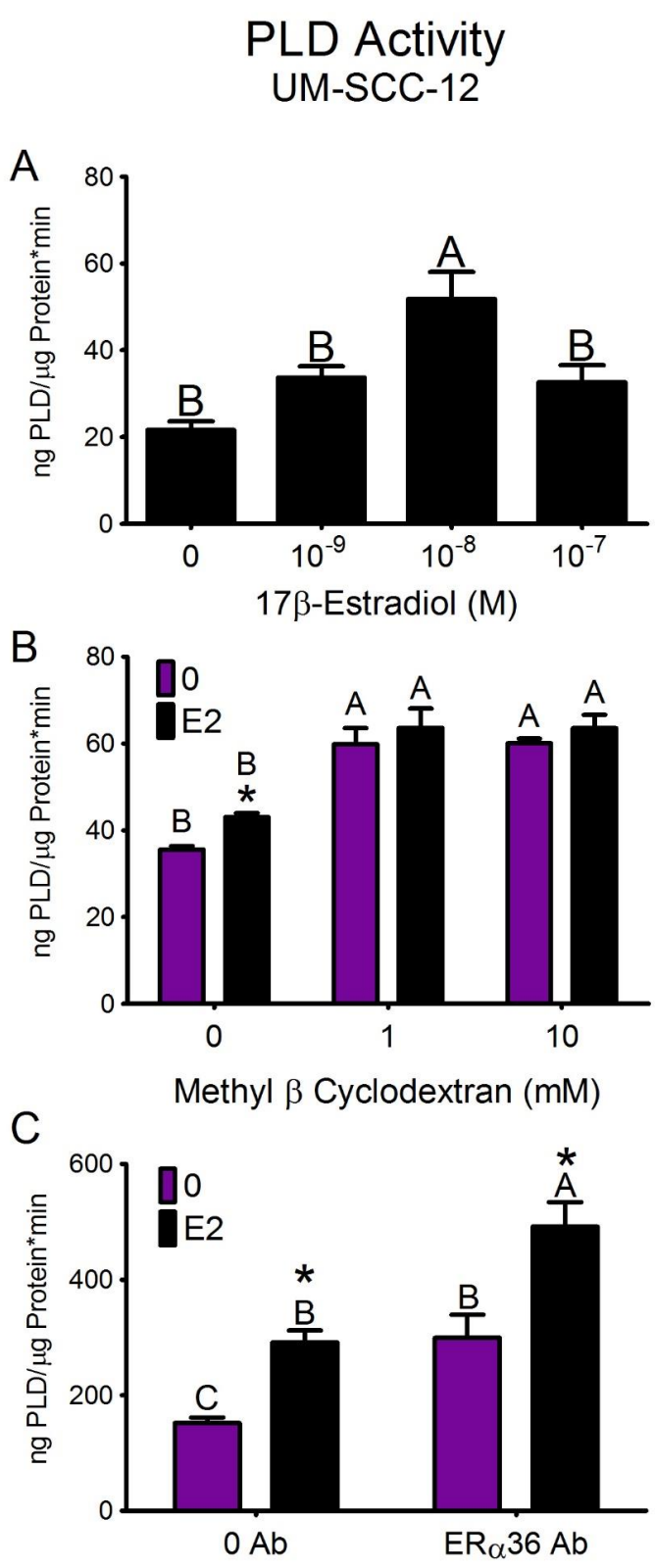

Figure 3.6 E2 stimulates PLD activity in UM-SCC-12 cell layer lysates.

[**A**] UM-SCC-12 cells were treated with E_2 for 9 minutes. [**B**] A second set of cultures was treated with methyl-β-cyclodextrin for 30 minutes, then treated with 10^{-8}M E_2 for 9 minutes. [**C**] A third set of cultures was treated with an antibody to ERα36 for 30 minutes, then treated with 10^{-8}M E_2 for 9 minutes. For all cultures, media were aspirated and monolayers were washed twice with 1X PBS. PLD activity in cell layer lysates was measured using a commercial kit and normalized to total protein content and reaction incubation time.

Discussion

E2 initiates multiple rapid signaling pathways from the cell membrane in different types of cells and via different membrane receptors, many of which remain the subject of active investigation. While there is evidence indicating that these receptors are in fact the traditional receptors residing in the cell membrane[36,40], novel orphan receptors have been identified and are being implicated in rapid membrane signaling by E_2[42,145]. Previously we showed that Hep2 laryngeal carcinoma epithelial cells express both traditional ERα66 and the recently identified splice variant, ERα36. ERα36, which was found to be a key cellular and transcriptional regulator of proliferation and enhanced aggressiveness in breast cancer [1,86], was shown to reside in the plasma membrane of Hep2 cells and to mediate the activation of PKC in response to E_2 via a mechanism comparable to that seen in the breast cancer cells[66]. ERα36 signaling had roles in tumorigenesis of laryngeal cancer enhancing proliferation and in the anti-apoptotic effect of E_2 against chemotherapeutics such as Taxol[66].

In the present study, we observed that the expression of ERs in laryngeal cancer cell lines is not uniform, which might explain the controversies in the literature regarding the presence and nature of the ER in laryngeal cancer. UM-SCC-11A expressed ERα36 and ERβ with no apparent ERα66, while UM-SCC-12 expressed both ERα66 and ERα36 with minimal ERβ. This diversity in ER expression translates to a disparate response to E_2. E_2 had a detrimental effect in UM-SCC-12 cells, enhancing proliferation and reducing apoptosis. UM-SCC-11 cells were much less responsive to E_2, inhibiting DNA synthesis at high concentrations, although not affecting the apoptotic rate.

UM-SCC-11A cells expressed high levels of ERβ, which might offer an explanation for the protective effect conferred by E_2. ERβ has been postulated to be a dominant-negative regulator of ERα modulating transcriptional responses to estrogens. The ratio of ERα vs. ERβ within a cell may determine the cell sensitivity to E_2 and its biological responses[26]. This protective effect of ERβ has been observed in breast cancer cells in which the expression of ERβ was found to inhibit proliferation and cell invasion[146], and in colorectal cancer in which the decrease of expression of ERβ was hypothesized to have a role in tumorigenesis[147] and might demonstrate the same effect in laryngeal cancer cells.

UM-SCC-12 cells demonstrated responses to E_2 similar to those seen in ERα-positive MCF7 and ERα-negative HCC38 breast cancer cells [1] as well as the Hep2 laryngeal cancer cell line[66]. E_2 caused dose dependent enhancement of proliferation and inhibition of apoptosis. These effects were mediated by the stimulation of the known PLD and PKC signaling cascades, as evidenced by the activation of both enzyme activities in UM-SCC-12 cells in response to E_2 and by the inhibition of proliferation when cultures were pre-treated with wortmannin, a specific PLD inhibitor at the concentrations used in this study. Pretreatment with methyl β-cyclodextrin, which depletes the membranes of cholesterol and thereby disrupts the caveolae, inhibited the activation of PKC and PLD and abolished the anti-apoptotic effect, indicating the importance of the specialized membrane compartment for E2-dependent signaling pathway in UM-SCC-12 laryngeal cancer cells.

Despite the clear similarity to the mechanism and effects of E_2 seen in our previous work, in UM-SCC-12 cells it seems that ERα36 plays only a part in the membrane

signaling pathways of E_2. While antibodies against ERα36 prevented the stimulatory effect of E_2 on the activation of PKC, they did not inhibit the effects of E_2 on proliferation rate or PLD activity. This suggests that E_2 causes an increase in PKC activity and proliferation by activating another estrogen receptor, rather than ERα36 as previously described in HCC38 breast cancer cells[66]. It should also be noted that while the antibody to ERα36 did not affect cell proliferation in UM-SCC-12 cells, it stimulated both PKC and PLD activity in these cells, suggesting that neutralizing ERα36 stimulates an unidentified mechanism which stimulates PKC and PLD in a compensatory pro-survival pathway. Furthermore, it is possible that the antibody to ERα36 simply stimulated PKC activity to a saturated point, preventing further increases in PKC activity by any stimulant rather than specifically blocking the effects of E_2.

The mechanism of E_2's action in the UM-SCC-12 laryngeal cancer cell line is intricate and not yet clarified completely. One hypothesis for the incongruity with previous results is that in UM-SCC-12 cells, the effects of E_2 are the result of the convergence and crosstalk of the different membrane receptor pathways, ERα66 and ERα36. An alternate hypothesis could be that the tumorigenic effects of E_2 are the result of E_2 binding to ERα46 or ERα66, has been shown previously in osteoblasts [148], or to an as-yet-uncharacterized novel membrane-bound estrogen receptor (Figure 3.7).

Classical sex hormone nuclear receptors have been found in the plasma membranes of hormone-responsive cancers where they elicit rapid signaling pathways, which enhance cancer cell survival and proliferation [46]. From the plasma membrane it is thought that the classical receptors exert their effect through transactivation of the EGF or IGF-1 tyrosine kinase receptors in order to stimulate kinase cascades[47]. It has been

suggested that the mechanism for trafficking of the classical sex hormones to the plasma membrane involves palmitoylation [35]; the attachment of palmitic acid to an internal cysteine residue, which promotes the association of the receptor with caveolin-1, a transporter protein, to caveolae rafts in the plasma membrane[49]. Once the receptor is incorporated in the caveolae it may interact with many signaling proteins incorporated in the caveolae rafts and activate various Gα and Gβ/γ proteins within seconds[52,149].

ERs have been the primary receptors studied in order to ascertain this theory of the nature of membrane steroid hormone receptors. Immunological studies found that the membrane-localized estrogen binding protein shared epitope homology to the nuclear receptors[150]. Endothelial cells from combined ERα/ERβ deleted mice and breast cancer MCF-7 cells that lack nuclear ERα as well as small interfering RNA directed against the classical ER, eliminated estrogen binding at the cell surface and the rapid hormone signaling elicited by E$_2$[36]. Transfection of ER cDNA of classical ERα or ERβ in ER-null cells resulted in induction of both nuclear and membrane signaling pathways [34]. Taken together there is evidence to support the role of classical nuclear receptors in membrane mediated rapid responses, which might clarify the effects seen in UM-SCC-12 cells of a synergistic effect of both ERα66 and ERα36 through membrane mediated signaling.

Another plausible explanation for the results found in UM-SCC-12 cells may originate from crosstalk between membrane ER signaling with growth factor receptors, which results in the activation of the common membrane delineated pathways such as ERK-MAPK, PI3k-Akt and Src[68]. Thus once ERα36 has been activated with resulting activation of PKC, the subsequent activation of growth factor receptor pathways may be responsible for the ensuing enhancement of proliferation. Such signaling cascades have been

implicated to have a major role in the carcinogenesis and progression of breast cancer independently and in collaboration with classical genomic E_2 signaling. The interaction between membrane ER and transmembrane growth factor signaling pathways such as insulin-like growth factor I receptor (IGF-IR), epidermal growth factor (EGFR), Src and HER2 and the upregulation of these signaling pathways has been accepted as being one of the mechanisms underlying resistance to endocrine therapy in breast cancer[151]. The activation of these signaling pathways has a variety of documented effects including inhibition of apoptosis, stimulation of cell proliferation, enhanced invasion and cell motility, and induction of angiogenesis[110,152].

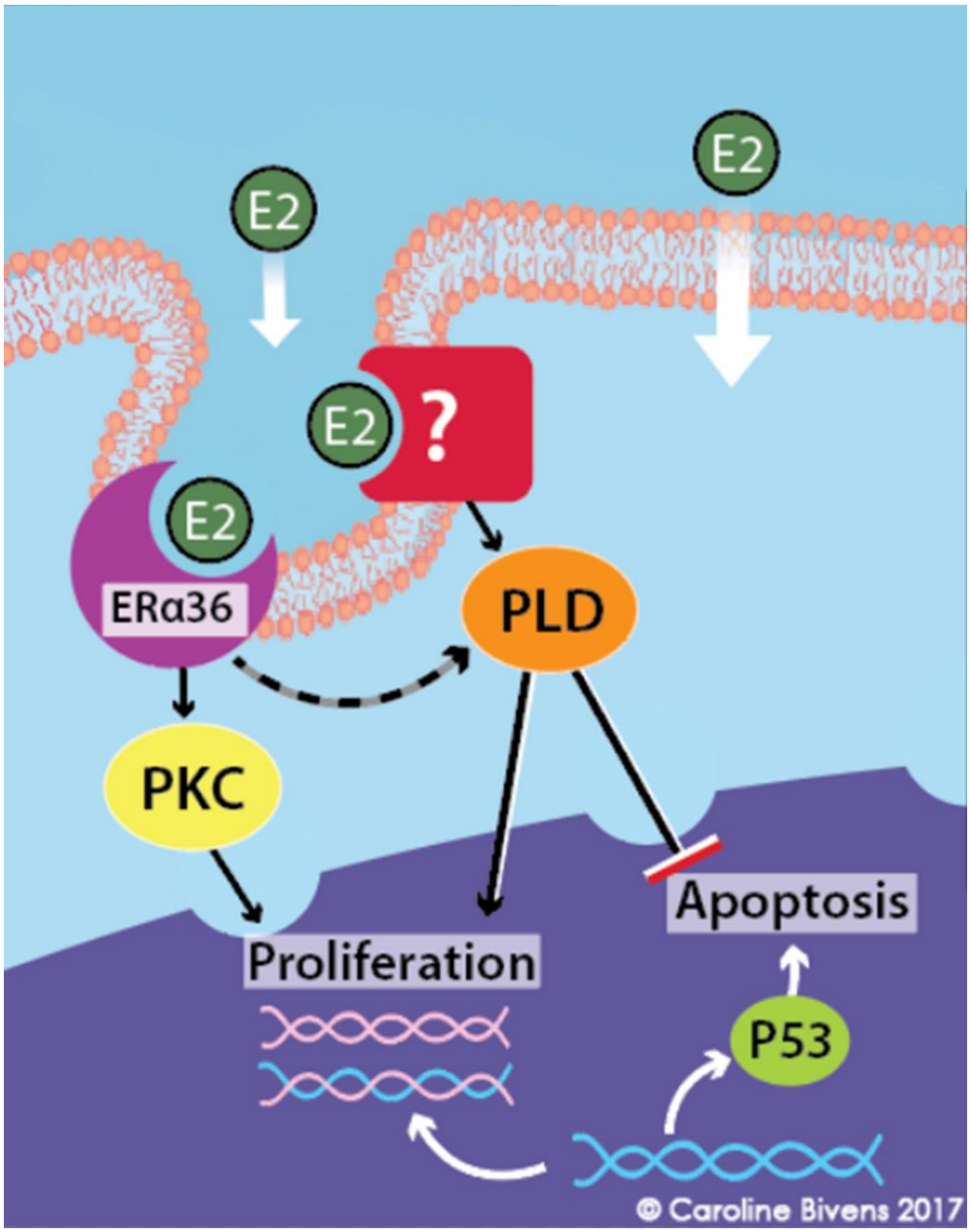

Figure 3.7 17β-estradiol activates PKC in UM-SCC-11A cells; and PKC and PLD in UM-SCC-12 cells by binding to ERα36 in the caveolae.

In UM-SCC-12, 17β-estradiol activation of PLD results in increased DNA synthesis. 17β-estradiol also activates PLD through an unknown caveolae-bound estrogen receptor to decrease total p53 levels and apoptosis.

The findings of this study present compelling evidence that laryngeal cancer is sex hormone responsive, specifically to E_2. Rapid non-genomic membrane signaling has been found to have an important role in mediating the effect of E_2 in laryngeal cancer cells. These effects are hypothesized to be mediated by the activation of different membrane receptors and subsequent activation of growth factor receptors and tyrosine kinase receptors. The full impact of steroid hormones is the result of the convergence and crosstalk of the membrane and classical nuclear receptor pathways. Their integrative, at times synergistic or alternatively antagonistic, effects confer a variability and complexity to steroid hormone function.

This is emphasized in the two laryngeal cell lines studied, in which one exhibited a protective effect of E_2 while in the other, E_2 had a deleterious effect augmenting proliferation and conferring anti-apoptotic potential to the cancer cells. These findings stress the importance of establishing the molecular and clinical characterization of the specific tumor in order to tailor treatment accordingly, thus optimizing treatment while reducing adverse effects for each individual patient. Further investigation is warranted in order to elucidate the versatile role of E_2 in laryngeal cancer pathogenesis and progression, the array of membrane-mediated mechanisms by which these effects come in to play, and to shed light on their impact on the treatment and management of laryngeal cancer.

Chapter 4.

Loss of estrogen receptors is associated with increased tumor aggression in laryngeal squamous cell carcinoma

[Chapter 4 is in preparation as: Verma A, Schwartz N, Cohen DJ, Patel V, Boyan BD, Schwartz Z. Loss of estrogen receptors is associated with increased tumor aggression in laryngeal squamous cell carcinoma. Scientific Reports. In Preparation]

Introduction

The larynx is an overlooked secondary sex hormone organ. Similar to other sex hormone organs, it undergoes trophic changes in response to hormonal changes during puberty, and morphological changes during adulthood. Steroid hormones have been reported to play a significant role in voice changes during maturation, as their effects mediate the lengthening and thickening of the male vocal folds.[153] In the female larynx, fluctuations in estrogen levels during the menstrual cycle are accompanied by variations in the pitch of the voice.[154] Atrophy and dystrophy have been found to be pronounced in the larynges of postmenopausal women as well as in the vocal fold tissue of ovariectomized rats.[155] These subjects are known to suffer from edema of the laryngeal lamina propria, inflammation in squamous and respiratory epithelia, pseudostratification, and cilia loss, but these symptoms were rectified with estrogen replacement therapy.[156]

Despite the obvious responsiveness of the larynx to estrogen, the presence and differential expression of estrogen receptors (ER) is a matter of debate, particularly in laryngeal cancer. ER, mainly ERα66, the traditional ER translated from the ESR1 gene, has been reported in laryngeal epithelia in both females[157] and males,[158] and changes in

ER are associated with inflammation and benign lesions.[159] ER expression has also been verified in laryngeal cancer[138,160] and at higher levels than in adjacent normal mucosa.[139] Moreover, the non-traditional transmembrane ERs G-protein coupled estrogen receptor (GPER1, sometimes called GPR30) and ERα36, a splice variant of the traditional ERα66, have been found in human vocal folds[71] and laryngeal cancer cells,[66] respectively. Another ER, ERβ, which is encoded by the ESR2 gene, has been inversely correlated with increased cancer aggression in laryngeal squamous cell carcinoma (LSCC).[70] However, opposing studies have not identified ER[161] or any other steroid hormone receptors[162,163] in the larynx or laryngeal cancer cells.[135] The clinical implication of ER expression in laryngeal cancer is equally confounding. In a previous study, we found a correlation between the number of ERs and regional lymph node metastasis.[66] This differs from other studies that reported a reduced prognosis[164] and lower rates of lymph node metastasis with increased ER expression.[139]

17β-estradiol (E$_2$) is produced from testosterone by the enzyme aromatase during normal physiological function. At the cellular level, E$_2$ elicits a wide array of nuclear and membrane signaling responses in different cells via different ERs. An assessment of estrogen's full impact on laryngeal cancer must consider the vast number of nuclear, cytosolic, and membrane-associated ERs, the differential expression of ER in different cell types, and the convergence and crosstalk of the membrane and classical ER pathways in each cell. It is their integrative, at times synergistic or alternatively antagonistic, effects that confer the variability and complexity of E$_2$ function in both normal and cancer cells.[68]

Estrogen exerts regionally specific effects on cell proliferation and mRNA expression of extracellular matrix (ECM)-associated genes in normal fibroblasts. Cervicothoracic fibroblasts from the vocal fold, trachea, and esophagus have been shown to respond differently to estrogen based on their specific estrogen profiles.[165] Studies examining the presence of ERα in vocal cord fibroblasts show that it is localized predominantly in the nucleus and cytoplasm.[159] Previous work by our group[66] and others[165] has shown that treatment with E_2 suppresses extracellular matrix gene expression in laryngeal and vocal fold tissue, but through a membrane-associated estrogen receptor rather than a nuclear ER. The complexity of E_2 function and its dependency on local ER expression are further emphasized in our previous study with laryngeal cancer cell lines, in which we found E_2 exhibited either a protective effect inhibiting DNA synthesis, or a deleterious effect augmenting proliferation and conferring anti-apoptotic potential to the cancer cells in a manner specific to the ER profile in each cell line.[67]

These findings stress the importance of further establishing the molecular and clinical characterization of laryngeal cancer in order to improve our understanding of the disease and its therapeutic options. The aim of our study was to further evaluate the different ER profiles that laryngeal cancer cells express and to correlate ER status with clinical prognoses. Furthermore, we implement our findings *in vivo* to evaluate how these cancers progress and behave with and without E_2 in an animal model.

Materials and Methods

Cell Culture

UM-SCC-12 cells and UM-SCC-11A were purchased from the Cancer Research Laboratory, Department of Otolaryngology/Head and Neck Surgery at the University of Michigan. Cells were maintained as previously described.[67] Estrogen receptor profiles were reported in a previous publication[67] and were compared against previously established estrogen receptor profiles[137]. The two cell lines were further characterized as described below.

Estradiol Production

Aromatase Activity.

Confluent cultures of UM-SCC-11A and UM-SCC-12 cells were harvested and assessed for aromatase activity (Aromatase (CYP19A) Activity Assay Kit (Fluorometric), Biovision, Milpitas, CA) according to manufacturer's instructions. Monolayers were also assessed for total protein content (Pierce 660nm Protein Assay, ThermoFisher, Waltham, MA), and aromatase activity was normalized to total protein.

17β-estradiol parameter assay.

UM-SCC-11A and UM-SCC-12 cell monolayers were cultured to confluence in hormone-free phenol-red media supplemented with 10% charcoal-dextran stripped fetal bovine serum (CD-FBS). At confluence, cell supernatants were collected and assessed for total 17β-estradiol content (Estradiol parameter assay kit, RnD Systems, Minneapolis, MN). Monolayers were washed twice in 1X PBS, lysed in 0.05% Triton X 100, and assessed for total double-stranded DNA content as described below. Total supernatant 17β-estradiol was normalized to total double-stranded DNA content.

Total p53 Content

p53 is a tumor suppressor gene that can induce apoptosis. Total p53 levels were measured 24 hours post-treatment with a sandwich ELISA (Human Total p53 DuoSet® IC, R&D Systems, Minneapolis, MN). Cell monolayers were cultured to confluence in 24W plates, then treated with fresh full media containing either 0 or 10^{-7}M E_2 for 9 minutes. These media were removed by aspiration and fresh media were added to the cultures for 24 hours. Cultures were then washed twice in 1X PBS and harvested in 200µL of p53 lysis buffer according to manufacturer's instructions, then assayed for total protein content (ThermoFisher, Pierce 660 nm Protein Assay), and normalized as previously described[67].

DNA Quantification

Cultures were treated with 0 or 10^{-7}M E_2 for 9 minutes as above and harvested with p53 lysis buffer. Cultures were then assessed for total double-stranded DNA content using the QuantiFluor® dsDNA System according to manufacturer's instructions (Promega, Madison, WI).

Production of UM-SCC-12 Cells Silenced for ESR1

Cells lines containing scramble control mRNA (TurboGFP Cat.# SHCOO4V, Millipore Sigma, Burlington, MA) and cells silenced for ESR1 (shESR1-UM-SCC-12) (Cat.# SHCLNV-NM_000125, Millipore Sigma) were created by transducing WT UM-SCC-12 cells with commercially available lentiviral shRNA plasmids and selecting the cells with 5µg/mL puromycin. Cells were maintained in full media containing 5µg/mL puromycin. Knockdown was assessed with western blots as described below.

Tumor Model

Subcutaneous xenograft laryngeal cancer mouse model.

UM-SCC-11A (n=16) and UM-SCC-12 (n=16) cell lines were mixed with 1X DPBS (Thermo Fisher Scientific, Waltham, MA) and phenol-red free Cultrex basement membrane extract (BME, Trevigen, Gaithersburg, MD) to a concentration of 7.5 mg/mL BME and 10 million cells/mL. The resulting cell suspension was kept on ice and 100µL (1 million cells) was injected subcutaneously into the left flank of a 6-week old male NOD.Cg-*Prkdc*^{scid} *Il2rg*^{tm1Wjl}/SzJ (NSG) mouse, Cancer Mouse Models Core, Massey Cancer Center, Virginia Commonwealth University, Richmond, VA) to create a subcutaneous xenograft model of laryngeal cancer.[166] At the time of cell injection, each animal was also subcutaneously implanted with a 0.96mg/60-day release E_2 pellet or a corresponding placebo pellet to create four experimental groups: UM-SCC-11A + Placebo, UM-SCC-11A + E_2, UM-SCC-12 + Placebo, UM-SCC-12 + E_2 (n=8 for each condition).[167] Tumors were allowed to grow for 8 weeks, and tumor measurements were taken with digital calipers starting at week 2 until the end of the study. After 8 weeks, mice were euthanized by CO_2 inhalation and cervical dislocation and tumors were extracted and preserved on wet ice (<6 hours) until µCT analysis. After µCT analysis, tumors were fixed in formalin and histologically analyzed as described below. All animal experiments were conducted in full compliance with the recommendations for the Care and Use of Laboratory Animals of the National Institutes of Health under a protocol approved by the Virginia Commonwealth University Institutional Animal Care and Use Committee (protocol number AD10000675).

In a second experiment, WT UM-SCC-12, and shESR1-UM-SCC-12 subcutaneous xenografts were created as described above (n=16 for each cell line). Animals were subcutaneously implanted with a 0.96mg/60-day release E_2 pellet or a corresponding placebo pellet as described above to create four experimental conditions: WT UM-SCC-12 + Placebo, WT UM-SCC-12 + E_2, shESR1-UM-SCC-12 + Placebo, shESR1-UM-SCC-12 + E_2 (n=8 for each condition). To preserve animal life, xenografts with scrambled control UM-SCC-12 cells were not created for this experiment. Tumors were monitored for 8 weeks until harvest. Animals were euthanized as described above and tumors were fixed in formalin.

μCT analysis.

After harvest, tumors were preserved for less than 6 hours on wet ice and scanned with a Bruker Skyscan 1173 μCT at 55kV and 70μA at a resolution of 560x560 pixels with an image pixel size of 40.26μm, an exposure time of 125ms and a rotation step of 0.8 degrees.[166] NRecon software version 1.6.10.4 (Kontich, Belgium) with a smoothing kernel of 0 and a beam hardening correction of 20% was used to reconstruct and analyze the tumors with a standard reconstruction protocol. Total tissue volume approximated total tumor volume.

Histology.

After harvest, xenograft tumors were fixed in 10% neutral formalin for 7 days, processed, and embedded in paraffin. Samples were then sectioned into 4μm thickness and stained with haemotoxylin and eosin as previously described.[168] Slides were imaged at 10X and 40X (Zeiss AxioVision Microscope, Carl Zeiss, Oberkuchen, Germany).

Clinical Sample Acquisition

Frozen tissue samples and prepared haematoxilin and eosin (H&E) slides were acquired from Meir Hospital, Kfar Saba, Israel under Institutional Review Board (IRB) protocol #0497-13-RMC or from Massey Cancer Center, Virginia Commonwealth University (VCU), Richmond, Virginia under an anonymization agreement in compliance with the Office for Human Research Protections' "Guidance on Research Involving Coded Private Information or Biological Specimens". Information on patient gender, age, tobacco and alcohol use, and tumor location (glottic/supraglottic), was provided by respective institutions. A value of '0' indicates no or infrequent use of tobacco or alcohol products as reported by the patient; a value of '1' indicates self-reported regular, heavy use of tobacco or alcohol products.

ID number	Origin	Gender	Age	Location	Tobacco	Alcohol
1	Meir Hospital, Israel	M	78	glottic	1	0
2	Meir Hospital, Israel	M	76	glottic	1	1
3	Meir Hospital, Israel	M	68	glottic	1	0
4	Massey Cancer Center, USA	M	73	glottic	1	0
5	Massey Cancer Center, USA	M	57	glottic	1	1
6	Massey Cancer Center, USA	M	59	supraglottic	1	0
7	Massey Cancer Center, USA	F	67	supraglottic	0	0
8	Massey Cancer Center, USA	M	69	supraglottic	1	1
9	Massey Cancer Center, USA	M	64	glottic	1	1
10	Massey Cancer Center, USA	M	51	supraglottic	1	1
11	Massey Cancer Center, USA	M	64	supraglottic	1	0
12	Meir Hospital, Israel	M	58	supraglottic	1	0
13	Meir Hospital, Israel	M	70	glottic	1	0
14	Meir Hospital, Israel	M	65	glottic	1	0

Table 4.1 Laryngeal squamous cell carcinoma samples and patient demographics

Number of Patients	14
Mean Age	65.6 ± 7.59
Female	1
Male	13
Supraglottic	6
Glottic	8
Heavy Tobacco User	13
Heavy Alcohol Consumer	5

Table 4.2 Summary of clinical laryngeal squamous cell carcinoma samples.

Preparation of Lysates

For samples obtained from Meir Hospital, Israel, tissue pieces were weighed, and >10mg of tissue was minced into pieces <1mm^3 with a No.11 scalpel blade. Tissue pieces were homogenized with a Dounce tissue grinder in Nonidet p-40 (NP-40) containing 5mM NaF and 20µL of protease inhibitor cocktail (Sigma-Aldrich #P3480) per mL of NP-40. After homogenization, samples were sonicated on ice at 40 amperes for 5 seconds to obtain tissue lysates as previously described.[169,170]

For samples from the VCU Tissue and Data Acquisition and Analysis Core Laboratory (TDAAC), frozen tissue shavings were obtained and washed twice with 2 mL of 1X PBS containing 40µL of protease cocktail inhibitor. Samples were vortexed and centrifuged at 1000 rpm for 5 minutes between each wash. Tissue pellets were then resuspended in 200µL of radioimmunoprecipitation assay (RIPA) buffer and sonicated on ice at 40 amperes for 5 seconds to obtain tissue lysates.

To assess ERα66 and ERα36 knockdown in shESR1-UM-SCC-12, WT UM-SCC-12, and Scramble Control UM-SCC-12, monolayer cultures were grown in T-75 flasks

(n=1 flask per cell line) until confluent, washed twice with 1X phosphate buffered saline (PBS), and harvested with 300µL RIPA as previously described to create cell lysates.[171]

Tissue and cell lysates were incubated on ice for 30 minutes and centrifuged at 13000g for 20 minutes at 4C. Supernatants were saved and assayed for total protein content and used in western blots as described below.

Western Blots

50µL of tissue or cell lysate containing 8-35µg protein were loaded onto 4-20% Mini-PROTEAN®TGX™ precast polyacrylamide gels (Bio-Rad, Hercules, CA). Proteins were transferred to low-fluorescence PVDF membranes using a Trans-Blot® Turbo™Transfer System (Bio-Rad). Membranes were blocked for 1 hour at room temperature in odyssey blocking buffer (LI-COR) and then incubated with antibodies against GAPDH (mouse monoclonal, Millipore, Burlington, MA) and ERα (rabbit polyclonal, Chi Scientific, Maynard, MA) or ERβ (rabbit polyclonal, Abcam, Cambridge, United Kingdom) for 24 hours at 4ºC. Membranes were then incubated with IRDye 700CW (goat anti mouse) and IRDye 800CW (goat anti-rabbit) conjugated secondary antibodies (LI-COR) for 45 minutes at room temperature and imaged using the LI-COR Odyssey® CLx Infrared Imaging System. Western blots were carried out at a central institution (VCU) to minimize variation and repeated once (a total of two experiments per assay) with 1 replicate per sample in each experiment. Signal intensity for proteins of interest (ERα66, ERα36, and ERβ) was normalized to GAPDH. Where no signal was detected, samples were considered to have '0' signal intensity and marked with 'N.D.', or no signal detected, on graphs (Figure 4.1, Figure 4.2).

Normalized signal intensity for ERα66, ERα36, and ERβ in each tumor sample was grouped by stage (stage 1, stage 2 & 3, stage 4) and graphed (Figure 4.3A-4C); or normalized to corresponding signal intensities in adjacent epithelial tissue (Figure 4.3D). A normalized ratio of greater than 1 was recorded with a blue upward-pointing arrow ↑, and a ratio less than 1 was recorded with a red downward-pointing arrow ↓ (Table 4.3). To generate heat maps, $\log_{10}$ of normalized signal intensities of tumor (Figure 4.3E) or normal epithelial tissue (Figure 4.3F) was calculated and graphed using the Graphpad Prism 7 Heatmap generator. Samples were grouped by stage and arranged in order of increasing cancer aggression (top-bottom) (Figure 4.3E-F).

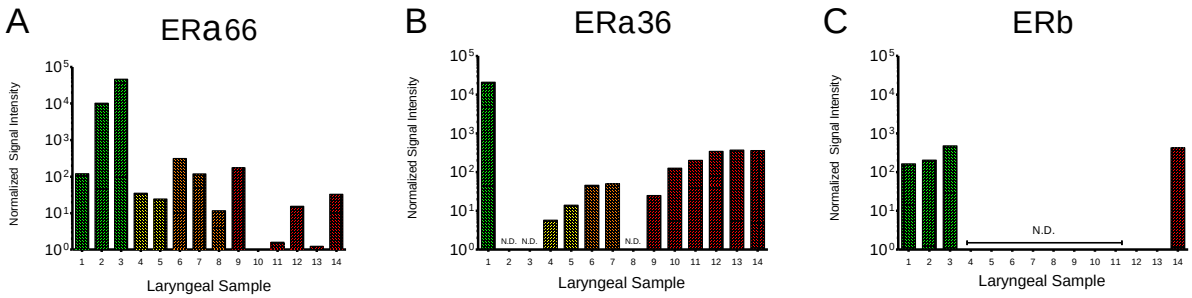

Figure 4.1 Expression of ERα in individual LSCC samples.

Quantification of western blots for [**A**] ERα66, [**B**] ERα36, and [**C**] ERβ for individual clinical tumor samples. Y-axes are given as log scales. Samples are color-coded according to clinical stage. Stage 1 samples are green, stage 2 yellow, stage 3 orange, and stage 4 red.

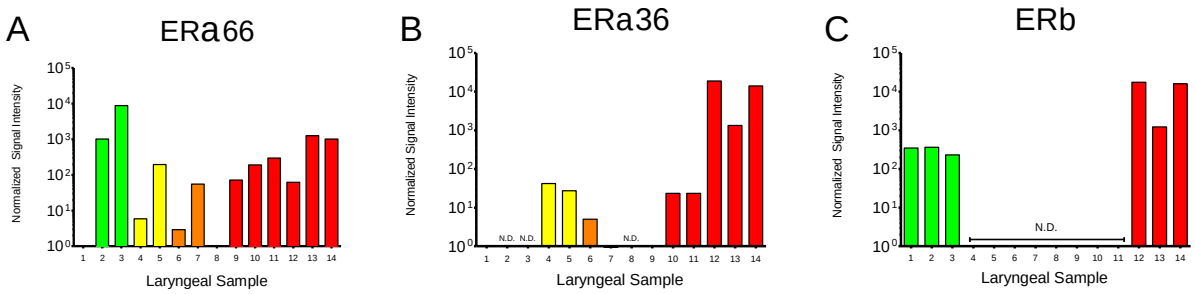

Figure 4.2 Expression of ERα in individual normal laryngeal tissue samples (LSCC surround).

Quantification of western blots for [**A**] ERα66, [**B**] ERα36, and [**C**] ERβ for normal epithelia adjacent to clinical tumor samples. Y-axes are given as log scales. Samples are color-coded according to clinical stage. Stage 1 samples are green, stage 2 yellow, stage 3 orange, and stage 4 red.

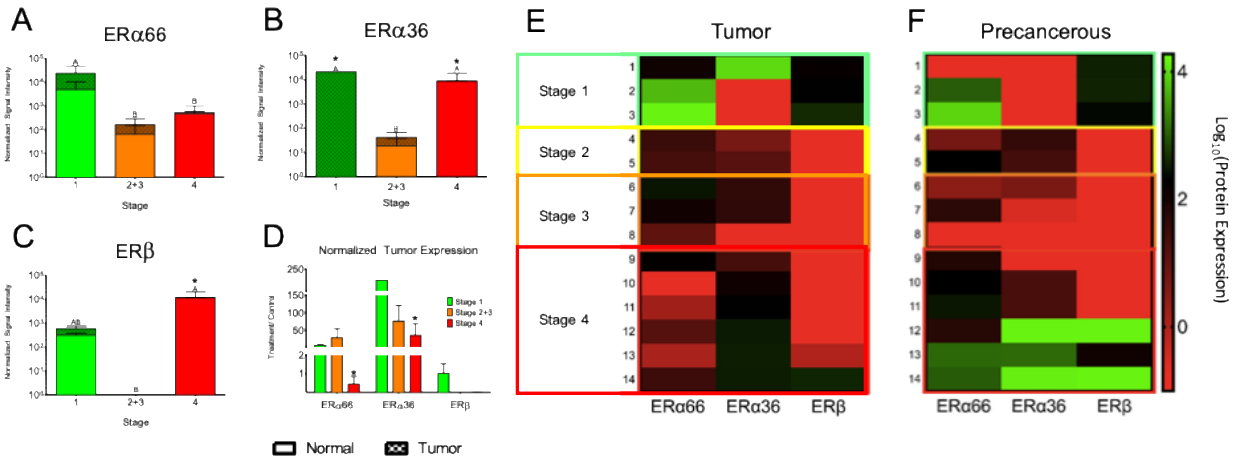

Figure 4.3 Expression of ERα isoforms in stage 1-4 clinical laryngeal cancer.

Quantification of western blots of [**A**] ERα66, [**B**] ERα36, and [**C**] ERβ. Samples were grouped by cancer stage (stage 1, stages 2 and 3, stage 4) and analyzed by one-way ANOVA with Tukey's correction. Bars not sharing a letter are significantly different from each other with $P < 0.05$. Bars are shown as total protein expression, with solid bars representing protein expression in normal epithelia and patterned bars representing protein expression in tumor tissue. Y-axes are given as log scales. [**D**] Protein expression in LSCC samples was normalized to expression in surrounding epithelia, grouped by stage, and graphed. * indicates significance against stage 1 within protein groups. Panels E and F: Heat maps showing [**E**] tumor and [**F**] surrounding epithelia expression of ERα66, ERα36, and ERβ for each sample. Individual protein expression was measured by western blot and graphed as log10 of normalized signal intensity.

ID number	Pathology	cT	cN	cM	Stage	Tumor/Normal		
						ERα66	ERα36	ERβ
1	invasive keratinizing SCC, NOS	1	0	0	1	↑	↑	↓
2	invasive keratinizing SCC, NOS	1	0	0	1	↑	N/A	↓
3	invasive keratinizing SCC, NOS	1	0	0	1	↑	N/A	↑
4	invasive keratinizing SCC moderate diff	2	x	x	2	↑	↓	N/A
5	invasive keratinizing SCC moderate diff	2	0	x	2	↓	↓	N/A
6	invasive keratinizing SCC moderate diff	3	0	x	3	↑	↑	N/A
7	invasive keratinizing SCC moderate diff	3	0	x	3	↑	↑	N/A
8	invasive keratinizing SCC moderate diff	3	0	x	3	↑	N/A	N/A
9	invasive keratinizing SCC moderate diff	4	x	x	4	↑	↑	N/A
10	invasive keratinizing SCC moderate to poorly diff	4	2b	x	4	↓	↑	N/A
11	invasive keratinizing SCC moderate diff	4	2c	x	4	↓	↑	N/A
12	invasive keratinizing SCC moderate diff	4	1	0	4	↓	↓	↓
13	invasive keratinizing SCC moderate to poorly diff	4	2	0	4	↓	↓	↓
14	invasive keratinizing SCC, NOS	4	0	0	4	↓	↓	↓

Ratio	Symbol
>1	↑
<1	↓

Table 4.3 Estrogen receptor protein expression in clinical laryngeal squamous cell carcinoma samples.

Accessing ESR1 and ESR2 Gene Transcript Expression Data

ESR1 and ESR2 expression data were publically available and were obtained from Total Cancer Genome Atlas (TCGA) cohort (Project Id: TCGA-HNSC) (n=525 patients) (https://portal.gdc.cancer.gov/projects/TCGA-HNSC) using University of California Santa Cruz (UCSC) Xena (http://xena.ucsc.edu/).[172,173] In brief, ESR1 and ESR2 expression data were downloaded from Xena and only samples taken from primary solid head and neck squamous cell carcinomas were included in overall head and neck cancer analyses. Samples were further separated by neoplasm tissue type, and only primary LSCC samples were included in the second analysis. Overall survival (OS) was defined as time of death by any cause and capped at fifteen years. Kaplan-Meir curves of OS were generated by GraphPad Prism v5.0 (GraphPad Software Inc.). Patients were grouped according to median gene expression as described previously.[174]

Statistical Analysis

µCT tumor volumes were compared with one-way ANOVA analysis with Tukey's correction. Tumor volume measurements over time were analyzed with a repeated-measures ANOVA. *Ex vivo* western blots were grouped by stage and analyzed with one-way ANOVA analysis with Tukey's correction to compare between stages and two-way ANOVA analysis with Bonferroni post-tests between stages to determine significance between precancerous and tumor tissue. Tumor protein expression for ERα66, ERα36, and ERβ was normalized to matched precancerous tissue and graphed as treatment/control. Two-way ANOVA analysis with Bonferroni post-tests between stages was done to determine significance between stages. Statistical analysis was performed by using GraphPad Prism v5.0. Comparison of high and low ESR survival curves was

done with a Log-rank Mantel-Cox χ^2 test. For all studies, p-values < 0.05 were considered significant.

Results

UM-SCC-12 and UM-SCC-11A locally produce 17β-estradiol.

Both ER positive (ER+) UM-SCC-12 cells, which express ERα66 and ERα36, and ER negative (ER-) UM-SCC-11A cells, which do not express ERα66 and only express ERα36, produce similar concentrations (~250 pg/mL supernatant) of 17β-estradiol (Figure 4.4A).[67] However, ER- UM-SCC-11A produced ~1.5 times more 17β-estradiol per cell than their ER+ UM-SCC-12 counterparts (Figure 4.4B). Similarly, UM-SCC-11A cells had higher basal aromatase activity than UM-SCC-12 cells (Figure 4.4C), with approximately 4nU of enzyme per mg of protein compared to UM-SCC-12's 1nU/mg protein.

17β-estradiol increased tumor aggression in estrogen receptor positive laryngeal cancer, but not estrogen receptor negative cancer in vivo.

ER positive UM-SCC-12 xenografts grown in placebo-treated mice initially increased in volume (slope ≠ 0, Table 4.4), but did not increase in size after 4 weeks of growth (slope ≈ 0, Table 4.5) and ultimately reached a volume of 250-500 mm^3 (Figure 4.5A,C). In contrast, UM-SCC-12 xenografts grown in E$_2$-treated mice increased in size over time (slope ≠ 0, Table 4.4, Table 4.5) and attained a final volume of 500-1000 mm^3, 2-fold larger than tumors grown in control-treated mice (Figure 4.5A,C). Most of this increase was observed after week 4. This effect was not observed in ER negative UM-SCC-11A

tumors, where both control and E_2 treated tumors increased in size at a similar rate and to a similar final volume (Figure 4.5B,C). Histology of UM-SCC-12 tumors revealed even cell shape, chromatin distribution, and uniform morphology in control tumors (Figure 4.5D), similar to stage 1 LSCC (Figure 4.6A,E). E_2 treated tumors stained with eosin and haematoxylin (H&E) had similar eosin staining but darker haematoxylin staining, more irregular nuclei, and uneven chromatin distribution as compared to control treated tumors (Figure 4.5E), similar to stage 2 LSCC (Figure 4.6B,F).

	11A Control	11A 17b-Estradiol	12 Control	12 17b-Estradiol
Best-fit values				
Slope	346.1 ± 46.88	428.2 ± 47.74	63.91 ± 12.24	164.9 ± 19.50
Y-intercept when X=0.0	-1091 ± 280.8	-1254 ± 263.7	47.39 ± 65.68	-352.4 ± 106.0
X-intercept when Y=0.0	3.152	2.929	-0.7415	2.138
1/slope	0.002890	0.002335	0.01565	0.006065
95% Confidence Intervals				
Slope	249.3 to 442.8	331.5 to 525.0	39.31 to 88.51	125.9 to 203.9
Y-intercept when X=0.0	-1671 to -511.3	-1789 to -719.8	-84.66 to 179.4	-564.6 to -140.3
X-intercept when Y=0.0	2.001 to 3.866	2.103 to 3.519	-4.449 to 0.9814	1.085 to 2.844
Goodness of Fit				
R square	0.6943	0.6850	0.3530	0.5478
Sy.x	417.0	612.1	180.6	306.4
Is slope significantly non-zero?				
F	54.50	80.46	27.28	71.48
DFn, DFd	1.000, 24.00	1.000, 37.00	1.000, 50.00	1.000, 59.00
P value	< 0.0001	< 0.0001	< 0.0001	< 0.0001
Deviation from zero?	Significant	Significant	Significant	Significant
Data				
Number of X values	7	7	7	7
Maximum number of Y replicates	5	7	8	9
Total number of values	26	39	52	61
Number of missing values	44	31	18	9

Table 4.4 Xenograft models of LSCC tumor growth curve: linear fit, weeks 2-8.

	11A Control	11A 17b-Estradiol	12 Control	12 17b-Estradiol
Best-fit values				
Slope	441.2 ± 69.19	684.9 ± 79.54	19.09 ± 22.63	209.0 ± 37.80
Y-intercept when X=0.0	-1728 ± 443.0	-2958 ± 503.3	343.3 ± 140.8	-638.4 ± 234.5
X-intercept when Y=0.0	3.917	4.318	-17.99	3.055
1/slope	0.002267	0.001460	0.05239	0.004785
95% Confidence Intervals				
Slope	296.9 to 585.5	521.4 to 848.4	-26.93 to 65.11	132.7 to 285.3
Y-intercept when X=0.0	-2653 to -804.3	-3992 to -1923	56.95 to 629.7	-1112 to -164.9
X-intercept when Y=0.0	2.664 to 4.606	3.627 to 4.784	-infinity to -0.8896	1.221 to 3.969
Goodness of Fit				
R square	0.6703	0.7404	0.02050	0.4213
Sy.x	417.2	574.1	194.5	350.3
Is slope significantly non-zero?				
F	40.66	74.15	0.7115	30.57
DFn, DFd	1.000, 20.00	1.000, 26.00	1.000, 34.00	1.000, 42.00
P value	< 0.0001	< 0.0001	0.4048	< 0.0001
Deviation from zero?	Significant	Significant	Not Significant	Significant
Data				
Number of X values	5	5	5	5
Maximum number of Y replicates	5	7	8	9
Total number of values	22	28	36	44
Number of missing values	28	22	14	6

Table 4.5 Xenograft models of LSCC tumor growth curve: linear fit, weeks 4-8.

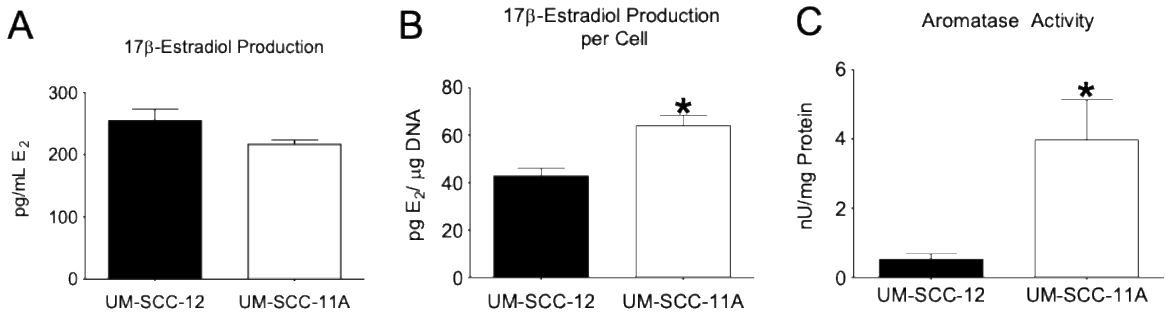

Figure 4.4 E2 is locally produced in vitro by UM-SCC-12 and UM-SCC-11A cultures.

Production of 17β-estradiol by ER+ UM-SCC-12 and ER- UM-SCC-11A [**A**] overall and [**B**] per cell. [**C**] Basal aromatase activity in laryngeal cancer cell lines. P-values less than 0.05 were considered significant. *indicates significance against UM-SCC-12.

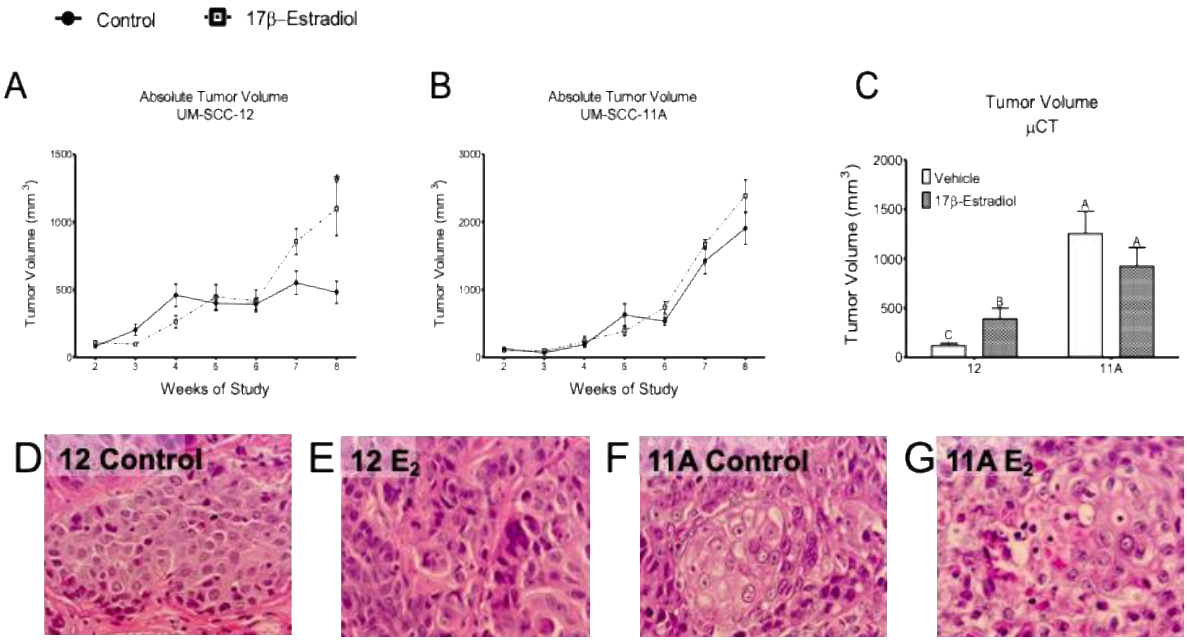

Figure 4.5 E$_2$ increases tumor burden in UM-SCC-12, but not UM-SCC-11A xenografts.

[**A,B**] Effect of 17β-estradiol on tumor growth of ER+ and ER- xenografts *in vivo*. Tumor growth of [**A**] UM-SCC-12 (ER+) and [**B**] UM-SCC-11A over time with and without estradiol supplementation. * indicates significance against week-matched control tumor volume. [**C**] Final tumor volume was measured with µCT Bars not sharing a letter have significantly different volumes with $P < 0.05$. [**D-F**] Representative histology of [**D,E**] ER+ and [**F,G**] ER- tumors [**E,G**] with and [**D,F**] without 17β-estradiol stained with hematoxylin and eosin and imaged at 40X. Scale bars = 20µm.

Estrogen receptor negative laryngeal cancer is more aggressive than estrogen receptor positive cancer.

UM-SCC-11A subcutaneous xenografts implanted into mice grew ~250 times their original size to a final volume of 1000-2000 mm^3 (Figure 4.5B). UM-SCC-11A tumors attained a final volume 2-4 times greater than that observed in UM-SCC-12 xenografts (Figure 4.5C). UM-SCC-11A also grew at a continuous exponential rate throughout the study (R^2=0.77-0.88, Table 4.6) with a faster doubling time than comparable UM-SCC-12 tumors (Table 4.6). Histology on UM-SCC-12 xenografts revealed moderately differentiated tumors with defined edges and uniform cell shapes (Figure 4.5D-E). Conversely, histology of UM-SCC-11A xenografts revealed anaplastic tumors with high variability in nucleus and cell size within the tumor. These tumors also showed a significant amount of invasion into the surrounding tissue (Figure 4.5F-G). The limited invasion and defined tumor edges observed in UM-SCC-12 cells are reminiscent of the defined tumor edges and even cell morphology observed in Stage 1 and 2 LSCC (Figure 4.6A,B,E,F). The increase in invasion in UM-SCC-11A tumors as compared to UM-SCC-12 tumors is similar to the increase in tumor invasion observed in samples of stages 3 and 4 (Figure 4.6C,D). The similar eosin staining, darker haematoxylin staining, irregular cell shape, and irregular nuclei structure observed in UM-SCC-11A tumors are similar to the cell morphology observed in stage 3 and 4 clinical LSCC samples (Figure 4.6G,H).

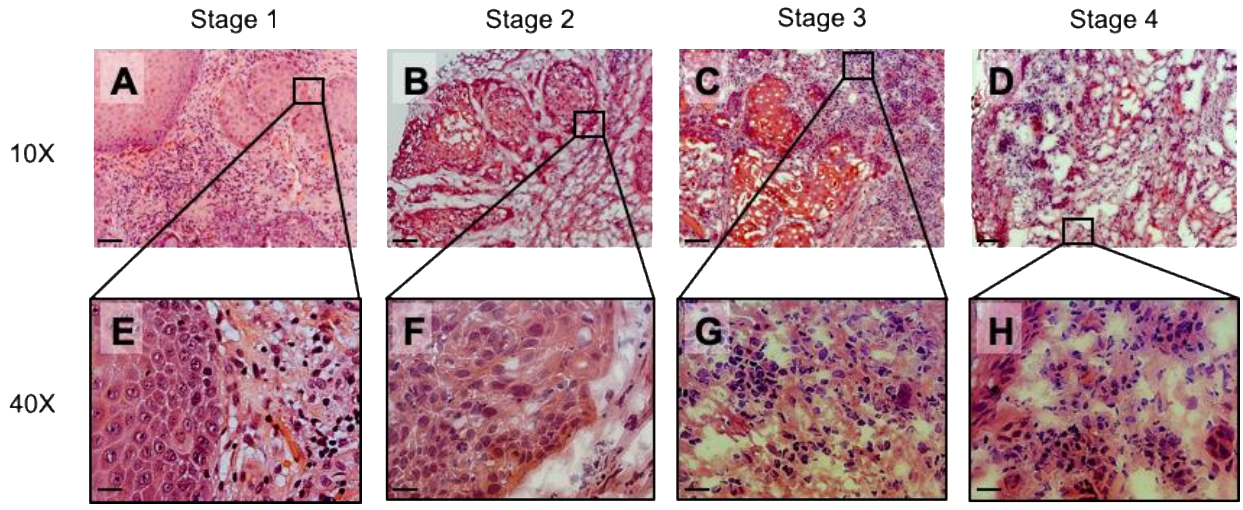

Figure 4.6 Representative Histology of Clinical Samples of Laryngeal Cancer.

Representative histology of [**A,E**] stage 1, [**B,F**] 2, [**C,G**] 3, and [**D,H**] 4 LSCC. Images were taken at [**A-D**] 10X and [**E-H**] 40X. [**A-D**] Scale bars = 100μm. [**E-H**] Scale bars = 20μm.

Exponential growth equation	11A Control	11A 17b-Estradiol	12 Control	12 17b-Estradiol
Best-fit values				
Y0	44.95	15.50	163.4	54.62
k	0.4723	0.6563	0.1533	0.3782
Tau	2.117	1.524	6.524	2.644
Doubling Time	1.468	1.056	4.522	1.833
Std. Error				
Y0	24.49	7.819	38.50	21.42
k	0.07290	0.06586	0.03665	0.05400
95% Confidence Intervals				
Y0	-5.601 to 95.49	-0.3556 to 31.35	86.01 to 240.8	11.77 to 97.48
k	0.3218 to 0.6227	0.5228 to 0.7898	0.07960 to 0.2270	0.2701 to 0.4862
Tau	1.606 to 3.108	1.266 to 1.913	4.406 to 12.56	2.057 to 3.702
Doubling Time	1.113 to 2.154	0.8776 to 1.326	3.054 to 8.708	1.426 to 2.566
Goodness of Fit				
Degrees of Freedom	24	37	50	59
R square	0.7679	0.8778	0.3106	0.5898
Absolute Sum of Squares	3.168e+006	5.376e+006	1.738e+006	5.025e+006
Sy.x	363.3	381.2	186.5	291.8
Number of points Analyzed	26	39	52	61

Table 4.6 Xenograft models of LSCC tumor growth curve: exponential fit, weeks 2-8.

Estrogen receptor expression in clinical cases of laryngeal squamous cell carcinoma is highly variable and regionally localized.

Quantification of western blots showed that ERα66 (Figure 4.1A, Figure 4.2A), ERα36 (Figure 4.1B, Figure 4.2B), and ERβ (Figure 4.1C, Figure 4.2C) signal intensity varied exponentially from samples to sample. While all samples taken from stage 4 patients had similar total levels of ERα66 (Figure 4.1A, Figure 4.2A) regardless of locality, ERα36 and ERβ expression was highly variable and appeared to be regionally localized. Stage 4 samples collected at Meir Hospital, Israel had greater ERα36 staining (Figure 4.1B, Figure 4.2B) and ERβ staining (Figure 4.1C, Figure 4.2C) than samples collected at Massey Cancer Center, U.S.A. All samples collected in Israel expressed high levels of ERβ, but none of the samples collected in the U.S.A. expressed ERβ (Figure 4.1C, Figure 4.2C). This regional variability was also apparent when considering the ratio of ER expression in tumor vs. precancerous tissue. All stage 3 and 4 samples collected in the U.S.A. had higher ratios of ERα36 in tumor tissue vs precancerous tissue (Table 4.3). However, stage 4 samples collected in Israel expressed less ERα36 in tumor tissue as compared to precancerous tissue (Table 4.3). If neither tumor nor matched normal tissue expressed protein for ERα66, ERα36, or ERβ as measured by western blot, a value of 'N/A' was recorded for that sample (Table 4.3).

Decreased absolute and normalized ERα66 expression is associated with advanced cancer stage in clinical samples of laryngeal squamous cell carcinoma.

A general trend of towards lower ERα66 expression was observed in more aggressive tumors (Stage 2-4) as compared to indolent tumors (Stage 1) (Figure 4.3A,E).

The total amount of ERα66 in these samples was greatest in stage 1 cancer (Figure 4.3A), and the proportion of ERα66 expressed by the tumor tissue as compared to matched precancerous tissue was also greater in stage 1 samples as compared to stage 4 samples (Figure 4.3D-F, Table 4.3). Samples from patients with stage 2-3 cancer had less ERα66 overall as compared to stage 1 samples (Figure 4.3A) but, like stage 1 samples, tumor tissues expressed more ERα66 than matched precancerous tissue (Figure 4.3D, Table 4.3). This trend did not hold true for Stage 4 cancer samples, where the ratio of ERα66 expression to precancerous tissue was flipped and precancerous tissue expressed more ERα66 than matched tumor tissue samples (Figure 4.3A,D-F; Table 4.3).

Patterns of relative ER expression among cancer stages described for ERα66 above also held true for ERα36 and ERβ (Figure 4.3B,C). Tumor tissue taken from patients with stage 4 cancer generally expressed less ERα36, and ERβ than matched precancerous samples (Figure 4.3B-F, Table 4.3). The ratio of ER expression in tumor vs. precancerous tissue was significantly lower in stage 4 samples as compared to stage 1 samples for all ERs: ERα66, ERα36, and ERβ (Figure 4.3D, Table 4.3).

Unlike ERα66, absolute expression of ERα36 and ERβ was similar in stage 1 and stage 4 cancers (Figure 4.3B,C). The most aggressive cancers (stage 4) generally had low ERα66 expression and high ERα36 expression (Figure 4.1A-B). Absolute ERα36 expression in stage 2 and 3 cancer samples was lower than stage 1, but ERα36 expression generally increased with stage in tumor samples taken from stage 2-4 patients (Figure 4.1B). Normal tissue surrounding stage 4 samples expressed higher ERα36 than matched normal tissue from lower stage cancers. Neither tumor nor precancerous samples taken from stage 2 and 3 samples patients expressed ERβ. However, it is

important to note that all stage 2 and 3 samples were collected in the U.S.A., while stage 4 samples were collected in both the U.S.A. and Israel.

Higher expression of ESR1 but not ESR2 is associated with increased survival in patients with primary laryngeal squamous cell carcinoma.

Analysis of RNAseq data taken from the TCGA study of 525 patients with primary head and neck cancer showed that patients with higher than median tumor ESR1 expression (ESR1 > 5.56) had significantly better survival rates than patients with lower tumor ESR1 expression (Figure 4.7A). This trend was also observed when patients were stratified by tumor ESR2 expression, with patients with higher than median ESR2 expression (ESR2 > 3.69) (Figure 4.7B) having significantly higher survival rates than patients with lower ESR2 expression after 15 years.

RNAseq data taken from a TCGA study of 128 patients with primary LSCC showed that patients with higher than median tumor ESR1 expression (ESR1 > 5.56) had significantly higher survival rates as compared to patients with lower tumor ESR1 expression (Figure 4.7C) with p-value < 0.0001 and a hazard ratio of 0.02845. However, no correlation between ESR2 expression and survival was observed when patients were stratified into groups of higher and lower than median ESR2 expression (Figure 4.7D) (p-value = 0.83).

Silencing ESR1 in estrogen receptor positive laryngeal squamous cell carcinoma eliminates the 17β-estradiol response and increases aggression.

Silencing the ESR1 gene, which encodes all known ERα isoforms, in UM-SCC-12 cells reduces ERα66 expression by 76% as compared to a 33.5% knockdown in scramble

control cells (Figure 4.8A,B). Similarly ESR1 silencing knocked down ERα36 expression by 75.2% as compared to 44.4% knockdown in scramble control cells (Figure 4.8A,C).

Silencing ESR1 in UM-SCC-12 did not change cell number *in vitro* as measured by total double-stranded DNA content (Figure 4.9A). However, silencing ESR1 altered total p53 content in these cells (Figure 4.9B). p53 protein production is associated with apoptosis. Total p53 content was significantly lower for shESR1-UM-SCC-12 cells as compared to WT and scramble control UM-SCC-12 cultures. Furthermore, silencing ESR1 in UM-SCC-12 eliminated the response of these cells to E_2. Both vehicle and E_2-treated shESR1-UM-SCC-12 cultures had approximately 1/3 the p53 content of WT vehicle-treated UM-SCC-12, whereas both vehicle and E_2-treated shESR1-UM-SCC-12 cultures levels of p53 similar to those observed in WT UM-SCC-12 cells treated with E_2 (Figure 4.9B).

UM-SCC-12 subcutaneous xenografts silenced for the ESR1 gene grew approximately 4 times larger than WT UM-SCC-12 xenograft tumors and twice as large as WT UM-SCC-12 xenografts treated with E_2. shESR1-UM-SCC-12 xenografts grew to similar sizes regardless of E_2 supplementation. Both silenced and WT xenografts grew in an approximately linear fashion, suggesting a faster doubling time *in vivo* for shESR1-UM-SCC-12 cells as compared to WT UM-SCC-12.

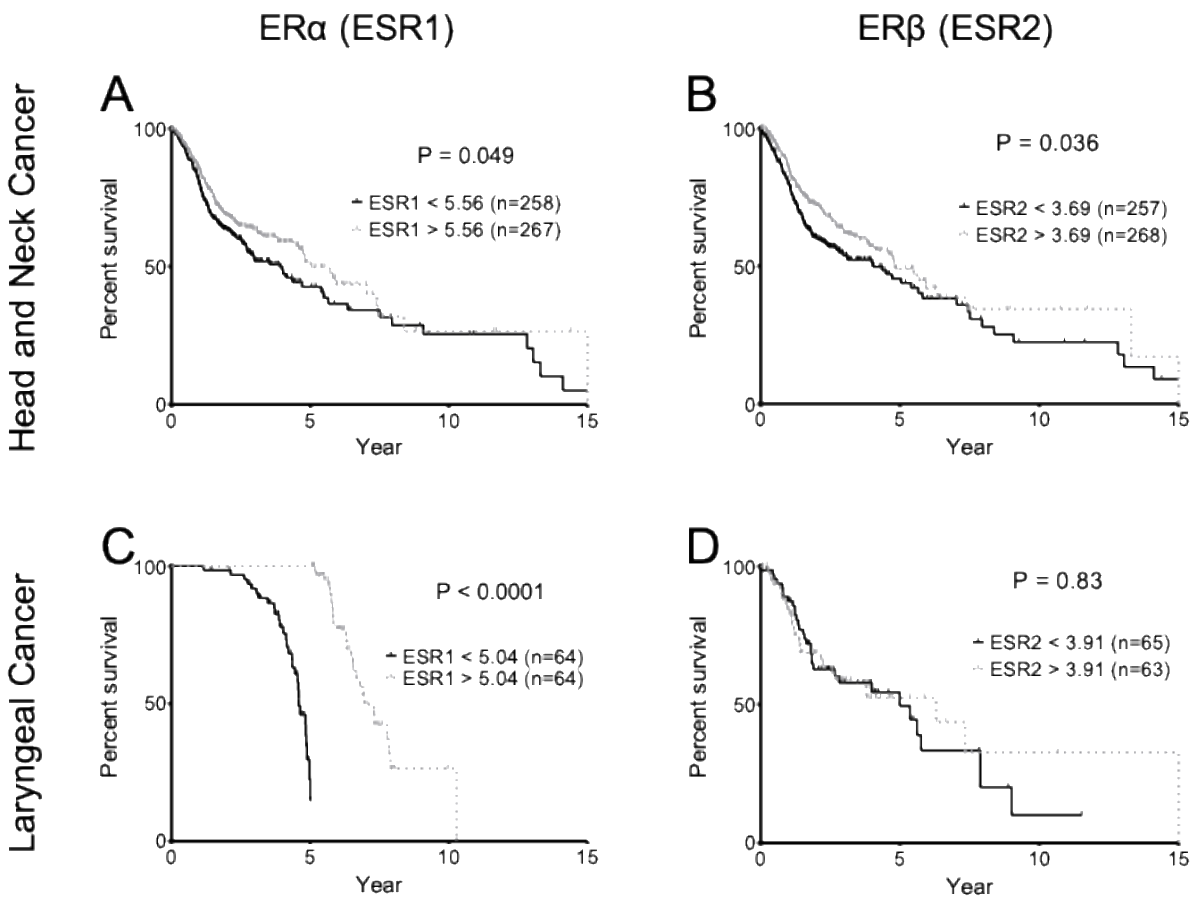

Figure 4.7 Intra-tumoral ESR1 expression correlates with survival.

Kaplan-Meier survival curves for patients with any [**A**,**B**] primary head and neck squamous cell carcinoma or [**C**,**D**] primary LSCC stratified by higher or lower than median [**A**,**C**] ESR1 or [**B**,**D**] ESR2 expression. Survival curves were analyzed with Log-rank Mantel-Cox $\chi 2$ tests. P-values less than 0.05 were considered significant.

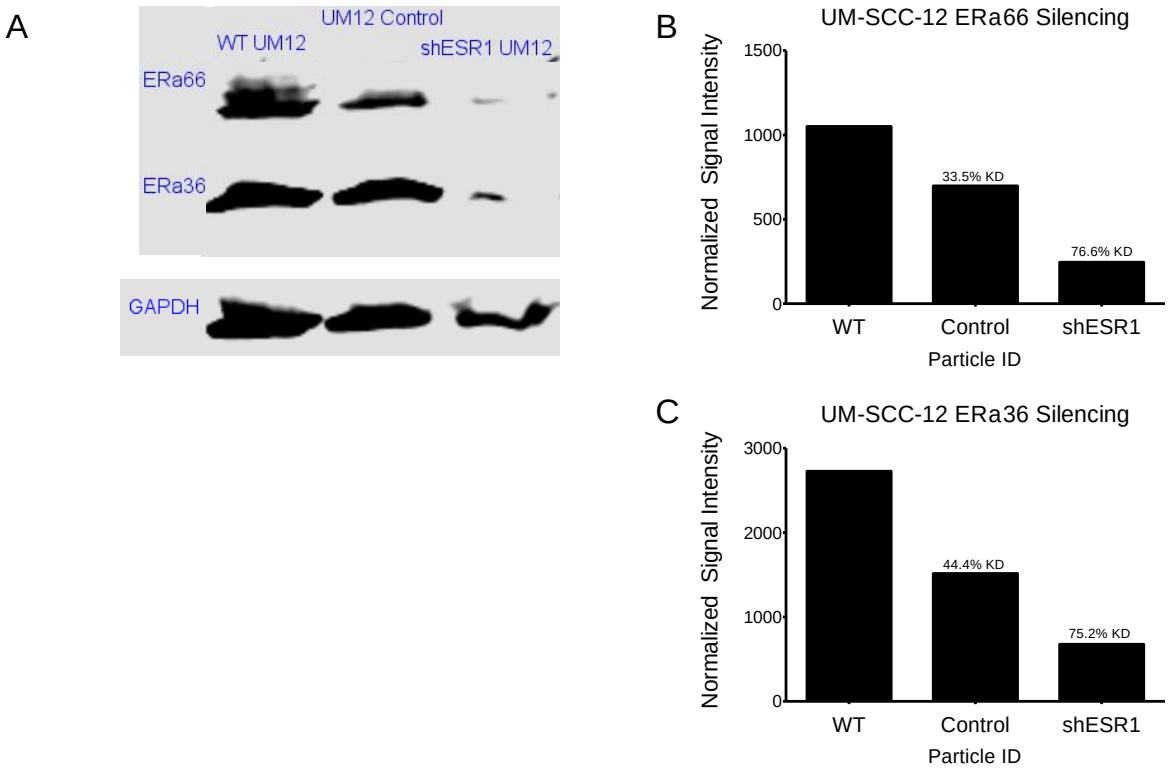

Figure 4.8 Knockdown of ERα in UM-SCC-12 cells.

A representative [**A**] western blot showing ERα expression in WT, scramble-control, and ESR1-silenced UM-SCC-12 cell lines. GAPDH was used as a protein loading control. [**B**] ERα66 and [**C**] ERα36 protein expression were normalized to GAPDH and quantified by normalized signal intensity. N=1.

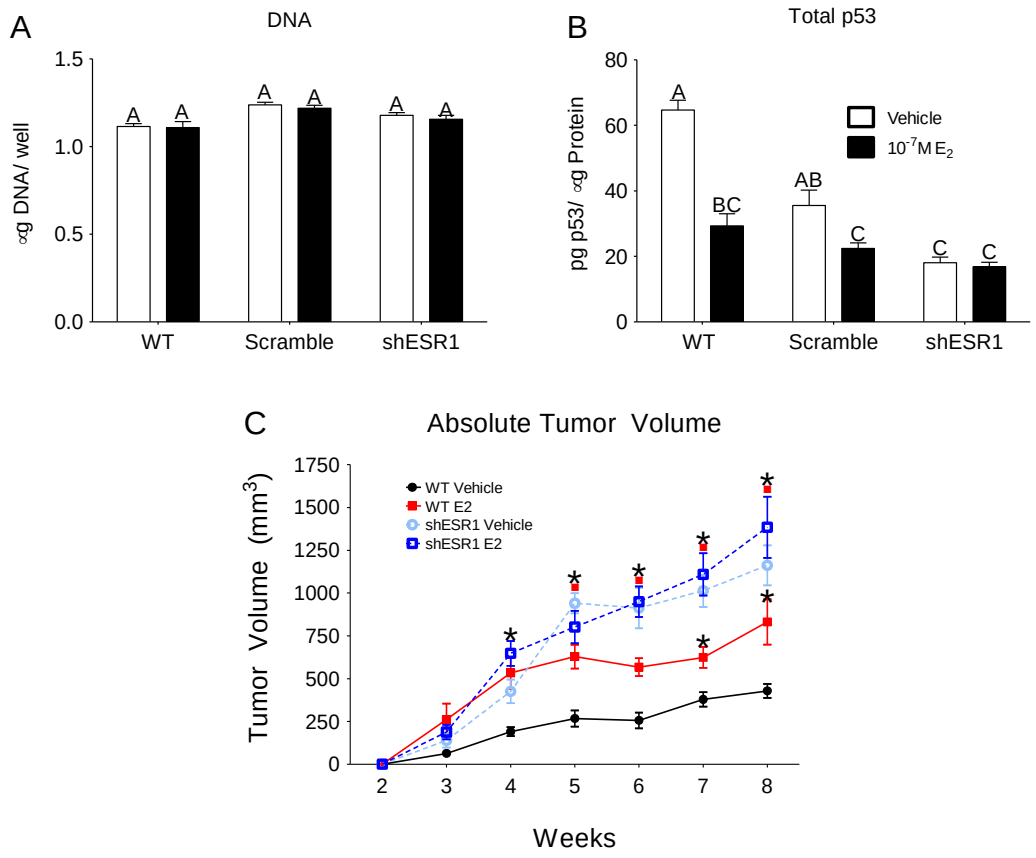

Figure 4.9 Silencing ESR1 in ERα+ LSCC increases tumor aggression.

Effect of silencing ESR1 in ERα66+ UM-SCC-12 cells *in vitro* on [**A**] cell number and the response to estrogen as measured by [**B**] total p53. Bars that do not share a letter are considered significant with p-values less than 0.05. *In vivo*, WT and ESR1-silenced UM-SCC-12 cell-line xenografts were implanted in a subcutaneous xenograft mouse model and [**C**] tumor burden was measured over time. Black * indicates significance against week-matched WT-vehicle tumor volume. Red squares ■ indicate significance against week-matched WT-E$_2$ tumor volumes. P-values less than 0.05 were considered significant.

Discussion

Accumulated evidence has substantiated that laryngeal cancer, a common head and neck cancer in the United States, is a hormone responsive cancer, comparable to other more renowned secondary sex hormone cancers. Despite the reports of E_2 detrimental effects in laryngeal cancer[89,90] and that anti-estrogen treatment has a beneficial effect[64] originating almost three decades ago,[62] there has been little advance in translating this recognition of the importance of E_2 to practical clinical implications. This might be explained by the cofounding and heterogeneous ER profile detected in these cancer cells. The cumulative effects of this heterogeneity translate to disparate responses to E_2 and must be clarified before implementation to clinical practice.

Local production of E_2 has been described in many steroid hormone responsive cancers, including breast,[175] endometrium,[176] cervical,[177] and testicular cancer.[178] Here, we observed a saturation in local E_2 production that occurred around 250 pg/mL, roughly 20 times previously reported levels of estradiol in serum from healthy adult males,[179] but not dissimilar from E_2 levels reported in plasma from pre-menopausal breast cancer patients.[180] Similar levels of E_2 production have also been observed in breast cancer-associated fibroblasts.[82] The tumorigenic properties of estrogen have been well-described in breast cancer,[55,76] and our previous work has shown that E_2 is also tumorigenic in ER+, but not in ER-, laryngeal cancer.[66,67] The increase in aromatase activity and corresponding increase in E_2 production per cell in ER- LSCC vs. ER+ LSCC was surprising; however similar disparities in E_2 production have been observed in ER+ and ER- breast cancer.[181] Increased serum E_2 is associated with compensatory mechanisms that arise in conjunction with defective estrogen signaling in normal breast

tissue,[182,183] and elevated serum E_2 has also been reported in estrogen insensitive triple-negative breast cancer (TNBC) patients as compared to those with ER+ tumors.[181] It is possible that the increase in aromatase activity and subsequent increase in E_2 production per cell was due to a saturation in E_2 concentration reminiscent of a classic negative signaling feedback loop[184]. However, it is also possible that the elevated E_2 production and aromatase activity observed in ER- LSCC is a result of similar compensatory signaling associated with these cells' insensitivity to estradiol.[67]

Consistent with previous reports,[138,139,157–160] evaluation of the laryngeal epithelia adjacent to laryngeal cancer reveals expression of both classical nuclear ERs and membrane ERs, specifically the ERα isoform ERα36. ERα36 is a well-established ERα splice variant which can mediate the effects of E_2 independent of nuclear ERα. This effect has been demonstrated in ERα66 null cells and in studies using antibodies against the nuclear and membrane isoforms of ERα.[109] The receptor initiates divergent pathways from the plasma membrane that re-converge downstream to affect cancer cell survivability.[27] In our study a striking difference is evident between the epithelia adjacent to advanced aggressive tumors and to more indolent tumors. While ERβ expression is highly variable, both ERα variants, the classical nuclear ERα66 and ERα36, are expressed in high levels in the epithelia adjacent to tumors displaying aggressive behavior, while absent in the indolent samples. In this, the ERα expression patterns in the epithelia adjacent to aggressively malignant samples (stage 4) is reminiscent of the ERα66 and ERα36 expression profiles generally seen in more indolent tumor samples.

It is well known that laryngeal squamous cell carcinoma arises from precancerous lesions, mainly dysplastic lesions. However, the exact molecular mechanisms of

malignant transformation of laryngeal mucosa are not clear. Moreover, the ability to identify patients who are most likely to progress into invasive laryngeal cancer or possess warning aggressive markers early in the course of their disease is paramount to early diagnosis and treatment to confer better prognoses. The presence of markers that correlate with pre-malignancy or early-stage cancer could have cardinal bearing on clinical decisions to observe or aggressively treat lesions.

Various classification systems have been crafted in an attempt to describe the histologic features of these laryngeal epithelial precursor lesions. Unfortunately, a universally accepted histopathological classification system and consensus on diagnostic criteria for LSCC are lacking. Different diagnostic techniques, specifically imaging modalities of laryngeal epithelial lesions, have been developed, but they do not offer a single system to make a differential diagnosis.[185] Consequently, new markers are required to reliably identify those high-risk precancerous lesions. Effort has been directed to identify molecular biomarkers that will enable the stratification of risk for malignant transformation and aggressive tumor behavior in patients with precancerous lesions. Some proposed biomarkers include the presence of chromosome instability markers,[186] cell cycle proteins,[187] β-catenin,[188] and microRNA-21.[189]

To our knowledge, ER characterization and profiling has not been studied in the context of precancerous lesions. Our findings imply that laryngeal epithelia expressing high levels of ERα66 and ERα36 are at risk for aggressive malignant transformation. Thus patients expressing this phenotype should be considered for more aggressive treatment and followed closely. Our sample number is too small to draw conclusions; however, in

this evolving field, ER should be considered as another biomarker that can shed light on the malignant potential of the tumor and direct treatment.

Evaluation of advanced and aggressive tumors, with clinical stage 4, revealed recovered high rates of ERα36, while remarkably losing or reducing their expression of ERα66. Indolent tumors, clinical stage 1, unexpectedly were found to upregulate the expression of both ERα66 and ERα36 compared to the adjacent epithelia. The majority of stage 2 and 3 tumors have reduced ERα66 expression as compared to more indolent samples, but retain their overexpression of ERα66 as compared to adjacent tissue. Conversely, there is a general trend of increasing ERα36 expression in more aggressive samples, suggesting that it is only in the final most aggressive stage 4 that tumors begin to loose ERα66 and regain ERα36 expression. In an attempt to interpret the differentiate ER expression between more indolent and aggressive tumors we turn to the prototype by which intricate ER cellular functions have been extensively studied, breast cancer.

The presence of the classical nuclear ERα66 has long been the most important molecular marker used in the diagnosis and as a predictor of prognosis in breast cancer. The presence of the receptor has a substantial role in dictating treatment, making anti-estrogen treatment a viable option for those patients with ERα overexpressing tumors. However, eventually most breast tumors become resistant to anti-estrogen treatment either through de-novo or acquired resistance.[190] One prevailing theory for the resistance to anti-estrogen treatment is the loss of the expression of ERα66, either as the presenting phenotype in ER negative tumors or in ER positive tumors during treatment, imparting loss of constraints and deleterious effects on tumor behavior. ER negative breast cancer, specifically the subclass of triple negative cancers, are renowned for their aggressive

nature and grave malignant potential.[191–193] Thus, in the case of the most renowned hormone responsive cancer, it is the loss of that responsiveness that causes the most aggressive behavior.

Interestingly, ER positive breast cancer acquired loss of the expression of ER precipitates the same aggressive phenotype. That same loss of ER expression has been described to incur trans-differentiation from epithelial to mesenchymal phenotype, which is responsible for increased aggressiveness and metastatic propensity.[194] More than a third of patients with recurrence and metastases from primary ER positive breast cancer were found to have lost their expression of ER upon recurrence,[195,196] which incurred a worse prognosis.[197] Coupled with the fact that almost half of patients with aggressive breast cancer characterized with high rates of recurrence and distant metastasis are classified as bearing primary triple negative cancers,[198] it seems evident that the lack of ER expression confers poor prognosis.

That loss of ER confers a poorer prognosis was further evidenced in our animal model. While the subcutaneous xenograft model we used does not traditionally metastasize,[199–201] the increased aggression associated with low ER and E_2 sensitivity in breast cancer was observed, with ER- LSCC reaching final tumor volumes more than twice as large as their ER+ LSCC counterparts regardless of estrogen supplementation. This was further borne out in a second LSCC xenograft model, which showed that natively ER+ LSCC silenced for the ESR1 gene behaves like ER- LSCC *in vivo*. shESR1-UM-SCC-12 xenografts grew to larger tumor sizes than either WT or E_2-treated ER+ LSCC xenografts regardless of estrogen supplementation.

In vitro studies confirm this, with silencing ESR1 in ER+ LSCC reducing total p53 levels to those on par with E_2-treated ER+ LSCC. This suggests that ERα loss mimics the effects of E_2 treatment on ER+ LSCC, implying that the presence of ERα, independent of its role as an estrogen receptor, affects some anti-tumorigenic signaling, which is superseded in the presence of supra-physiological doses of E_2. E_2-ERα signaling has been well established as pro-tumorigenic[190] in breast cancer, but the role of ERα independent of its actions as an E_2 conduit has not been widely studied. However, other studies in breast and other hormonally response cancers have shown that loss of ER contributes to tumor aggression [195,196,202].

Although ER expression profiles were not confirmed in the harvested xenograft, expression of ERα and ERβ isoforms pre-implantation suggests that both UM-SCC-12 and UM-SCC-11A have similar levels of ERα36 expression, but only UM-SCC-12 express ERα66. This is in line with observations from clinical and TCGA data, which suggest that increased ERα is associated with lower aggression in LSCC. It should also be noted that silencing ESR1 in UM-SCC-12 reduces both ERα66 and ERα36 expression in these cells, making it difficult to determine if the increase in aggression in shESR1-UM-SCC-12 is due to a reduction in ERα66, ERα36, or some combination of the two. The similar levels of ERα36 in UM-SCC-11A and UM-SCC-12 suggest that the increased aggression observed in shESR1-UM-SCC-12 is due to a reduction in ERα66 expression, but further studies are needed to determine which isoform(s) of ERα are involved in ERα-silencing induced increases in tumor aggression.

Survival data from head and neck cancer and LSCC patients further suggest that lack of ERα is associated with poorer prognoses, again in a manner similar to breast

cancer. It is well known that loss of ER correlates with reduced survival in breast cancer patients[69], and similar trends were observed in our meta-analysis of recent head and neck cancer cohorts. Although all head and neck cancer patients show a slight correlation between increased ERα or ERβ expression and improved survival odds; this trend is not mirrored in laryngeal cancer, where ERα is the predominant determinate of ER-associated survival. It should be noted that the majority of the samples in this data set came from patients with stage 4 cancer (n = 81 of 140), suggesting that the prognostic value of ESR1 expression as a marker of LSCC aggression may exist independent of any association with late-stage cancer. It is also interesting to note the discrepancy between the whole head and neck cancer dataset and laryngeal cancer survival specifically. RNAseq data necessarily lacks information about post-transcriptional modification of transcribed proteins and can offer limited insights about splice variants and alternative isoforms of the traditional ERα and ERβ, many of which have been identified.[36,68,203,204] A lack of correlation between ESR1 and ESR2 expression may indicate a mechanistic difference in the ERα and ERβ membrane and cytosolic signaling pathways that could be dependent on alternative isoforms of both ERs.

The mechanism underlying the loss of ER expression in primary ER positive tumors has not yet been clarified. Genomic and posttranscriptional silencing mechanisms offer an explanation for the loss of ER expression. One proposed mechanism is the inactivation of ER gene transcription due to methylation of cytosine-rich areas termed CpG islands.[205] This mechanism has also been described in another hormone responsive tumor, endometrial cancer.[206] Similar silencing of ER gene transcription is the basis of the mechanism underlying the action of micro-RNA. The micro-RNA are a class of regulatory

molecules that have been shown to control gene expression such as ERα in breast cancer,[207,208] and have been implicated in ovarian,[209] endometrial[210] and laryngeal cancer.[211] An alternative genomic mechanism has been proposed, that entails the loss of heterogeneity in ER genes such as allelic loss in microsatellites located in regulatory regions of ER genes,[212] which was verified as an independent prognostic factor for relapse free survival.[213]

These mechanisms of loss of ER expression resemble the findings we have observed in laryngeal cancer. The indolent laryngeal cancer cells express both ERα66 and ERα36, and their ER profile resembles that of the epithelia adjacent the aggressive tumors, being part of a spectrum from precancerous lesions to low grade tumors. Stage 2 and 3 samples begin to loose ERα66 and gain ERα36 expression, and, the aggressive tumors are distinctly characterized by the loss of ERα66 and high expressing ERα36.

There is growing interest in the clinical implication of the membrane ERα36, particularly in regard to its role in mediating E$_2$ responsiveness in ER negative tumors and anti-estrogen resistance in ER positive tumors. About 40% of ER positive and ER negative breast cancer cells express ERα36 in the plasma membrane.[214] High levels of ERα36 expression correlate with an unfavorable prognosis, independent of ER status and have been suggested as an important novel marker for breast cancer clinical characterization.[88] In our previous studies and in this recent study we have consistently identified high rates of ERα36 expression in laryngeal cancer cells.[66,67] Furthermore, in a previous study, we demonstrated that activation of ERα36 resulted in an upregulation of angiogenic and metastatic factors and observed an association between the amount of ERα36, VEGF, and lymph node metastasis in laryngeal cancer patients, indicating that

ERα36 has a role in metastasis.[66] In laryngeal cancer it seems that ERα36 has a pivotal role in tumorigenesis and tumor progression, with both indolent laryngeal cancer samples and epithelia adjacent to aggressive samples expressing high levels of ERα36.

The epithelia adjacent to all the tumors collected from Meir Hospital, Israel in our study expressed high levels of ERβ, and the level of expression of ERβ was maintained in the indolent tumor. In contrast the aggressive tumors from this sample set demonstrated a marked decline or full suppression of the expression of ERβ. These results indicate that ERβ confers protective effect in laryngeal cancer cells, an effect that has also been reported in previous studies of head and neck carcinoma.[70] ERβ has been postulated to be a dominant-negative regulator of ERα modulating transcriptional responses to estrogens. The ratio of ERα vs. ERβ within a cell may determine the cell sensitivity to E_2 and its biological responses.[26] This protective effect of ERβ has been observed in breast cancer cells in which the expression of ERβ was found to inhibit proliferation and cell invasion.[146,215] Further, ERβ expression has been clinically correlated with low grade tumors, low S phase fraction, negative axillary node status and most importantly higher likelihood to respond to hormonal therapy.[216] These findings coincide with our observation that advanced laryngeal tumors with metastasis to regional lymph nodes, fully suppress the expression of ERβ. The relative conservation of ERβ was correlated with a more indolent tumor behavior. Up to 90% of triple negative breast cancer have been found to express ERβ,[217] the activation of which resulted in suppression of cell proliferation, presumably due to suppression of cyclin kinase 1 and 7 and blockage of cell cycle progression.[218] ERβ target genes have been postulated to regulate apoptosis and cell survival, cell development and movement, growth and proliferation as well as genes

involved in β-catenin and cell cycle checkpoint pathways.[217] Knockdown of the ERβ expression in triple negative breast cancer cells increased the invasiveness of the cells about three fold,[219] while ERβ agonists had the opposite effect,[220] raising the possibility of their role in the treatment of these cancers.

A number of studies have identified geographic and racial disparities in ERα and ERβ expression in other hormonally responsive cancers, particularly breast cancer and prostate cancer. Geographic incidences of ER negative breast cancer are highly variable both within the U.S. and internationally,[221–225] and this disparity has been associated with higher incidences of ERα negative, ERβ positive, and triple-negative breast cancer in women of African descent.[226–231] The opposite trend has been observed in prostate cancer, with one study of 300 prostate cancer samples from African American (AA) and Caucasian American (CA) men identifying increased ERβ expression in tumor and precancerous samples from AA patients as compared to CA men.[232] However, both sets of patients had increased intra-tumor ERβ staining as compared to matched precancerous samples.

The proportion of ERα positive breast cancer incidence relative to the total diagnoses is similar for patients in the United States and Northern Israel;[224,225] however, our data suggest that ERβ positive cancer incidence may be more regionally localized. Other studies have reported high variability of ERβ expression in laryngeal cancer samples, similar to the trends we observed in our samples.[233] It is important to note that, although western blots were conducted in a centralized lab, our samples were originally fixed and processed at two different institutions, which could have caused 'batch processing effects' that could also account for the regional variation we observed in our

samples. Additional demographic data on race and ethnicity were not available for our samples; however, the wide variability of ERα and ERβ expression in our data could be indicative of variability in race and ethnicity among our sample set. While our sample size is too small to draw conclusions, further investigation into geographic variability of ERα and ERβ expression in laryngeal cancer is needed to further understand the potential of ERs as diagnostic and prognostic markers of laryngeal cancer.

Chapter 5.

24R,25-Dihydroxyvitamin D$_3$ regulates breast cancer cells *in vitro* and *in vivo*

[Chapter 5 is published as: Verma A, Cohen DJ, Muktipaty C, Schwartz N, Boyan BD, Schwartz Z. Loss of estrogen receptors is associated with increased tumor aggression in laryngeal squamous cell carcinoma. BBA-Gen. 2019]

Introduction

Interest in anti-tumorigenic effects of vitamin D$_3$ began with reports of an inverse association between sunlight exposure and age-adjusted breast cancer mortality [234]. Subsequent studies have demonstrated a connection between serum 25-hydroxyvitamin D$_3$ (25(OH)D$_3$) and breast cancer risk and prognosis, with low serum levels correlating with increased incidence of breast cancer and high serum levels correlating with reduced recurrence and increased survival in breast cancer patients [112,235,236]. Despite this, studies evaluating the effectiveness of vitamin D supplementation on cancer progression and survival have been inconclusive [236–240]. Interestingly, one study examining post-remission vitamin D supplementation showed that supplement use was associated with reduced recurrence rates among patients with estrogen receptor (ER) positive breast cancer, but not patients with ER negative breast cancer [8]. Similarly, high serum 25(OH)D$_3$ levels correlate with improved survival as measured by reduced hazard ratios in post-menopausal patients (statistically associated with higher rates of ER positive cancer [241]), but no correlation was identified in pre-menopausal patients (statistically associated with ER negative or triple-negative breast cancer [242]) [243].

Many physicians prescribe vitamin D$_3$ to breast cancer patients, and even more breast cancer patients are believed to supplement their dietary vitamin D intake with over-the-counter supplements [244,245]. Vitamin D$_3$ is hydroxylated in the liver to form 25(OH)D$_3$ [246], which binds to albumin and vitamin D-binding protein in the blood and is subsequently transported to the kidney where it is metabolized to 1,25-dihydroxyvitamin D$_3$ (1,25(OH)$_2$D$_3$) and 24,25-dihydroxyvitamin D$_3$ (24,25(OH)$_2$D$_3$) [13]. Although the kidney produces the bulk of circulating 1,25(OH)$_2$D$_3$ and 24,25(OH)$_2$D$_3$, 25(OH)D$_3$ metabolism also occurs locally in some cell types [247–249].

Preclinical studies indicate that 1,25(OH)$_2$D$_3$ and its precursor 25(OH)D$_3$ may have potential as a preventive therapy for breast cancer. Oral vitamin D3 increased autophagy and cell turnover in normal murine mammary gland [114] and both oral vitamin D$_3$ and intravenous 1α,25(OH)$_2$D$_3$ reduced tumor growth in estrogen receptor (ER) positive breast cancer xenograft models [14]. *In vitro*, 1α,25(OH)$_2$D$_3$ reduced cancer cell growth, angiogenesis, and metastasis, and induced apoptosis in ER positive breast cancer cells [115–117] but not in normal breast epithelial cells [118]. This may be a function of 1α,25(OH)$_2$D$_3$'s genomic [120] or non-genomic [118,250] actions. 1α,25(OH)$_2$D$_3$-liganded vitamin D receptor (VDR) suppresses transcription of the ESR1 gene [120;] and both 1α,25(OH)$_2$D$_3$ [118] and its non-VDR binding analogs 1,24,25(OH)$_3$D$_3$ and 1,25,26(OH)$_3$D$_3$ inhibit growth of breast cancer cells *in vitro* [122].

While these studies are promising, there is some concern about the risk of hypercalcemia that accompanies treatment with high doses of 1α,25(OH)$_2$D$_3$. Both 25(OH)D$_3$ and 1α,25(OH)$_2$D$_3$ have narrow therapeutic windows when given intravenously, with serum levels of ~1x10^{-6}M 25(OH)D$_3$ and ~9x10^{-10}M 1,25(OH)$_2$D$_3$ being

associated with clinical hypercalcemia [126]. The potentially toxic effect of 1α,25(OH)$_2$D$_3$ with regard to calcium handling and its narrow therapeutic window prompted the search for synthetic vitamin D analogs that share its anti-cancer properties while bearing a less calcemic profile [251,252].

We propose an alternative endogenous metabolite of vitamin D, 24R,25(OH)$_2$D$_3$. This naturally occurring steric epimer of 24,25(OH)$_2$D$_3$ plays an active role in developing skeletal tissue [23,253]. Furthermore, 24,25(OH)$_2$D$_3$ is less calcemic than 1,25(OH)$_2$D$_3$, with doses up to 500 times greater than 1,25(OH)$_2$D$_3$ toxicity thresholds having no effect on serum calcium in rats [125].

The identity of the 24R,25(OH)$_2$D$_3$ receptor remains elusive. Larsson et al. reported specific receptors for this vitamin D metabolite in lysosomal membranes in intestinal cells [21] and Seo et al. [19] and Kato et al. [20] have shown evidence for a membrane-bound receptor for 24,25(OH)$_2$D$_3$ in chick fracture healing callus. Martineau et al. recently identified a novel 24R,25(OH)$_2$D$_3$ receptor, FAM57B2, which may regulate the 24R,25(OH)$_2$D$_3$ response in chondrocytes [22]. Analysis of the crystal structure of the classical VDR suggests that conformational changes in the receptor may accommodate binding of a variety of 1,25(OH)$_2$D$_3$ analogues, raising the possibility that 24,25(OH)$_2$D$_3$ might also occupy the ligand binding pocket on the receptor, at least transiently [54]. Studies using rat growth plate resting zone chondrocytes have characterized specific membrane-associated signal transduction pathways that mediate both rapid non-genomic, and genomic responses [17,23,93], supporting the presence of receptor(s) for 24R,25(OH)$_2$D$_3$ but whether one or more of the receptors identified above are involved is not known.

Steroid hormones act through both traditional and non-traditional receptors, which operate in parallel pathways and collaborate to exert the hormone's full effect [68]. Such a model exists in the case of 1α,25(OH)$_2$D$_3$; VDR and membrane-associated Pdia3 co-localize with the caveolae scaffolding protein, caveolin-1, in osteoblasts. Ligand binding changes the interactions of the two receptors and rapidly activates phospholipase A$_2$ (PLA$_2$) and Src [254,255]. 24R,25(OH)$_2$D$_3$ acts via membrane-associated phospholipid metabolism, resulting in activation of phospholipase D (PLD)-mediated signaling and protein kinase C, amplifying the complexity of the actions of this secosteroid [15,105].

24R,25(OH)$_2$D$_3$ is produced via hydroxylation of 25(OH)D3 on C-24 by CYP24A1 [256]. Overexpression of CYP24A1 increases 24,25(OH)$_2$D$_3$, which may have growth modulating effects independently and in combination with 1,25(OH)$_2$D$_3$ on various cancers, including ovarian cancer [257], colon cancer [98], lung cancer [258] and breast cancer [128,259]. One such study showed that 24R,25(OH)$_2$D$_3$ treatment prolonged survival of mice with Lewis lung carcinoma *in vivo* [260,261]. In rats, 24R,25(OH)$_2$D$_3$ reduced the development of cancerous and precancerous lesions in the glandular stomach in a dose-dependent manner by altering calcium pharmacodynamics during the post-initiation phase of glandular stomach carcinogenesis [262]. In the colon, a similar chemopreventive effect was observed via anti-proliferative actions. Pretreatment and, more markedly, continuous administration of 24R,25(OH)$_2$D$_3$ reduced the total numbers of aberrant crypt foci and putative pre-neoplastic lesions to inhibit development of colon cancer foci [263]. Alterations in c-fos, c-myc, and c-jun oncogene expression were proposed as potential mechanisms for incurring these anti-proliferative actions, suggesting that rapid actions of the vitamin D metabolite were involved.

In the search for compounds that mimic the growth regulating effects of vitamin D$_3$ independent from its calcium mobilizing actions, 24R,25(OH)$_2$D$_3$ has emerged as an exceptional candidate as it incorporates the anti-proliferative and anti-tumorigenic effects of 1α,25(OH)$_2$D$_3$ without disrupting calcium homeostasis by elevating calcium blood levels [262]. To further improve the understanding of the role of 24R,25(OH)$_2$D$_3$ in the tumorigenesis and progression of breast cancer we established an *in vivo* model of tumor growth and metastasis in mice using MCF7 breast cancer xenografts. In addition, we examined the underlying mechanism of 24R,25(OH)$_2$D$_3$'s effect *in vitro* using MCF7. We hypothesized that the effect exerted by 24R,25(OH)$_2$D$_3$ on breast cancer cells involves protecting against proliferation, promoting apoptosis and suppressing migration and metastatic gene expression, resulting in reduced invasion and metastasis. To validate the hypothesis that the secosteroid can modulate breast cancer cell survival, we also assessed the response of two breast cancer cell lines.

Materials & Methods

Cell Lines

MCF7, T-47D, and HCC38 breast cancer cells were authenticated by ATCC (Manassas, VA) using STR profiling and were used within 6 months of purchase as described previously [1]. Cells were maintained in media and passaged in accordance with ATCC guidelines. Red fluorescent protein (RFP) expressing-MCF7 cells (RFP-MCF7) were created by transfecting cells with an RFP-encoding plasmid (pMirTarget, #PS100062, Origene, Rockville, MD) using TurboFectin 8.0 (Origene #TF81001) according to manufacturers' protocol.

In Vivo Studies

Female NSG mice skeletally mature (6-8 weeks old) were obtained from the Virginia Commonwealth University (VCU) Cancer Mouse Models Core Laboratory at Massey Cancer Center, (Richmond, VA). All animal experiments were approved by VCU's Institutional Animal Care and Use Committee.

MCF7 Xenograft Model.

To create MCF7 tumors, female 6-8 weeks old mice (N = 8) were injected intraperitoneally with 2.5mg/kg of 17β-estradiol (#E8875; Sigma-Aldrich, St. Louis, MO) or 2% ethanol:1X distilled phosphate buffered saline (DPBS) vehicle one week prior to tumor initiation. These injections continued twice a week for the remainder of the study (11 weeks in total). One week after the first 17β-estradiol or vehicle injection, tumors were initiated by injecting 1 million MCF7 cells in 50μL of 1:1 DPBS:BME (Cultrex Pathclear basement membrane extract Type 3, 14.5mg/mL; #3632; R&D Systems, Minneapolis, MN) solution into the lactiferous duct of the right fourth mammary gland of the mouse[264–266]. Beginning at 2 weeks post-cell injection, tumors were measured along two perpendicular axes (length and width) with digital calipers, and tumor volume was calculated using the following formula: $Volume = \frac{Length * Width^2}{2}$ [264,265,267,268]. Tumor volume was plotted against time and comparisons between vehicle and control mice were made using a repeated-measured analysis of variance (ANOVA). P-values <0.05 were considered significant. Tumor measurements were taken once a week for 10 weeks until harvest.

Mice were euthanized at 10 weeks via CO_2 inhalation. Tumors were harvested and preserved in 10% neutral buffered formalin. Fixed tissues were processed, embedded in paraffin, and cut into 3-5μm sections. Sections were stained with H&E to examine cell morphology[109].

In a second study, 5-week old female NSG mice were ovariectomized[167]. Two weeks post-operatively, mice were injected with 17β-estradiol (N=6) or vehicle (N=6) twice a week for 11 weeks as described above. One week after the first 17β-estradiol or vehicle injection, mice were implanted with MCF7 cells in the right fourth mammary gland as described above. Tumor size was measured once a week with digital calipers and tumor volume was calculated using the established system described above. Tumors grown in ovariectomized mice were harvested after 10 weeks, analyzed with μCT, and preserved in formalin. Histologic sections were stained with H&E and analyzed. Tumor volume and percent growth of tumor were graphed vs. time. Animals in both studies were monitored for signs of estrogen toxicity, such as urinary bladder distension and skin rash.

μCT Tumor Volume Measurements.

Tumors were harvested and immediately scanned with a Bruker Skyscan 1173 μCT at 55kV and 70μA, with a resolution of 560x560 pixels with an image pixel size of 40.26μm, an exposure time of 125ms and a rotation step of 0.8^o [166]. A standard reconstruction was conducted on the tumors using the NRecon software version 1.6.10.4 (Kontich, Belgium) with a smoothing kernel of 0 and a beam hardening correction of 20%. μCT reconstructions of the tumors were analyzed using the CTAn software version 1.16.1.0 (Kontich, Belgium). Total tumor volume was measured as the total tissue volume.

Calculated tumor volumes as measured by digital calipers and total tumor volumes from μCT scans were compared using a 2-way ANOVA with Bonferroni post-tests with α=0.05.

Effect of 24R,25(OH)2D3.

Two weeks after subcutaneous implantation of zero-order release 17β-estradiol pellets (0.96mg/45 days) (Innovative Research of America, Sarasota, FL) [167] at 'week 0', female NSG mice (N=24) were injected with 1 million RFP-MCF7 cells in the right lactiferous duct of the fourth mammary fat pad. MCF7 tumors were allowed to grow for 5 weeks. At that time, mice were divided into 3 groups (n=8) and each group was injected intraperitoneally 3 times a week with 0, 25ng, or 100ng of 24R,25(OH)$_2$D$_3$ (#BML-DM300-0050; Enzo Life Sciences, Farmington, NY) in a 2% ethanol: DPBS vehicle. Mammary fat pad tumors were measured with calipers throughout the study. Tumor volume and tumor accretion rate (tumor volume over time normalized to original tumor volume) were graphed vs. time. Tumor growth rate from weeks 6-10 was analyzed with a linear regression model for each group (0, 25, and 100ng of 24R,25(OH)$_2$D$_3$). Animal survival was tracked throughout the study and percent surviving mice vs. length of survival was recorded. Animal survival was plotted on a hazard curve and analyzed with the chi-squared logrank test for trend at α=0.05. Throughout the study, animals were monitored for signs of hypercalcemia, such as changes in appetite or lethargy.

On the day of harvest, animals were euthanized with CO_2 and metastases was identified by the presence of RFP (443/581nm) using a Zeiss SteroDiscovery.V12 fluorescence dissecting microscope with an AxioCam MRm digital camera. Tumors were harvested and analyzed with μCT. Axial and inguinal lymph nodes, lungs, and livers were grossly examined for RFP expression. Fluorescing organs were harvested and fresh

flash-frozen on block dry ice in optimal cutting temperature compound (OCT) (#25608; VWR, Radnor, PA) for histological analysis. After μCT analysis, tumors were fresh flash-frozen in OCT as above. OCT-embedded samples were cut into 3-5μm sections on a cryostat, post-fixed with fresh 4% paraformaldehyde for 10 minutes, and stained with H&E to confirm metastasis. Total metastatic incidence and metastatic incidence by organ were recorded.

In vitro Studies

Response to Vitamin D3 Metabolites.

To assess specificity of the response of MCF7 cells to 24R,25(OH)$_2$D$_3$ confluent cultures were treated with media containing 1α,25(OH)$_2$D$_3$ (10^{-10}-10^{-8}M, Enzo #BML-DM200-0050); 24R,25(OH)$_2$D$_3$ (10^{-9}-10^{-7}M); 24S,25(OH)$_2$D$_3$ (10^{-9}-10^{-7}M, Sigma Aldrich #29447); 25(OH)D$_3$ (10^{-9}-10^{-7}M, Sigma Aldrich #17938); or vehicle. All vitamin D metabolites were reconstituted to 1mM stock solutions in absolute ethanol. Stock solutions were diluted in warm complete media to final treatment concentrations. Media were removed by aspiration at 15 min or 24 hours and cells were incubated with fresh complete media until harvest as indicated below.

Signaling Pathway Inhibition.

In these experiments, cells were pre-treated for 30 minutes with inhibitors or vehicle in warm complete media. At that time, fresh media containing 24R,25(OH)$_2$D$_3$ or vehicle were added on top of inhibitor treatments, and cells were incubated for a further 15 minutes before the conditioned media were aspirated. Cultures were then incubated in fresh complete media until harvest. To determine if the effect of 24R,25(OH)$_2$D$_3$ was

mediated by palmitoylation, cultures were pretreated with 1-10μM 2-bromopalmitate (Sigma-Aldrich #21604)[269]. PLD was inhibited by pretreatment with 0.1 to 1 μM wortmannin (VWR #80055508, Radnor, PA) [15]. To assess whether intact caveolae were required, cultures were pretreated with 1 or 10mM methyl β-cyclodextrin (Sigma-Aldrich #C4555) in serum-free media to deplete cell membranes of cholesterol [169,270,271]. In order to assess the role of ERα66, cultures were pretreated with 10^{-7}M ICI-182780, an inhibitor to cytosolic and nuclear ERs (Sigma-Aldrich #I4409) [272,273]. The contribution of ERα36 was determined by pretreating MCF7 cells with 1μg of a neutralizing antibody to the membrane-associated estrogen receptor (Chi Scientific #8-80113, purchased from VWR) [55].

Outcome Measures

DNA synthesis. Cells were cultured to 70% confluence, then serum-starved for 48 hours in phenol-red free MEM supplemented with 1% charcoal-dextran filtered FBS and 50U/50U penicillin-streptomycin. At that time, cells were treated with 24R,25(OH)$_2$D$_3$, 24S,25(OH)$_2$D$_3$, 25(OH)D$_3$, or 1α25(OH)$_2$D$_3$ for 15 minutes and incubated with fresh complete media for 24 hours. In a separate experiment, cells were treated with these vitamin D3 metabolites for 24 hours. At the 20 hour mark, cells in both experiments were pulsed with 10μL of a 1:100 dilution of 5-ethynyl-2'-deoxyuridine (EdU) and incubated for 4 hours. Cells were harvested and assayed for EdU incorporation according to manufacturer's instructions (ThermoFisher Scientific #C10214).

Gene expression. Cells were cultured to confluence, then treated with 24R,25(OH)$_2$D$_3$ or 24S,25(OH)$_2$D$_3$ or vehicle in complete media for 15 minutes as described above. Cultures were then aspirated and incubated with complete media for 12

hours. RNA was extracted using TRIzol (Invitrogen, Carlsbad, CA) and quantified (Take3 Micro-Volume Plate, Biotek, Winooski, VT) before being used to synthesize cDNA libraries (High Capacity cDNA Reverse Transcription kit, Promega, Madison, WI). Apoptosis markers were B cell lymphoma protein 2-associated X protein (BAX) to B cell lymphoma protein 2 (BCL2) mRNA expression. Epithelial to mesenchymal transition markers were C-X-C- motif chemokine 12 (CXCL12), chemokine receptor type 4 (CXCR4), snail family transcriptional repressor 1 (SNAI1), erythroblastic oncogene B (ERBB2), and matrix metalloproteinase 1 (MMP1). Markers of metastasis were osteoprotegerin (OPG), and nuclear factor kappa-B ligand (RANKL)[274–277].

mRNAs were quantified with real-time quantitative PCR using *Power* SybrGreen® Master Mix (Applied Biosystems) and gene-specific primers described in Table 5.1. Commercially available primers (Qiagen, Hilden, Germany) were used to quantify BCL2 (Hs_BCL2-1-SG QuantiTect Primer #249900), ESR1 (Hs_ESR1-1-SG QuantiTect Primer #044492), RANKL (Hs_TNFSF11-1-SG QuantiTect Primer #PPH01048F), and SNAI1 (Hs_SNAI1-1-SG QuantiTect Primer #010010) mRNA. All other primers were self-designed using the National Center for Biotechnology Information PrimerBLAST [278] and ordered from ThermoFisher Scientific (Waltham, MA). Exact sequences for all ThermoFisher primers are given in Table 5.1. RNA quantities were determined by the standard curve method. mRNA levels were normalized to levels of glyceralde-3-phosphate dehydrogenase (GAPDH) mRNA. mRNA for BAX, BCL2, CXCR4, and CXCL12 are presented as ratios of BAX to BCL2 and CXCR4 to CXCL12.

Gene	Primer Sequence	
BAX	F	GACGAACTGGACAGTAACATGG
	R	AAAGTAGAAAAGGGCGACAACC
CXCL12	F	GCCTCTGAAGCCTATGTATG
	R	GACGAACTGGACAGTAACATGG
CXCR4	F	TAGCAAAGTGACGCCGAGGG
	R	TGGTTCTCCAGATGCGGTGG
ERBB2	F	CCGCTGAAGTCCACACAGTT
	R	AAAGGTTCTACCCCGCATGG
GAPDH	F	CTATAAATTGAGCCCGCAGCC
	R	TGGCGACGCAAAAGAAGATG
MMP1	F	AGAAAGAAGACAAAGGCAAGTTGA
	R	TCCCCAGTCACTTTCAGCCC
OPG	F	GTGTGCGAATGCAAGGAAGG
	R	CACTCCAAATCCAGGAGGGC

Table 5.1 Human primers used in real-time PCR analysis.

Total p53 content. Total p53 was measured 24 hours post-cell treatment with vitamin D metabolites as described above using a sandwich enzyme-linked immunosorbent assay (ELISA) (R&D Systems, Human Total p53 DuoSet® IC). Cells were plated in 24 well plates, treated with vitamin D3 metabolite for 15 minutes, and incubated for 24 hours in complete media. Conditioned media were collected and cell layers were lysed by sonication (40A for 5 seconds) in 200µL lysis buffer according to manufacturer's protocol. Lysates were centrifuged at 10,000*g* for 15 minutes; the supernatant was collected and assayed for total protein content (ThermoFisher, Pierce 660 nm Protein Assay) and total p53 content following the manufacturer's instructions. Data are presented as a ratio of nanograms of total p53 to total protein content.

DNA fragmentation. DNA fragmentation was assessed by colorimetric terminal deoxynucleotidyl transferase (TdT)-mediated dUTP nick end labeling (Trevigen, TiterTAC™ *in situ* microplate TUNEL assay). Cells were incubated with vehicle, 24R,25(OH)$_2$D$_3$, or 24S,25(OH)$_2$D$_3$ for 15 minutes followed by incubation in fresh media for 24 hours. After fixing the cultures with 3.7% sucrose-buffered formaldehyde, samples were processed for TUNEL staining following manufacturer's instructions. Final absorbance was detected at 450 nm using a microplate spectrophotometer.

Enzyme-linked immunosorbent assays for secreted proteins. Confluent cultures of MCF7 cells were plated in 6 well plates, treated with vehicle or 24R,25(OH)$_2$D$_3$ for 15 minutes as described above, aspirated, and then incubated in complete media. After 24 hours, conditioned media were collected in 5mL polypropylene tubes, frozen at -80^{o}C and lyophilized (Labconco, Kansas City, Missouri, Freezone Freeze Dryer #7740020). Lyophilized samples were reconstituted in 200 µL of filtered 1XPBS containing 1% BSA and assayed for OPG and RANKL using sandwich ELISAs (R&D Systems, Human TRANCE/RANK L/TNFSF11 DuoSet ELISA #DY626, Human Osteoprotegerin/TNFRSF11B DuoSet ELISA #DY805). Cell monolayers were lysed in 1mL 0.5% Triton™ X-100. Cell lysates were assayed for total DNA content (Promega, QuantiFluor dsDNA, #E6150). OPG and RANKL content are expressed as a ratio of OPG/RANKL.

Matrix metalloproteinase 1. Collagenase (MMP1) content in the cultures was measured using an MMP1 assay kit (SensoLyte® Plus 520 MMP-1 Assay Kit *Fluorimetric and Enhanced Selectivity*, Anaspec #AS-72012). Cells were plated in 24 well plates and treated with vehicle or 24R,25(OH)$_2$D$_3$ as described above. At harvest

conditioned media were collected; cell monolayers were lysed in 500µL 0.05% Triton-X-100 and total DNA content measured. Total MMP1 was measured in the media and normalized to total DNA content. Data are presented as a ratio of ng MMP1/µg DNA.

Wound closure assay. A wound closure assay was used to demonstrate metastasis. Confluent cultures of MCF7 cells were treated for 15 min with media containing vehicle or 24R,25(OH)$_2$D$_3$. Another set of cultures was treated with 10^{-7}M 17β-estradiol as a positive control. Following treatment, a scratch was drawn from one end of the well to the other using a sterile 1 mL pipette tip. The loosened cells were aspirated along with the treatment media, and fresh media added to the cultures. A phase-contrast microscope was used to take pictures of each well at 0, 3, 6, 9, 12, and 24 hours after the scratch was made. Wound area was calculated using Adobe Photoshop™ 2 software, normalized to the original wound closure area, and presented as percent wound closure. Data presented are from one of two repeated experiments.

Statistical Analysis

Data shown are from single representative experiments of two or more repeats and are presented as mean ± standard error of six independent cultures per treatment group. Data were analyzed by ANOVA with Tukey's post-test to determine significance between groups. Experiments with two independent variables (DNA synthesis, total DNA content, and total p53 time courses) were analyzed with two-way ANOVA with Bonferroni's modification of Student's t-test post-tests to determine the variance between row and column factors. The wound closure assay was analyzed with a repeated measures ANOVA test with comparisons between time points. P-values <0.05 were considered significant.

Results

17β-Estradiol supplementation stimulated MCF7 breast cancer tumor growth in mice.

MCF7 (estrogen receptor positive, ER+, progesterone receptor positive, PR+) breast cancer cells were injected into the duct of the fourth mammary gland. Mice receiving 17β-estradiol injections grew tumors 3-5 times their original size. In contrast, tumors grown in animals given a vehicle control injection showed minimal growth over 10 weeks (Figure 5.1). Tumors in mice given 17β-estradiol increased from approximately 40mm^3 to an average of 200mm^3, approximately 500% of their original volume, with a linear growth increase over the course of 8 weeks (week 2 to week 10). However, tumors grown in mice given a vehicle injection reached an average size of 55mm^3, an increase of approximately 10% of their original volume (Figure 5.1A). In ovariectomized animals, the difference between vehicle versus 17β-estradiol injected mice was even more pronounced, with tumors grown in 17β-estradiol injected mice reaching an average size of 100mm^3 versus only 25mm^3 in vehicle-injected ovariectomized mice (Figure 5.1B,C). Tumor morphology was similar in both 17β-estradiol and vehicle-injected mice, and there was no observed difference in tumor morphology in samples taken from normal vs. ovariectomized mice [representative image, (Figure 5.1D)]. At harvest, final tumor volume in 17β-estradiol animals was approximately 4 times greater than tumor volume in vehicle-treated animals in both the normal and ovariectomized mouse models (Figure 5.1E). None of the animals in either experiment showed signs of estrogen toxicity.

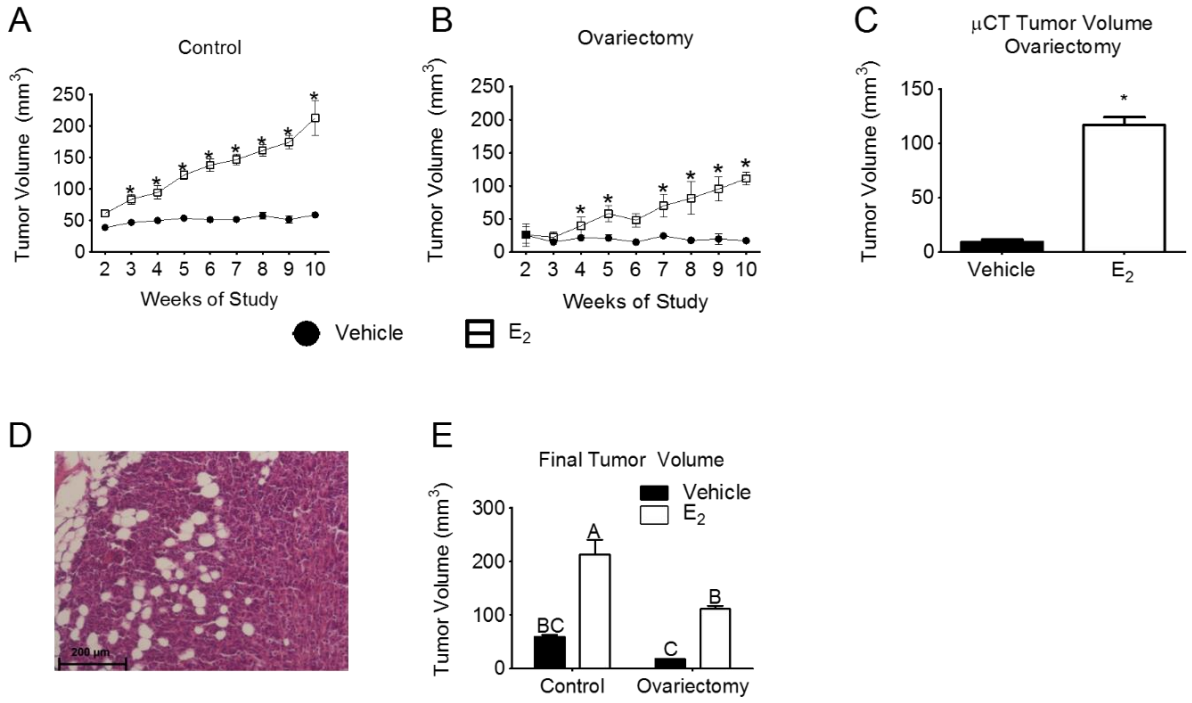

Figure 5.1 17β-estradiol stimulates MCF7 tumor growth in a mammary fat pad xenograft model in NSG mice.

[**A**] Non-ovariectomized mice injected with 17β-estradiol showed a significant increase in tumor growth as compared to the vehicle after 3 weeks of injection until the end of the study at week 10. [**B**] Similar trends were observed in a separate study with ovariectomized animals, with animals treated with 17β-estradiol showing a significant increase in tumor growth as compared to vehicle at weeks 4 and 5 and weeks 7-10 of the study. [**C**] At harvest, tumors grown in ovariectomized mice supplemented with 17β-estradiol reached an average volume of 120mm^3, nearly 6 times greater than tumors grown in vehicle-treated mice. [**D**] Histology of the fourth mammary fat pad revealed neoplastic tissue characteristic of MCF7 tumors.

(continued from page 124) [**E**] Final tumor volume was largest in control mice supplemented with 17β-estradiol. Ovariectomized mice supplemented with 17β-estradiol had tumor volumes that were smaller than those from normal mice, but still larger than tumors grown in ovariectomized mice given a vehicle control. Groups that share a letter are not statistically significant at α=0.05 with two-way ANOVA.

Treatment with 24R,25(OH)2D3 reduced tumor aggression and increased animal survival.

Red fluorescent protein (RFP)-overexpressing MCF7 mammary fat pad tumors were grown in female NSG mice for 10 weeks. Estrogen supplementation was given for 2 weeks prior to tumor initiation, then continued for the first 4 weeks of tumor growth. Dose-dependent 24R,25(OH)$_2$D$_3$ was initiated at the beginning of week 5, and continued for the rest of the 10 week study. Mice receiving either 25ng or 100ng per injection of 24R,25(OH)$_2$D$_3$ survived longer than mice injected with vehicle alone. 6/8 and 7/8 animals in the 25ng and 100ng groups, respectively, survived until harvest, while only 3/8 animals survived in the control group (Figure 5.2A). Animals in the control group also started dying earlier (at day 38) than animals given 24R,25(OH)$_2$D$_3$ (day 56) (Figure 5.2B). Both 25ng and 100ng treated tumors exhibited a lower percent increase in size compared to vehicle-treated mice. Tumors in both 24R,25(OH)$_2$D$_3$ treated groups achieved approximately 500% of their original volume, while vehicle-treated tumors grew to approximately 1000% of their original volume (Figure 5.2C). Tumors in mice given 25ng 24R,25(OH)$_2$D$_3$ reached volumes of approximately 400mm^3 at harvest, roughly 80% the size of the tumors in

vehicle-treated mice, which reached a volume of 500mm^3 on average. Tumors in mice given 100ng showed an even steeper growth depression, reaching final volumes of 200mm^3 on average, roughly 40% of vehicle-treated tumors (Figure 5.2D,E).

The difference in tumor volume was due to growth that occurred in the last 4 weeks of the study, after 24R,25(OH)$_2$D$_3$ injections were begun. All tumors were approximately the same size at week 6, at the onset of treatment. From week 6-10, vehicle-treated tumors had a growth rate of 79.54 ± 9.40 mm^3/week (R^2 =0.96); 25 ng-treated tumors had a growth rate of 57.90 ± 8.70 mm^3/week (R^2 =0.94); and 100ng-treated tumors had a growth rate of 40.61 ± 6.60 mm^3/week (R^2 =0.93). The slopes were significantly different (P=0.0213). Calculated tumor volumes from caliper measurements were not significantly different from tumor volumes generated by μCT analysis (Figure 5.2E). Haematoxylin and eosin (H&E) staining revealed similar tumor morphology in tumors from each group [representative image, (Figure 5.2F)].

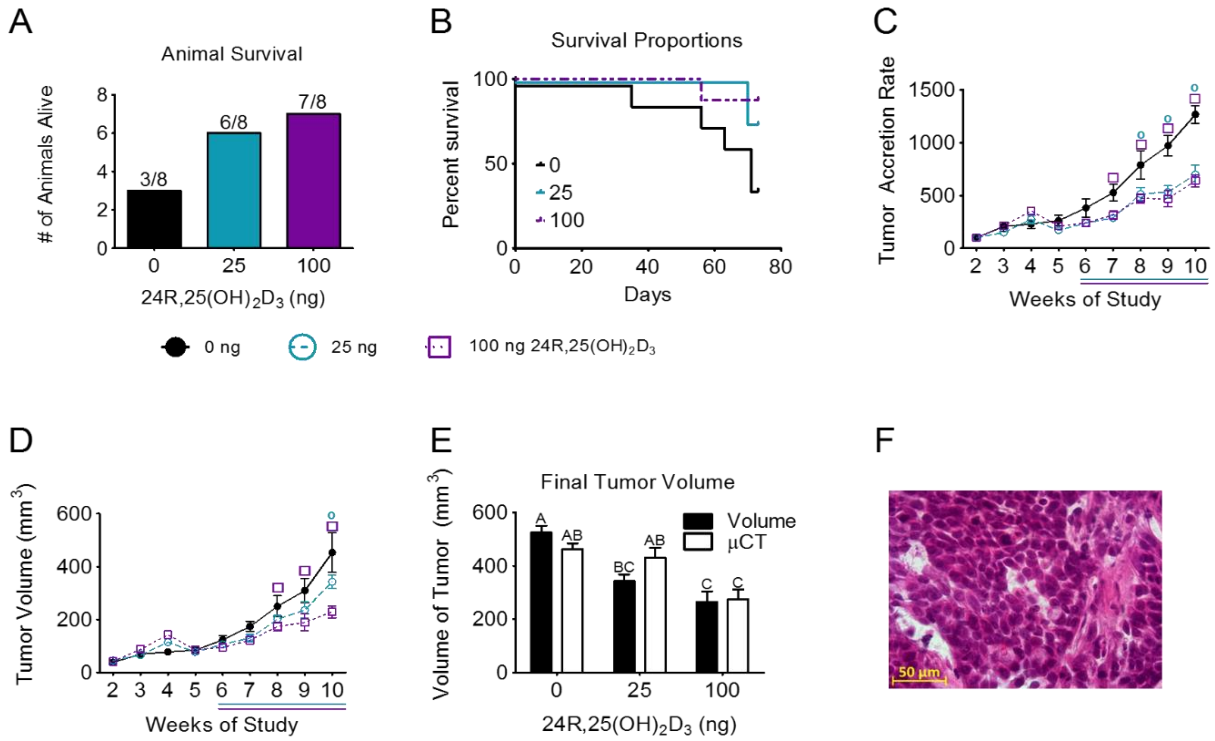

Figure 5.2 24R,25(OH)2D3 reduces MCF7 tumor burden and increases animal survival.

[**A**] After 8 weeks, 3 animals from the vehicle group, 6 animals from the low-dose 24R,25(OH)$_2$D$_3$ group, and 7 animals from the 24R,25(OH)$_2$D$_3$ group survived out of an original n of 8. [**B**] Animals in the vehicle group had a statistically significant reduced survival rate as compared to animals in the low or high dose groups by the chi-squared logrank test for trend (P=0.0433). [**C**] Tumor accretion rate was calculated by normalizing tumor volumes at each week to the original tumor volume calculated at week 2.

(continued from page 122) [**D**] Animals given 24R,25(OH)$_2$D$_3$ showed a decreased rate of growth after vitamin D$_3$ injections were begun at week 6 of the study. Statistics were done using a repeated-measures ANOVA test to compare between the vehicle, low, and high-dose groups within weeks.

(continued from page 127) Purple squares □ indicate significance against the high-dose group, and blue open circles ○ indicate significance against the low-dose group. [**E**] After harvest, tumor volume was quantified using µCT analysis. Calculated caliper volumes and µCT-derived volumes were graphed together, and statistics were done using ANOVA with Tukey's correction. Bars that share a letter are not significant at α=0.05. Both caliper measurements and µCT analyses showed statistically significant decreases in final tumor volume between the high-dose 24R,25(OH)$_2$D$_3$ group and the vehicle control; and µCT analysis showed a statistically significant difference between both the vehicle and the low-dose 24R,25(OH)$_2$D$_3$ group as compared to the high-dose 24R,25(OH)$_2$D$_3$ group. [**F**] Histology of the fourth mammary fat pad showed cells with a dense epithelial-like phenotype consistent with MCF7 morphology and previous MCF7 xenograft studies, bar 50 µm.

Metastatic burden was detected in animals by assessing individual organs for RFP expression using a fluorescent dissection microscope at harvest. Animals treated with 24R,25(OH)$_2$D$_3$ had a lower metastatic burden than vehicle-injected controls, with fewer organs that were positive for RFP-tagged MCF7 cells. Animals treated with 25ng 24R,25(OH)$_2$D$_3$ had, on average, 1-2 incidences of metastasis/animal, while 100ng treated animals averaged 0-1 metastatic incidence per animal. Control group animals averaged 3-4 incidences of metastasis per animal (Figure 5.3A). Animals treated with 24R,25(OH)$_2$D$_3$ also had fewer incidences of local and distant metastasis than control group animals, with animals injected with 25ng 24R,25(OH)$_2$D$_3$ having fewer incidences of multiple lymph node, lung, and liver metastases. This effect was even greater in

animals treated with higher doses of 24R,25(OH)$_2$D$_3$ (100ng). These animals had fewer lymph node and lung metastases and no incidences of multiple lymph node or liver metastases (Figure 5.3B). Metastatic sites were characterized by round clusters of RFP-positive cells with defined edges, characteristic of MCF7 metastases [279] (Figure 5.3C-E). Morphology of metastatic sites was similar to the morphology of the primary tumor (Figure 5.3F-H). None of the animals showed signs of hypercalcemia throughout the study or upon dissection at harvest.

24R,25(OH)$_2$D$_3$ induced both proliferation and apoptosis in ER+ cells in vitro.

When MCF7 cells were treated for 15 minutes with 24R,25(OH)$_2$D$_3$, its enantiomer 24S,25(OH)$_2$D$_3$, or its precursor 25(OH)D$_3$, proliferation was increased after 24 hours. The effect of 24R,25(OH)$_2$D$_3$ and 24S,25(OH)$_2$D$_3$ was dose-dependent with the greatest increase at 10^{-8}M 24R,25(OH)$_2$D$_3$ (Figure 5.4A) and 10^{-7}M 24S,25(OH)$_2$D$_3$ (Figure 5.4B); all doses (10^{-9}-10^{-7}M) of 25(OH)D$_3$ increased proliferation (Figure 5.4C). In contrast, 1α,25(OH)$_2$D$_3$, did not increase proliferation at 24 hours (Figure 5.4D). None of these metabolites increased proliferation in MCF7 monolayers that were treated with vitamin D metabolites for 24 hours (Figure 5.5), and only 24R,25(OH)$_2$D$_3$ increased apoptosis in these cells after 24 hours (Figure 5.6).

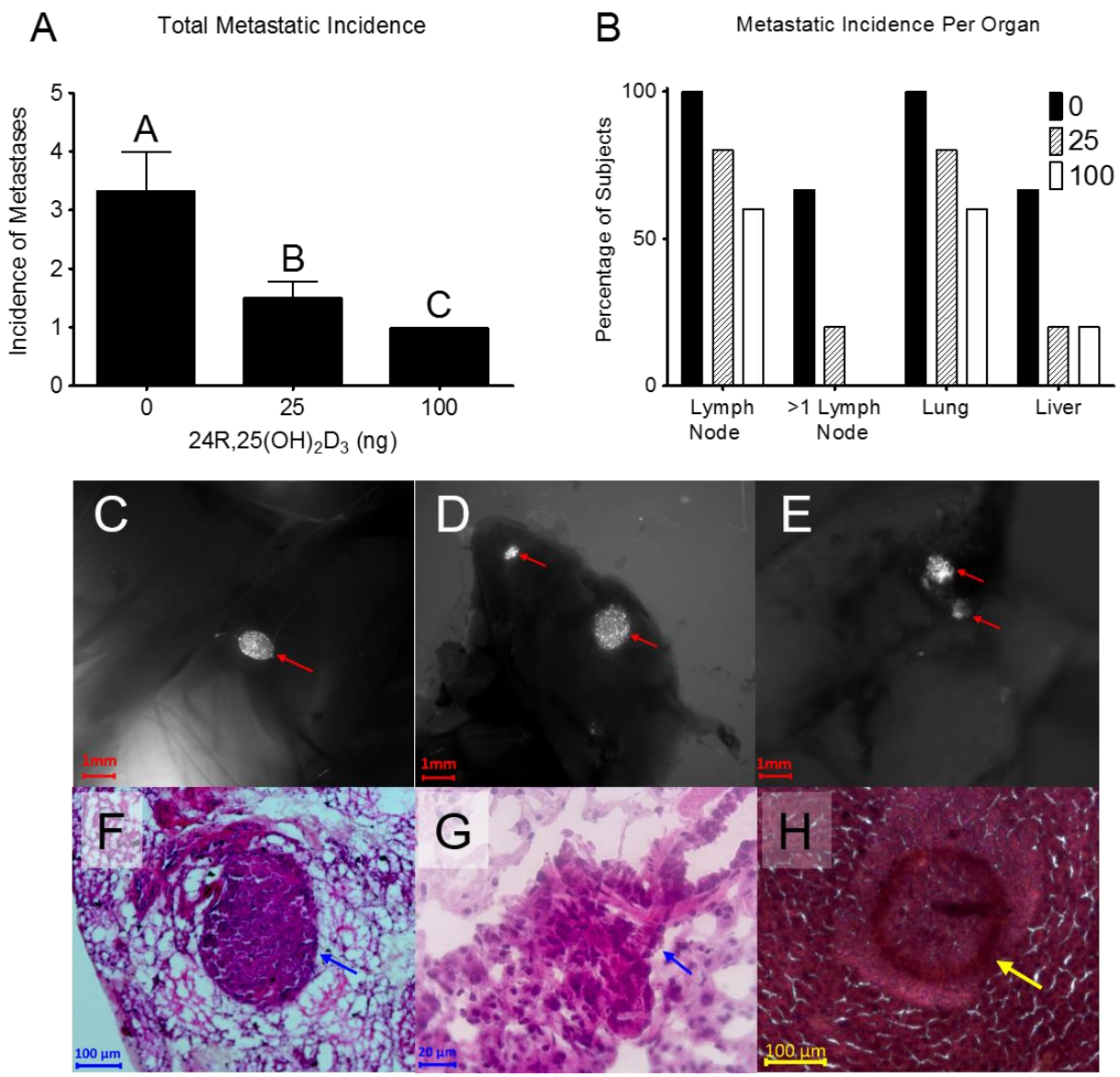

Figure 5.3 24R,25(OH)2D3 reduces metastatic burden in MCF7 xenograft mouse models.

[**A**] High-dose 24R,25(OH)$_2$D$_3$ reduced the total metastatic burden of red fluorescent protein-expressing MCF7 tumors and [**B**] reduced the number of metastatic incidences to the lymph nodes, lungs, and liver. Statistics were not done on metastatic incidence per organ data due to the ordinal nature of the data collected and the small sample size of the surviving animals in the vehicle group (n=3).

(continued from page 125) In fig [**A**], groups that share a letter are not significant at α=0.05. Metastatic organs – [**C**,**E**] lymph node, [**D**,**G**] lungs, and [**E**,**H**] liver – were identified at harvest with a fluorescent microdissection scope set [**C**,**E**] an RFP/ tdTomato filter at 10X magnification and [**D**] 40X magnification. Metastases were confirmed with [**F**-**H**] H&E staining, and images are displayed at [**F**] 10X or [**G**,**H**] 40X magnification.

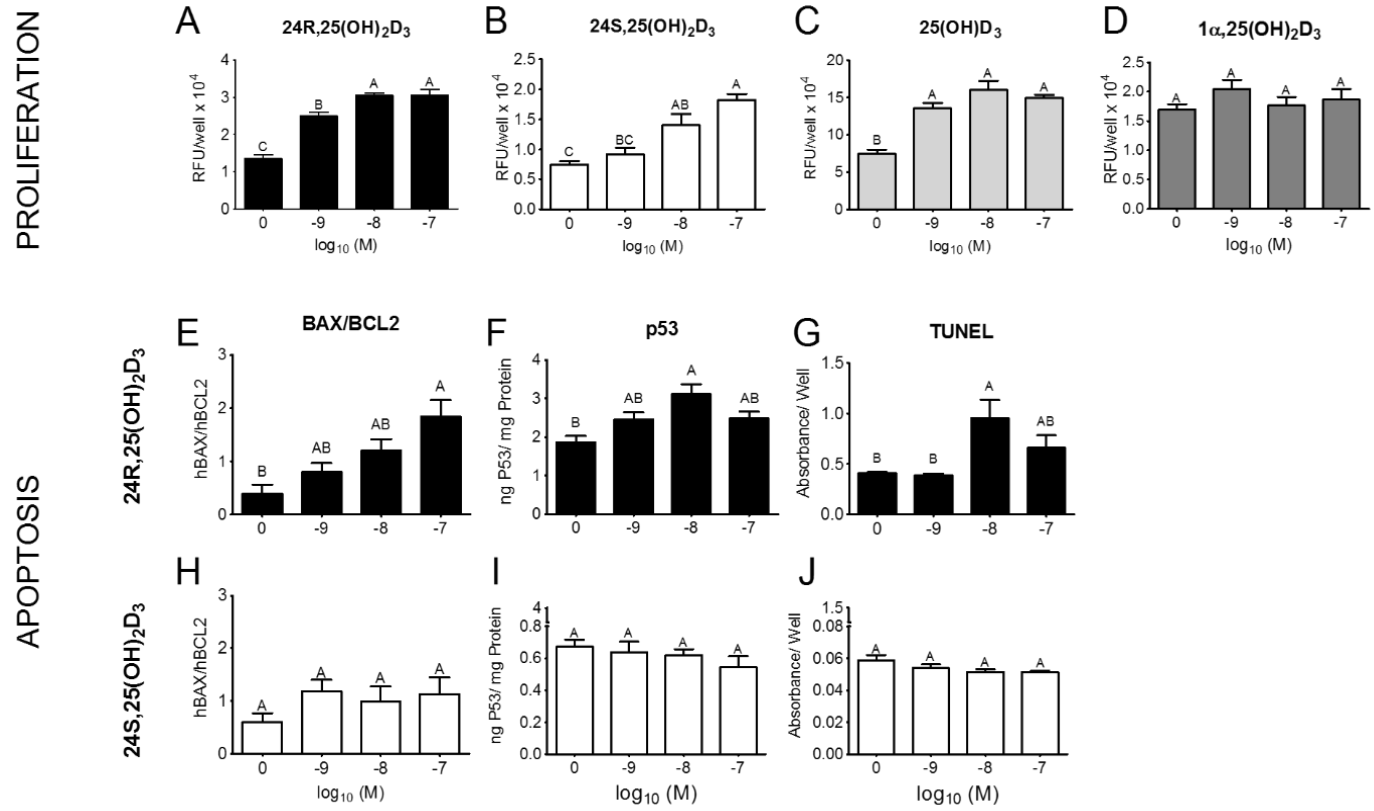

Figure 5.4 24,25(OH)2D3 induces both proliferation and apoptosis in MCF7 cells with varying specificities.

[**A**] 24R,25(OH)$_2$D$_3$ induced proliferation in MCF7 cells 24 hours after a 15-minute treatment. [**B**] Its enantiomer 24S,25(OH)$_2$D$_3$ also increased proliferation in this system [**C**] and so did their precursor 25(OH)D$_3$. [**D**] The vitamin D isoform 1α,25(OH)$_2$D$_3$ did not increase proliferation in these cells. [**E**-**G**] In contrast, 24R,25(OH)$_2$D$_3$ induced apoptosis in MCF7 cells 24 hours after a 15-minute treatment, [**H**-**J**] but its enantiomer 24S,25(OH)$_2$D$_3$ did not. [**E**,**H**] Apoptosis was measured by BAX/BCL2 expression, [**F**,**I**] total p53 levels, [**G**,**J**] and TUNEL staining. Groups that do not share a letter are statistically significant at α=0.05.

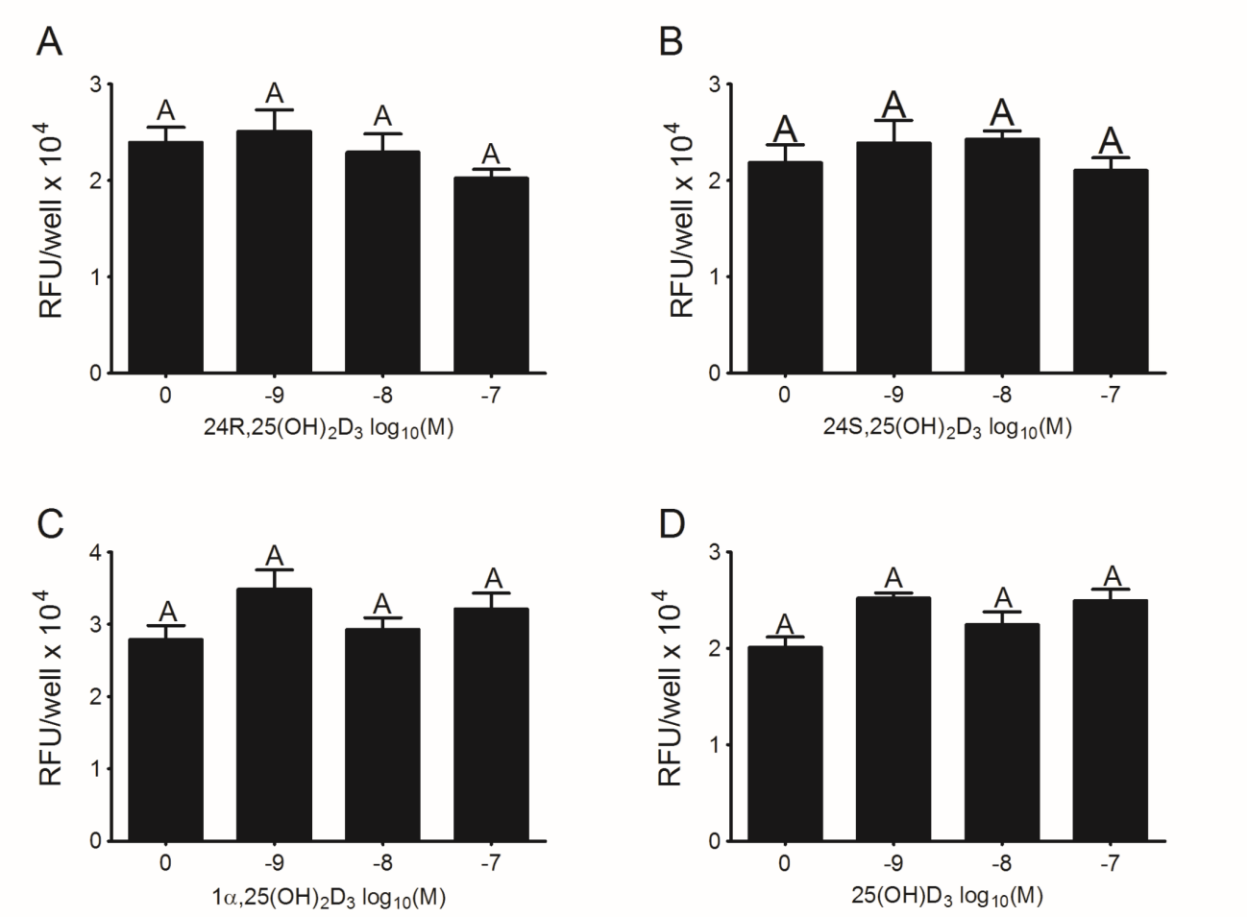

Figure 5.5 Treatment with vitamin D3 metabolites for 24 hours does not alter MCF7 cell proliferation.

[**A**] 24R,25(OH)$_2$D$_3$, [**B**] 24S,25(OH)$_2$D$_3$, [**C**] 1α,25(OH)$_2$D$_3$, and [**D**] 25(OH)D$_3$ did not induce DNA synthesis in MCF7 cells after 24 hours of treatment.

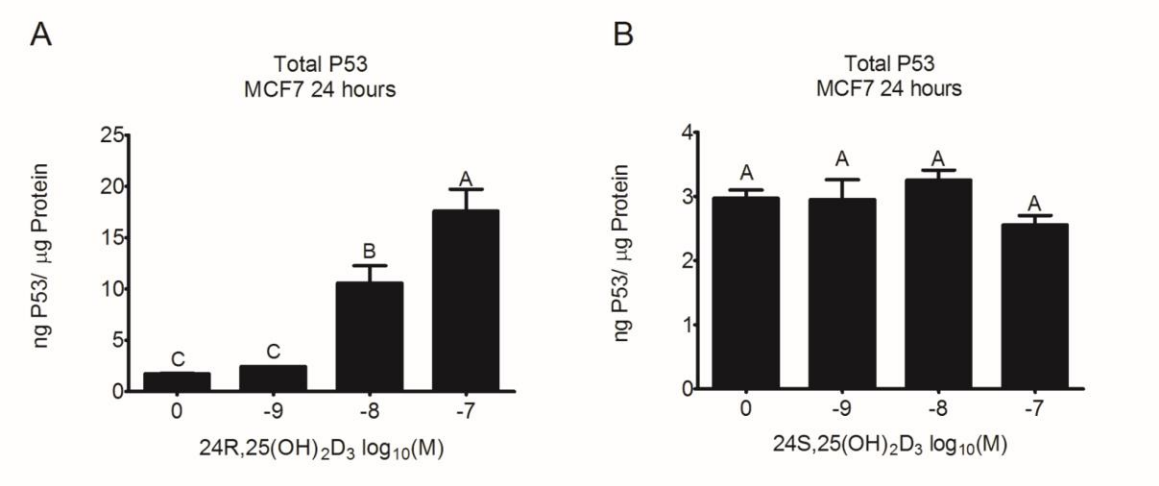

Figure 5.6 24R,25(OH)$_2$D$_3$ specifically induces apoptosis in MCF7 cells after 24 hours of treatment.

[**A**] 24R,25(OH)$_2$D$_3$ increased total p53 production after 24 hours of treatment in MCF7 cells but [**B**] 24S,25(OH)$_2$D$_3$ did not.

24R,25(OH)$_2$D$_3$ caused a dose-dependent increase in BAX to BCL2 expression ratios (BAX/BCL2), which was significant at 10^{-7}M (~4-fold) (Figure 5.4E). 24R,25(OH)$_2$D$_3$ had a bi-phasic effect on total p53 levels and TUNEL staining, with the 10^{-8}M dose producing the maximum increase in p53 levels (~1.5 fold) (Figure 5.4F)and TUNEL (~2 fold) (Figure 5.4G). The enantiomer 24S,25(OH)$_2$D$_3$ did not affect apoptosis in these cells, as measured by BAX/BCL2 expression (Figure 5.4H), total p53 levels (Figure 5.4I), and TUNEL staining (Figure 5.4J). In another ER+ cell line, T-47D cells, 10^{-7}M 24R,25(OH)$_2$D$_3$ increased total p53 content (Figure 5.7A), TUNEL staining (Figure 5.8A) , and proliferation (Figure 5.8B) after 15 minutes of treatment. In contrast, in a third breast cancer cell line, HCC38, which are ER-, all doses of 24R,25(OH)$_2$D$_3$ decreased total p53 content (Figure 5.7).

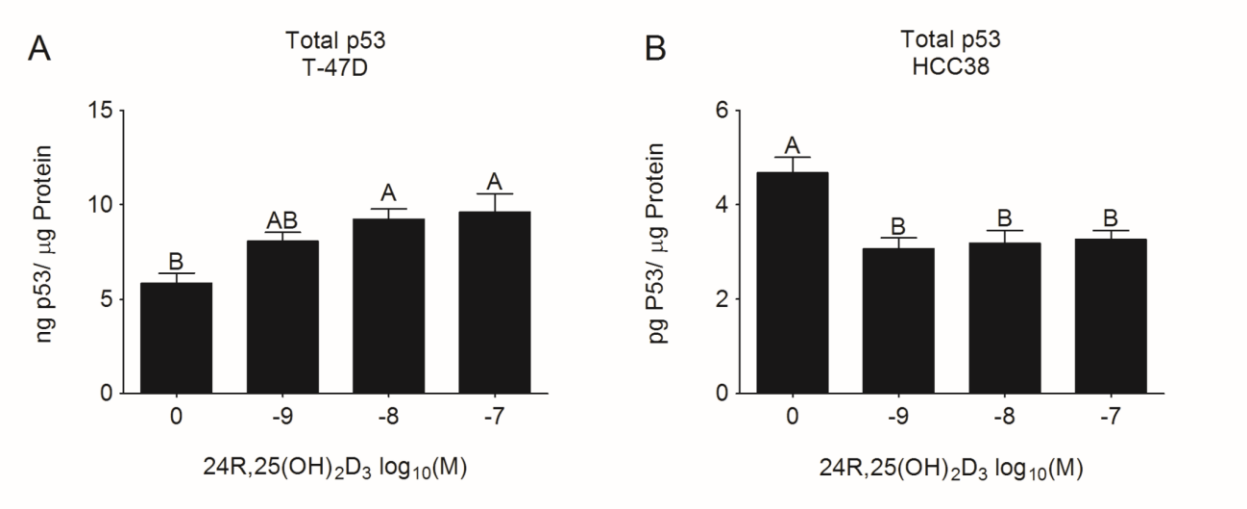

Figure 5.7 24R,25(OH)$_2$D$_3$ differentially changes apoptosis in other breast cancer cell lines.

Treatment of cultures for 15 minutes with 24R,25(OH)$_2$D$_3$ increased total p53 production in [**A**] T-47D cells and [**B**] HCC38 cells.

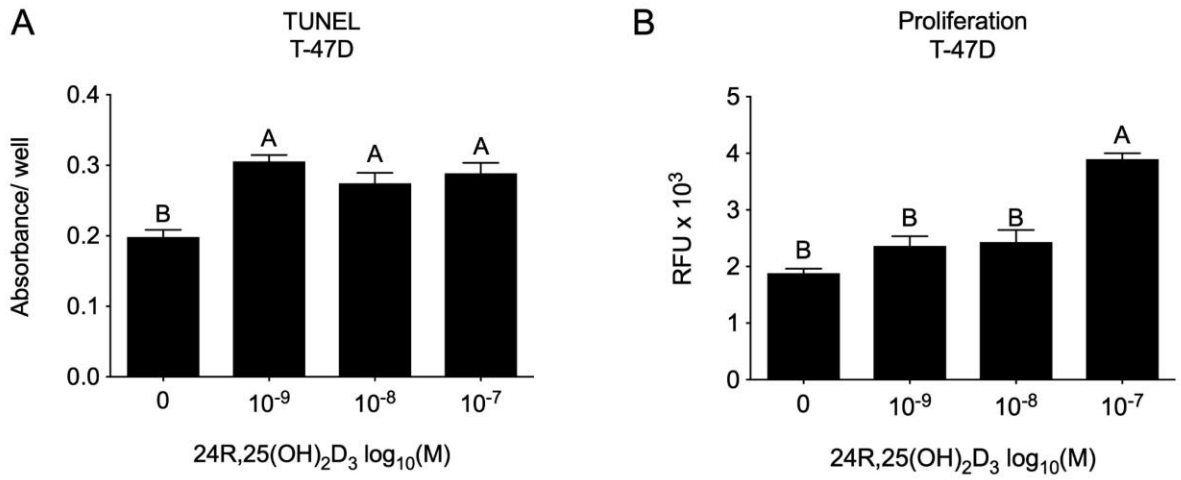

Figure 5.8 24R,25(OH)$_2$D$_3$ increases apoptosis and proliferation in T47D, an ER+ breast cancer cell line.

Treatment of cultures for 15 minutes with 24R,25(OH)$_2$D$_3$ increased [**A**] total TUNEL staining and [**B**] proliferation in T-47D cell monolayers.

24R,25(OH)$_2$D$_3$ decreased epithelial-to-mesenchymal transition, metastasis, and migration in MCF7 cells in vitro.

MCF7 monolayers were treated with dose-dependent 24R,25(OH)$_2$D$_3$ for 15 minutes, then harvested after 12 hours to assess gene expression. Treatment with 10^{-8}M and 10^{-7}M 24R,25(OH)$_2$D$_3$ significantly reduced expression of the mesenchymal-associated transcription factor SNAI1 compared to cells treated with vehicle (Figure 5.9A). ERBB2 and MMP1, which are associated with tumor aggression and matrix turnover respectively, were also reduced. 24R,25(OH)$_2$D$_3$ (10^{-7}M) caused a 50% reduction in ERBB2 expression (Figure 5.9B), and both 10^{-8}M and 10^{-7}M 24R,25(OH)$_2$D$_3$ reduced expression of MMP1 expression by more than 75% (Figure 5.9C).

24R,25(OH)$_2$D$_3$ had a biphasic effect on collagenase with the most significant reduction observed in cultures treated with 10^{-8}M (Figure 5.9D). 24R,25(OH)$_2$D$_3$ decreased cell migration in the scratch test assay; 10^{-7}M 24R,25(OH)$_2$D$_3$ increased wound size to 300% of its original area while both the vehicle control and the positive control (10^{-7}M 17β-estradiol) reduced wound size to 50% of original area (Figure 5.9E). 24R,25(OH)$_2$D$_3$ also decreased metastatic markers. 24R,25(OH)$_2$D$_3$ decreased CXCR4 to CXCL12 ratios (CXCR4/CXCL12) in a dose-dependent manner, with 10^{-7}M 24R,25(OH)$_2$D$_3$ decreasing CXCR4/CXCL12 expression in MCF7 cells 8-fold as compared to cells treated with vehicle (Figure 5.9F). 24R,25(OH)$_2$D$_3$ also increased OPG to receptor activator of RANKL ratios (OPG/RANKL) - which is contraindicative of osteoclast activity - in both gene expression and protein. 24R,25(OH)$_2$D$_3$ increased OPG/RANKL gene expression 5-fold at 10^{-7}M (Figure 5.9G), and both 10^{-8}M and 10^{-7}M 24R,25(OH)$_2$D$_3$ increased OPG/RANKL protein by 100% (Figure 5.9H).

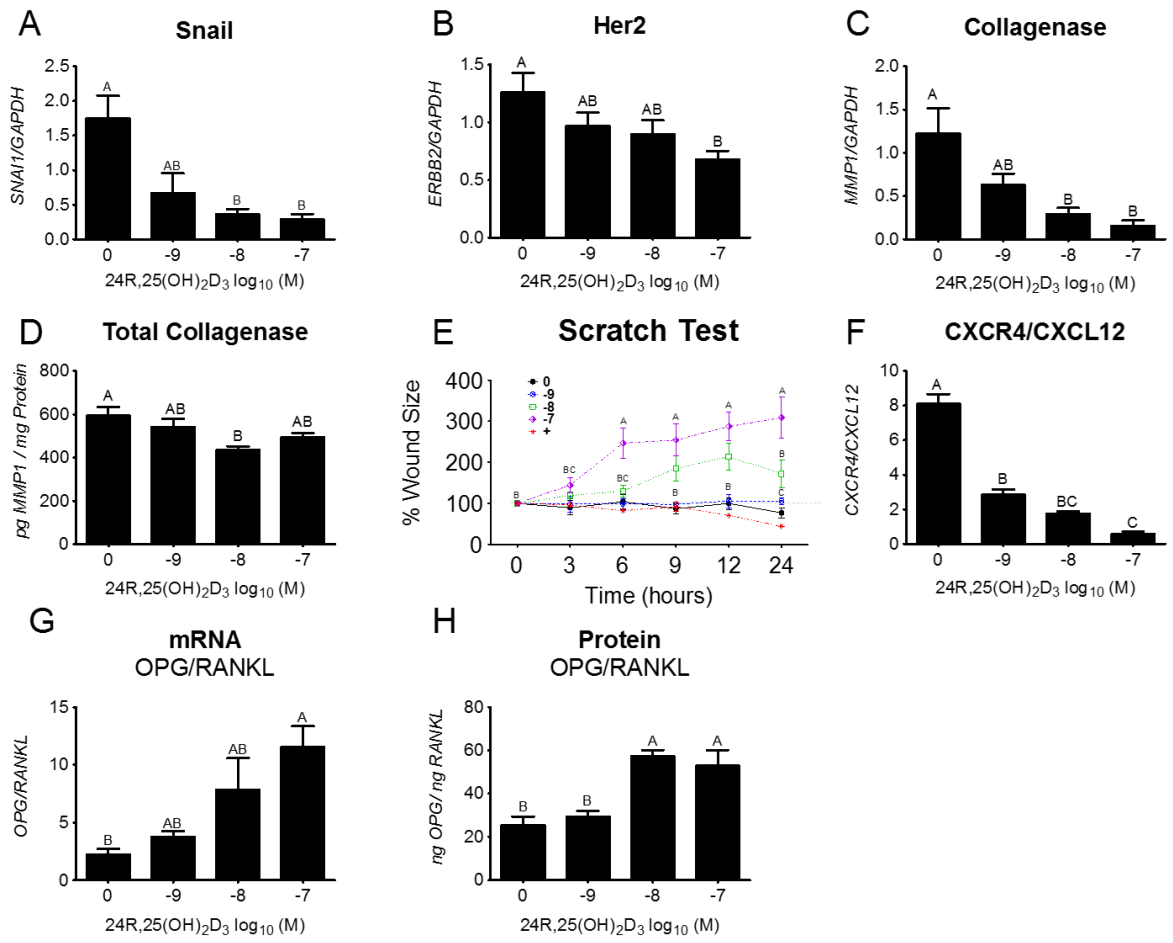

Figure 5.9 24R,25(OH)2D3 reduces epithelial-to-mesenchymal transition and migration in MCF7 cultures.

[**A**] 24R,25(OH)$_2$D$_3$ decreases the gene expression of snail [**B**], her2 [**C**], collagenase and [**D**] total collagenase protein. [**E**] 24R,25(OH)$_2$D$_3$ also inhibited migration in MCF7 monolayers and significantly increased wound size in a scratch test assay as compared to vehicle and E$_2$-treated cultures, and [**F**] decreased the gene expression ratio of migratory markers CXCR4/CXCL12. [**G**] 24R,25(OH)$_2$D$_3$ also inhibited bone resorption and distant metastasis marker OPG/RANKL as measured by gene expression and [**H**] protein. Groups that do not share a letter are statistically significant at α=0.05.

24R,25(OH)$_2$D$_3$ increased proliferation and apoptosis through a membrane-mediated, PLD-dependent pathway.

MCF7 cell monolayers were treated for 30 minutes with increasing concentrations of inhibitors of membrane-associated steroid hormone signaling mechanisms, then treated with high-dose 24R,25(OH)$_2$D$_3$ for 15 minutes. After 24 hours, proliferation and apoptosis markers were assessed. Inhibition of palmitoylation with 2-bromopalmitate blocked the stimulatory effect of 24R,25(OH)$_2$D$_3$ on DNA synthesis (Figure 5.10A), TUNEL staining (Figure 5.10I), and p53 production (Figure 5.10E), indicating that the 24R,25(OH)$_2$D$_3$ effect on both proliferation and apoptosis required docking of protein receptors to the membrane. Treatment of the cultures with wortmannin blocked the 24R,25(OH)$_2$D$_3$ dependent increase in DNA synthesis (Figure 5.10B) and p53 production (Figure 5.10F). The PLD inhibitor increased TUNEL staining in control cultures to levels comparable to 24R,25(OH)$_2$D$_3$ treated cultures (Figure 5.10J). Depletion of membrane cholesterol by methyl β-cyclodextrin blocked 24R,25(OH)$_2$D$_3$ stimulated increases in DNA synthesis (Figure 5.10C). At the higher concentration, it increased p53 levels in control cultures to levels seen in 24R,25(OH)$_2$D$_3$-treated cultures (Figure 5.10G); all methyl-β cyclodextrin treated cultures had TUNEL staining comparable to the 24R,25(OH)$_2$D$_3$-treated cells (Figure 5.10K). Antibodies blocking ERα36 prevented 24R,25(OH)$_2$D$_3$-stimulated proliferation but the treatment of the culture with 10^{-7}M ICI-182780, a cytosolic and nuclear ERα inhibitor, had no effect (Figure 5.10D). Both anti-ERα36 and ICI-182780 blocked the stimulatory effect of 24R,25(OH)$_2$D$_3$ on p53 (Figure 5.10H) and TUNEL (Figure 5.10L).

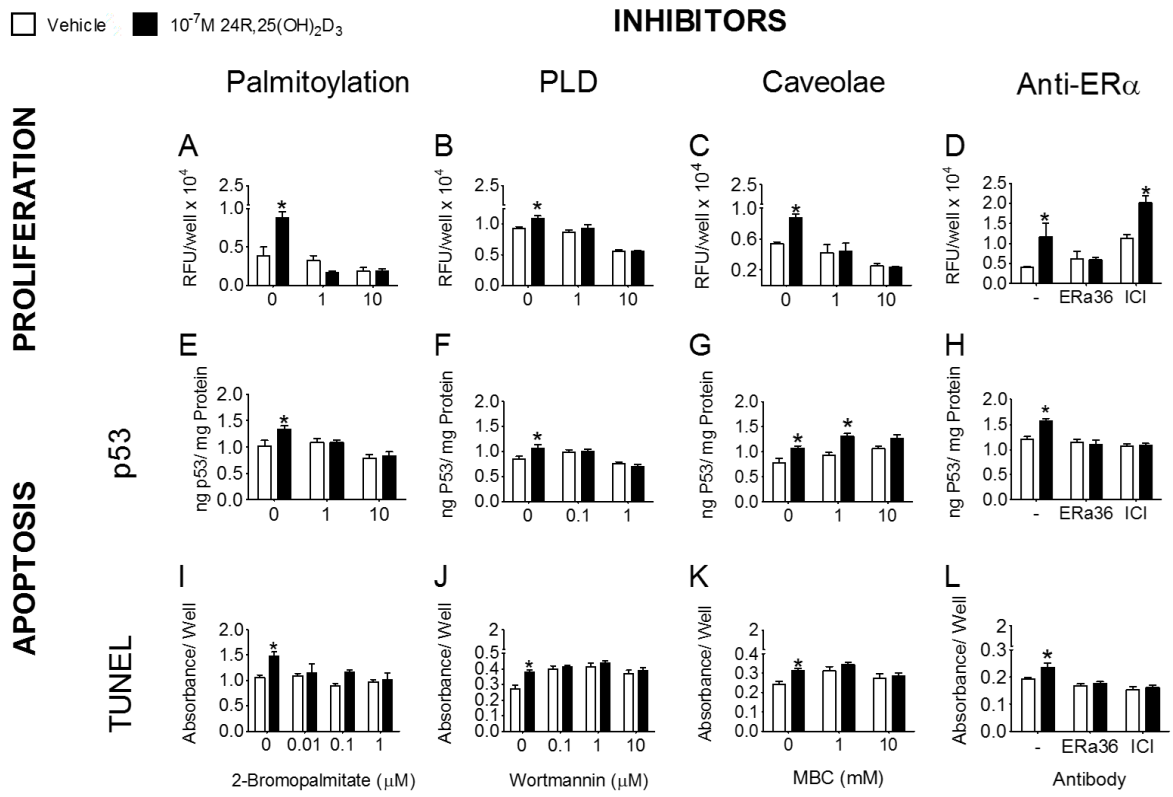

Figure 5.10 24R,25(OH)2D3 induces proliferation and apoptosis in MCF7 cells through a membrane-mediated mechanism.

Inhibitors against palmitoylation ([**A**], [**E**], [**I**], 2-bromopalmitate), phospholipase D ([**B**], [**F**], [**J**], wortmannin), caveolae ([**C**], [**G**], [**K**], methyl β-cyclodextrin), membrane estrogen receptor α 36 ([**D**], [**H**], [**L**], anti-ERα36 antibody) and cytosolic and nuclear estrogen receptor α ([**D**], [**H**], [**L**]) (ICI-182780) were used to gain insight into the mechanism by which 24R,25(OH)$_2$D$_3$ acts on apoptosis and proliferation in MCF7 cells. Proliferation was measured by [**A-D**] DNA synthesis assay and apoptosis was measured by [**E-H**] total p53 ELISA and [**I-L**] TUNEL staining. All doses of 2-bromopalmitate, which inhibits palmitoylation, inhibited a 24R,25(OH)$_2$D$_3$ induced increase in [**A**] proliferation, [**E**] p53 content, and [**I**] TUNEL staining. Wortmannin, a non-specific phospholipase-D inhibitor,

(continued from page 135) [**B**] inhibited a 24R,25(OH)$_2$D$_3$ induced increase in proliferation, [**F**] p53 content, and [**J**] TUNEL staining in a similar manner. Methyl β-cyclodextrin, which depletes the cell membrane of cholesterol to inhibit caveolae function, [**C**] inhibited a 24R,25(OH)$_2$D$_3$ induced increase in proliferation at 1 and 10mM, [**G**] p53 content at 10mM, and [**K**] TUNEL staining at 0.1-10mM. The anti-ERα36 antibody to block membrane-ERα isoforms also [**D**] inhibited a 24R,25(OH)$_2$D$_3$ increase in proliferation, [**H**] p53 content, and [**L**] TUNEL staining. [**D**, **H**, and **L**] To confirm membrane ER involvement, ICI-182780 was included as a control in anti-ERα36 experiments. However, [**D**] while ICI-182780 did not inhibit 24R,25(OH)$_2$D$_3$-induced proliferation, it did inhibit apoptosis as measured by both [**H**] TUNEL staining and [**L**] total p53 content. All graphs were analyzed by two-way ANOVA at α=0.05 with Bonferroni's correction.

Discussion

Vitamin D has been shown to have a significant anti-tumorigenic effect against breast cancer in epidemiological, pre-clinical, cellular and molecular studies [111,280–282]. The expanding body of evidence using new synthetic analogs of vitamin D has demonstrated the possibility of developing compounds that can regulate cellular processes independently from their calcemic effects, enabling the expansion of the therapeutic window of vitamin D-related compounds [280].

We have identified an alternative active endogenous metabolite of vitamin D, 24R,25(OH)$_2$D$_3$. 24R,25(OH)$_2$D$_3$ has a marked inhibitory action on bone resorption [283,284], reducing calcium release and thus not causing hypercalcemia [285]. In the present study, we have established its anti-tumor and pro-apoptotic effects in MCF7 breast cancer cells.

Our results clearly demonstrate an anti-cancer effect indicated by reduced tumor growth, improved prognosis, and longer survival rates. Treatment with 24R,25(OH)$_2$D$_3$ significantly reduced tumor volumes in mice implanted with MCF7 breast cancer xenografts. 17β-estradiol supplementation was required to initiate MCF7 tumor growth in these mice, but after 4 weeks of 17β-estradiol supplementation, tumors continued growing without additional supplementation. Supplementation with 24R,25(OH)$_2$D$_3$ caused a dose-dependent decrease in the rate of tumor growth, with improvement in survival and final tumor volume. Furthermore, increasing concentrations of 24R,25(OH)$_2$D$_3$ correlated with a significant reduction in total metastatic burden, loco-regional and distant metastatic incidence. These effects resemble the correlation described in the literature between increasing serum vitamin D$_3$ and improved survival in breast cancer [251,286], and support the hypothesis that 24R,25(OH)$_2$D$_3$ does, in fact, possess anti-tumorigenic properties.

These findings are further supported by the observation that 24R,25(OH)$_2$D$_3$ inhibited expression of metastatic markers, including expression of Snail, Her2, and collagenase, as well as the ratio of CXCR4 to CXCL12. Migration was inhibited in a dose-dependent manner when testing wound closure using the scratch test, and the ratio of OPG to RANKL, both in terms of expression and protein production, was stimulated by high-dose 24R,25(OH)$_2$D$_3$. Total collagenase was not affected to the same extent as MMP1 expression, probably due to the experimental design, where mRNA was assessed at 12 hours and enzyme content was assessed at 24 hours.

In contrast with our *in vivo* observations, and the evidence shown above that 24R,25(OH)$_2$D$_3$ had an anti-tumor effect, 24R,25(OH)$_2$D$_3$ enhanced proliferation of MCF7

cells *in vitro*. The effect of 24R,25(OH)$_2$D$_3$ on proliferation of MCF7 cells was not stereospecific as a similar response was seen with 24S,25(OH)$_2$D$_3$. Although the precursor 25(OH)D$_3$ had the same stimulatory effect on proliferation as 24R,25(OH)$_2$D$_3$, 1α,25(OH)$_2$D$_3$ had no effect, indicating that the site of the second hydroxyl on either C-24 or C-1 was the important differentiator, but whether the hydroxyl on C-24 was in a R or S configuration did not matter. It is possible that the addition of the C-1 hydroxyl caused a stereospecific inhibition in the binding of the molecular to an as-yet-unidentified receptor. The study did not take into account, however, that vitamin D3 metabolism occurs in a cyclic manner *in vivo*, both locally in cells that possess appropriate hydroxylases, and in the kidney [13,287]. MCF7 cells normally express 1-hydroxylase, but do not typically express 24-hydroxylase unless stimulated by 1,25(OH)$_2$D$_3$ [288]. It is possible that either local levels or systemic levels of 1α,25(OH)$_2$D$_3$ may have been sufficient to reduce or prevent the proliferative effect of 24R,25(OH)$_2$D$_3$, particularly in response to indirect upregulation of Cyp27B1 and production of 1,25(OH)$_2$D$_3$ due to the 24R,25(OH)$_2$D$_3$ treatment. None of these vitamin D$_3$ metabolites had any effect on cell proliferation after 24 hours of treatment *in vitro*, which could also indicate another undiscovered pathway that counteracts the initial pro-proliferative pathway stimulated by the 15 minute treatment.

Our in vitro studies were performed using MCF7 cells in order to have a direct correlation with our in vivo observations. In order to determine whether our results using this well-studied ER+ breast cancer cell line were also found using other breast cancer cell lines, we examined the responses of ER+ T-47D cells and ER- HCC38 cells to 24R,25(OH)$_2$D$_3$. At least with respect to p53 abundance, the effect of 24R,25(OH)$_2$D$_3$ was not consistent between MCF7, T-47D, and HCC38 cells, suggesting that the response to

this secosteroid may be cell-type dependent. 24R,25(OH)$_2$D$_3$ increased p53 content in both MCF7 and T-47D cell lines, which express similar levels of ERα66 and its isoforms [43]. HCC38, on the other hand, expresses high levels of ERα36 and no ERα66 [27]. It is possible that each cell line's ERα profile has a modulating effect on the tumorigenicity of 24R,25(OH)$_2$D$_3$. This could provide an explanation for conflicting reports on the tumorigenicity of 24R,25(OH)$_2$D$_3$ and 24-hydroxylase. In ERα+ Lewis lung carcinoma cells [72], 24R,25(OH)$_2$D$_3$ was reported to have an anti-tumorigenic effect [260], but in ERα-ERβ-expressing HT29 colorectal cancer cells [11], CYP24A1 overexpression enhanced tumor volume, an effect that was further compounded by a diet high in soy-based phytoestrogens [98]. Further studies are ongoing to investigate the universality of 24R,25(OH)$_2$D$_3$'s therapeutic effect against breast cancer in other cell types. However, it is clear from our data that 24R,25(OH)$_2$D$_3$ has a cell survival modulating effect on breast cancer.

Our results using MCF7 cells indicate that the stimulatory effects of 24R,25(OH)$_2$D$_3$ and 24S,25(OH)$_2$D$_3$ involved membrane-associated signaling pathways. Pretreatment with 2-bromopalmitate, which blocks palmitoylation of membrane receptors, and inhibition of PLD activity as well as destruction of caveolae structural integrity with β-cyclodextrin abolished their effects. The stimulatory effect of both 24,25(OH)$_2$D$_3$ enantiomers on DNA synthesis was only evident in cultures treated for 15 minutes, suggesting a rapid signaling mechanism was involved, although a specific membrane receptor for either the R or S form of the secosteroid might not be required. The effect on DNA synthesis was not evident in cultures treated for 24 hours, raising the possibility that the augmentation of

proliferation was not specific to either enantiomer and might reflect a crosstalk with other membrane or nuclear signaling pathways, as seen extensively in steroid hormones [34,68].

Treatment with 24R,25(OH)$_2$D$_3$ induced apoptosis in MCF7 cell monolayers as evidenced by elevated levels of Bax/Bcl2 gene expression, total p53 production, and DNA fragmentation (as measured by TUNEL staining). This effect was stereo-specific, as the enantiomer 24S,25(OH)$_2$D$_3$ did not alter Bax/Bcl2 expression, p53 content, or TUNEL staining after treatment for either 15 minutes or 24 hours. The mechanism by which 24R,25(OH)$_2$D$_3$ induced apoptosis is not yet known, although our findings indicate that a membrane-mediated pathway was involved. The 24R,25(OH)$_2$D$_3$-dependent increase in p53 production and TUNEL staining required palmitoylation, PLD activation, and intact caveolae. It should be noted that although the effect of 24R,25(OH)$_2$D$_3$ on apoptosis was stereo-specific and the effect on proliferation was not specific to the 'R' isoform, inhibitor studies suggest that both effects use similar pathways.

Treatment with 24R,25(OH)$_2$D$_3$ not only retarded breast cancer tumor growth, but also lead to the suppression of the primary tumor from metastasizing to other secondary sites. This may be due to an inhibitory effect on the epithelial-to-mesenchymal transition associated with metastasis as previously observed in MCF7 cells [194]. 24R,25(OH)$_2$D$_3$ reduced the expression of several epithelial-mesenchymal transition and tumor aggression-associated factors such as Snail1, which leads to a down-regulation of cell-cell interaction proteins such as cadherins to assist the cell's transition from a static epithelial cell to a migratory mesenchymal cell [289,290]. 24R,25(OH)$_2$D$_3$ also suppressed migration-associated markers, such as the ratio of gene expression of metastatic factor CXC chemokine receptor type 4 (CXCR4) to its ligand CXC ligand 12 [291–294], and the

migration of cells *in vitro*. Matrix metalloproteinases (MMPs), a family of zinc-dependent endopeptidases, which are involved in the degradation of extracellular matrix [295], have also been associated with cancer invasion, metastasis and angiogenesis [296]. 24R,25(OH)$_2$D$_3$ caused a reduction in MMP1 expression. Together with its effect in reducing chemotaxis, as evidenced by reducing the rate of wound closure in a two-dimensional culture, our results indicate that 24R,25(OH)$_2$D$_3$ mediates a reduction in breast cancer cell invasion.

Overexpression of Her2, which is regarded as a growth factor receptor oncogene [297], plays an essential role in the development and progression of certain aggressive types of breast cancer. Expression of Her2 has become an important biomarker and target of therapy for approximately 30% of breast cancer patients [298], as its downregulation is correlated with growth inhibition of breast cancer cells [299]. Studies with antibodies against Her2 demonstrated improved survival and response rates to chemotherapy [300]. 24R,25(OH)$_2$D$_3$ downregulated expression of Her2, supporting its potential as a negative regulator of tumor growth, by inhibiting the ability of breast cancer cells to detach from the primary tumor and migrate to distant sites of the body. This anti-metastatic effect was further observed *in vivo*, in the reduction of loco-regional and distant metastasis observed in animals treated with 24R,25(OH)$_2$D$_3$. Thus, the reduction of migratory factors observed with 24R,25(OH)$_2$D$_3$ treatment suggests that it confers a protective effect opposing the growth of breast cancer cells.

The pro-apoptotic effect of 24R,25(OH)$_2$D$_3$ was stereo-specific; 24S,25(OH)$_2$D$_3$ failed to elicit a response from the cells. This effect was rapid, with 15 minutes of 24R,25(OH)$_2$D$_3$ treatment inducing the pro-apoptotic response in cultures harvested 12

to 24 hours later. The effect of 24R,25(OH)$_2$D$_3$ on proliferation was similarly rapid, although it was not stereo-specific. This prompted us to determine the role of the membrane in the 24R,25(OH)$_2$D$_3$ pro-apoptotic response, as membrane-associated actions of 24R,25(OH)$_2$D$_3$ have been shown to affect apoptosis and DNA synthesis in other cell types [17,18,93,105,301]. Pretreatment with methyl β-cyclodextrin, which depletes the membranes of cholesterol and thereby disrupts the caveolae [169], abolished the pro-apoptotic effect, indicating the importance of the specialized membrane compartment for the 24R,25(OH)$_2$D$_3$-dependent signaling pathway in MCF7 breast cancer cells.

24R,25(OH)$_2$D$_3$ is a steroid hormone, and like 1□,25(OH)$_2$D$_3$ and ERα, acts by a set of membrane-associated mechanisms to exert its effect. Steroid hormone receptors are trafficked to the plasma membrane to serve as transmembrane receptors via a uniform mechanism involving palmitoylation [35], the attachment of palmitic acid to an internal cysteine residue, which promotes the association of the receptor with caveolin-1, a transporter protein, to caveolae rafts in the plasma membrane [49]. Palmitoylation plays a role in signaling through the membrane-associated ERα [78,302]. The canonical vitamin D receptor (VDR), which binds 1α,25(OH)$_2$D$_3$, can act through rapid membrane associated signaling pathways [39,254]. Our results show that the apoptotic effects of 24R,25(OH)$_2$D$_3$ require palmitoylation, as they were blocked by 2-bromopalmitate, which is an inhibitor of palmitoylacetyl-transferase and prevents palmitoylation of steroid hormone receptors [269].

Previous studies in our lab using chondrocytes show that 24R,25(OH)$_2$D$_3$ increases proliferation (DNA synthesis) and differentiation while inhibiting apoptosis [303]. These actions involved PLD-mediated increases in PKC, as well as through inhibition of the phospholipase A$_2$ (PLA$_2$) pathway [15,16,255]. It has been suggested that the point of

regulation in the mechanism of 24R,25(OH)$_2$D$_3$ stimulated PKC is PLA$_2$, which controls the availability of substrate for Cox-1 [17]. Further, the activation of PLD resulted in increased production of lysophosphatidic acid (LPA) and consequently LPA-mediated proliferation, maturation, inhibition of phosphate-induced apoptosis, and reduction of p53 [18,92,93]. Both genomic and non-genomic signaling pathways have been implicated in the actions of 24R,25(OH)$_2$D$_3$ and it has been suggested that it exerts its effects via more than one signaling pathway. These pathways may be interrelated via the modulation of PLA$_2$ [17]. In our study, both the pro-apoptotic and proliferative effects incurred by 24R,25(OH)$_2$D$_3$ in MCF7 breast cancer cells were abolished by pretreatment with wortmannin, a non-specific inhibitor of PLD [15,142]. Thus, a PLD mediated signaling pathway is implicated in both 24R,25(OH)$_2$D$_3$'s pro-apoptotic and proliferative effects in breast cancer cells.

The full impact of 24R,25(OH)$_2$D$_3$ is the result of the convergence and crosstalk of the different signaling pathways, which at times are antagonistic, and its interaction with other steroid hormones such as other vitamin D metabolites [18] or sex hormones. However, it is important to note that wortmannin is also a weak inhibitor of PKC and PI3K, which have both been shown to be involved in rapid signaling by steroid hormones and resultant regulation of proliferation and apoptosis [31,68]. Further investigation is necessary to determine whether this effect is cell type specific or if the PLD, PLA$_2$ mechanism shown in chondrocytes universally governs 24R,25(OH)$_2$D$_3$'s apoptotic effects. 24R,25(OH)$_2$D$_3$ function is variable and complex and necessitates further research to clarify the signaling pathways involved and to clarify the effects of 24R,25(OH)$_2$D$_3$ on breast cancer cells.

Finally, we assessed the relationship between the effect of 24R,25(OH)$_2$D$_3$ and ERα, the classical nuclear receptor for the sex steroid 17β-estradiol (E$_2$). A known correlation between 1α,25(OH)$_2$D$_3$ and E$_2$ exists. 1α,25(OH)$_2$D$_3$ downregulates E$_2$ receptor abundance by binding to VDR and activating negative response elements in the ESR1 promoter [120]; suppresses E$_2$ actions in MCF7 breast cancer cells [120,304;] and restores antiestrogen responsiveness [129]. Our findings stress a striking resemblance in the signaling pathways of the two steroid hormones despite having antagonist actions in breast cancer cells. E$_2$ signaling is pivotal in the initiation and progression of breast cancer; it functions as a potent mitogen inducing the activation of c-Myc and an array of cyclin genes promoting cell cycle progression from G1 to S phase [305]. The novel membrane receptor ERα36 is gaining interest as a key player in breast cancer, especially in conferring aggressive features and resistance to hormonal treatment.

ERα36 mediates the anti-apoptotic effect of E$_2$ by activating PLD at the membrane leading to activation of LPA signaling and PI3K, which in turn leads to attenuation of the caspase cascade that promotes apoptosis [1]. E$_2$-ERα36 signaling has also been implicated in the activation of other rapid pathways such as ERK-MAPK, PI3K-Akt, and PKC-ERK, and may have downstream effects on the employment of IGF-IR, EGFR, HER2 [306], resulting in a decrease in apoptosis and an increase in proliferation and metastatic potential in a variety of cancer cells, including breast cancer cells [68,109]. These pathways have been reported to stimulate tumorigenicity in both ER positive and negative breast cancer tumors [27,55]. These rapid signaling mechanisms mediated by ERα36 are insensitive to anti-estrogens and have even been shown to employ agonist activities in response to anti-estrogens, such as tamoxifen and ICI-182,780, which are both known

inhibitors of the classical ERα66 [129]. Both antibodies that block the ER□36 mediated effect of E_2 and ICI 182,780 (which blocks cytosolic and nuclear ERs) abolished the pro-apoptotic effect of 24R,25(OH)$_2$D$_3$. However, only the antibody to ERα36 blocked the proliferative effect. This implies that 24R,25(OH)$_2$D$_3$ and both the canonical and membrane-associated signaling pathways of E_2 share a common downstream pathway, the exact mechanism of which remains to be revealed (Figure 5.11).

Upon activating a signaling cascade at the membrane, 24R,25(OH)$_2$D$_3$ stimulates the secondary messenger PLD. PLD stimulates the LPAR1/3 receptor and downstream signaling stimulates PI3K, upregulates Bax, and downregulates Bcl2 expression to increase p53 production and induce apoptosis in MCF7 cells. A similar mechanism is responsible for the proliferative actions of 24R,25(OH)$_2$D$_3$, which is regulated by a membrane-mediated receptor in the caveolae niche via a PLD-dependent mechanism. 24R,25(OH)$_2$D$_3$ also decreases invasion and metastatic markers through an as yet unidentified mechanism.

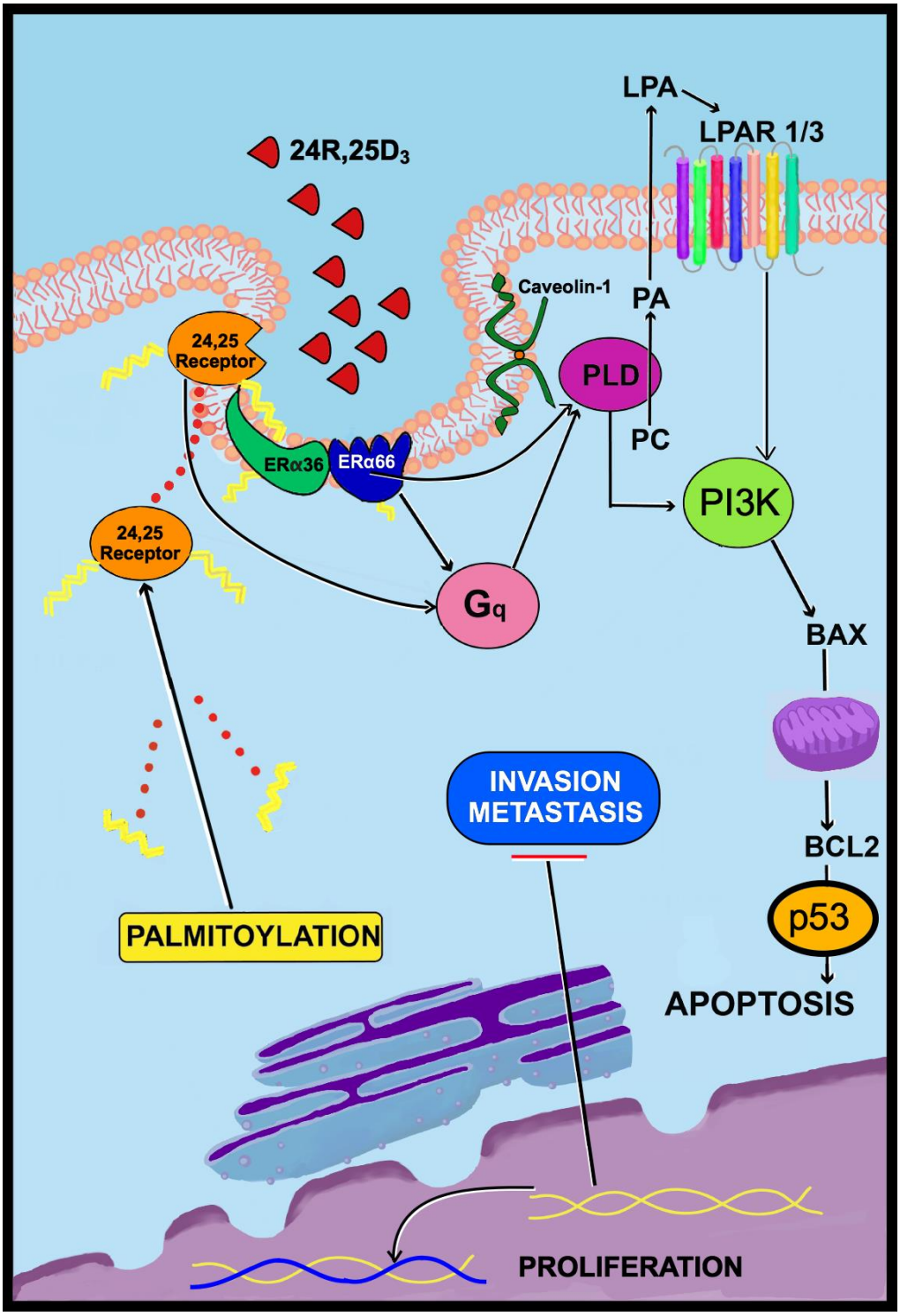

Figure 5.11 24R,25(OH)2D3 induces apoptosis and proliferation through a membrane-mediated caveolae-dependent mechanism involving one or more as yet undescribed palmitoylated nuclear receptors.

Chapter 6.

24R,25-dihydroxyvitamin D$_3$ regulates breast cancer progression in an estrogen receptor α 66-dependent manner.

[Chapter 6 is in preparation as: Verma A, Cohen DJ, Jacobs TW, Boyan BD, Schwartz Z. Loss of estrogen receptors is associated with increased tumor aggression in laryngeal squamous cell carcinoma. Mol. Can. Res. In preparation]

Introduction

Vitamin D$_3$ has been of interest as an anti-tumorigenic agent for decades. Interest in vitamin D$_3$ first peaked when epidemiologists noticed that the incidence of certain cancers, including breast cancer, inversely correlated with daily sun exposure [307,308]. Vitamin D$_3$ is an essential pro-hormone that is synthesized in response to UVB radiation from sunlight. Retrospective clinical studies have shown that reduced exposure to UVB correlates with low levels of serum vitamin D$_3$, and low serum vitamin D$_3$ correlates with an increased risk for breast cancer [113]. Similarly, epidemiological studies have shown vitamin D$_3$ supplementation is associated with a reduced risk of breast cancer recurrence [8]. However, recent large-scale double-blind clinical trials have concluded that there is no connection between vitamin D$_3$ supplementation and breast cancer incidence in the general population [6,7].

There are two possible reasons for this discrepancy. One reason may be that most clinical studies that examine the efficacy of vitamin D$_3$ treat breast cancer as a homogenous disease with uniform presentation. In actuality, breast cancer is a heterogeneous disease that can present with several distinct molecular subtypes.

Detailed clinical and retrospective analyses have shown that low serum vitamin D$_3$ is associated with an increased risk of developing estrogen receptor positive (ER+) cancer, but not estrogen receptor negative (ER-) cancer [309]. Furthermore, vitamin D supplementation is associated with a reduced risk of developing new or recurrent tumors in patients with estrogen receptor positive (ER+) cancer, but not patients with estrogen receptor negative (ER-) cancer) [8,310].

Another reason may be that most studies that examine the anti-cancer properties of vitamin D$_3$ limit their investigations by correlating cancer incidence with oral vitamin D$_3$ intake or serum 25-hydroxyvitamin D$_3$ (25(OH)D$_3$) [112,240,311]. Serum 25(OH)$_2$D$_3$ is an incomplete picture of the active vitamin D metabolome. Once ingested, vitamin D3 is metabolized in the liver into 25(OH)D$_3$ [246]. From there it circulates in the blood as serum 25(OH)D$_3$ until it reaches the kidney, where it is hydroxylated into a number of active vitamin D$_3$ metabolites, including the well-described metabolite 1α,25-dihydroxyvitamin D$_3$ (1α,25(OH)$_2$D$_3$) and the understudied 24R,25-dihydroxyvitamin D$_3$ (24R,25(OH)$_2$D$_3$) [13]. 1α,25(OH)$_2$D$_3$ is partially responsible for maintaining calcium homeostasis and bone mineralization and has been shown to have some anti-cancer properties. However, it has a narrow therapeutic window and can induce hypercalcemia. 24R,25(OH)$_2$D$_3$ is a less studied, less calcemic vitamin D$_3$ metabolite. Previous studies in our lab and others have shown that 24R,25(OH)$_2$D$_3$ is responsible for maintaining cartilage differentiation and may regulate the cell cycle in chondrocytes [23,93,312].

24,25(OH)$_2$D$_3$ has been shown to have anti-tumorigenic properties in certain cancers [260], including lung and stomach carcinomas [260,262]. However, an increase in 24-hydroxylase, the enzyme that increases 24R,25(OH)$_2$D$_3$ *in vivo*, has been associated with

increased tumorigenicity in models of colorectal carcinoma [98]. Recently, our lab has shown that 24R,25(OH)$_2$D$_3$ is active in breast cancer cell lines and that 100 ng of 24R,25(OH)$_2$D$_3$ given three times a week is non-calcemic and anti-tumorigenic in a model of ER+ breast cancer [313]. However, while 24R,25(OH)$_2$D$_3$ was anti-tumorigenic in ER+ breast cancer cell lines, it was pro-tumorigenic in HCC38, an ER- breast cancer cell line [313]. *In vitro* studies revealed that the actions of 24R,25(OH)$_2$D$_3$ are modulated by a rapid, membrane-associated, mechanism in breast cancer [313].

Breast cancer cells that are 'ER+' express the classical estrogen receptor α (ERα) isoform ERα66, while 'ER-' cells do not express ERα66. Both cell types may express other ERα isoforms, including the membrane isoform ERα36 [27,55]. HCC38 does not express ERα66, however, it expresses ERα36 [1]. ERα36 mediates rapid signaling by 17β-estradiol (E$_2$) in cancer cells [55]. We hypothesized that the pro-apoptotic effects of 24R,25(OH)$_2$D$_3$ might be regulated in part by the canonical receptor, ERα66, rather than the rapid signaling receptor, ERα36, thus implying a role for the canonical receptor ERα66 in the rapid signaling of 24R,25(OH)$_2$D$_3$.

Materials & Methods

Cell Lines

MCF7 and HCC38 breast cancer cell lines and C2C12, a muscle cell line, were purchased from ATCC (Manassas, VA). Experiments were conducted within 6 months of cell purchase. Cells were maintained in media and passaged following ATCC guidelines as previously described[1].

Caveolin-1 knockdown.

Stable knockdown of Cav-1 was achieved by transducing wild-type HCC38 cells with CAV-1 shRNA lentiviral transduction particles packaged in Mission® shRNA lentiviral particles as previously described[314]. Four shRNAs targeted to the CAV1 gene (Millipore-Sigma, Burlington, MA, cat#SHCLNV-NM_0001753, clone TRCN0000000310, clone TRCN00000000508, clone TRCN 00000008000 and clone TRCN0000008002) were cloned into a cassette containing a puromycin-resistance gene and packaged as lentiviral particles. Empty control cells were created with MISSION® pLKO.1 puro Empty Vector Control Transduction Particles (Sigma MISSION® cat#SHC001V). HCC38 cells were transduced with shRNA-containing lentiviral particles according to manufacturer's protocol and a pure population of cells was enriched by using 50μg/mL as a selection agent. CAV1-knocked down-HCC38 cells were tested for effective Caveolin-1 knockdown, and the two clones with the best knockdown, clone TRCN0000000508 and clone TRCN0000008002, were chosen for subsequent experiments and labeled "clone 1" and "clone 2" respectively. Caveolin-1 knockdown was confirmed with western blot as previously described [169]. Antibodies for all western blots are given in Table 6.1. All transduced-HCC38 cells were maintained in full media supplemented with 50μg/mL puromycin.

ERα isoform overexpression in cell lines

ERα isoforms were overexpressed in HCC38 and C2C12 cells with a commercially available ESR1, GFP-tagged open-reading-frame (ORF) plasmid (Origene, cat# RG213277) as previously described [315,316]. Empty vector controls were created with open

reading frame (ORF) control particles (Origene, cat# PS100093) according to Origene protocols.

HCC38 monolayer cultures were transiently transduced for 48 hours with the ESR1 or control particles according to manufacturer's instructions. In brief, a solution of 5μg of plasmid per 1mL of opti-mem serum-free media per 6μL turbofectin 8.0 (Origene, cat# TF81001) was added drop-wise to T25 (1mL plasmid solution/well), 24W (100μL/well) or 48W (50μL/well) monolayer cultures. Transfection was confirmed 48 hours after particle addition by visualizing GFP expression in wells with a Zeiss SteroDiscovery.V12 fluorescence microscope with an AxioCam MRm digital camera. In a representative set of cultures, 48 hours after transient transfection a T25 culture of cells was harvested with radioimmunoprecipitation assay (RIPA) buffer and ERα66 overexpression was confirmed by western blot as described previously[1].

C2C12, a mesenchymal cell line derived from myoblasts, were stably transfected with ESR1 or empty control cells using the ORF particles described above. 48 hours after transfection, cells were selected with full media supplemented with 1mg/mL G418 as previously described[313]. ESR1 overexpression was confirmed by western blot as described previously[1].

ERα66 silencing in MCF7 cell lines

ERα66 was stably knocked down in MCF7 cells with a commercially available short hairpin ESR1 lentiviral vector from Sigma MISSION® (cat# TRCN0000003301). Scrambled control cells were created with MISSION® TurboGFP® Control Transduction Particles (Sigma MISSION® cat#SHC016V). Both vectors included a coding region for a puromycin resistance gene. Cells were transduced according to manufacturer's protocol

and a pure cell population was enriched using 50µg/mL puromycin selection media. Cells were maintained in 50µg/mL puromycin full media and ERα66 silencing was confirmed via western blot as previously described [169].

Table 6.1 Antibodies used in western blots.

Protein	Source	Catalog #
Caveolin-1	Abcam	Ab2910
ERα66	Chi Scientific	8-80119
ERα36	Chi Scientific	8-80119
GAPDH	Millipore-Sigma	MAB374

In Vivo Studies

All *in vivo* experiments were done on female 6-8 week old Nod-Scid-gamma IL2γ (NSG) mice obtained from the Virginia Commonwealth University (VCU) Cancer Mouse Models Core Laboratory at Massey Cancer Center (Richmond, VA). All animal experiments were approved by VCU's Institutional Animal Care and Use Committee. Animals were monitored for signs of hypercalcemia and other health and behavioral changes throughout the course of the study.

Mammary fat pad xenograft model.

Two mammary fat pad xenograft models were tested for this study. The first study was done with un-operated mice. A second study was conducted at a later date with ovariectomized mice. 5-6 week old female NOD.Cg-Prkdc^{scid}Il2rgt^{m1Wjl}/SzJ (NSG) mice were ovariectomized as previously described [167]. Two weeks after ovariectomy, tumors were initiated as previously described[313]. In brief, intact or ovariectomized NSG mice were injected twice weekly intraperitoneally with 2.5mg/kg of 17β-estradiol (n=6) (Millipore-Sigma cat#E8875) or vehicle (n=6) (2% ethanol:1X distilled phosphate buffered saline [DPBS]) starting at 1 week prior to tumor initiation and continuing until the end of the study 10 weeks later. To initiate tumors, 1 million HCC38 cells in 50µL of 1:1 DPBS:BME (Cultrex Pathclear basement membrane extract Type 3, 14.5 mg/mL; #3632; RnD Systems, Minneapolis, MN) were injected into the lactiferous duct of the right fourth mammary gland of 5-6 week old NSG mice as previously described [313]. Tumors were measured with digital calipers starting at 2 weeks post cell injection and continued to be measured once a week until harvest at 10 weeks.

Effect of 24R,25(OH)$_2$D$_3$ on xenograft tumor growth.

One million HCC38 cells in 50µL of 1:1 DPBS: BME were injected into the lactiferous duct of the right fourth mammary gland of un-operated female NSG mice to initiate tumors as described in the **Error! Reference source not found.**. The next day, m ice were injected with 0, 25 ng, or 100 ng of 24R,25(OH)$_2$D$_3$ dissolved in 2% ethanol:1X DPBS. Injections continued 3 times a week for the remainder of the study. Tumors were measured with digital calipers, and tumor volume was calculated as previously described [313]. After 8 weeks, mice were euthanized and tumors were harvested as described above. Immediately after harvesting, tumors were scanned for µCT analysis and then fixed in 10% neutral-buffered formalin. µCT tumor measurements were normalized to vehicle-treated tumors and compared to µCT measurements taken from MCF7 tumors from a previous study [313] and similarly analyzed to assess changes in tumor volume relative to their respective controls [313]. Animal survival was assessed with a Mantel-Cox logrank survival curve analysis, and P-values <0.05 were considered significant as previously described [313].

In vitro Studies

Response to vitamin D$_3$ metabolites.

24R,25(OH)$_2$D$_3$, and 1α,25(OH)$_2$D$_3$ were purchased from Enzo Life Sciences (Farmingdale, NY); 24S,25(OH)$_2$D$_3$ was purchased from Millipore-Sigma (cat# 29447). Stock solutions were prepared in absolute ethanol and diluted in culture medium as previously described [15].

Confluent cultures were treated with dose-dependent 24R,25(OH)$_2$D$_3$ (10^{-10}-10^{-7}M) as previously described [313]. To assess specificity of the response to 24R,25(OH)$_2$D$_3$,

confluent cultures were also treated with 1α,25(OH)$_2$D$_3$ (10^{-10}-10^{-8}M), 24S,25(OH)$_2$D$_3$ (10^{-9}-10^{-7}M), or 25(OH)D$_3$ (10^{-9}-10^{-7}M), or a vehicle (10^{-4}M ethanol). All vitamin D metabolites were reconstituted in ethanol, as previously described [15]. Stock solutions were diluted in warm complete media to final treatment concentrations. Media were removed by aspiration at 15 min or 24 hours, and cells were incubated with fresh complete media until harvest as indicated below.

Signaling Pathway Inhibition.

In these experiments, cells were pre-treated for 30 minutes with inhibitors or vehicle in warm complete media as previously described [313]. In brief, cultures were pretreated with 1-10μM 2-bromopalmitate (Millipore-Sigma #21604)[269] to inhibit palmitoylation, 0.1-1 μM wortmannin (VWR, Radnor, PA, cat# 80055508) [15] to inhibit PLD, or 1-10mM methyl β-cyclodextrin (Millipore-Sigma #C4555) in serum-free media to deplete cell membranes of cholesterol and inhibit intact caveolae [169,270,271]. Cultures were pretreated with 10^{-7}M ICI-182780, an inhibitor to cytosolic and nuclear ERs (Millipore-Sigma #I4409) [272,273], or 1μg of a neutralizing antibody to the membrane-associated estrogen receptor (Alpha Diagnostic, San Antonio, Texas, cat#ERA361-A), to assess the role of ERα66 or ERα36 respectively on the actions of 24R,25(OH)$_2$D$_3$ [55].

Outcome Measures

DNA synthesis

Cells were cultured to 70% confluence, then serum-starved for 48 hours as previously described [313]. At that time, cells were treated with 24R,25(OH)$_2$D$_3$, 24S,25(OH)$_2$D$_3$, or 1α25(OH)$_2$D$_3$ for 15 minutes and incubated with fresh complete media for 24 hours, harvested, and assayed for EdU incorporation according to manufacturer's

instructions (ThermoFisher Scientific, Waltham, Massachusetts, #C10214) as previously described [313].

Gene expression

Cells were cultured to confluence, then treated with 24R,25(OH)$_2$D$_3$ or vehicle in complete media for 15 minutes as described above. Cultures were then aspirated, incubated with complete media for 12 hours. RNA was extracted using TRIzol (Invitrogen, Carlsbad, CA) and quantified (Take3 Micro-Volume Plate, Biotek, Winooski, VT) before being used to synthesize cDNA libraries (High Capacity cDNA Reverse Transcription kit, Promega, Madison, WI) and assessed for gene expression using qRT-PCR as previously described [313]. Gene-specific primers were designed as previously described and are given in Table 6.2 [313]. HCC38, a triple-negative breast cancer cell line that does not express ERα66 [1] but does express ERα36, and MCF7, a luminal breast cancer cell line that expresses all ERα isoforms [1], were both assessed for hydroxylase enzyme mRNA expression.

Table 6.2 Gene expression primers used in quantitative real-time PCR.

Species	Gene	Primer Sequence	
Human	BAX	F	GACGAACTGGACAGTAACATGG
		R	AAAGTAGAAAAGGGCGACAACC
Human	BCL2	Hs_BCL2-1-SG QuantiTect Primer #249900	
Mouse	BCL2	F	TTTGAGTTCGGTGGGGTCAT
		R	CTGGGGCCATATAGTTCCACAA
Human	CXCL12	F	GCCTCTGAAGCCTATGTATG
		R	GACGAACTGGACAGTAACATGG
Human	CXCR4	F	TAGCAAAGTGACGCCGAGGG
		R	TGGTTCTCCAGATGCGGTGG
Human	CYP24A1	F	GACATCCAGGCCACAGACAA
		R	ACCACCATCTGAGGCGTATT
Human	CYP27B1	F	AGAGTTGCTATTGGCGGGAG
		R	AGAACAGTGGCTGAGGGGTA
Human	ERBB2	F	CCGCTGAAGTCCACACAGTT
		R	AAAGGTTCTACCCCGCATGG
Human	ESR1	Hs_ESR1-1-SG QuantiTect Primer #044492	
Human	GAPDH	F	CTATAAATTGAGCCCGCAGCC
		R	TGGCGACGCAAAAGAAGATG
Human	MMP1	F	AGAAAGAAGACAAAGGCAAGTTGA
		R	TCCCCAGTCACTTTCAGCCC
Human	OPG	F	GTGTGCGAATGCAAGGAAGG
		R	CACTCCAAATCCAGGAGGGC
Human	RANKL	Hs_TNFSF11-1-SG QuantiTect Primer #PPH01048F	
Human	SNAI1	Hs_SNAI1-1-SG QuantiTect Primer #010010	

p53 content

Total p53 was measured 24 hours post-cell treatment in human cells with 24R,25(OH)$_2$D$_3$ as described above using a sandwich enzyme-linked immunosorbent assay (ELISA) (R&D Systems, cat# DYC1043) and phosphorylated p53 was measured using a sandwich ELISA specific to the serine-15 residue (R&D Systems, cat# DYC1839). Total p53 content was measured in C2C12 cells with a p53 pan ELISA (Millipore-Sigma cat# 11828789001). For all cell types, cells were plated in 24 well plates, treated with

24R,25(OH)$_2$D$_3$ for 15 minutes, and incubated for 24 hours in complete media. Conditioned media were collected, and cell layers were lysed by sonication (40A for 5 seconds) in 200µL lysis buffer according to manufacturer's protocol. Lysates were centrifuged at 10,000*g* for 15 minutes; the supernatant was collected and assayed for total protein content (ThermoFisher, Pierce 660 nm Protein Assay) and total p53 content following the manufacturer's instructions. Data are presented as a ratio of nanograms of total p53 to total protein content.

DNA fragmentation

DNA fragmentation was assessed by colorimetric terminal deoxynucleotidyl transferase (TdT)-mediated dUTP nick end labeling (Trevigen, TiterTAC™ *in situ* microplate TUNEL assay). Cells were incubated with vehicle or 24R,25(OH)2D3 for 15 minutes, followed by incubation in fresh media for 24 hours. Samples were harvested and processed for TUNEL staining following the manufacturer's instructions [313].

Enzyme-linked immunosorbent assays for secreted proteins

Confluent cultures cells were plated in 6 well plates, treated with vehicle or 24R,25(OH)$_2$D$_3$ for 15 minutes as described above, aspirated, and then incubated in complete media. After 24 hours, conditioned media were collected in 5mL polypropylene tubes, frozen at -80^{o}C and lyophilized (Labconco, Kansas City, Missouri, Freezone Freeze Dryer #7740020). Lyophilized samples were reconstituted in 200 µL of filtered 1XPBS containing 1% BSA and assayed for OPG and RANKL using sandwich ELISAs (R&D Systems, Human TRANCE/RANK L/TNFSF11 DuoSet ELISA #DY626, Human Osteoprotegerin/TNFRSF11B DuoSet ELISA #DY805) as previously described [313]. Cell monolayers were lysed in 1mL 0.5% Triton™ X-100. Cell lysates were assayed for total

DNA content (Promega, QuantiFluor dsDNA, #E6150). OPG and RANKL content are expressed as a ratio of OPG/RANKL.

Collagenase

Collagenase content in the cultures was measured using an MMP1 assay kit (SensoLyte® Plus 520 MMP-1 Assay Kit *Fluorimetric and Enhanced Selectivity*, Anaspec #AS-72012). Cells were plated in 24 well plates and treated with vehicle or 24R,25(OH)$_2$D$_3$ as described above. At harvest conditioned media were collected; cell monolayers were lysed in 500µL 0.05% Triton-X-100 and total DNA content measured. Total MMP1 was measured in the media and normalized to total DNA content. Data are presented as a ratio of ng MMP1/µg DNA [313].

Osteoclast Activity

Osteoclast (OC) activity was measured using a commercially available europium-conjugated human type I collagen-coated OsteoLyse™ Assay Kit, as previously described[317]. Human OC precursors (OCPs; Lonza Biosciences, Walkersville, MD, cat# 2T-110) were cultured on a human type I collagen-coated, 96-well OsteoLyse™ Assay Kit (Lonza Biosciences). OCPs were differentiated into mature OCs using osteoclast precursor growth medium (OCGM, Lonza Biosciences, cat# PT-8001) supplemented with 33ng/mL macrophage colony stimulating factor (M-CSF) and 66ng/mL RANKL as previously described for 7 days[317]. OCPs were also cultured in OCGM supplemented with M-CSF without RANKL for use as a negative control.

HCC38 cells were plated in 6 well plates. At confluence, cultures were treated with vehicle or dose-dependent 24R,25(OH)$_2$D$_3$ for 15 minutes as described above. 24 hours after treatment, conditioned media were collected. OC cultures were aspirated and

treated with conditioned media. OCs were cultured for another 7 days in conditioned media. After 7 days of culturing with HCC38-conditioned media (14 days total), OC activity was measured using the OsteoLyse™ Assay Kit, as previously described[317].

Wound closure assay

A wound closure assay was used to demonstrate metastasis. Confluent cultures of HCC38 cells were treated for 15 min with media containing vehicle or 24R,25(OH)$_2$D$_3$. Another set of cultures was treated with 10^{-7}M 17β-estradiol as a positive control. Following treatment, a scratch was drawn from one end of the well to the other using a sterile 1 mL pipette tip. The loosened cells were aspirated along with the treatment media, and fresh media added to the cultures. A phase-contrast microscope was used to take pictures of each well at 0, 3, 6, 9, 12, and 24 hours after the scratch was made. Wound area was calculated using Adobe Photoshop™ 2 software, normalized to the original wound closure area, and presented as percent wound closure. Data presented are from one of two repeated experiments [313].

Enzyme Activity Assays

Cells were plated in 24-well plates and treated with dose-dependent 24R,25(OH)$_2$D$_3$ as described above for 9 minutes. Immediately after treatment, cells were aspirated, washed twice with 1X DPBS, and harvested with 200µL/well of phospholipase D (PLD) or protein kinase C (PKC) assay buffer according to manufacturer's instructions. PLD activity was measured using the Amplex Red PLD assay (Fisher Scientific, Hampton, NH, cat# A12219) as previously described[55]. PKC activity was measured using the PKC Activity Kit (Abcam, Cambridge, UK, cat# ab139437) as previously described[67].

Statistical Analysis

Data shown are from single representative experiments of two or more repeats and are presented as the mean ± standard error of six independent cultures per treatment group. Data were analyzed by ANOVA with Tukey's post-test to determine significance between groups. Animal studies were analyzed with a repeated-measures two-way ANOVA with $\alpha = 0.05$. Tumor growth curves were analyzed with linear regression analysis to determine whether tumor growth was linear and non-zero. μCT data were analyzed with a one-way ANOVA within xenograft model types (i.e., MCF7 and HCC38 experiments were analyzed separately). Animal survival was assessed with a Kaplan-Meier log-rank analysis.

In vitro experiments with two independent variables (DNA synthesis, total DNA content, and total p53 time courses) were analyzed with two-way ANOVA with Bonferroni's modification of Student's t-test post-tests to determine the variance between row and column factors. The wound closure assay was analyzed with a repeated measures ANOVA test with comparisons between time points. P-values <0.05 were considered significant. Treatment over control data were calculated as the mean fold change of treated groups as compared to vehicle-treated cultures (dashed lines) from three or more experiments and analyzed with Wilcoxon signed-rank non-parametric paired t-tests as compared to control. All other experiments were analyzed with a one-way ANOVA with Tukey's correction. All statistics were conducted in Graphpad Prism 6™. For all experiments, P-values < 0.05 were considered significant.

Results

Breast cancer cell lines differentially express 24-hydroxylase enzyme.

HCC38 expressed both 24-hydroxylase (CYP24A1) and 1α-hydroxylase (CYP27B1) (Figure 6.1A), while MCF7 did not express CYP24A1. Both HCC38 and MCF7 expressed similar levels of CYP27B1 (Figure 6.1B).

17β-Estradiol supplementation is not required to support HCC38 mammary fat pad xenografts in NSG mice.

HCC38 xenografts were created in the 4th mammary fat pad of un-operated or ovariectomized NSG mice given systemic 17β-estradiol (E$_2$) or a vehicle. E$_2$ did not significantly alter HCC38 tumor burden until week 8 (ovariectomized mice) or week 9 (un-operated mice) (Figure 6.1C-6.1D). At weeks 9, 11, and 12, E$_2$ statistically increased HCC38 tumor burden in un-operated mice. In ovariectomized mice, E$_2$ statistically decreased tumor burden at week 8, but did not significantly alter tumor burden at any other time point in the study. Tumors grown in mice with intact ovaries (un-operated mice) were slightly larger at 3 weeks in un-operated mice (~50-75 mm^3) as compared to ovariectomized mice (~30 mm^3). This slight increase in tumor burden in un-operated mice continued throughout both studies, with tumors in un-operated mice being slightly larger (~200 mm^3) than tumors in ovariectomized mice (~150 mm^3) at the end of the study at 10 weeks (**Error! Reference source not found.**C-6.1D).

Tumors grew at a linear rate in vehicle-treated (R^2=0.7857) and E$_2$-treated (R^2=0.7638) un-operated mice with slopes of 2.660 $\pm$ 0.1824 mm^3/day and 3.206 $\pm$ 0.2341 mm^3/day, respectively. The slopes of the vehicle-treated and E$_2$-treated tumors were significantly different from each other with E$_2$-treated tumors growing faster than vehicle-

treated tumors in un-operated mice. In ovariectomized mice, tumors also grew at a linear rate with vehicle-treated (R^2=0.8257) and E_2-treated (R^2=0.7916) tumors having slopes of 2.579 ± 0.1767 mm^3/day and 2.034 ± 0.1539 mm^3/day respectively. The slopes of the vehicle-treated and E_2-treated tumors were also significantly different from each other, but E_2 treated tumors grew more slowly than vehicle-treated tumors in ovariectomized mice. A linear regression analysis found that both vehicle and E_2-treated tumors had significantly non-zero slopes in both un-operated and ovariectomized mice.

Treatment with 24R,25(OH)$_2$D$_3$ increased tumor burden in an HCC38 xenograft model of breast cancer.

Mice receiving either 25 ng or 100 ng per injection of 24R,25(OH)$_2$D$_3$ had a greater HCC38 tumor burden than mice given a vehicle control injection (Figure 6.1E). This increase in tumor volume in 24R,25(OH)$_2$D$_3$ treated mice began at week 6 and continued until harvest at week 8. In previous HCC38 mammary fat pad xenograft studies, vehicle-treated HCC38 tumors reached a final volume of 150-200 mm^3 (Figure 6.1C, 6.1D), consistent with vehicle-treated HCC38 tumors in this study. Tumors in mice given 100ng of 24R,25(OH)$_2$D$_3$ per injection were significantly larger than tumors in mice given 25 ng at weeks 7 & 8. At harvest at week 8, tumors in mice given 100 ng were ~33% larger (final volume ~400 mm^3) than tumors in mice given 25ng of 24R,25(OH)$_2$D$_3$ per injection, which reached a final volume of ~300 mm^3. As in previous HCC38 mammary fat pad xenograft studies, HCC38 tumors were linear with non-zero slopes of 1.635 ± 0.4265 mm^3/day (vehicle), 5.48 ± 0.4642 mm^3/day (25 ng 24R,25(OH)$_2$D$_3$) and 7.575 ± 1.241 mm^3/day (100 ng 24R,25(OH)$_2$D$_3$). All three slopes were significantly non-zero and different from each other. Treatment with high-dose 24R,25(OH)$_2$D$_3$ increased tumor growth rate and

tumor burden in HCC38 xenografts by approximately 50%, as compared to a 50% decrease in tumor burden by 24R,25(OH)$_2$D$_3$ in MCF7 xenografts as measured by μCT (**Error! Reference source not found.**Figure 6.1F). Signs of hypercalcemia, such as anorexia, vomiting, lethargy, fatigue, and polyuria, were not detected in animals treated with a vehicle or with either dose of 24R,25(OH)$_2$D$_3$. In the high-dose 24R,25(OH)$_2$D$_3$ HCC38 xenograft group, only 6 out of 8 animals survived to the end of the study as compared to 8 out of 8 animals in the vehicle and low-dose 24R,25(OH)$_2$D$_3$ groups. However, this reduction in animal survival was not statistically significant (Figure 6.1G).

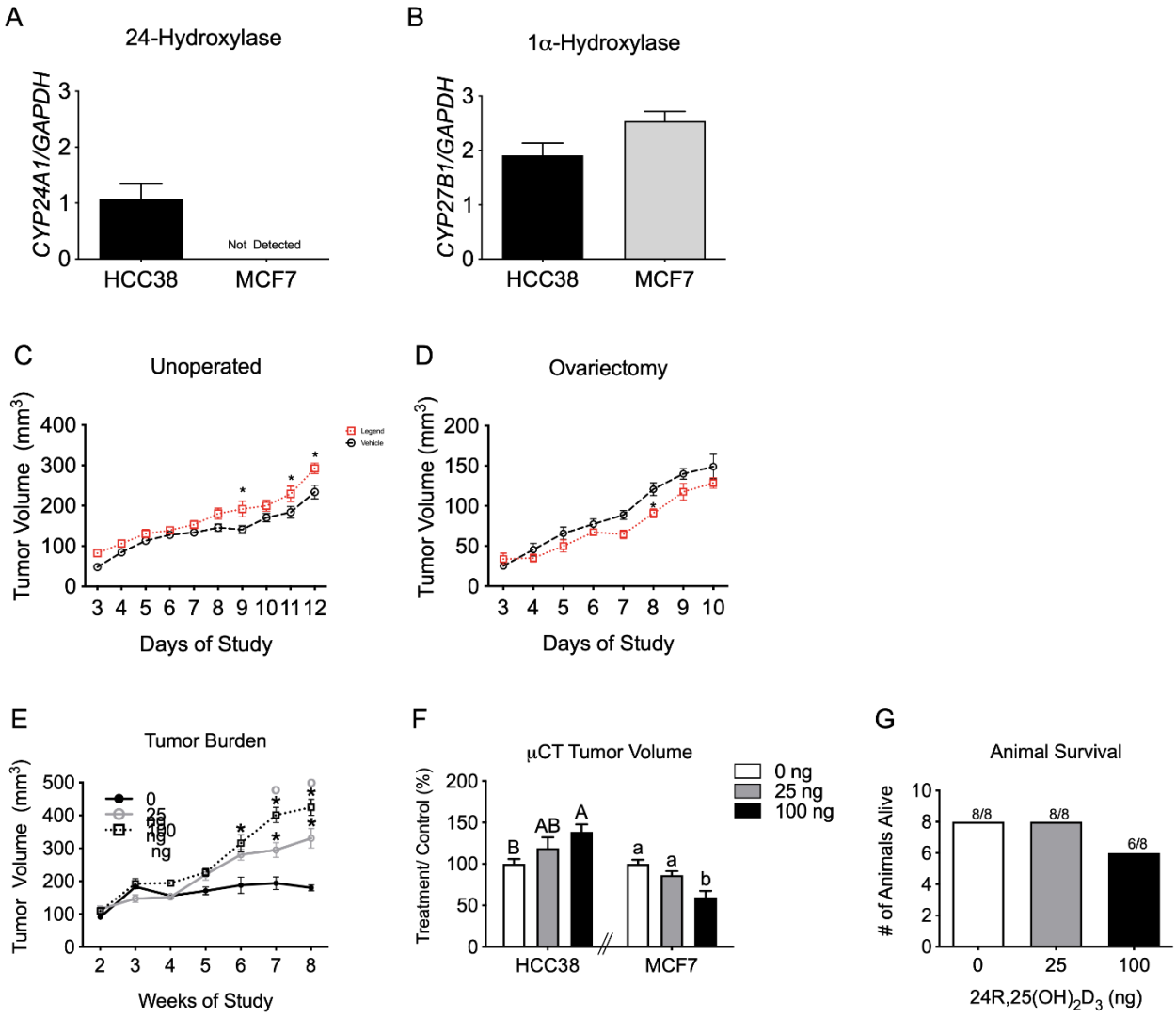

Figure 6.1 Breast cancer cell lines differentially expression hydroxylase enzymes

HCC38 and MCF7 breast cancer cells were cultured to confluence and harvested after 12 hours for gene expression. Cells were assessed for [**A**] CYP24A1 or [**B**] CYP27B1 expression and normalized to GAPDH as a housekeeping gene. [**C**] Unoperated female NSG mice implanted with HCC38 xenograft mammary fat pad tumors were intraperitoneally injected with 2.5mg/kg 17β-estradiol or a vehicle

twice a week for 12 weeks. Tumor burden was measured twice a week throughout the course of the study and plotted against time. [**D**] A similar study was done with ovariectomized NSG mice. HCC38 xenografts were treated with the same dose (2.5mg/kg) or 17β-estradiol) or a vehicle and tumors were measured twice a week until harvest at 10 weeks. *indicates statistical significance against week-matched vehicle tumors at α=0.05 with two-way ANOVA. [**E**] NSG mice with HCC38 mammary fat pad xenograft tumors were intraperitoneally injected with 25 or 100 ng of 24R,25(OH)$_2$D$_3$ 3 times a week for 8 weeks. Tumor burden was measured with digital calipers and plotted against time. Animals given 24R,25(OH)$_2$D$_3$ had increased tumor burden as measured by digital calipers. *indicates significance as compared to vehicle-treated animals within the same time point. ^{O} indicates significance as compared to animals treated with 25 ng of 24R,25(OH)$_2$D$_3$ within the same time point. [**F**] Animals given 24R,25(OH)$_2$D$_3$ had increased tumor burden as measured by μCT as compared to tumor burden in vehicle-treated mice. Capital letters were used to indicate significance within HCC38 xenograft tumor groups, while lower-case letters were used to indicate significance within MCF7 tumor groups. Groups that do not share a letter are statistically significant. [**G**] After 8 weeks, 8 animals from the vehicle group, 8 animals from the low-dose (25 ng per injection) 24R,25(OH)$_2$D$_3$ group, and 6 animals from the high-dose (100 ng per injection) 24R,25(OH)$_2$D$_3$ group survived out of an original n of 8. Animals in the high-dose group did not have a statistically significant reduced survival rate as compared to animals in low dose or vehicle groups.

24R,25(OH)$_2$D$_3$ specifically induced proliferation in HCC38 cells in vitro.

When HCC38 cells were treated for 15 minutes with 24R,25(OH)$_2$D$_3$ proliferation increased after 24 hours (Figure 6.2A) as measured by DNA synthesis. However, treatment with 24S,25(OH)$_2$D$_3$, an enantiomer of 24R,25(OH)$_2$D$_3$, or 1α,25(OH)$_2$D$_3$ for 15 minutes did not change proliferation after 24 hours (Figure 6.2B, C). The effect of 24R,25(OH)$_2$D$_3$ was dose-dependent with the greatest increase at 10^{-7}M 24R,25(OH)$_2$D$_3$. The effect of 24R,25(OH)$_2$D$_3$ was also observed in MCF7 cells [313], with both 10^{-8} and 10^{-7} 24R,25(OH)$_2$D$_3$ increasing DNA synthesis (Figure 6.2D). In both HCC38 and MCF7 cells, 10^{-7}M 24R,25(OH)$_2$D$_3$ increased DNA synthesis ~two-fold above vehicle-treated cultures.

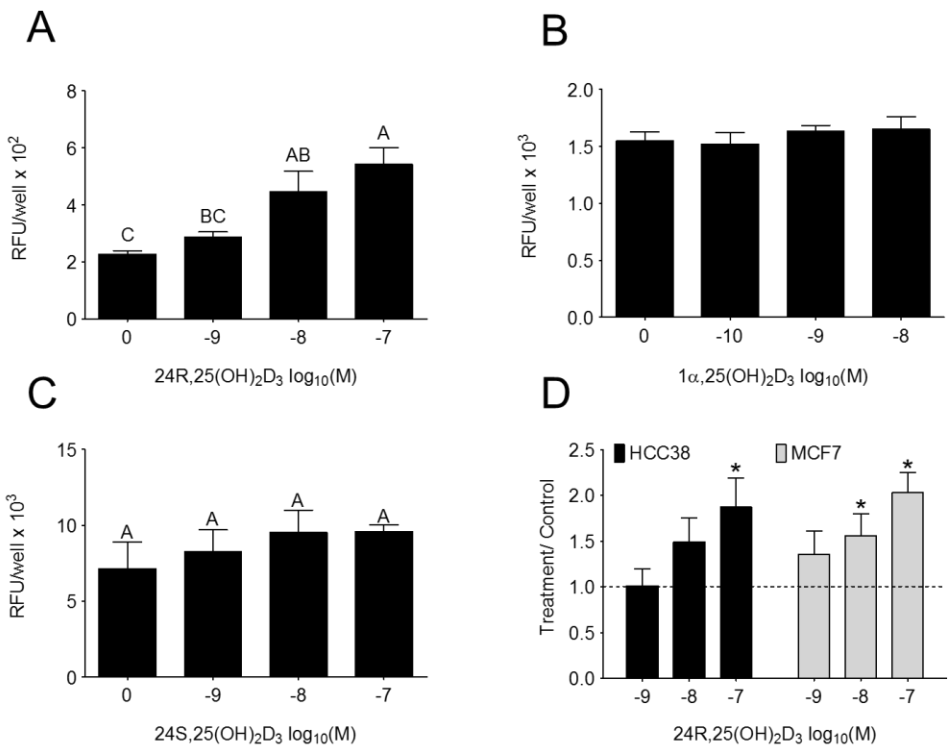

Figure 6.2: 24R,25(OH)2D3 specifically induces proliferation in HCC38 cells.

HCC38 monolayer cultures were serum-starved for 48 hours, treated with 24R,25(OH)$_2$D$_3$, 24S,25(OH)$_2$D$_3$, or 1α,25(OH)$_2$D$_3$ for 15 minutes and assayed 24 hours later for EdU incorporation. [**A**] 24R,25(OH)$_2$D$_3$, but not [**B**] 24S,25(OH)$_2$D$_3$ nor [**C**] 1α,25(OH)$_2$D$_3$, induced proliferation in HCC38 cell monolayers 24 hours after a 15-minute treatment. [**D**] Treatment over control was calculated as the average fold-change of treatment as compared to vehicle-treated cultures in three or more experiments and analyzed with a paired t-test against normalized vehicle controls *indicates significance at P<0.05 as compared to vehicle-treated cultures. High-dose 24R,25(OH)$_2$D$_3$ induced proliferation in HCC38 and MCF7 cell monolayers 2-fold over control.

24R,25(OH)$_2$D$_3$ reduces apoptotic markers in HCC38 cell monolayers, contrary to its effect in MCF7 cultures.

24R,25(OH)$_2$D$_3$ caused a dose-dependent decrease in B cell lymphoma protein 2-associated X protein (BAX) to B cell lymphoma protein 2 (BCL2) expression ratios (BAX/BCL2), which was significant at 10^{-8}M and 10^{-7}M doses (an ~8-fold decrease) (Figure 6.3A). 24R,25(OH)$_2$D$_3$ had a similar reducing effect on total p53 levels (Figure 6.3B) and TUNEL staining (Figure 6.3C), with the 10^{-7}M dose producing the maximum decrease in p53 levels (~2 fold decrease) and TUNEL (~.25 fold decrease). 24R,25(OH)$_2$D$_3$-induced fold-change decreases in apoptosis in HCC38 cultures are similar in proportion to 24R,25(OH)$_2$D$_3$-induced fold change *increases* in apoptosis observed in MCF7 cultures (Figure 6.3D-F). However, in HCC38 cells, 24R,25(OH)$_2$D$_3$ has the greatest effect at 10^{-7}M on BAX/BCL2, total p53, and TUNEL staining; unlike MCF7, where maximal effect sizes are observed at 10^{-8}M 24R,25(OH)$_2$D$_3$.

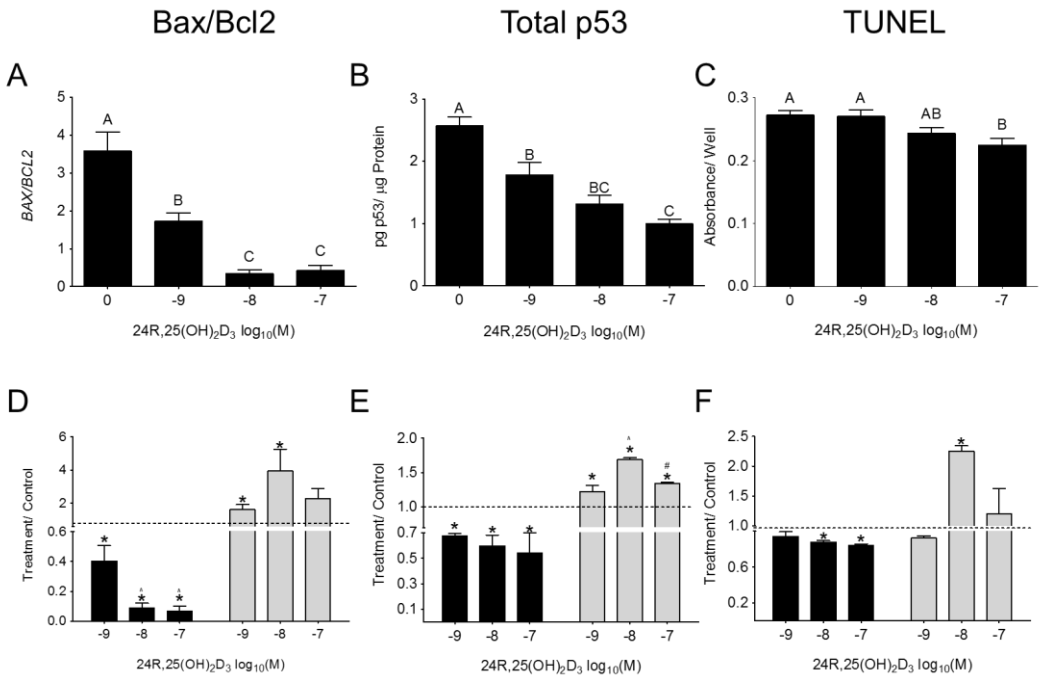

Figure 6.3: 24R,25(OH)2D3 prevents apoptosis in HCC38 cells, but induces apoptosis in MCF7 cells.

HCC38 monolayer cultures were treated with 24R,25(OH)$_2$D$_3$ for 15 minutes, and harvested 12 hours later for gene expression and 24 hours later for protein and TUNEL staining. Cultures were assessed for apoptosis as measured by [**A, D**] BAX/BCL2 gene expression, [**B, E**] total p53 protein, and [**C, F**] TUNEL staining. [**A-C**] 24R,25(OH)$_2$D$_3$ reduced apoptosis in HCC38 cells. Groups that share a letter are not significant at $p<0.05$. [**D-F**] HCC38 or MCF7 monolayer cultures were treated with 24R,25(OH)$_2$D$_3$ for 15 minutes and assessed for apoptosis 12-24 hours later. Treatment over control was calculated as the average fold-change of treatment as compared to vehicle-treated cultures in three or more experiments and analyzed with a paired t-test against normalized vehicle controls *indicates significance at $P<0.05$ as compared to vehicle-treated cultures.

24R,25(OH)$_2$D$_3$ increased epithelial-to-mesenchymal transition, metastatic markers, and migration in HCC38 cells in vitro.

Treatment with 10^{-8}M and 10^{-7}M 24R,25(OH)$_2$D$_3$ significantly increased expression of the mesenchymal-associated transcription factor snail family transcriptional repressor 1 (SNAI1) compared to cells treated with vehicle (Figure 6.4A). Expression of receptor tyrosine-protein kinase erbB-2 (ERBB2) and matrix metalloproteinase 1 (MMP1), which are associated with tumor aggression and matrix turnover respectively, was also increased by similar doses of 24R,25(OH)$_2$D$_3$, with the maximal effect at 10^{-7}M(Figure 6.4B, 6.4C). 24R,25(OH)$_2$D$_3$ had a biphasic effect on collagenase enzyme protein expression, with statistically significant induction of collagenase protein observed in cultures treated with 10^{-8}M 24R,25(OH)$_2$D$_3$ (Figure 6.4D), and a non-significant increase in cultures treated with 10^{-7}M 24R,25(OH)$_2$D$_3$. 24R,25(OH)$_2$D$_3$ (10^{-7}M) stimulated a 4-fold increase in SNAI1 (Figure 6.4E), a 6-fold increase in ERBB2 expression (Figure 6.4F), a 6-fold increase in MMP1 expression (Figure 6.4G), and a 10-fold increase in collagenase protein expression (Figure 6.4H) as compared to vehicle-treated cultures (Figure 6.4E-H). This is in direct contrast to the effect of 24R,25(OH)$_2$D$_3$ on MCF7 cultures, where 10^{-7}M 24R,25(OH)$_2$D$_3$ reduced SNAI1, and all doses of 24R,25(OH)$_2$D$_3$ reduced ERBB2 and MMP1 transcript expression and reduced collagenase protein expression (Figure 6.4E-H).

24R,25(OH)$_2$D$_3$ also increased metastatic markers in HCC38 cultures. 10^{-7}M 24R,25(OH)$_2$D$_3$ increased chemokine receptor type 4 (CXCR4) to C-X-C- motif chemokine 12 (CXCL12) ratios (CXCR4/CXCL12) (Figure 6.4I). 10^{-8}M 24R,25(OH)$_2$D$_3$ decreased the ratio of osteoprotegerin (OPG) to receptor activator of nuclear factor

kappa-B ligand (RANKL) transcripts (OPG/RANKL) (Figure 6.4J) , and both 10^{-8}M and 10^{-7}M 24R,25(OH)$_2$D$_3$ decreased OPG/RANKL protein expression (Figure 6.4K). Conditioned media from 24R,25(OH)$_2$D$_3$-treated HCC38 cells increased osteoclast activity more than conditioned media from vehicle-treated HCC38 cells (Figure 6.4L). 24R,25(OH)$_2$D$_3$ increased osteoclast activity by 100% as compared to vehicle-treated cells. 10^{-7}M 24R,25 induced a 10-fold increase CXCR4/CXCL12 ratios (Figure 6.4M), and a 2-fold decrease in OPG/RANKL ratios (Figure 6.4N, 6.4O) in HCC38 cells. Both 10^{-8}M and 10^{-7}M 24R,25(OH)$_2$D$_3$ decreased CXCR4/CXCL12 ratios and 10^{-9}M and 10^{-7}M increased OPG/RANKL transcript and protein expression ratios, respectively in MCF7 cells.

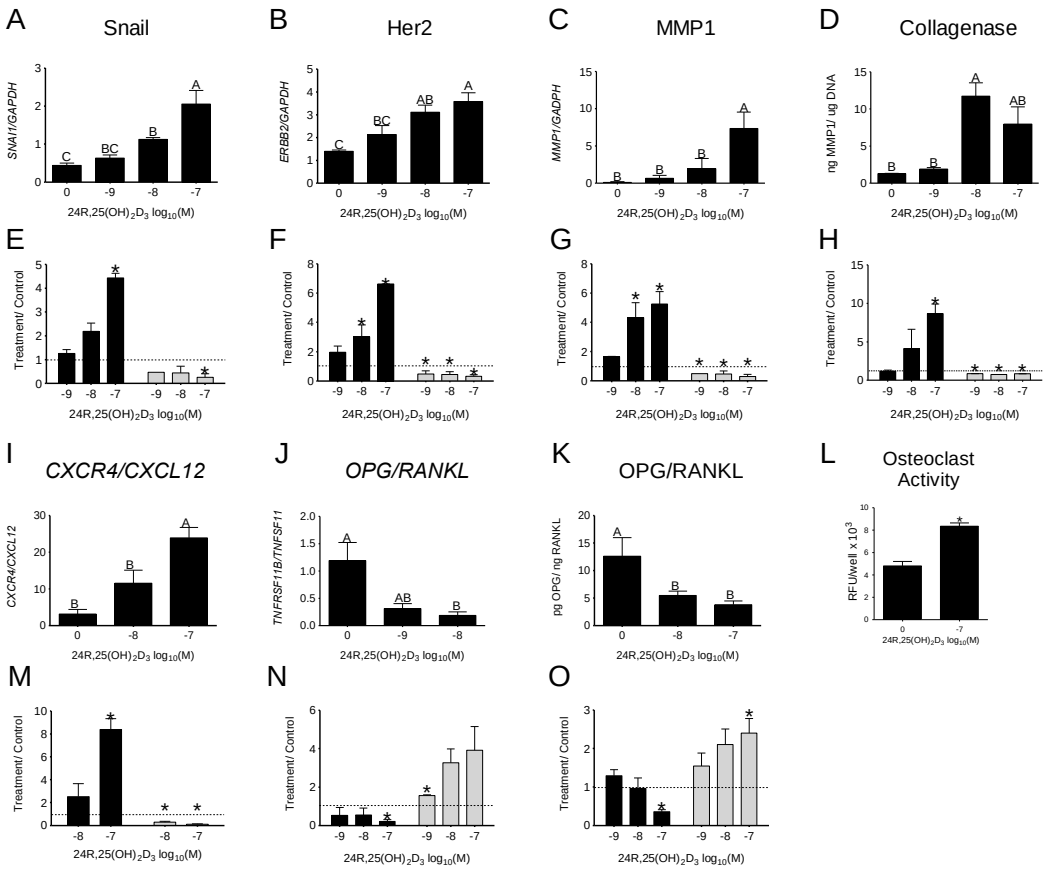

Figure 6.4: 24R,25(OH)2D3 increases epithelial-to-mesenchymal transition and metastatic markers in HCC38 cultures.

(Figure 4, cont. from the previous page): HCC38 and MCF7 monolayer cultures were treated with 24R,25(OH)$_2$D$_3$ for 15 minutes and harvested 12 hours later for gene expression. Effect of dose-dependent 24R,25(OH)$_2$D$_3$ on gene expression of [**A, E**] snail, [**B, F**] her2, [**C, G**] MMP1, [**D**, **H**] collagenase protein, [**I, M**] CXCR4/ CXCL12 ratios, [**J, N**] OPG/ RANKL ratios, and [**K, O**] OPG/RANKL protein in **[A-D, I-L**] HCC38 cells, but reduces them in MCF7 cells [**E-H, M-O**]. [**L**] 24R,25(OH)$_2$D$_3$ increases osteoclast activity in osteoclasts treated with HCC38 conditioned media from cultures treated with 24R,25(OH)$_2$D$_3$. Groups that share a letter are not significant at $p<0.05$. Treatment over control was calculated as the average fold-change of treatment as compared to vehicle-treated cultures in three or more experiments and analyzed with a paired t-test against normalized vehicle controls *indicates significance at $P<0.05$ as compared to vehicle-treated cultures.

24R,25(OH)$_2$D$_3$ increased cell migration in a scratch test assay. 12 hours after a wound was made on a confluent culture of HCC38 cells, wound size in cultures given a vehicle treatment had not significantly altered, while 10^{-10}M 24R,25(OH)$_2$D$_3$ had slightly decreased wound size, and 10^{-7}M 24R,25(OH)$_2$D$_3$ had reduced wound size to ~25% of its original area (Figure 6.5). 24 hours after the scratch test was initiated, all cultures had closed their wounds.

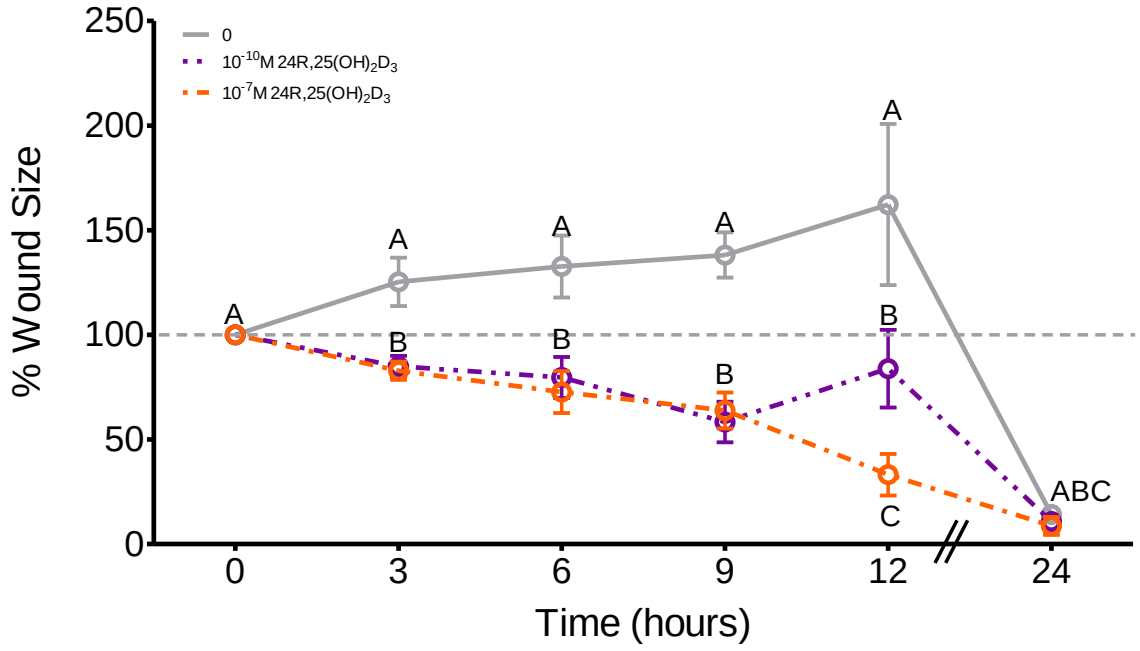

Figure 6.5: Effect of 24R,25(OH)2D3 on cell migration in HCC38 cell monolayers.

HCC38 monolayer cultures were treated with 24R,25(OH)$_2$D$_3$ for 15 minutes and incubated with fresh media. A scratch was made across the culture with a 1mL pipette tip, and monolayer cultures were observed over 24 hours for wound closure.

24R,25(OH)$_2$D$_3$ differentially regulates PLD and PKC activity in HCC38 and MCF7 cells.

24R,25(OH)$_2$D$_3$ dose-dependently increases PLD activity in HCC38 cells, with the maximal effect occurring at 10^{-7}M 24R,25(OH)$_2$D$_3$ (~3-fold increase as compared to vehicle-treated control cultures) (Figure 6.6A). However, 24R,25(OH)$_2$D$_3$ dose-dependently decreases PLD activity in MCF7 cells, with 10^{-7}M reducing PLD activity to 25% that of vehicle-treated control cultures (Figure 6.6A). Treatment with 24R,25(OH)$_2$D$_3$ did not change PKC activity in HCC38 cells (Figure 6.6B); however, it did slightly increase PKC activity in MCF7 cells (Figure 6.6B). Baseline PKC activity in MCF7 cells was ~2-fold higher in MCF7 cells (~60 μU/μg protein/min) than in HCC38 cells (~30 μU/μg protein/min) (Figure 6.6B).

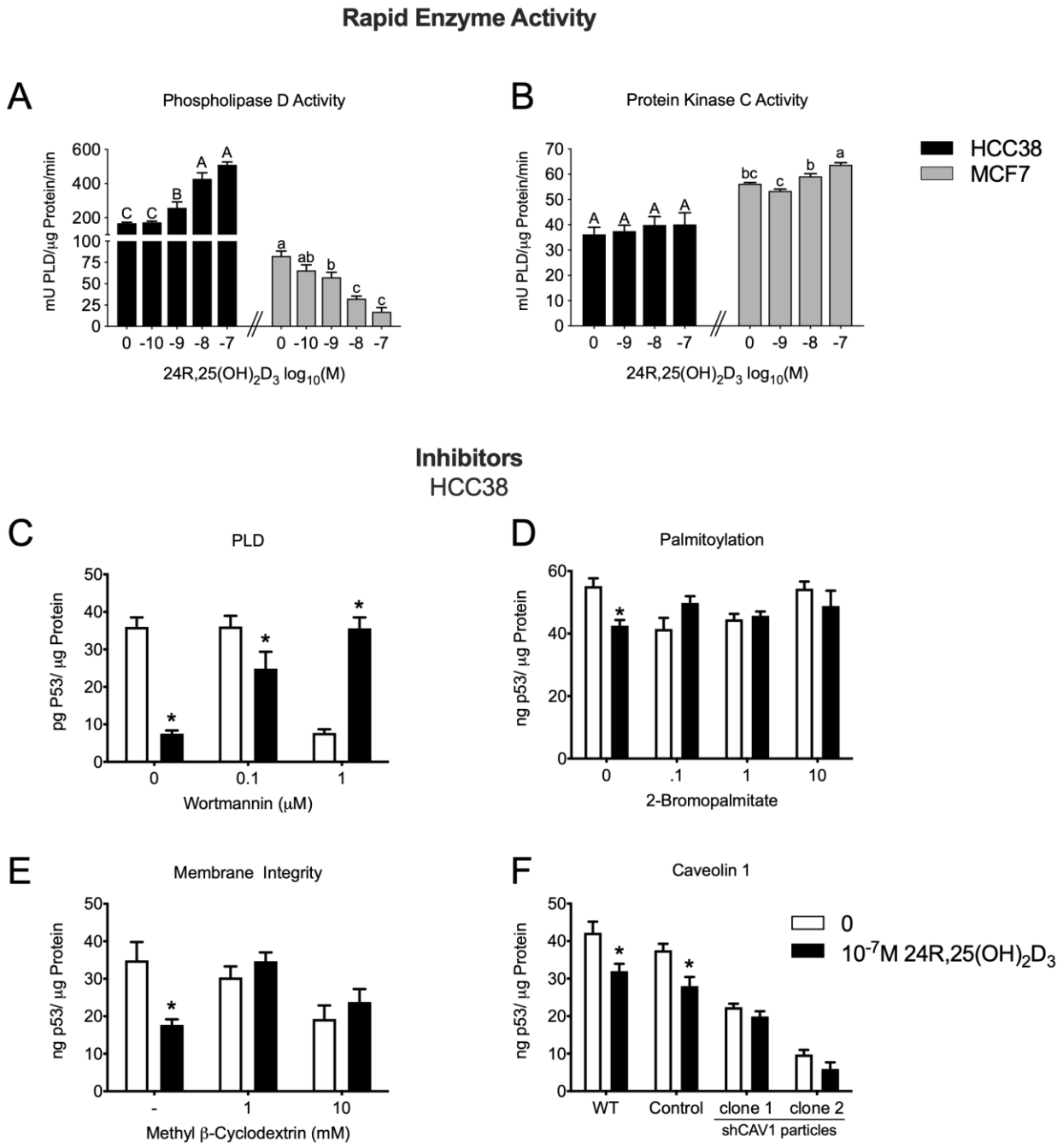

Figure 6.6 24R,25(OH)2D3 reduces total p53 levels through a caveolae-associated, PLD-dependent mechanism.

HCC38 or MCF7 monolayer cultures were treated with 24R,25(OH)$_2$D$_3$ for 15 minutes, and assessed for [**A**] PLD activity decreases or [**B**] PKC activity. In a

separate set of experiments, HCC38 monolayer cultures were treated with inhibitors for 30 minutes before treatment with 24R,25(OH)$_2$D$_3$ for 15 minutes and assessed for total p53 content. 24R,25(OH)2D3 reduced p53 levels in HCC38 cell monolayers, but this effect was prevented by treatment with [**C**] wortmannin to inhibit PLD activity, [**D**] 2-bromopalmitate to inhibit palmitoylation of nuclear receptors trafficked to the membrane, [**E**] methyl beta-cyclodextrin to deplete the membrane of cholesterol, and [**F**] short-hairpin RNA to silence caveolin-1.

24R,25(OH)$_2$D$_3$ inhibited apoptosis through a caveolae-associated, PLD-dependent pathway.

PLD inhibition with low-dose wortmannin prevented a 24R,25(OH)$_2$D$_3$-induced reduction in p53 (Figure 6.6**Error! Reference source not found.**C). High-dose wortmannin reduced p53 levels in HCC38 cultures, but treatment with 24R,25(OH)$_2$D$_3$ reversed this effect and increased p53 levels back to baseline p53 levels in vehicle-treated control HCC38 cultures (Figure 6.6**Error! Reference source not found.**C). 2-bromopalmitate (2BP) was used to prevent trafficking of palmitoylated nuclear receptors to the membrane. Treatment with all doses of 2BP prevented a 24R,25(OH)$_2$D$_3$-induced reduction in total p53 levels (Figure 6.6**Error! Reference source not found.**D). Methyl β-cyclodextrin (MBC) was used to deplete the cell membrane of cholesterol and destroy caveolae and lipid rafts. Treatment with 1mM and 10mM MBC prevented a 24R,25(OH)$_2$D$_3$-induced reduction in total p53 levels (**Error! Reference source not found.**Figure 6.6E).

To evaluate the role of the caveolae on 24R,25(OH)$_2$D$_3$ signaling in HCC38 cells, HCC38 cells were stably knocked down for caveolin-1 with shRNA (Figure 6.7). Caveolin-1 knocked down HCC38 cells (shCAV1-HCC38) had <10% of wild-type caveolin-1 protein, while empty control-transduced cells had >100% of wild-type caveolin-1 protein expression (Figure 6.7A). Caveolin-1 levels were similar for both clone #1 and clone #2 shCAV1-HCC38 cells (Figure 6.7A, 6.7B). 24R,25(OH)$_2$D$_3$ reduced total p53 protein expression in wild-type and scramble control HCC38 cells, but did not affect shCAV1-HCC38 cells. Baseline levels of p53 in shCAV1-HCC38 cultures were lower than wild-type, and empty-control transduced HCC38 cultures (**Error! Reference source not found.**Figure 6.6F).

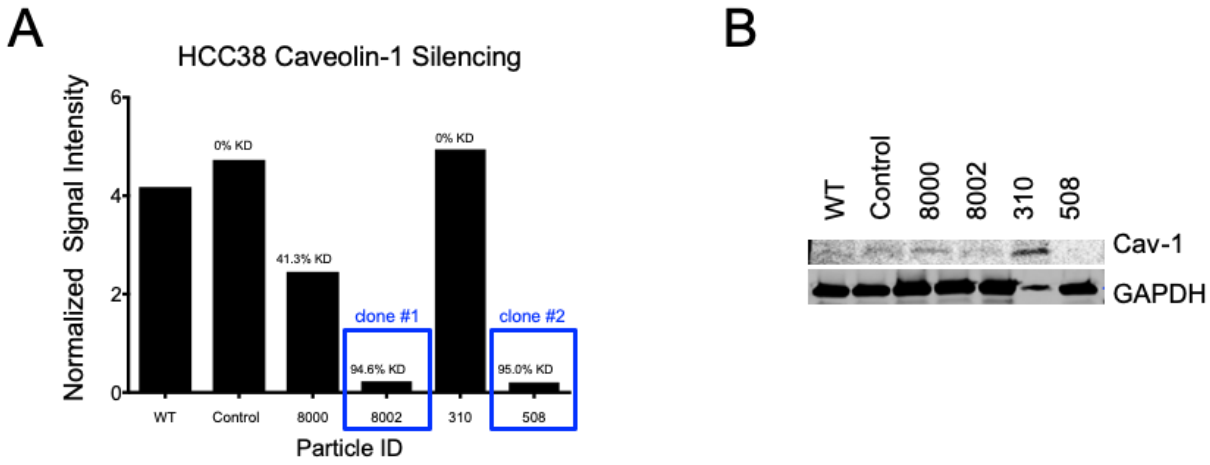

Figure 6.7 Silencing CAV1 in HCC38 cells.

Caveolin-1 was stably knocked down in HCC38 using a recombinant plasmid with a puromycin antibiotic selection marker. Four short-hairpin clones targeting the CAV1 gene were screened for caveolin-1 silencing, and the two best clones (8002, “clone 1”, and 508, “clone 2”) were sub-cultured and expanded for further experiments. A separate set

of HCC38 cultures was also transfected with an empty cassette vector as a control. [**A**] Caveolin-1 silencing by shRNA particles and [**B**] Representative western blot (n=1).

Overexpressing and silencing ERα changes the 24R,25(OH)2D3 response.

ERα was transiently overexpressed in HCC38 cells (Figure 6.8A-D) and stably overexpressed in C2C12 (Figure 6.9A-C). ERα66 expression in ESR1-transfected HCC38 cells (ovERα-HCC38) was 20-times greater than wild-type HCC38 cells and 16-times greater than empty-control HCC38 cells (Figure 6.8C). ERα36 was 2.3-times greater in ESR1-transfected vs. wild-type HCC38 and 3-times greater than ORF-control HCC38 cells (Figure 6.8D). In C2C12 cells, ESR1-transfected C2C12 cells (ovERα-C2C12) expressed 11-times more ERα66 protein expression than wild-type C2C12 cells (Figure 6.9A), and 2.8-times more ERα36 than wild-type C2C12 (Figure 6.9B, 6.9C).

24R,25(OH)$_2$D$_3$ induced apoptosis in cells that do not express ERα66 but induced apoptosis in cells that express ERα66. In wild-type and ORF-control HCC38 cells, which express very low levels of ERα66 (Figure 6.8B, 6.8C), all doses of 24R,25(OH)$_2$D$_3$ prevented apoptosis as measured by BAX/BCL2 (Figure 6.11A) and total p53 levels (Figure 6.11B). However, treatment with 10^{-8}M 24R,25(OH)$_2$D$_3$ induced apoptosis in ovERα-HCC38 cells (Figure 6.11A, 6.11B) as measured by both BAX/BCL2 and total p53. 10^{-7}M 24R,25(OH)$_2$D$_3$ upregulated BAX/BCL2 ratios in ovERα-HCC38 (Figure 6.11A). 24R,25(OH)$_2$D$_3$ had a biphasic effect on total p53 levels in ovERα-HCC38. 10^{-8} 24R,25(OH)$_2$D$_3$ increased total p53 protein in ovERα-HCC38, but 10^{-7}M 24R,25(OH)$_2$D$_3$ did not affect p53 (Figure 6.11). Wild-type and ORF-control HCC38 cells had similar baseline ratios of BAX/BCL2 mRNA (Figure 6.11A) and similar baseline levels of total p53 protein (Figure 6.11B), but ovERα-HCC38 cells had lower ratios of BAX/BCL2 mRNA and lower baseline p53 than wild-type HCC38 (Figure 6.11A, 6.11B).

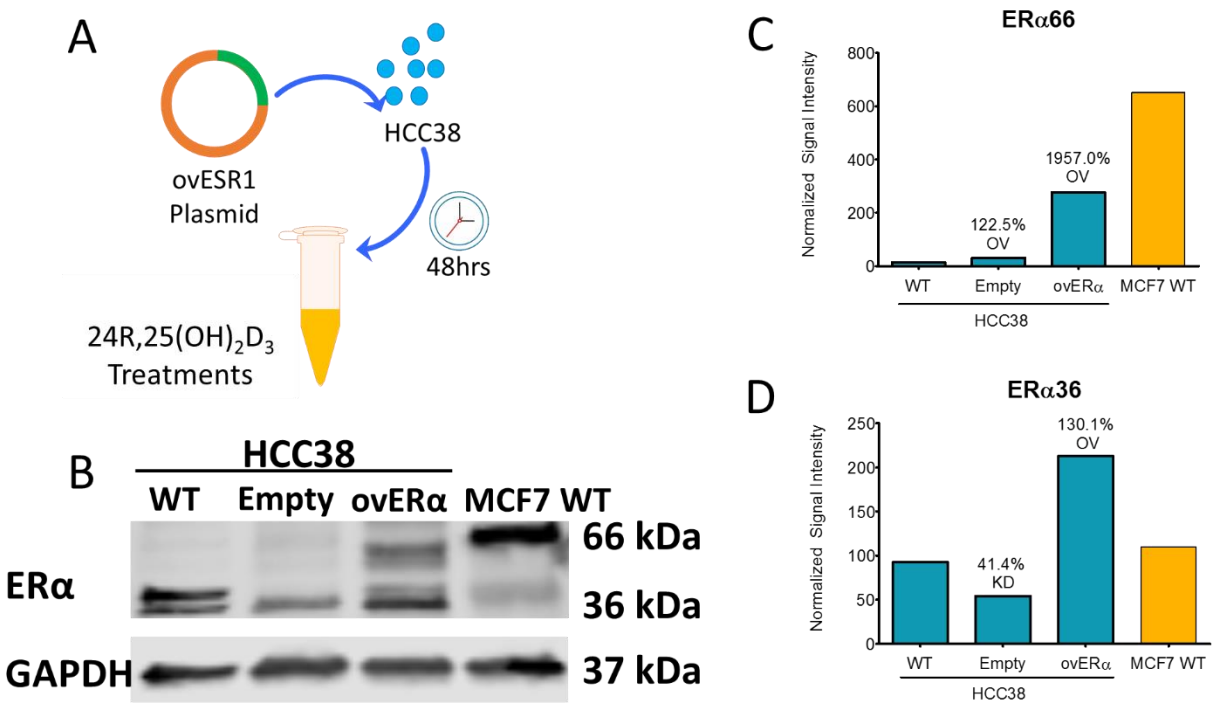

Figure 6.8 Overexpression of ESR1 in HCC38 changes ERα isoform expression.

[**A**] ERα and an empty control were transiently transfected in HCC38 using a recombinant plasmid with a GFP reporter gene. 48 hours after transfection, cells were assessed for ERα isoform expression by [**B**] western blot (representative image, n=1) and [**C**] ERα66 and [**D**] ERα36 protein expression were quantified (OV = overexpressed; KD = knockdown as compared to WT).

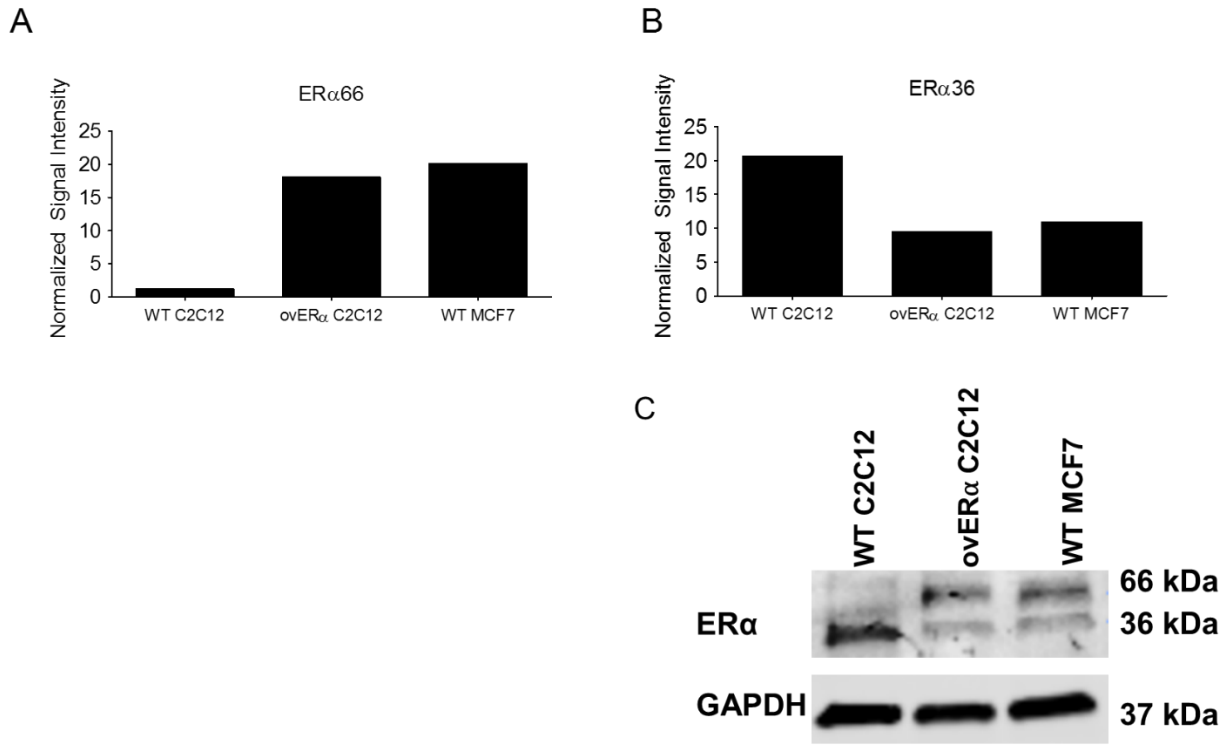

Figure 6.9 Overexpression of ESR1 in C2C12.

ERα was stably overexpressed in C2C12 using a recombinant plasmid with a G418 antibiotic selection marker. ovERα-C2C12 cells were selected for G418 resistance and assessed for protein expression via western blot. [**A**] ERα66 and [**B**] ERα36 protein expression were quantified (n=1) to confirm overexpression of ERα isoforms as compared to WT. [**C**] Representative western blot (n=1).

In C2C12 muscle cells, which express low levels of ERα66 (Figure 6.9A), 24R,25(OH)$_2$D$_3$ had an anti-apoptotic effect as measured by BAX/BCL2 mRNA ratios, but upregulated BAX/BCL2 mRNA ratios in ovERα-C2C12 cells (Figure 6.11C). Wild-type C2C12 cultures had higher baseline BAX/BCL2 mRNA ratios than ovERα-C2C12 cultures (Figure 6.11C). 24R,25(OH)$_2$D$_3$ did not affect total p53 levels in wild-type C2C12 cells but

increased total p53 in ovERα-C2C12 (Figure 6.11D). Baseline total p53 was higher in ovERα-C2C12 cells than in wild-type C2C12 (Figure 6.11D). In both C2C12 and HCC38 cells, transfecting with ESR1 to overexpress the ERα isoforms changed the cell response to 24R,25(OH)$_2$D$_3$. 24R,25(OH)$_2$D$_3$ stimulated apoptosis in all HCC38 and C2C12 cultures that overexpressed ERα66 (Figure 6.11A-D).

ERα66 was stably knocked down in MCF7 cells (Figure 6.10A, 6.10C). Knocked down MCF7 (shESR1-MCF7) cells had approximately one-third the ERα66 expression of wild-type MCF7 cells, while scrambled controls had >80% of wild-type MCF7 cells expression Figure 6.10A. ERα36 levels were similar for wild-type, scramble control, and shESR1-MCF7 cells, with the scrambled control and the shESR1-MCF7 cells expressing ~90% as much ERα36 as wild-type cells (Figure 6.10B, 6.10C).

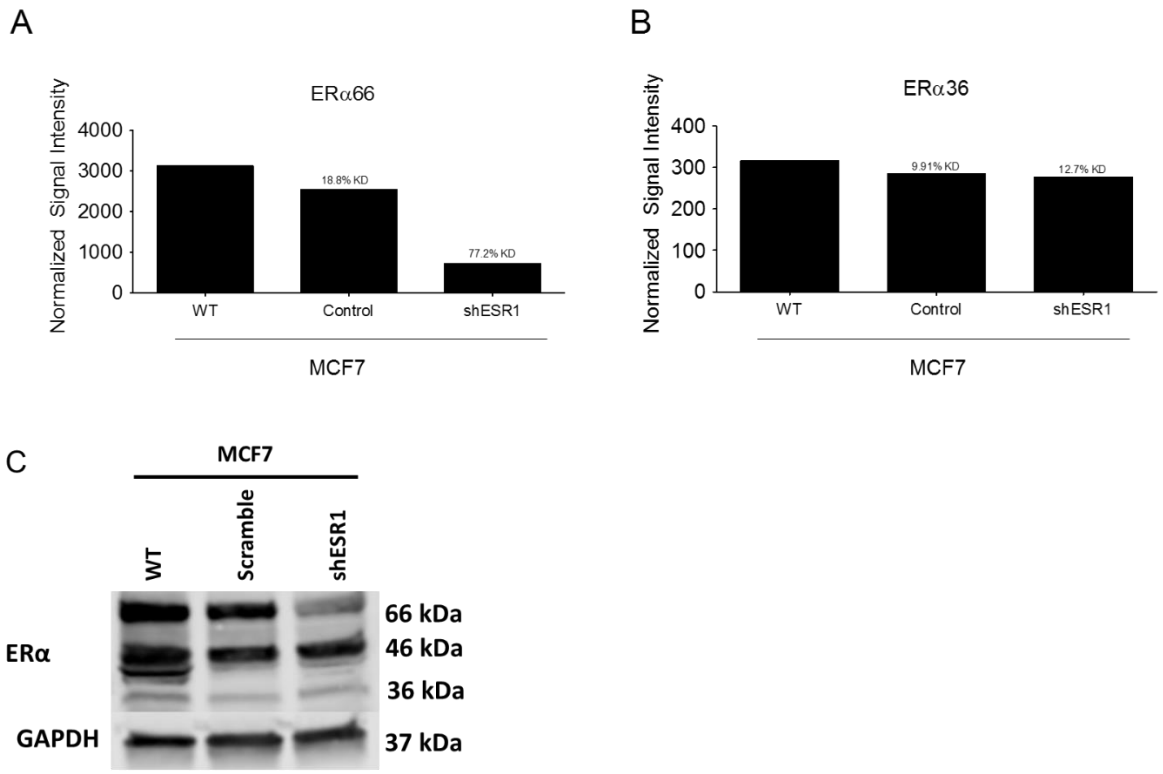

Figure 6.10 ERα66 was stably knocked down in MCF7 using a recombinant plasmid with a puromycin antibiotic resistant selection marker.

shESR1 and scramble-control cells were selected for puromycin resistance and assessed for protein expression via western blot. [**A**] ERα66 and [**B**] ERα36 protein expression were quantified (n=1) to confirm silencing of ERα66 as compared to WT. [**C**] Representative western blot (n=1).

24R,25(OH)$_2$D$_3$ upregulated BAX/BCL2 mRNA ratios and increased total p53 levels in wild-type and scrambled MCF7 cells at 10^{-8}M (Figure 6.11E, 6.11F). 24R,25(OH)$_2$D$_3$ had no effect on BAX/BCL2 mRNA ratios or total p53 levels in shESR1-MCF7 cells (Figure 6.11E, 6.11F). Baseline BAX/BCL2 mRNA ratios and total p53 were the same in wild-type, scrambled, and shESR1 MCF7 cells. In wild-type, MCF7 cells, 10^{-7}M 24R,25(OH)$_2$D$_3$ also increased phosphorylated p53 but did not increase phosphorylated p53 in cultures that were knocked down for ERα66 (Figure 6.12). While 24R,25(OH)$_2$D$_3$ increased the average amount of phosphorylated p53 in scramble-control MCF7 cells as compared to vehicle-treated scramble-control MCF7 cells, this change was not statistically significant. Similarly, 10^{-7}M 24R,25(OH)$_2$D$_3$ reduced average phosphorylated p53 in shESR1-MCF7 cells as compared to vehicle-treated shESR1-MCF7 cells; however, this difference was not statistically significant. Baseline phosphorylated p53 was not statistically different between wild-type, scrambled, and shESR1-MCF7 cells (Figure 6.12).

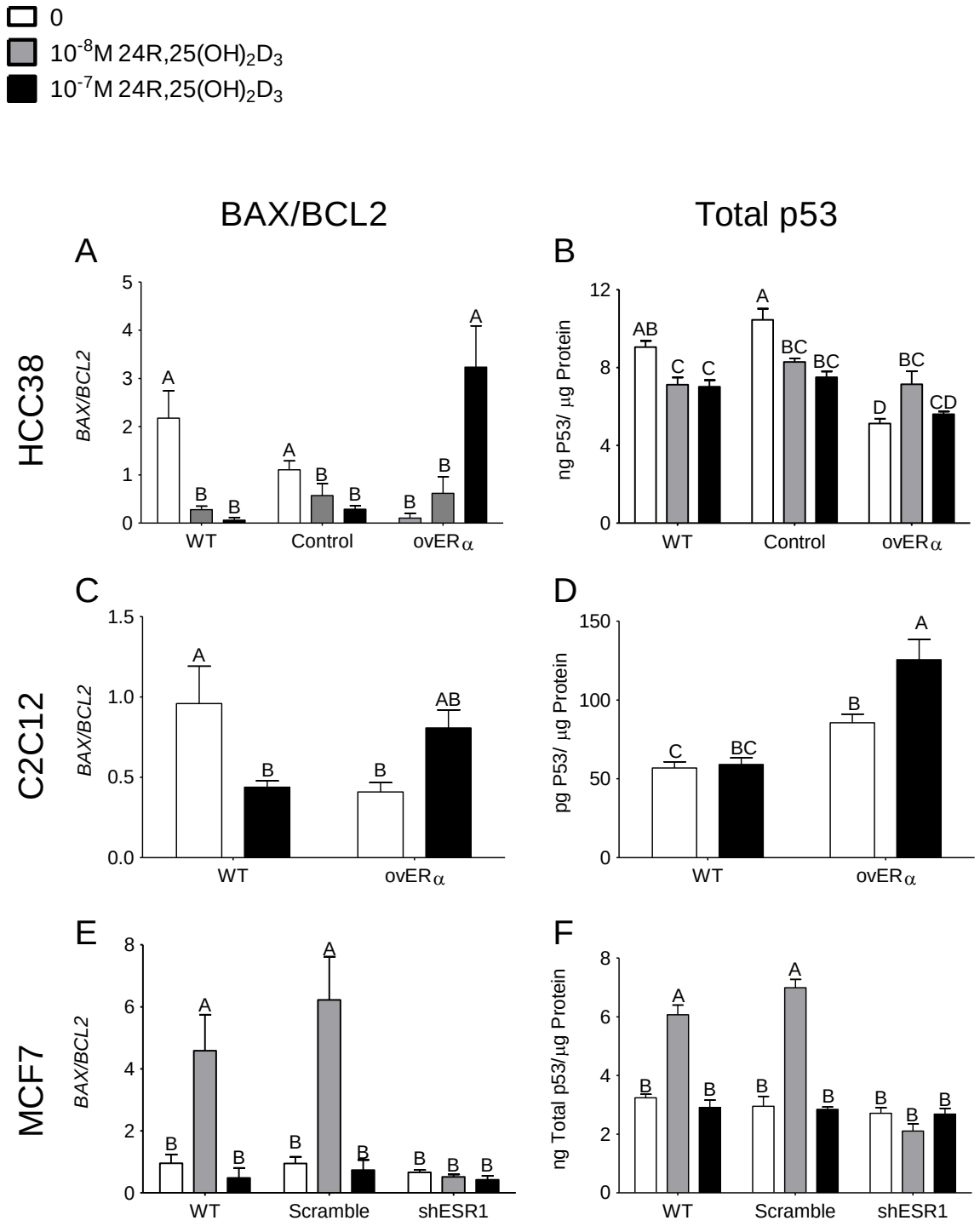

Figure 6.11: Expression and silencing of ERα isoforms change the 24R,25(OH)2D3 response.

(Figure 7, cont. from the previous page):

Overexpressing all ERα isoforms reversed the 24R,25(OH)$_2$D$_3$ anti-apoptotic effect in [**A, B**] HCC38 cells and [**C, D**] C2C12 cells. 24R,25(OH)$_2$D$_3$ prevented apoptosis as measured by [**A**] BAX/BCL2 and [**B**] total p53 levels in wild-type HCC38 and HCC38 cells transfected with an empty control vector, but induced apoptosis in ERα-transfected HCC38 cells. In C2C12 muscle cells, 24R,25(OH)$_2$D$_3$ prevented or did not induce apoptosis in wild-type cells but induced apoptosis in ERα-transfected cells as measured by [**C**] BAX/BCL2 and had no effect on apoptosis as measured by [**D**] total p53 levels in wild-type cells. Silencing the ERα66 isoform reversed the pro-apoptotic effect of 24R,25(OH)$_2$D$_3$ on [**E, F**] MCF7 cells. 24R,25(OH)$_2$D$_3$ induced apoptosis as measured by [**E**] BAX/BCL2 and [**F**] total p53 levels in wild-type and scramble-control MCF7 cells, but had no effect on apoptosis in ERα66-knocked down MCF7 cells.

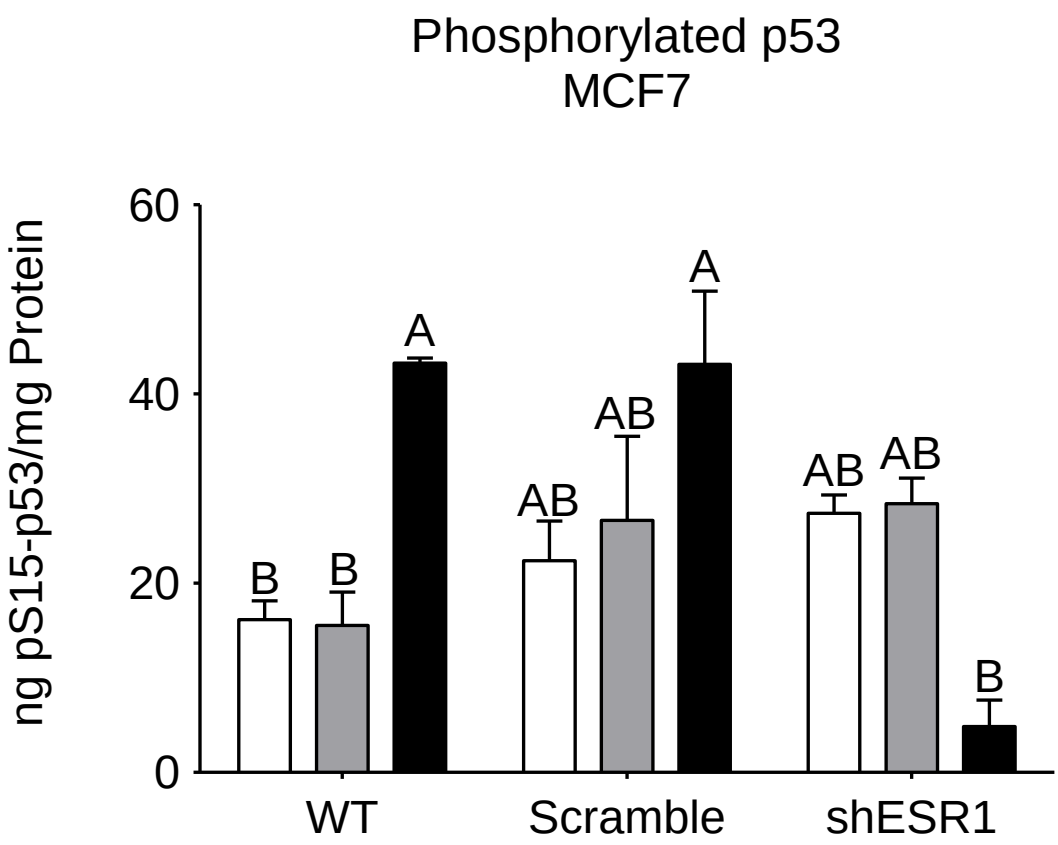

Figure 6.12 Silencing the ERα66 isoform reversed the pro-apoptotic effect of 24R,25(OH)2D3 on MCF7 cells.

24R,25(OH)$_2$D$_3$ significantly increased phosphorylated p53 levels in wild-type MCF7 cells and qualitatively increased phosphorylated p53 in scramble-control MCF7 cells. In MCF7 cells knocked down for ERα66, 24R,25(OH)$_2$D$_3$ qualitatively decreased average phosphorylated p53.

Discussion

Vitamin D metabolites may have anti-tumorigenic properties in breast cancer; however, many vitamin D3 metabolites are highly calcemic and have narrow therapeutic windows (34). Previously we identified an alternative endogenous vitamin D3 metabolite, 24R,25(OH)$_2$D$_3$, which has anti-tumorigenic and pro-apoptotic effects in the ERα66-positive breast cancer cell lines MCF7 and T47D(21) but, unlike other vitamin D3 metabolites, 24R,25(OH)$_2$D$_3$ is not calcemic at therapeutic doses (21,35). However, recent studies have shown that vitamin D supplementation may not be beneficial for all cancer patients (5,6), and some studies have shown that patients with estrogen receptor positive (ERα66+) breast cancer benefit from vitamin D supplements, but patients with estrogen receptor negative (ERα66-) breast cancer do not (4,7,36). The dependence of the estrogen receptor and its isoforms on the tumorigenicity of vitamin D metabolites is an understudied area of breast cancer research, and more investigation into the crosstalk between estrogen receptors and vitamin D metabolites is necessary to refine treatment protocols and vitamin D supplement regimens.

In this paper, the effects of 24R,25(OH)$_2$D$_3$ were investigated *in vivo* in an HCC38 xenograft orthotopic mammary fat pad model of breast cancer in an immuno-compromised NSG mouse, and *in vitro* in cell monolayer cultures of HCC38. The effects of 24R,25(OH)$_2$D$_3$ on models of HCC38 (ERα66-) breast cancer were contrasted with the effects of 24R,25(OH)$_2$D$_3$ in MCF7 (ERα66+); the ERα66 receptor was overexpressed and silenced in HCC38, MCF7, and a third unrelated cell line, C2C12, to understand how the expression of ERα66 modulates the effect of 24R,25(OH)$_2$D$_3$. Although 24R,25(OH)$_2$D$_3$ was not calcemic *in vivo*, treatment with 24R,25(OH)$_2$D$_3$ increased tumor

burden and decreased animal survival in mice with HCC38 (ERα66-) xenografts. *In vitro*, 24R,25(OH)$_2$D$_3$ specifically decreased apoptosis and increased proliferation, metastasis, and migration in HCC38 (ERα66-) cells. This pro-tumorigenic effect is in direct contrast to the pro-apoptotic and anti-metastatic effects of 24R,25(OH)$_2$D$_3$ on MCF7 cells (ERα66+). Overexpressing and silencing ERα66 found that in cells that do not express ERα66, 24R,25(OH)$_2$D$_3$ does not stimulate apoptosis and may be tumorigenic. In cells that express ERα66, 24R,25(OH)$_2$D$_3$ is pro-apoptotic and anti-tumorigenic. Our results suggest that ERα66 directly modulates the apoptotic effects of 24R,25(OH)$_2$D$_3$.

Our previous work showed that 24R,25(OH)$_2$D$_3$ is anti-tumorigenic in mammary fat pad xenografts of MCF7 (ERα66+) in NOD.*Cg-Prkdc^{scid}Il2rg^{tm1Wjl}*/SzJ (NSG) mice. Here, we use a similar *in vivo* model to test the effects of 24R,25(OH)$_2$D$_3$ on tumor burden in mammary fat pad xenografts of HCC38 (ERα66-) in NSG mice. These models allowed us to study the effects of 24R,25(OH)$_2$D$_3$ directly on the tumor, rather than the direct and indirect effects of 24R,25(OH)$_2$D$_3$ on the tumor and concomitant immunity. However, it is important to note that 24R,25(OH)$_2$D$_3$ has been shown to modulate the immune system, and clinically 24R,25(OH)$_2$D$_3$ could also indirectly affect tumor invasion and metastasis. Other studies have shown that both 1,25(OH)$_2$D$_3$ and 24R,25(OH)$_2$D$_3$ can alter the production of pro-and anti-inflammatory cytokines (16,17). 1α,25(OH)$_2$D$_3$ reduced the production of tumor necrosis factor α (TNFα) and interleukin-10 (IL-6) by tumor-associated monocytes (17). In our lab, we have shown that 24R,25(OH)$_2$D$_3$ reduced serum levels of TNFα, IL-6, interleukin-1α, interleukin-1β, and other pro-inflammatory factors in Sprague-Dawley rats with surgically transected anterior crucial ligaments (16). While studies in this paper with immune compromised animals have shown that

24R,25(OH)$_2$D$_3$ is capable of directly modulating tumor growth *in vivo*, it is possible that 24R,25(OH)$_2$D$_3$ may also alter the immune-regulation of carcinomas in immunocompetent animals, and more studies are required to explore this possibility further.

Previous results by our lab and others have shown that 24R,25(OH)$_2$D$_3$ has anti-carcinogenic properties, particularly in models of breast, lung, and glandular stomach carcinomas (18,19,21). However, high expression of 24-hydroxylase (CYP24A1), the enzyme responsible for metabolizing 25(OH)D$_3$ into 24R,25(OH)$_2$D$_3$, is associated with increased tumor aggression in several cancers including breast cancer (18–20,37). 24R,25(OH)$_2$D$_3$ has been shown to act both directly on several cell types such as bone, cartilage, kidney, and cancer cells, and indirectly by increasing the production of 1α-hydroxylated vitamin D$_3$ metabolites *in vivo* (38,39). Physiologically, 24R,25(OH)$_2$D$_3$ increases the expression of 1α-hydroxylase (CYP27B1) and 1α,25(OH)$_2$D$_3$, in turn, increases the expression of 24-hydroxylase (CYP24A1) (40). While HCC38 cells express both CYP24A1 and CYP27B1, our results and others have shown that MCF7 cells express CYP27B1 but do not express CYP24A1 (37,41). 1α,25(OH)$_2$D$_3$, a product of CYP27B1 activity, has been shown to have anti-tumorigenic activity in MCF7 *cells in vivo* and *in vitro* (42,43). CYP24A1 is a commonly mutated gene in cancers (44), and further study is needed to determine whether the tumorigenicity of 24R,25(OH)$_2$D$_3$ is related to native CYP24A1 expression within the tumor. It is possible that the MCF7 cells respond anti-tumorigenically to 24R,25(OH)$_2$D$_3$ because they are CYP24A1 negative, and this point should be explored further in future studies. Previous studies in our lab show that MCF7 cells respond with the greatest fold-change to 10^{-8}M 24R,25(OH)$_2$D$_3$ (21), while in

this paper we show that HCC38 cells are more sensitive to 10^{-7}M 24R,25(OH)$_2$D$_3$. This, coupled with the lack of CYP24A1 expression in MCF7, may indicate that MCF7 cells are more sensitive to 24R,25(OH)$_2$D$_3$ than HCC38 cells. This sensitivity may be a result of an increase in CYP27B1 and 1α-hydroxylated vitamin D$_3$ metabolite. Furthermore, our results with 24R,25(OH)$_2$D$_3$ on MCF7 and HCC38 cells may not be reflective of the direct effects of 24R,25(OH)$_2$D$_3$, but could be a result of shifting proportions of other vitamin D$_3$ metabolites caused by an influx of 24R,25(OH)$_2$D$_3$.

However, our data on the effect of 24R,25(OH)$_2$D$_3$ on phospholipase D (PLD) and protein kinase C (PKC) activity in breast cancer cells suggest that 24R,25(OH)$_2$D$_3$ can directly affect breast cancer cells. In male rat resting zone chondrocytes, the rapid actions of 24R,25(OH)$_2$D$_3$ are mediated by PLD, while the rapid actions of both 17β-estradiol and 1α,25(OH)$_2$D$_3$ are mediated by protein kinase C (PKC) (45). Our data show a similar effect, with 24R,25(OH)$_2$D$_3$ rapidly changing PLD activity in both HCC38 and MCF7, but not affecting PKC activity in HCC38 cells at the same time point. 24R,25(OH)$_2$D$_3$ slightly increased PKC activity in MCF7 cells at high doses, but this effect had a smaller fold change than the effect size of 24R,25(OH)$_2$D$_3$ on PLD activity in MCF7 cells. The rapid effect of 24R,25(OH)$_2$D$_3$ on PLD rather than PKC activity in HCC38 and MCF7 cells suggests that *in vitro*, 24R,25(OH)$_2$D$_3$ acts directly on both HCC38 cells and MCF7 cells rather than stimulating the production of another vitamin D$_3$ metabolite which is responsible for the effects of 24R,25(OH)$_2$D$_3$ on apoptosis, epithelial-to-mesenchymal transition, migration, and metastatic markers in these cells.

The connection between 24R,25(OH)$_2$D$_3$ and ERα66 has implications for many different cell types and tissues. Firstly, 24R,25(OH)$_2$D$_3$ has an established

chondroprotective effect and may prevent bone resorption by limiting calcium efflux in cartilage and bone cells (46). Post-menopausal women have a higher incidence of osteoarthritis than men of similar ages (47,48), and the extremely low levels of circulating estradiol in post-menopausal women have been implicated in this discrepancy (48,49); estradiol has a protective effect on bone, bone resorption, cartilage (48,50). Treatment with 24R,25(OH)$_2$D$_3$ has been proposed as a potential therapeutic for osteoarthritis patients, as 24R,25(OH)$_2$D$_3$ prevents oxidative damage and apoptosis in chondrocytes (16). However, all previous research on the chondroprotective effects of 24R,25(OH)$_2$D$_3$ has previously been done in male chondrocytes (16), who have higher circulating estradiol than post-menopausal women and lower expression of ERα66 (48,51,52). Further research on 24R,25(OH)$_2$D$_3$ and ERα66 should be done to ensure that the chondroprotective effects of 24R,25(OH)$_2$D$_3$ are clinically applicable to both men and women, and male and female chondrocytes may be an appropriate model to further investigate crosstalk between 24R,25(OH)$_2$D$_3$ and ERα.

Secondly, 24R,25(OH)$_2$D$_3$ is a naturally occurring ubiquitous metabolite of vitamin D$_3$. Serum 24R,25(OH)$_2$D$_3$ is present at higher levels in the blood than 1α,25(OH)$_2$D$_3$, the more commonly studied active metabolite of vitamin D$_3$ (53). Women with breast cancer have been reported to take vitamin D$_3$ supplements at a higher rate than the general population (4), and some of that supplemental vitamin D$_3$ is undoubtedly getting metabolized into 24R,25(OH)$_2$D$_3$ (54). Further investigation into the benefits of taking vitamin D$_3$ supplements for patients with ERα66+ and ERα66- breast cancer needs to be conducted, as our results imply that women with ERα66- breast cancer may be aggravating their tumors by taking excess vitamin D$_3$.

Conclusion

In summary, 24R,25(OH)$_2$D$_3$ modulates apoptosis and tumorigenicity in breast cancer cells through an ERα66-associated pathway. In ERα66-negative breast tumors, 24R,25(OH)$_2$D$_3$ increases tumor burden, migration, and metastasis, and may decrease survival. In ERα66-positive tumors, 24R,25(OH)$_2$D$_3$ induces apoptosis and reduces tumor burden. Our results show that overexpressing ERα66 in wild-type ERα66-negative HCC38 cells reverses the anti-apoptotic effect of 24R,25(OH)$_2$D$_3$ and causes treatment with 24R,25(OH)$_2$D$_3$ to induce apoptosis; likewise, silencing ERα66 in wild-type ERα66-positive MCF7 cells eliminates the pro-apoptotic effect of 24R,25(OH)$_2$D$_3$. Our results with C2C12, an unrelated cell line, showed that the regulation of the 24R,25(OH)$_2$D$_3$ effect by ERα66 is not limited to breast cancer cells; rather, treatment with 24R,25(OH)$_2$D$_3$ induced apoptosis in ERα66-overexpressing C2C12 cells. Our data show that ERα66 is a modulator of the apoptotic effect of 24R,25(OH)$_2$D$_3$ in a diverse array of cell lines, and should inform diverse research areas such as the implications of vitamin D supplementation in breast cancer patients and the potential of 24R,25(OH)$_2$D$_3$ as a therapeutic in male vs. female osteoarthritis patients.

Chapter 7.

Conclusions and Future Perspectives

Although high serum 25(OH)D$_3$ is often associated with improved prognosis and reduced risk of tumor recurrence in breast cancer patients, double-blind clinical trials investigating the efficacy of vitamin D$_3$ supplementation in cancer have been inconclusive. This is in part because breast cancer is a multifaceted disease with genetic and phenotypic variations. As such, the idea of making blanket treatment recommendations on vitamin D$_3$ supplementation may be as impractical as suggesting a single, defined cure for all types of breast cancer. Preliminary research on vitamin D$_3$ supplementation in breast cancer suggests that ER+ patients may benefit from vitamin D$_3$ supplementation, but ER- patients may not. This thesis demonstrates that 24R,25(OH)$_2$D$_3$ is functionally active in breast cancer cells and that the tumorigenicity of 24R,25(OH)$_2$D$_3$ is regulated in part by ERα66.Furthermore, this work suggests that crosstalk between 24R,25(OH)$_2$D$_3$ and ERα66 may not be cell-type specific, and the actions of 24R,25(OH)$_2$D$_3$ on apoptosis may have implications for other disease states.

Like other steroid hormones, 24R,25(OH)$_2$D$_3$ has been found to initiate multiple rapid signaling pathways from the cell membrane in chondrocytes, and a membrane receptor has been implicated, which remains the subject of active investigation. Here, we show evidence that the rapid actions of 24R,25(OH)$_2$D$_3$ are conserved across cell types, with 24R,25(OH)$_2$D$_3$ regulating proliferation and apoptosis in MCF7, HCC38, and C2C12 cells – three unrelated cell lines from different species, tissues, and with different ERα profiles. Furthermore, the regulation of proliferation and apoptosis by 24R,25(OH)$_2$D$_3$ was

specific to the 'R' enantiomer. 24S,25(OH)$_2$D$_3$ did not have an effect on apoptosis in either MCF7 or HCC38 cells.

Our results also demonstrated that in MCF7 and HCC38 cells, 24R,25(OH)$_2$D$_3$ stimulates PLD at 9 minutes. Extensive studies in chondrocytes have shown that 24R,25(OH)$_2$D$_3$ also stimulates PLD after 9 minutes[15]. In proliferative chondrocytes, 24R,25(OH)$_2$D$_3$ has been shown to prevent apoptosis through a PLD-dependent mechanism by promoting p53 degradation via ubiquitination. This is similar to the mechanism we observed in HCC38 breast cancer cells, where 24R,25(OH)$_2$D$_3$ prevented apoptosis by decreasing p53 production. This suggests that 24R,25(OH)$_2$D$_3$ regulates apoptosis in proliferating chondrocytes and ERα66-negative breast cancer cells through the same PLD, p53-dependent mechanism.

Many of the second messengers of the rapid signaling pathway of 24R,25(OH)$_2$D$_3$, such as PLD and PKC, are also implicated in 17β-estradiol (E$_2$) signaling through the membrane receptor ERα36. Our results show that E$_2$ signaling through ERα36 is tumorigenic in laryngeal cancer as well as breast cancer, suggesting that E$_2$ signaling through ERα36 might also regulate apoptosis in other disease states. We also show that, as in breast cancer, ERα66-, ERα36+ laryngeal cancer is more aggressive than its ERα66+, ERα36+ counterparts.

Many of the rapid signaling pathways activated by E$_2$ binding to ERα36 in laryngeal cancer are also activated by 24R,25(OH)$_2$D$_3$ in breast cancer. Our results suggest that the rapid actions of 24R,25(OH)$_2$D$_3$ in MCF7 (ERα66+, ERα36+) breast cancer cells may be modulated by a membrane-mediated, caveolae-localized pathway employing a palmitoylated nuclear receptor to stimulate PLD with downstream regulatory effects on

apoptosis, proliferation, migration, and metastasis. In MCF7 (ERα66+, ERα36+), 24R,25(OH)$_2$D$_3$ confers a chemoprotective effect against breast cancer cells *in vitro* and *in vivo* to prevent tumorigenesis and reduce metastasis.

Our work with MCF7 (ERα66+, ERα36+) showed that the chemoprotective effects of 24R,25(OH)$_2$D$_3$ were dependent upon activation of isoforms of ERα in this cell line. This suggested that ERα isoforms may modulate 24R,25(OH)$_2$D$_3$ in breast cancer cells. The effects of 24R,25(OH)$_2$D$_3$ on tumorigenicity were examined in a second cell line, HCC38, which does not express ERα66 (ERα66-, ERα36+). 24R,25(OH)$_2$D$_3$ was tumorigenic in HCC38 (ERα66-, ERα36+), and this tumorigenicity was initiated by a PLD-dependent signaling mechanism. Overexpressing ERα66 in HCC38 (ERα66-, ERα36+) reversed the tumorigenic effects of 24R,25(OH)$_2$D$_3$, suggesting that ERα66 may modulate the rapid actions of 24R,25(OH)$_2$D$_3$. We also overexpressed ERα66 and ERα36 in an unrelated cell line, C2C12, and found that 24R,25(OH)$_2$D$_3$ increased apoptosis in C2C12 cells that overexpressed ERα66 and ERα36. And wild-type MCF7 (ERα66+, ERα36+) and ERα66-silenced MCF7 (ERα66-, ERα36+) were tested for 24R,25(OH)$_2$D$_3$-induced apoptosis, and we found that in wild-type and scramble-transfected MCF7 cells, 24R,25(OH)$_2$D$_3$ induced apoptosis; however in ERα66-silenced MCF7 cells, 24R,25(OH)$_2$D$_3$ did not stimulate apoptosis. This demonstrates that the pro-apoptotic effect of 24R,25(OH)$_2$D$_3$ is dependent upon the ERα66 isoform across cell lines.

The implications of this in the wake of similarities between 24R,25(OH)$_2$D$_3$ signaling in chondrocytes, MCF7, and HCC38 cells are interesting. The 24R,25(OH)$_2$D$_3$ signaling pathway was discovered and tested in male rat chondrocytes, where 24R,25(OH)$_2$D$_3$ was found to prevent apoptosis. Male rat chondrocytes express all

isoforms of ERα, including ERα66 and ERα36. However, female rat chondrocytes express roughly equal amounts of ERα66 in the plasma membrane, caveolae, and nucleus[324]. Male rat chondrocytes expressed more ERα66 in the plasma membrane and caveolae fraction than in the nucleus. Furthermore, ERα36 was found at similar levels in the plasma membrane and nucleus of female rat chondrocytes. However male rat chondrocytes only expressed ERα36 in the nucleus, and did not express detectable levels of ERα36 in the plasma membrane or the caveolae[324]. It is worth noting that ERβ levels were the same in female and male rat chondrocytes[324]. Similarly, MCF7 cells express high levels of ERα isoforms in the plasma membrane and nucleus, while HCC38 cells only express ERα isoforms in the membrane[1,27]. Perhaps the pro-apoptotic effects of 24R,25(OH)$_2$D$_3$ are regulated not by ERα66 itself, but by an abundance of nuclear ERα isoforms rather than an abundance of membrane ERα isoforms.

This work provides a foundation for the further investigation of 24R,25(OH)$_2$D$_3$ as a modulator of tumorigenicity in breast cancer, and suggests that vitamin D$_3$ supplementation should only be considered for patients with ER+, or ERα66+, breast cancer. Our lab has begun developing a means of assessing 24R,25(OH)$_2$D$_3$ metabolite expression by HPLC. We plan to use this technique to measure the local production of 24R,25(OH)$_2$D$_3$ in breast tissue. Later on, we plan to assess 24R,25(OH)$_2$D$_3$ metabolite levels in banked serum samples from breast cancer patients. A meta-analysis can be conducted to assess correlations between circulating 24R,25(OH)$_2$D$_3$ metabolite expression and ERα66 and ERα36 expression in breast cancer.

Preliminary results from these studies also suggest that 24R,25(OH)$_2$D$_3$ can alter markers of osteoclast activation in breast tumors. In MCF7 (ERα66+, ERα36+)

24R,25(OH)$_2$D$_3$ reduced markers of osteoclast activation and in HCC38 (ERα66-, ERα36+) 24R,25(OH)$_2$D$_3$ enhanced markers of osteoclast activation and osteoclast activity in HCC38. Stage 4 ER+ breast cancer commonly metastasizes to the long bone and spine, and 5-year survival rates for patients with late-stage bone metastasis are around 22%. 24R,25(OH)$_2$D$_3$ may have potential as a therapeutic for these patients. Our lab has established a model of breast tumor osteolysis in murine femurs, and we are planning to examine the effect of 24R,25(OH)$_2$D$_3$ on models of ER+ and ER-breast cancer metastasis in mice. If these pre-clinical studies show that 24R,25(OH)$_2$D$_3$ is efficacious against ER+ breast cancer metastasis, we would suggest a clinical trial on the use of 24R,25(OH)$_2$D$_3$ supplementation in breast cancer patients.

References

1. Chaudhri RA, Olivares-Navarrete R, Cuenca N, Hadadi A, Boyan BD, Schwartz Z. Membrane estrogen signaling enhances tumorigenesis and metastatic potential of breast cancer cells via estrogen receptor α 36 (ERα36). J Biol Chem 2012;287(10):7169-7181.
2. Howlader N, Noone A, Krapcho M. *SEER Cancer Statistics Review*. Bethesda, MD
3. Rooney MR, Harnack L, Michos ED, Ogilvie RP, Sempos CT, Lutsey PL. Trends in use of high-dose vitamin D supplements exceeding 1000 or 4000 international units daily, 1999-2014. JAMA - J Am Med Assoc 2017;317(23):2448-2450.
4. Crew KD, Shane E, Cremers S, McMahon DJ, Irani D, Hershman DL. High prevalence of vitamin D deficiency despite supplementation in premenopausal women with breast cancer undergoing adjuvant chemotherapy. J Clin Oncol 2009;27(13):2151-2156.
5. Yao S, Sucheston LE, Millen AE, et al. Pretreatment serum concentrations of 25-hydroxyvitamin D and breast cancer prognostic characteristics: A case-control and a case-series study. PLoS One 2011;6(2).
6. Scragg R, Khaw K-T, Toop L, et al. Monthly high-dose vitamin D supplementation and cancer risk. JAMA Oncol 2018;4(11):e182178.
7. Manson JE, Cook NR, Lee I-M, et al. Vitamin D supplements and prevention of cancer and cardiovascular disease. N Engl J Med 2019;380(1):33-44.
8. Poole EM, Shu X, Caan BJ, et al. Postdiagnosis supplement use and breast cancer prognosis in the After Breast Cancer Pooling Project. Breast Cancer Res Treat 2013;139(2):529-537.

9. Sheikh MS, Garcia M, Pujol P, Fontana JA, Rochefort H. Why are estrogen-receptor-negative breast cancers more aggressive than the estrogen-receptor-positive breast cancers? Invasion Metastasis 1994;14(1-6):329-336.
10. Dalmau E, Armengol-Alonso A, Muñoz M, Seguí-Palmer MÁ. Current status of hormone therapy in patients with hormone receptor positive (HR+) advanced breast cancer. Breast 2014;23(6):710-720.
11. Niv Y. Estrogen receptor β expression and colorectal cancer: A systematic review and meta-analysis. Eur J Gastroenterol Hepatol 2015;27(12):1438-1442.
12. Prossnitz ER, Barton M. Estrogen biology: New insights into GPER function and clinical opportunities. Mol Cell Endocrinol 2014;389(1-2):71-83.
13. Jones G, Prosser DE. The activating enzymes of vitamin D metabolism (25- and 1α-hydroxylases). In: Feldman D, Pike JW, Adams JS, eds. *Vitamin D*. 3rd ed. Academic Press; 2013:23-42.
14. Swami S, Krishnan A V, Wang JY, et al. Dietary vitamin D$_3$ and 1,25-dihydroxyvitamin D$_3$ (calcitriol) exhibit equivalent anticancer activity in mouse xenograft models of breast and prostate cancer. Endocrinology 2012;153(6):2576-2587.
15. Sylvia VL, Schwartz Z, Y Y, et al. Regulation of phospholipase D (PLD) in growth plate chondrocytes by 24R ,25-(OH)2D3 is dependent on cell maturation state (resting zone cells) and is specific to the PLD2 isoform. Biochim Biophys Acta 2001;1499(3):209-221.
16. Schwartz Z, Sylvia VL, Luna MH, et al. The effect of 24R,25-(OH)$_2$D$_3$ on protein kinase C activity in chondrocytes is mediated by phospholipase D whereas the

effect of 1α,25-(OH)$_2$D$_3$ is mediated by phospholipase C. Steroids 2001;66(9):683-694.

17. Schwartz Z, Sylvia VL, Del Toro F, Hardin RR, Dean DD, Boyan BD. 24R,25-(OH)2D3 mediates its membrane receptor-dependent effects on protein kinase C and alkaline phosphatase via phospholipase A$_2$ and cyclooxygenase-1 but not cyclooxygenase-2 in growth plate chondrocytes. J Cell Physiol 2000;182(3):390-401.
18. Hurst-Kennedy J, Zhong M, Gupta V, Boyan BD, Schwartz Z. 24R,25-dihydroxyvitamin D3, lysophosphatidic acid, and p53: a signaling axis in the inhibition of phosphate-induced chondrocyte apoptosis. J Steroid Biochem Mol Biol 2010;122(4):264-271.
19. Seo E, Kato A, Norman AW. Evidence for a 24R,25(OH)2-vitamin D3 receptor/ binding protein in a membrane fraction isolated from a chick tibial fracture-healing callus. Biochem Biophys Res Commun 1996;208(225):203-208.
20. Kato A, Seo E-G, Einhorn T., Bishop J., Norman A. Studies on 24R,25-dihydroxyvitamin D3: Evidence for a nonnuclear membrane receptor in the chick tibial fracture-healing callus. Bone 1998;23(2):141-146.
21. Larsson D, Anderson D, Smith NM, Nemere I. 24,25-Dihydroxyvitamin D$_3$ binds to catalase. J Cell Biochem 2006;97(6):1259-1266.
22. Martineau C, Naja RP, Husseini A, et al. Optimal bone fracture repair requires 24R,25-dihydroxyvitamin D$_3$ and its effector molecule FAM57B2. J Clin Invest 2018;25(8):3546-3557.
23. Boyan BD, Sylvia VL, Dean DD, Schwartz Z. 24,25(OH)$_2$D$_3$ regulates cartilage and

bone via autocrine and endocrine mechanisms. Steroids 2001;66(3-5):363-374.

24. Prossnitz E, Arterburn JB, Sklar LA. GPR30: a G protein-coupled receptor for estrogen. Mol Cell Endocrinol 2007;265-266(505):138-142.
25. Deroo BJ, Buensuceso A V. Minireview: Estrogen Receptor-β: Mechanistic Insights from Recent Studies. Mol Endocrinol 2010;24(9):1703-1714.
26. Böttner M, Thelen P, Jarry H. Estrogen receptor beta: Tissue distribution and the still largely enigmatic physiological function. J Steroid Biochem Mol Biol 2014;139:245-251.
27. Chaudhri RA, Schwartz N, Elbaradie K, Schwartz Z, Boyan BD. Role of ERα36 in membrane-associated signaling by estrogen. Steroids 2014;81(1):74-80.
28. Buschke S, Stark H-J, Cerezo A, et al. A decisive function of transforming growth factor-β/Smad signaling in tissue morphogenesis and differentiation of human HaCaT keratinocytes. Mol Biol Cell 2011;22(6):782-794.
29. Mangelsdorf DJ, Thummel C, Beato M, et al. The nuclear receptor superfamily: The second decade. Cell 1995;83:835-839.
30. Kousteni S, Bellido T, Plotkin LI, et al. Nongenotropic, sex-nonspecific signaling through the estrogen or androgen receptors: dissociation from transcriptional activity. Cell 2001;104(5):719-730.
31. Vertino AM, Bula CM, Chen J-RR, et al. Nongenotropic, anti-apoptotic signaling of 1α,25(OH)2-vitamin D3 and analogs through the ligand binding domain of the vitamin D receptor in osteoblasts and osteocytes. J Biol Chem 2005;280(14):14130-14137.
32. Grazzini E, Guillon G, Mouillac B, Zingg HH. Inhibition of oxytocin receptor function

by direct binding of progesterone. Nature 1998;392(6675):509-512.

33. Peluso JJ. Multiplicity of progesterone's actions and receptors in the mammalian ovary. Biol Reprod 2006;75(1):2-8.
34. Hammes SR, Levin ER. Extranuclear steroid receptors: Nature and actions. Endocr Rev 2007;28(7):726-741.
35. Pedram A, Razandi M, Sainson RCA, Kim JK, Hughes CC, Levin ER. A conserved mechanism for steroid receptor translocation to the plasma membrane. J Biol Chem 2007;282(31):22278-22288.
36. Pedram A, Razandi M, Levin ER. Nature of functional estrogen receptors at the plasma membrane. Mol Endocrinol 2006;20(9):1996-2009.
37. Boonyaratanakornkit V, McGowan E, Sherman L, Mancini MA, Cheskis BJ, Edwards DP. The role of extranuclear signaling actions of progesterone receptor in mediating progesterone regulation of gene expression and the cell cycle. Mol Endocrinol 2007;21(2):359-375.
38. Gaudet HM, Cheng SB, Christensen EM, Filardo EJ. The G-protein coupled estrogen receptor, GPER: The inside and inside-out story. Mol Cell Endocrinol 2015;418 Pt 3:207-219.
39. Norman AW. Minireview: Vitamin D receptor: New assignments for an already busy receptor. Endocrinology 2006;147(12):5542-5548.
40. Levin ER. Minireview: Extranuclear steroid receptors: Roles in modulation of cell functions. Mol Endocrinol 2011;25(3):377-384.
41. Boyan BD, Chen J, Schwartz Z. Mechanism of Pdia3-dependent 1α,25-dihydroxy vitamin D3 signaling in musculoskeletal cells. Steroids 2012;77(10):892-896.

42. Wang Z, Zhang X, Shen P, Loggie BW, Chang Y, Deuel TF. Identification, cloning, and expression of human estrogen receptor-α36, a novel variant of human estrogen receptor-α66. Biochem Biophys Res Commun 2005;336(4):1023-1027.

43. Al-Bader M, Ford C, Al-Ayadhy B, Francis I. Analysis of estrogen receptor isoforms and variants in breast cancer cell lines. Exp Ther Med 2011;2(3):537-544.

44. Gros R, Ding Q, Sklar LA, et al. GPR30 expression is required for the mineralocorticoid receptor-independent rapid vascular effects of aldosterone. Hypertension 2011;57(3):442-451.

45. Gellersen B, Fernandes MS, Brosens JJ. Non-genomic progesterone actions in female reproduction. Hum Reprod Update 2008;15(1):119-138.

46. Kampa M, Pelekanou V, Castanas E. Membrane-initiated steroid action in breast and prostate cancer. Steroids 2008;73(9-10):953-960.

47. Santen RJ, Fan P, Zhang Z, Bao Y, Song RX-D, Yue W. Estrogen signals via an extra-nuclear pathway involving IGF-1R and EGFR in tamoxifen-sensitive and -resistant breast cancer cells. Steroids 2009;74(7):586-594.

48. Bagchi G, Wu J, French J, Kim J, Moniri NH, Daaka Y. Androgens transduce the G alphas-mediated activation of protein kinase A in prostate cells. Cancer Res 2008;68(9):3225-3231.

49. Pedram A, Razandi M, Deschenes RJ, Levin ER. DHHC-7 and -21 are palmitoylacyltransferases for sex steroid receptors. Mol Biol Cell 2012;23(1):188-199.

50. Razandi M, Pedram A, Levin ER. Heat shock protein 27 is required for sex steroid receptor trafficking to and functioning at the plasma membrane. Mol Cell Biol

2010;30(13):3249-3261.

51. Moriarty K, Kim KH, Bender JR. Minireview: Estrogen receptor-mediated rapid signaling. Endocrinology 2006;147(12):5557-5563.
52. Razandi M, Oh P, Pedram A, Schnitzer J, Levin ER. ERs associate with and regulate the production of caveolin: Implications for signaling and cellular actions. Mol Endocrinol 2002;16(1):100-115.
53. Huhtakangas JA, Olivera CJ, Bishop JE, Zanello LP, Norman AW. The vitamin D receptor is present in caveolae-enriched plasma membranes and binds 1 alpha,25(OH)2-vitamin D3 in vivo and in vitro. Mol Endocrinol 2004;18(11):2660-2671.
54. Mizwicki MT, Keidel D, Bula CM, et al. Identification of an alternative ligand-binding pocket in the nuclear vitamin D receptor and its functional importance in 1α,25(OH)$_2$-vitamin D$_3$ signaling. Proc Natl Acad Sci U S A 2004;101(35):12876-12881.
55. Chaudhri RA, Hadadi A, Lobachev KS, Schwartz Z, Boyan BD. Estrogen receptor-α 36 mediates the anti-apoptotic effect of estradiol in triple negative breast cancer cells via a membrane-associated mechanism. Biochim Biophys Acta 2014;1843(11):1-11.
56. Wang Q, Jiang J, Ying G, et al. Tamoxifen enhances stemness and promotes metastasis of ERα36+ breast cancer by upregulating ALDH1A1 in cancer cells. Cell Res 2018;28(3):336-358.
57. Zhang X, Ding L, Kang L, Wang Z-Y. Estrogen receptor-alpha 36 mediates mitogenic antiestrogen signaling in ER-negative breast cancer cells. PLoS One

2012;7(1):e30174.

58. Chantalat E, Boudou F, Laurell H, et al. The AF-1-deficient estrogen receptor ERα46 isoform is frequently expressed in human breast tumors. Breast Cancer Res 2016;18(1):1-16.

59. Gozgit JM, Pentecost BT, Marconi SA, Otis CN, Wu C, Arcaro KF. Use of an aggressive MCF-7 cell line variant, TMX2-28, to study cell invasion in breast cancer. Mol Cancer Res 2006;4(12):905-913.

60. Hunakova L, Sedlakova O, Cholujova D, Gronesova P, Duraj J, Sedlak J. Modulation of markers associated with aggressive phenotype in MDA-MB-231 breast carcinoma cells by sulforaphane. Neoplasma 2009;56(6):548-556.

61. Verma A, Schwartz Z, Boyan BD. 24R,25-dihydroxyvitamin D3 modulates tumorigenicity in breast cancer in an estrogen receptor-dependent manner. Steroids (Under Rev.

62. Grenman R, Virolainen E, Shapira A, Carey T. In vitro effects of tamoxifen on UM-SCC head and neck cancer cell lines: Correlation with the estrogen and progesterone receptor content. Int J Cancer 1987;39(1):77-81.

63. Shapira A, Virolainen E, Jameson JJ, Ossakow SJ, Carey TE. Growth inhibition of laryngeal UM-SCC cell lines by tamoxifen. Comparison with effects on the MCF-7 breast cancer cell line. Arch Otolaryngol Head Neck Surg 1986;112(11):1151-1158.

64. Robbins KT, Vu TP, Diaz A, Varki NM. Growth effects of tamoxifen and estradiol on laryngeal carcinoma cell lines. Arch Otolaryngol Head Neck Surg 1994;120(11):1261-1266.

65. Urba SG, Carey TE, Kudla-Hatch V, Wolf GT, Forastiere AA. Tamoxifen therapy in

patients with recurrent laryngeal squamous carcinoma. Laryngoscope 1990;100.

66. Schwartz N, Chaudhri RA, Hadadi A, Schwartz Z, Boyan BD. 17β-estradiol promotes aggressive laryngeal cancer through membrane-associated estrogen receptor-α 36. Horm Cancer 2014;5(1):22-32.
67. Schwartz N, Verma A, Muktipaty C, Bivens C, Schwartz Z, Boyan BD. Estradiol receptor profile and estrogen responsiveness in laryngeal cancer and clinical outcomes. Steroids 2019;142(2):34-42.
68. Schwartz N, Verma A, Bivens CB, Schwartz Z, Boyan BD. Rapid steroid hormone actions via membrane receptors. Biochim Biophys Acta - Mol Cell Res 2016;1863(9):2289-2298.
69. Clarke R, Tyson JJ, Dixon JM. Endocrine resistance in breast cancer- an overview and update. Mol Cell Endocrinol 2015;418(3):220-234.
70. Gouliomis AK, Fuxe J, Varakis J, Repanti M, Goumas P, Papadaki H. Estrogen receptor-ß expression in human laryngeal carcinoma: Correlation with the expression of epithelial-mesenchymal transition specific biomarkers. Oncol Rep 2009;22(5):1063-1068.
71. Wu D, Jiang JJ, Fang R, Swinarski K, Cui X. G protein-coupled estrogen receptor 1 expression in human vocal fold. Laryngoscope 2013;123(4):948-951.
72. Zhao XZ, Liu Y, Zhou LJ, Wang ZQ, Wu ZH, Yang XY. Role of estrogen in lung cancer based on the estrogen receptor-epithelial mesenchymal transduction signaling pathways. Onco Targets Ther 2015;8:2849-2863.
73. Collins P, Webb C. Estrogen hits the surface. Nat Med 1999;5(10):1130-1131.
74. Shi X, Peng Y, Du X, et al. Estradiol promotes epithelial-to-mesenchymal transition

in human benign prostatic epithelial cells. Prostate 2017;77(14):1424-1437.

75. Hall JM, Couse JF, Korach KS. The Multifaceted Mechanisms of Estradiol and Estrogen Receptor Signaling. J Biol Chem 2001;276(40):36869-36872.
76. Katzenellenbogen BS, Kendra KL, Norman MJ, Berthois Y. Proliferation, hormonal responsiveness, and estrogen receptor content of MCF-7 human breast cancer cells grown in the short-term and long-term absence of estrogens. Cancer Res 1987;47(16):4355-4360.
77. Bredfeldt TG, Greathouse KL, Safe SH, Hung M-C, Bedford MT, Walker CL. Xenoestrogen-induced regulation of EZH2 and histone methylation via estrogen receptor signaling to PI3K/AKT. Mol Endocrinol 2010;24(5):993-1006.
78. Adlanmerini M, Solinhac R, Abot A, et al. Mutation of the palmitoylation site of estrogen receptor α in vivo reveals tissue-specific roles for membrane versus nuclear actions. Proc Natl Acad Sci U S A 2014;111(2):E283-90.
79. Marino M, Galluzzo P, Ascenzi P. Estrogen signaling multiple pathways to impact gene transcription. Curr Genomics 2006;7(8):497-508.
80. Dunbier AK, Anderson H, Ghazoui Z, et al. Relationship between plasma estradiol levels and estrogen-responsive gene expression in estrogen receptor-positive breast cancer in postmenopausal women. J Clin Oncol 2010;28(7):1161-1167.
81. Treilleux, Peloux N, Brown MS, Sergeant A. Human estrogen receptor (ER) gene promoter-P1: Estradiol-independent activity and estradiol inducibility in ER+ and ER- cells. Mol Endocrinol 1997;11(9):1319-1331.
82. Luo H, Yang G, Yu T, et al. GPER-mediated proliferation and estradiol production in breast cancer-associated fibroblasts. Endocr Relat Cancer 2014;21(2):355-369.

83. Zhang XT, Kang LG, Ding L, Vranic S, Gatalica Z, Wang Z-Y. A positive feedback loop of ER-α36/EGFR promotes malignant growth of ER-negative breast cancer cells. Oncogene 2011;30(7):770-780.

84. Verma A, Schwartz N, Boyan BD, Schwartz Z. Estrogen signaling and estrogen receptors as prognostic indicators in laryngeal cancer. Steroids (Under Rev.

85. Almeida M, Han L, O'Brien CA, Kousteni S, Manolagas SC. Classical genotropic versus kinase-initiated regulation of gene transcription by the estrogen receptor alpha. Endocrinology 2006;147(4):1986-1996.

86. Wang Z, Zhang X, Shen P, Loggie BW, Chang Y, Deuel TF. A variant of estrogen receptor-α, hER-α36: Transduction of estrogen- and antiestrogen-dependent membrane-initiated mitogenic signaling. Proc Natl Acad Sci U S A 2006;103(24):9063-9068.

87. Pelekanou V, Notas G, Kampa M, et al. ERα36, a new variant of the ERα is expressed in triple negative breast carcinomas and has a specific transcriptomic signature in breast cancer cell lines. Steroids 2012;77(10):928-934.

88. Chamard-Jovenin C, Jung AC, Chesnel A, et al. From ERα66 to ERα36: a generic method for validating a prognosis marker of breast tumor progression. BMC Syst Biol 2015;9(28):1-7.

89. Somers KD, Koenig M, Schechter GL. Growth of head and neck squamous cell carcinoma in nude mice: Potentiation of laryngeal carcinoma by 17 beta-estradiol. J Natl Cancer Inst 1988;80(9):688-691.

90. Dorsey M, Benghuzzi H, Tucci M, Cason Z. Growth and cell viability of estradiol and IP-6 treated Hep-2 laryngeal carcinoma cells. Biomed Sci Instrum

2005;41:205-210.

91. Resta L, Marsigliante S, Leo G, Fiorella R, Di Nicola V, Maiorano E. Molecular biopathology of metaplastic, dysplastic, and neoplastic laryngeal epithelium. Acta Otolaryngol Suppl 1997;527:39-42.
92. Hurst-Kennedy J, Boyan BD, Schwartz Z. Lysophosphatidic acid signaling promotes proliferation, differentiation, and cell survival in rat growth plate chondrocytes. Biochim Biophys Acta 2009;1793(5):836-846.
93. Boyan BD, Hurst-Kennedy J, Denison TA, Schwartz Z. 24R,25-dihydroxyvitamin D3 [24R,25(OH)$_2$D$_3$] controls growth plate development by inhibiting apoptosis in the reserve zone and stimulating response to 1α,25(OH)$_2$D$_3$ in hypertrophic cells. J Steroid Biochem Mol Biol 2010;121(1-2):212-216.
94. Díaz L, Díaz-Muñoz M, García-Gaytán AC, Méndez I. Mechanistic effects of calcitriol in cancer biology. Nutrients 2015;7(6):5020-5050.
95. St-Arnaud R. CYP24A1-deficient mice as a tool to uncover a biological activity for vitamin D metabolites hydroxylated at position 24. J Steroid Biochem Mol Biol 2010;121(1-2):254-256.
96. Seo E-G, Schwartz Z, Dean DD, Norman a W, Boyan BD. Preferential accumulation *in vivo* of 24R,25-dihydroxyvitamin D3 in growth plate cartilage of rats. Endocrine 1996;5(2):147-155.
97. Luo W, Karpf AR, Deeb KK, et al. Epigenetic regulation of vitamin D 24-hydroxylase/CYP24A1 in human prostate cancer. Cancer Res 2010;70(14):5953-5962.
98. Höbaus J, Tennakoon S, Heffeter P, et al. Impact of CYP24A1 overexpression on

growth of colorectal tumour xenografts in mice fed with vitamin D and soy. Int J cancer 2016;138(2):440-450.

99. Scheible C, Thill M, Baum S, Solomayer E, Friedrich M. Implication of CYP24A1 splicing in breast cancer. 2014;49(0):109-114.
100. Luo W, Hershberger PA, Trump DL, Johnson CS. 24-Hydroxylase in cancer: Impact on vitamin D-based anticancer therapeutics. J Steroid Biochem Mol Biol 2013;136:252-257.
101. Yamato H, Matsumoto T, Fukumoto S, Ikeda K, Ishizuka S, Ogata E. Effect of 24,25-Dihydroxyvitamin D3 on 1,25- Dihydroxyvitamin D3 [1,25-(OH)2D3] metabolism in vitamin D-deficient rats infused with 1,25-(OH)2D3. Endocrinology 2014;124(1):511-517.
102. Ohyama Y, Yamasaki T. Eight cytochrome P450s catalyze vitamin D metabolism. Front Biosci 2004;9:3007-3018.
103. Swain LD, Schwartz Z, Boyan BD. 1,25-(OH)$_2$D$_3$ and 24,25-(OH)$_2$D$_3$ regulation of arachidonic acid turnover in chondrocyte cultures is cell maturation-specific and may involve direct effects on phospholipase A$_2$. Biochim Biophys Acta 1992;1136(1):45-51.
104. Schwartz Z, Boyan BD. The effects of vitamin D metabolites on phospholipase A2 activity of growth zone and resting zone cartilage cells in vitro. Endocrinology 1988;122(5).
105. Schwartz Z, Sylvia VL, Curry D, Luna MH, Dean DD, Boyan BD. Arachidonic acid directly mediates the rapid effects of 24,25-dihydroxyvitamin D$_3$ via protein kinase C and indirectly through prostaglandin production in resting zone chondrocytes.

Endocrinology 1999;140(7):2991-3002.

106. Schwartz Z, Schlader DL, Swain LD, Boyan BD. Direct effects of 1,25-dihydroxyvitamin D_3 and 24,25- dihydroxyvitamin D_3 on growth zone and resting zone chondrocyte membrane alkaline phosphatase and phospholipase-A_2 specific activities. Endocrinology 1988;123(6):2878-2884.
107. Swain LD, Schwartz Z, Caulfield K, Brooks BP, Boyan BD. Nongenomic regulation of chondrocyte membrane fluidity by 1,25-$(OH)_2D_3$ and 24,25-$(OH)_2D_3$ is dependent on cell maturation. Bone 1993;14(4):609-617.
108. Boyan BD, Dean DD, Sylvia VL, Schwartz Z. Steroid hormone action in musculoskeletal cells involves membrane receptor and nuclear receptor mechanisms. Connect Tissue Res 2003.
109. Zhang X, Deng H, Wang Z-Y. Estrogen activation of the mitogen-activated protein kinase is mediated by ER-α36 in ER-positive breast cancer cells. J Steroid Biochem Mol Biol 2014;143:434-443.
110. Clarke R, Liu MC, Bouker KB, et al. Antiestrogen resistance in breast cancer and the role of estrogen receptor signaling. Oncogene 2003;22(47):7316-7339.
111. Garland CF, Gorham ED, Mohr SB, et al. Vitamin D and prevention of breast cancer: Pooled analysis. J Steroid Biochem Mol Biol 2007;103(3-5):708-711.
112. Mohr SB, Gorham ED, Kim J, Hofflich H, Garland CF. Meta-analysis of vitamin D sufficiency for improving survival of patients with breast cancer. Anticancer Res 2014;34(3):1163-1166.
113. Garland CF, Garland FC, Gorham ED, et al. The role of vitamin D in cancer prevention. Am J Public Health 2006;96(2):252-261.

114. Tavera-Mendoza LE, Westerling T, Libby E, et al. Vitamin D receptor regulates autophagy in the normal mammary gland and in luminal breast cancer cells. Proc Natl Acad Sci 2017:E2186-E2194.

115. Simboli-Campbell M, Narvaez CJ, van Weelden K, Tenniswood M, Welsh J. Comparative effects of 1,25(OH)$_2$D$_3$ and EB1089 on cell cycle kinetics and apoptosis in MCF-7 breast cancer cells. Breast Cancer Res Treat 1997;42(1):31-41.

116. Yuan L, Jiang R, Yang Y, Ding S, Deng H. 1,25-Dihydroxyvitamin D$_3$ inhibits growth of the breast cancer cell line MCF-7 and downregulates cytochrome P4501B1 through the COX-2/PGE2 pathway. Oncol Rep 2012;28(6):2131-2137.

117. Leyssens C, Verlinden L, Verstuyf A. Antineoplastic effects of 1,25(OH)$_2$D$_3$ and its analogs in breast, prostate and colorectal cancer. Endocr Relat Cancer 2013;20(2):R31-R47.

118. Richard CL, Farach-Carson MC, Rohe B, Nemere I, Meckling KA. Involvement of 1,25D$_3$-MARRS (membrane associated, rapid response steroid-binding), a novel vitamin D receptor, in growth inhibition of breast cancer cells. Exp Cell Res 2010;316(5):695-703.

119. Jiang YJ, Teichert AE, Fong F, Oda Y, Bikle DD. 1α,25(OH)$_2$-dihydroxyvitamin D$_3$/VDR protects the skin from UVB-induced tumor formation by interacting with the β-catenin pathway. J Steroid Biochem Mol Biol 2013;136:229-232.

120. Swami S, Krishnan A V., Peng L, Lundqvist J, Feldman D. Transrepression of the estrogen receptor promoter by calcitriol in human breast cancer cells via two negative vitamin D response elements. Endocr Relat Cancer 2013;20(4):565-577.

121. Zhou W, Srinivasan S, Nawaz Z, Slingerland JM. ERα, SKP2 and E2F-1 form a feed forward loop driving late ERα targets and G1 cell cycle progression. Oncogene 2014;33(18):2341-2353.

122. Frampton RJ, Omond SA, Eisman JA. Inhibition of human cancer cell growth by 1,25-dihydroxyvitamin D3 metabolites. Cancer Res 1983;43:4443-4447.

123. Stewart AF. Hypercalcemia associated with cancer. N Engl J Med 2005;352(4):373-379.

124. Mirrakhimov AE. Hypercalcemia of malignancy: An update on pathogenesis and management. N Am J Med Sci 2015;7(11):483-493.

125. Jones G. Pharmacokinetics of vitamin D toxicity. Am J Clin Nutr 2008;88(2):582-586.

126. Pettifor JM, Bikle DD, Cavaleros M, Zachen D, Kamdar MC, Ross FP. Serum levels of free 1,25-dihydroxyvitamin D toxicity. Ann Intern Med 1995;122(7):511-513.

127. García-Becerra R, Díaz L, Camacho J, et al. Calcitriol inhibits ether-à go-go potassium channel expression and cell proliferation in human breast cancer cells. Exp Cell Res 2010;316(3):433-442.

128. García-Quiroz J, García-Becerra R, Barrera D, et al. Astemizole synergizes calcitriol antiproliferative activity by inhibiting CYP24A1 and upregulating VDR: A novel approach for breast cancer therapy. PLoS One 2012;7(9):e45063.

129. Santos-Martínez N, Díaz L, Ordaz-Rosado D, et al. Calcitriol restores antiestrogen responsiveness in estrogen receptor negative breast cancer cells: A potential new therapeutic approach. BMC Cancer 2014;14:230.

130. Leyssens C, Verlinden L, Verstuyf A. The future of vitamin D analogs. Front Physiol

2014;5(4):1-18.

131. Yager JD, Leihr JG. Molecular mechanisms of estrogen carcinogenesis. Annu Rev Pharmacol Toxicol 1996;36(1):203-232.
132. Carruba G. Estrogen and prostate cancer: an eclipsed truth in an androgen-dominated scenario. J Cell Biochem 2007;102(4):899-911.
133. van den Brûle FA, Engel J, Stetler-Stevenson WG, Liu FT, Sobel ME, Castronovo V. Genes involved in tumor invasion and metastasis are differentially modulated by estradiol and progestin in human breast-cancer cells. Int J cancer 1992;52(4):653-657.
134. Diamond MI, Miner JN, Yoshinaga SK, Yamamoto KR. Transcription factor interactions: selectors of positive or negative regulation from a single DNA element. Science 1990;249(4974):1266-1272.
135. Hagedorn HG, Nerlich AG. Analysis of sex-hormone-receptor expression in laryngeal carcinoma. Eur Arch Otorhinolaryngol 2002;259(4):205-210.
136. Ferguson BJ, Hudson WR, McCarty KS. Sex steroid receptor distribution in the human larynx and laryngeal carcinoma. Arch Otolaryngol Head Neck Surg 1987;113(12):1311-1315.
137. Virolainen E, Vanharanta R, Carey TE. Steroid hormone receptors in human squamous carcinoma cell lines. Int J Cancer 1984;33(1):19-25.
138. Reiner Z, Cvrtila D, Petric V. Cytoplasmic steroid receptors in cancer of the larynx. Oto-Rhino- Laryngol 1988;245:47-49.
139. Bianchini C, Pastore A, Pelucchi S, et al. Sex hormone receptor levels in laryngeal carcinoma: A comparison between protein and RNA evaluations. Eur Arch

Otorhinolaryngol 2008;265(9):1089-1094.

140. Ferrandina G, Almadori G, Maggiano N, et al. Growth-inhibitory effect of tamoxifen and quercetin and presence of type II estrogen binding sites in human laryngeal cancer cell lines and primary laryngeal tumors. Int J Cancer 1998;77(5):747-754.
141. Natarajan V, Vepa S, al-Hassani M, Scribner WM. The enhancement by wortmannin of protein kinase C-dependent activation of phospholipase D in vascular endothelial cells. Chem Phys Lipids 1997;86(1):65-74.
142. Carrasco-Marín E, Alvarez-Domínguez C, Leyva-Cobián F. Wortmannin, an inhibitor of phospholipase D activation, selectively blocks major histocompatibility complex class II-restricted antigen presentation. Eur J Immunol 1994;24(9):2031-2039.
143. Gottlieb TM, Oren M. p53 and apoptosis. Semin Cancer Biol 1998;8(5):359-368.
144. Hyzy SL, Olivares-Navarrete R, Schwartz Z, Boyan BD. BMP2 induces osteoblast apoptosis in a maturation state and noggin-dependent manner. J Cell Biochem 2012;113(10):3236-3245.
145. Klinge CM, Riggs KA, Wickramasinghe NS, et al. Estrogen receptor alpha 46 is reduced in tamoxifen resistant breast cancer cells and re-expression inhibits cell proliferation and estrogen receptor alpha 66-regulated target gene transcription. Mol Cell Endocrinol 2010;323(2):268-276.
146. Lazennec G, Bresson D, Lucas A, Chauveau C, Vignon F. ERβ inhibits proliferation and invasion of breast cancer cells. Endocrinology 2001;142(9):4120-4130.
147. Niv Y. Estrogen receptor β expression and colorectal cancer. Eur J Gastroenterol Hepatol 2015;27(12):1438-1442.

148. Longo M, Brama M, Marino M, et al. Interaction of estrogen receptor alpha with protein kinase C alpha and c-Src in osteoblasts during differentiation. Bone 2004;34(1):100-111.

149. Kumar P, Wu Q, Chambliss KL, et al. Direct interactions with Gαi and Gβγ mediate nongenomic signaling by estrogen receptor α . Mol Endocrinol 2007;21(6):1370-1380.

150. Pappas TC, Gametchu B, Watson CS. Membrane estrogen receptors identified by multiple antibody labeling and impeded-ligand binding. FASEB J 1995;9(5):404-410.

151. Osborne CK, Shou J, Massarweh S, Schiff R. Crosstalk between estrogen receptor and growth factor receptor pathways as a cause for endocrine therapy resistance in breast cancer. Clin Cancer Res 2005;11(2 Pt 2):865s-70s.

152. Krasilnikov MA. Phosphatidylinositol-3 kinase dependent pathways: The role in control of cell growth, survival, and malignant transformation. Biochemistry 2000;65(1):59-67.

153. Harries M, Hawkins S, Hacking J, Hughes I. Changes in the male voice at puberty: Vocal fold length and its relationship to the fundamental frequency of the voice. J Laryngol Otol 1998;112(5):451-454.

154. Fischer J, Semple S, Fickenscher G, et al. Do women's voices provide cues of the likelihood of ovulation? The importance of sampling regime. PLoS One 2011;6(9):e24490.

155. Caruso S, Roccasalva L, Sapienza G, Zappalá M, Nuciforo G, Biondi S. Laryngeal cytological aspects in women with surgically induced menopause who were treated

with transdermal estrogen replacement therapy. Fertil Steril 2000;74(6):1073-1079.

156. Tatlipinar A, Günes P, Ozbeyli D, Cimen B, Gökçeer T. Effects of ovariectomy and estrogen replacement therapy on laryngeal tissue: A histopathological experimental animal study. Otolaryngol Head Neck Surg 2011;145(6):987-991.
157. Brunings JW, Schepens JJBFG, Peutz-Kootstra CJ, Kross KW. The expression of estrogen and progesterone receptors in the human larynx. J Voice 2013;27(3):376-380.
158. Newman SR, Butler J, Hammond EH, Gray SD. Preliminary report on hormone receptors in the human vocal fold. J Voice 2000;14(1):72-81.
159. Voelter C, Kleinsasser N, Joa P, et al. Detection of hormone receptors in the human vocal fold. Eur Arch Oto-Rhino-Laryngology 2008;265(10):1239-1244.
160. Virolainen E, Tuohimaa P, Aitasalo K, Kyttä J, Vanharanta-Hiltunen R. Steroid hormone receptors in laryngeal carcinoma. Otolaryngol Neck Surg 1986;94(4):512-517.
161. Rios OAB, Duprat A de C, Santos AR dos. Immunohistochemical searching for estrogen and progesterone receptors in women vocal fold epithelia. Braz J Otorhinolaryngol 2008;74(4):487-493.
162. Schneider B, Cohen E, Stani J, et al. Towards the expression of sex hormone receptors in the human vocal fold. J Voice 2007;21(4):502-507.
163. Nacci A, Fattori B, Basolo F, et al. Sex hormone receptors in vocal fold tissue: a theory about the influence of sex hormones in the larynx. Folia Phoniatr Logop 2011;63(2):77-82.
164. Lukits J, Remenár E, Rásó E, Ladányi A, Kásler M, Tímár J. Molecular

identification, expression and prognostic role of estrogen- and progesterone receptors in head and neck cancer. Int J Oncol 2007;30(1):155-160.

165. Mukudai S, Matsuda KI, Nishio T, et al. Differential responses to steroid hormones in fibroblasts from the vocal fold, trachea, and esophagus. Endocrinology 2015;156(3):1000-1009.
166. Jensen MM, Jørgensen JT, Binderup T, Kjær A. Tumor volume in subcutaneous mouse xenografts measured by microCT is more accurate and reproducible than determined by 18F-FDG-microPET or external caliper. BMC Med Imaging 2008;8:1-9.
167. Ström JO, Theodorsson A, Ingberg E, Isaksson I-M, Theodorsson E. Ovariectomy and 17β-estradiol Replacement in Rats and Mice: A Visual Demonstration. J Vis Exp 2012;(64):3-7.
168. Pan Q, O'Connor MI, Coutts RD, et al. Characterization of osteoarthritic human knees indicates potential sex differences. Biol Sex Differ 2016;7:27.
169. Doroudi M, Olivares-Navarrete R, Hyzy SL, Boyan BD, Schwartz Z. Signaling components of the 1α,25(OH)2D3-dependent Pdia3 receptor complex are required for wnt5a calcium-dependent signaling. Biochim Biophys Acta 2014;1843(11):2365-2375.
170. Swaminathan S, Huang C, Geng H, et al. BACH2 mediates negative selection and p53-dependent tumor suppression at the pre-B cell receptor checkpoint. Nat Med 2013;19(8):1014-1022.
171. Chen J, Lobachev KS, Grindel BJ, et al. Chaperone properties of pdia3 participate in rapid membrane actions of 1α,25-dihydroxyvitamin d3. Mol Endocrinol

2013;27(7):1065-1077.

172. Lawrence MS, Sougnez C, Lichtenstein L, et al. Comprehensive genomic characterization of head and neck squamous cell carcinomas. Nature 2015;517(7536):576-582.
173. University of California SC. USCS Xena. 2015.
174. Dolezal JM, Dash AP, Prochownik E V. Diagnostic and prognostic implications of ribosomal protein transcript expression patterns in human cancers. BMC Cancer 2018;18(1):275.
175. Miller WR, Hawkins RA, Forrest APM. Significance of aromatase activity in human breast cancer. Cancer Res 1982;42(8 Suppl.):3365-3369.
176. Yamamoto T, Kitawaki J, Urabe M, et al. Estrogen productivity of endometrium and endometrial cancer tissue; influence of aromatase on proliferation of endometrial cancer cells. J Steroid Biochem Mol Biol 1991;40(1):405-409.
177. Nair HB, Luthra R, Kirma N, et al. Induction of aromatase expression in cervical carcinomas: Effects of endogenous estrogen on cervical cancer cell proliferation. Cancer Res 2005;65(23):11164-11173.
178. Sato B, Spomer W, Huseby RA, Samuels LT. The testicular estrogen receptor system in two strains of mice differing in susceptibility to estrogen-induced leydig cell tumors. Endocrinology 1979;104(3):822-831.
179. Handelsman DJ, Newman JD, Jimenez M, McLachlan R, Sartorius G, Jones GRD. Performance of direct estradiol immunoassays with human male serum samples. Clin Chem 2014;60(3):510-517.
180. Pasqualini JR. The selective estrogen enzyme modulators in breast cancer: A

review. Biochim Biophys Acta - Rev Cancer 2004;1654(2):123-143.

181. Ajayi O, Charles-Davies M, Anetor J, Ademola A. Pituitary, gonadal, thyroid hormones and endocrine disruptors in pre and postmenopausal nigerian eomen with ER-, PR- and HER-2 positive and negative breast cancers. Med Sci 2018;6(2):37.
182. Suba Z. Diverse pathomechanisms leading to the breakdown of cellular estrogen surveillance and breast cancer development: New therapeutic strategies. Drug Des Devel Ther 2014;8:1381-1390.
183. Onland-Moret NC, Van Gils CH, Roest M, Grobbee DE, Peeters PHM. The estrogen receptor α gene and breast cancer risk (the Netherlands). Cancer Causes Control 2005;16(10):1195-1202.
184. Norman AW, Henry HL, Litwack G. Hormones : An introduction. In: *Hormones*. Vol 1953. ; 1969:1-27.
185. Mannelli G, Cecconi L, Gallo O. Laryngeal preneoplastic lesions and cancer: Challenging diagnosis. Qualitative literature review and meta-analysis. Crit Rev Oncol Hematol 2016;106:64-90.
186. Bergshoeff VE, Van der Heijden SJA, Haesevoets A, et al. Chromosome instability predicts progression of premalignant lesions of the larynx. Pathology 2014;46(3):216-224.
187. Pavlovic B, Djukic V, Milovanovic J, Tomanovic N, Milovanovic A, Trivic A. Morphometric analysis of Ki-67 and p16 expression in laryngeal precursor lesions. Eur Arch Otorhinolaryngol 2013;270(4):1405-1410.
188. López F, Alvarez-Marcos C, Alonso-Guervós M, et al. From laryngeal epithelial

precursor lesions to squamous carcinoma of the larynx: The role of cell cycle proteins and β-catenin. Eur Arch Otorhinolaryngol 2013;270(12):3153-3162.

189. Wei L, Mao M, Liu H. Droplet digital PCR and qRT-PCR to detect circulating miR-21 in laryngeal squamous cell carcinoma and pre-malignant laryngeal lesions. Acta Otolaryngol 2016;136(9):923-932.
190. Ring A, Dowsett M. Mechanisms of tamoxifen resistance. Endocr Relat Cancer 2004;11(4):643-658.
191. Sørlie T, Perou CM, Tibshirani R, et al. Gene expression patterns of breast carcinomas distinguish tumor subclasses with clinical implications. Proc Natl Acad Sci U S A 2001;98(19):10869-10874.
192. Correa Geyer F, Reis-Filho JS. Microarray-based gene expression profiling as a clinical tool for breast cancer management: are we there yet? Int J Surg Pathol 2009;17(4):285-302.
193. Weigelt B, Baehner FL, Reis-Filho JS. The contribution of gene expression profiling to breast cancer classification, prognostication and prediction: a retrospective of the last decade. J Pathol 2010;220(2):263-280.
194. Al Saleh S, Al Mulla F, Luqmani YA. Estrogen receptor silencing induces epithelial to mesenchymal transition in human breast cancer cells. PLoS One 2011;6(6):e20610.
195. Kuukasjärvi T., Kononen J., Helin H., Holli K. IJ. Loss of estrogen receptor in recurrent breast cancer is associated with poor response to endocrine therapy. J Clin Oncol 1996;14(9):2584-2589.
196. Matsumoto A, Jinno H, Murata T, et al. Prognostic implications of receptor

discordance between primary and recurrent breast cancer. Int J Clin Oncol 2015;20(4):701-708.

197. Yang Y-F, Liao Y-Y, Yang M, Peng N-F, Xie S-R, Xie Y-F. Discordances in ER, PR and HER2 receptors between primary and recurrent/metastatic lesions and their impact on survival in breast cancer patients. Med Oncol 2014;31(10):214.
198. Edenfield J, Schammel C, Collins J, Schammel D, Edenfield WJ. Metaplastic breast cancer: Molecular typing and identification of potential targeted therapies at a single institution. Clin Breast Cancer 2017;17(1):e1-e10.
199. Sano D, Myers JN. Xenograft models of head and neck cancers. Head Neck Oncol 2009;1:32.
200. Murata T, Mekada E, Hoffman RM. Reconstitution of a metastatic-resistant tumor microenvironment with cancer-associated fibroblasts enables metastasis. Cell Cycle 2017;16(6):533-535.
201. Zhang Y, Toneri M, Ma H, et al. Real-time GFP intravital imaging of the differences in cellular and angiogenic behavior of subcutaneous and orthotopic nude-mouse models of human PC-3 prostate cancer. J Cell Biochem 2016;2551(3):2546-2551.
202. Leav I, Lau K-M, Adams JY, et al. Comparative studies of the estrogen receptors β and α and the androgen receptor in normal human prostate glands, dysplasia, and in primary and metastatic carcinoma. Am J Pathol 2001;159(1):79-92.
203. Kim KH, Bender JR. Membrane-initiated actions of estrogen on the endothelium. Mol Cell Endocrinol 2009;308(1-2):3-8.
204. Kang L, Zhang X, Xie Y, et al. Involvement of estrogen receptor variant ER-alpha36, not GPR30, in nongenomic estrogen signaling. Mol Endocrinol 2010;24(4):709-

721.

205. Ottaviano YL, Issa JP, Parl FF, Smith HS, Baylin SB, Davidson NE. Methylation of the estrogen receptor gene CpG island marks loss of estrogen receptor expression in human breast cancer cells. Cancer Res 1994;54(10):2552-2555.
206. Piva R, Kumar VL, Hanau S, et al. Abnormal methylation of estrogen receptor gene and reduced estrogen receptor RNA levels in human endometrial carcinomas. J Steroid Biochem 1989;32(1):1-4.
207. Adams BD, Furneaux H, White BA. The micro-ribonucleic acid (miRNA) miR-206 targets the human estrogen receptor-α (ERα) and represses ERα messenger RNA and protein expression in breast cancer cell lines. Mol Endocrinol 2007;21(5):1132-1147.
208. Yoshimoto N, Toyama T, Takahashi S, et al. Distinct expressions of microRNAs that directly target estrogen receptor α in human breast cancer. Breast Cancer Res Treat 2011;130(1):331-339.
209. Li S, Li Y, Wen Z, Kong F, Guan X, Liu W. microRNA-206 overexpression inhibits cellular proliferation and invasion of estrogen receptor α-positive ovarian cancer cells. Mol Med Rep 2014;9(5):1703-1708.
210. Chen X, Yan Q, Li S, et al. Expression of the tumor suppressor miR-206 is associated with cellular proliferative inhibition and impairs invasion in ERα-positive endometrioid adenocarcinoma. Cancer Lett 2012;314(1):41-53.
211. Zhang T, Liu M, Wang C, Lin C, Sun Y, Jin D. Down-regulation of miR-206 promotes proliferation and invasion of laryngeal cancer by regulating VEGF expression. Anticancer Res 2011;31(11):3859-3863.

212. Iobagiu C, Lambert C, Raica M, et al. Loss of heterozygosity in tumor tissue in hormonal receptor genes is associated with poor prognostic criteria in breast cancer. Cancer Genet 2015;208(4):135-142.

213. Tokunaga E, Okada S, Yamashita N, et al. High incidence and frequency of LOH are associated with aggressive features of high-grade HER2 and triple-negative breast cancers. Breast Cancer 2012;19(2):161-169.

214. Shi L, Dong B, Li Z, et al. Expression of ERα36, a novel variant of estrogen receptor α, and resistance to tamoxifen treatment in breast cancer. J Clin Oncol 2009;27(21):3423-3429.

215. Reese JM, Bruinsma ES, Nelson AW, et al. ERβ -mediated induction of cystatins results in suppression of TGFβ signaling and inhibition of triple-negative breast cancer metastasis. Proc Natl Acad Sci 2018;115(41):1-10.

216. Järvinen TA, Pelto-Huikko M, Holli K, Isola J. Estrogen receptor beta is coexpressed with ERalpha and PR and associated with nodal status, grade, and proliferation rate in breast cancer. Am J Pathol 2000;156(1):29-35.

217. Shanle EK, Zhao Z, Hawse J, et al. Research resource: global identification of estrogen receptor β target genes in triple negative breast cancer cells. Mol Endocrinol 2013;27(10):1762-1775.

218. Reese JM, Bruinsma ES, Monroe DG, et al. ERβ inhibits cyclin dependent kinases 1 and 7 in triple negative breast cancer. Oncotarget 2017;8(57):96506-96521.

219. Schüler-Toprak S, Häring J, Inwald EC, Moehle C, Ortmann O, Treeck O. Agonists and knockdown of estrogen receptor β differentially affect invasion of triple-negative breast cancer cells in vitro. BMC Cancer 2016;16(1):951.

220. Hinsche O, Girgert R, Emons G, Gründker C. Estrogen receptor β selective agonists reduce invasiveness of triple-negative breast cancer cells. Int J Oncol 2015;46(2):878-884.

221. Sengal AT, Mukhtar NSH, Vetter M, et al. Comparison of receptor-defined breast cancer subtypes between German and Sudanese women: a facility-based cohort study. J Glob Oncol 2017:1-12.

222. Carvalho FM, Bacchi LM, Pincerato KM, Van De Rijn M, Bacchi CE. Geographic differences in the distribution of molecular subtypes of breast cancer in Brazil. BMC Womens Health 2014;14(102):1-8.

223. Laden F, Spiegelman D, Neas LM, et al. Geographic variation in breast cancer incidence rates in a cohort of U.S. women. J Natl Cancer Inst 1997;89(18):1373-1378.

224. Li CI, Daling JR, Malone KE. Incidence of invasive breast cancer by hormone receptor status from 1992 to 1998. J Clin Oncol 2003;21(1):28-34.

225. Rennert G, Pinchev M, Rennert HS. Use of bisphosphonates and risk of postmenopausal breast cancer. J Clin Oncol 2010;28(22):3577-3581.

226. Newman LA. Disparities in breast cancer and african ancestry : A global perspective. Breast J 2015;21(2):133-139.

227. Dietze EC, Sistrunk C, Miranda-Carboni G, O'Regan R, Seewaldt VL. Triple-negative breast cancer in African-American women: disparities versus biology. Nat Rev Cancer 2015;15(4):248-254.

228. Ren Y, Black DM, Mittendorf EA, et al. Crossover effects of estrogen receptor status on breast cancer-specific hazard rates by age and race. PLoS One 2014;9(10):1-

11.

229. Joslyn SA. Hormone receptors in breast cancer: Racial differences in distribution and survival. Breast Cancer ResTreat 2002;73(1):45-59.
230. Wright JL, Reis IM, Zhao W, et al. Racial disparity in estrogen receptor positive breast cancer patients receiving trimodality therapy. The Breast 2012;21(3):276-283.
231. Rauscher GH, Campbell RT, Wiley EL, Hoskins K, Stolley MR, Warnecke RB. Mediation of racial and ethnic disparities in estrogen/progesterone receptor–negative breast cancer by socioeconomic position and reproductive factors. Am J Epidemiol 2016;183(10):884-893.
232. Abd Elmageed ZY, Moroz K, Srivastav SK, et al. High circulating estrogens and selective expression of ERβ in prostate tumors of Americans: Implications for racial disparity of prostate cancer. Carcinogenesis 2013;34(9):2017-2023.
233. Grsic K, Opacic IVAL, Sitic S. The prognostic significance of estrogen receptor β in head and neck squamous cell carcinoma. Oncol Lett 2016;12:3861-3865.
234. Garland FC, Garland CF, Gorham ED, Young JF. Geographic variation in breast cancer mortality in the United States: A hypothesis involving exposure to solar radiation. Prev Med (Baltim) 1990;19(6):614-622.
235. Bilinski K, Boyages J. Association between 25-hydroxyvitamin D concentration and breast cancer risk in an Australian population: An observational case–control study. Breast Cancer Res Treat 2013;137(2):599-607.
236. Atoum M, Alzoughool F. Vitamin D and breast cancer: Latest evidence and future steps. Breast Cancer (Auckl) 2017;11.

237. Neuhouser ML, Manson JE, Millen A, et al. The influence of health and lifestyle characteristics on the relation of serum 25-hydroxyvitamin D with risk of colorectal and breast cancer in postmenopausal women. Am J Epidemiol 2012;175(7):673-684.

238. Bolland MJ, Grey A, Gamble GD, Reid IR. Calcium and vitamin D supplements and health outcomes: A reanalysis of the Women's Health Initiative (WHI) limited-access data set. Am J Clin Nutr 2011;94(4):1144-1149.

239. Grant WB, Boucher BJ. Randomized controlled trials of vitamin D and cancer incidence: A modeling study. PLoS One 2017;12(5):e0176448.

240. Chlebowski RT, Johnson KC, Kooperberg C, et al. Calcium plus vitamin D supplementation and the risk of breast cancer. J Natl Cancer Inst 2008;100(22):1581-1591.

241. Tarone RE, Chu KC. The greater impact of menopause on ER- than ER+ breast cancer incidence: A possible explanation. Cancer Causes Control 2002;13(1):7-14.

242. Klauber-DeMore N. Tumor biology of breast cancer in young women. Breast Dis 23:9-15.

243. Hatse S, Lambrechts D, Verstuyf A, et al. Vitamin D status at breast cancer diagnosis: Correlation with tumor characteristics, disease outcome, and genetic determinants of vitamin D insufficiency. Carcinogenesis 2012;33(7):1319-1326.

244. Office of Dietary Supplements. *Vitamin D Fact Sheet for Health Professionals*.; 2016.

245. Bailey RL, Dodd KW, Goldman JA, et al. Estimation of total usual calcium and vitamin D intakes in the United States. J Nutr 2010;140(4):817-822.

246. Deluca HF. Historical overview of vitamin D. In: Feldman D, Pike JW, Adams JS, eds. *Vitamin D*. 3rd ed. Academic Press; 2013:3-12.

247. Adams JS, Hewison M. Extrarenal expression of the 25-hydroxyvitamin D-1-hydroxylase. Arch Biochem Biophys 2012;523(1):95-102.

248. Weisman Y, Harell A, Edelstein S, David M, Spirer Z, Golander A. 1α 25-dihydroxyvitamin D3, and 24,25-dihydroxyvitamin D3 in vitro synthesis by human decidua and placenta. Nature 1979;281(5729):317-319.

249. Schwartz Z, Brooks B, Swain L, Del Toro F, Norman AW, Boyan BD. Production of 1,25-dihydroxyvitamin D3 and 24,25-dihydroxyvitamin D3 by growth zone and resting zone chondrocytes is dependent on cell maturation and is regulated by hormones and growth factors. Endocrinology 1992;130(5):2495-2504.

250. Costa JL, Eijk PP, van de Wiel MA, et al. Anti-proliferative action of vitamin D in MCF7 is still active after siRNA-VDR knock-down. BMC Genomics 2009;10:499.

251. Colston KW, Hansen CM. Mechanisms implicated in the growth regulatory effects of vitamin D in breast cancer. Endocr Relat Cancer 2002;9(1):45-59.

252. Murray A, Madden SF, Synnott NC, et al. Vitamin D receptor as a target for breast cancer therapy. Endocr Relat Cancer 2017;24(4):181-195.

253. Somjen D, Somjen GJ, Weisman Y, Binderman I. Evidence for 24,25-dihydroxycholecalciferol receptors in long bones of newborn rats. BiochemJ 1982;204(1):31-36.

254. Doroudi M, Chen J, Boyan BD, Schwartz Z. New insights on membrane mediated effects of 1α,25-dihydroxy vitamin D$_3$ signaling in the musculoskeletal system. Steroids 2014;81:81-87.

255. Chen J, Doroudi M, Cheung J, Grozier AL, Schwartz Z, Boyan BD. Plasma membrane Pdia3 and VDR interact to elicit rapid responses to 1α,25(OH)$_2$D$_3$. Cell Signal 2013;25(12):2362-2373.

256. Madhok TC, Schnoes HK, DeLuca HF. Mechanism of 25-hydroxyvitamin D3 24-hydroxylation: Incorporation of oxygen-18 into the 24 position of 25-hydroxyvitamin D3. Biochemistry 1977;16(10):2142-2145.

257. Miettinen S, Ahonen MH, Lou YR, et al. Role of 24-hydroxylase in vitamin D$_3$ growth response of OVCAR-3 ovarian cancer cells. Int J Cancer 2004;108(3):367-373.

258. Chen G, Kim SH, King AN, et al. CYP24A1 is an independent prognostic marker of survival in patients with lung adenocarcinoma. Clin Cancer Res 2011;17(4):817-826.

259. Fischer D, Becker S, Cordes T, et al. Vitamin D-24-hydroxylase in benign and malignant breast tissue and cell lines. Anticancer Res 2009;29(9):3641-3645.

260. Maeda Y, Yamato H, Kobori N, et al. Antitumor and other effects of 24R,25-dihydroxycholecalciferol in lewis lung carcinoma causing abnormal calcium metabolism in tumor-bearing mice. Oncology 1988;205:202-205.

261. Maeda Y, Hirai T, Yamato H, Koborl N. Animal pharmacological effects of 24R,25-dihydroxyvitamin D3 one of the endogenous substances regulating calcium metabolism. J Int Med Res 1988;16(January):125-133.

262. Ikezaki S, Nishikawa A, Furukawa F, et al. Chemopreventive effects of 24R,25-dihydroxyvitamin D3, a vitamin D3 derivative, on glandular stomach carcinogenesis induced in rats by N-methyl-N'-nitro-N- nitrosoguanidine and sodium chloride. Cancer Res 1996;56(12):2767-2770.

263. Salim EI, Wanibuchi H, Taniyama T, et al. Inhibition of development of N,N'-dimethylhydrazine-induced rat colonic aberrant crypt foci by pre, post and simultaneous treatments with 24R,25-dihydroxyvitamin D$_3$. Japanese J Cancer Res 1997;88(11):1052-1062.

264. Werbeck JL, Thudi NK, Martin CK, et al. Tumor microenvironment regulates metastasis and metastasis genes of mouse MMTV-PymT mammary vancer vells in vivo. Vet Pathol 2014;51(4):868-881.

265. Iorns E, Hnatyszyn HJ, Seo P, Clarke J, Ward T, Lippman M. The role of SATB1 in breast cancer pathogenesis. JNCI J Natl Cancer Inst 2010;102(16):1284-1296.

266. Xu J, Prosperi JR, Choudhury N, Olopade OI, Goss KH. β-Catenin is required for the tumorigenic behavior of triple-negative breast cancer cells. PLoS One 2015;10(2):e0117097.

267. Chung E, Yamashita H, Au P, Tannous BA, Fukumura D, Jain RK. Secreted *Gaussia* luciferase as a biomarker for monitoring tumor progression and treatment response of systemic metastases. Najbauer J, ed. PLoS One 2009;4(12):e8316.

268. Tai L-H, Tanese de Souza C, Sahi S, et al. A mouse tumor model of surgical stress to explore the mechanisms of postoperative immunosuppression and evaluate novel perioperative immunotherapies. J Vis Exp 2014;(85).

269. Webb Y, Hermida-Matsumoto L, Resh MD. Inhibition of protein palmitoylation, raft localization, and T cell signaling by 2-bromopalmitate and polyunsaturated fatty acids. J Biol Chem 2000;275(1):261-270.

270. Ulloth JE, Almaguel FG, Padilla A, Bu L, Liu J-W, De Leon M. Characterization of methyl-beta-cyclodextrin toxicity in NGF-differentiated PC12 cell death.

Neurotoxicology 2007;28(3):613-621.

271. Boyan BD, Wang L, Wong KL, Jo H, Schwartz Z. Plasma membrane requirements for 1α,25(OH)$_2$D$_3$ dependent PKC signaling in chondrocytes and osteoblasts. Steroids 2006;71(4):286-290.
272. Gunther DF, Calikoglu AS, Underwood LE. The effects of the estrogen receptor blocker, Faslodex (ICI 182780), on estrogen-accelerated bone maturation in mice. Pediatr Res 1999;46(3):269-273.
273. Zhong M, Carney DH, Boyan BD, Schwartz Z. 17β-estradiol regulates rat growth plate chondrocyte apoptosis through a mitochondrial pathway not involving nitric oxide or mapks. Endocrinology 2011;152(1):82-92.
274. Ibrahim T, Ricci M, Scarpi E, et al. RANKL: A promising circulating marker for bone metastasis response. Oncol Lett 2016;12(4):2970-2975.
275. Holen I, Shipman CM. Role of osteoprotegerin (OPG) in cancer. Clin Sci 2006;110(3):279-291.
276. Park HS, Lee A, Chae BJ, Bae J-S, Song BJ, Jung SS. Expression of receptor activator of nuclear factor kappa-B as a poor prognostic marker in breast cancer. J Surg Oncol 2014;110(7):807-812.
277. Van Poznak C, Cross SS, Saggese M, et al. Expression of osteoprotegerin (OPG), TNF related apoptosis inducing ligand (TRAIL), and receptor activator of nuclear factor κB ligand (RANKL) in human breast tumours. J Clin Pathol 2006;59(1):56-63.
278. Ye J, Coulouris G, Zaretskaya I, Cutcutache I, Rozen S, Madden TL. Primer-BLAST: A tool to design target-specific primers for polymerase chain reaction. BMC

Bioinformatics 2012;13(1):134.

279. Iorns E, Drews-Elger K, Ward TM, et al. A new mouse model for the study of human breast cancer metastasis. PLoS One 2012;7(10):e47995.
280. Chiang K-C, Chen S-C, Yeh C-N, et al. MART-10, a less calcemic vitamin D analog, is more potent than 1α,25-dihydroxyvitamin D$_3$ in inhibiting the metastatic potential of MCF-7 breast cancer cells in vitro. J Steroid Biochem Mol Biol 2014;139:54-60.
281. Simboli-Campbell M, Narvaez CJ, Tenniswood M, Welsh J. 1,25-Dihydroxyvitamin D$_3$ induces morphological and biochemical markers of apoptosis in MCF-7 breast cancer cells. J Steroid Biochem Mol Biol 1996;58(4):367-376.
282. Trivedi T, Zheng Y, Fournier PGJ, et al. The vitamin D receptor is involved in the regulation of human breast cancer cell growth via a ligand-independent function in cytoplasm. Oncotarget 2017;8(16):26687-26701.
283. Mahgoub A. Interaction between 24R,25-dihydroxycholecalciferol and 1,25-dihydroxycholecalciferol on 45Ca release from bone *in vitro*. Calcif Tissue Int 1981;33(6):663-666.
284. Ono T, Tanaka H, Yamate T, Nagai Y, Nakamura T, Seino Y. 24R,25-dihydroxyvitamin D$_3$ promotes bone formation without causing excessive resorption in hypophosphatemic mice. Endocrinology 1996;137(6):2633-2637.
285. Maeda Y, Yamato H, Katoh T, Orimo H. Hypocalcemic effect of 24R,25-dihydroxyvitamin D3 in rats. In Vivo (Brooklyn) 1987;1(6):347-350.
286. Narvaez CJ, Zinser G, Welsh JE. Functions of 1α,25-dihydroxyvitamin D$_3$ in mammary gland: from normal development to breast cancer. Steroids 2001;66(3-5):301-308.

287. Segersten U, Holm PK, Björklund P, et al. 25-Hydroxyvitamin D3 1α-hydroxylase expression in breast cancer and use of non-1α-hydroxylated vitamin D analogue. Breast Cancer Res 2005;7(6):R980-R986.

288. Alimirah F, Vaishnav A, McCormick M, et al. Functionality of unliganded VDR in breast cancer cells: Repressive action on CYP24 basal transcription. Mol Cell Biochem 2012;29(6):997-1003.

289. Tomaskovic-Crook E, Thompson EW, Thiery JP. Epithelial to mesenchymal transition and breast cancer. Breast Cancer Res 2009;11(6):213.

290. Blick T, Widodo E, Hugo H, et al. Epithelial mesenchymal transition traits in human breast cancer cell lines. Clin Exp Metastasis 2008;25(6):629-642.

291. Guo F, Wang Y, Liu J, Mok SC, Xue F, Zhang W. CXCL12/CXCR4: A symbiotic bridge linking cancer cells and their stromal neighbors in oncogenic communication networks. Oncogene 2015;(154):1-11.

292. León X, Diez S, García J, et al. Expression of the CXCL12/CXCR4 chemokine axis predicts regional control in head and neck squamous cell carcinoma. Eur Arch Oto-Rhino-Laryngology 2016;273(12):4525-4533.

293. Sun Y, Mao X, Fan C, et al. CXCL12-CXCR4 axis promotes the natural selection of breast cancer cell metastasis. Tumour Biol 2014;35(8):7765-7773.

294. Mukherjee D, Zhao J. The role of chemokine receptor CXCR4 in breast cancer metastasis. Am J Cancer Res 2013;3(1):46-57.

295. Przybylowska K, Kluczna A, Zadrozny M, et al. Polymorphisms of the promoter regions of matrix metalloproteinases genes MMP-1 and MMP-9 in breast cancer. Breast Cancer Res Treat 2006;95(1):65-72.

296. Ren F, Tang R, Zhang X, et al. Overexpression of MMP family members functions as prognostic biomarker for breast cancer patients: A systematic review and meta-analysis. PLoS One 2015;10(8):1-18.

297. Andrechek ER. HER2/Neu tumorigenesis and metastasis is regulated by E2F activator transcription factors. Oncogene 2015;34(2):217-225.

298. Mitri Z, Constantine T, O'Regan R. The HER2 receptor in breast cancer: Pathophysiology, clinical use, and new sdvances in therapy. Chemother Res Pract 2012;2012:1-7.

299. Davis NM, Sokolosky M, Stadelman K, et al. Deregulation of the EGFR/PI3K/PTEN/Akt/mTORC1 pathway in breast cancer: Possibilities for therapeutic intervention. Oncotarget 2014;5(13):4603-4650.

300. Nahta R, Esteva FJ. HER-2-targeted therapy: lessons learned and future directions. Clin Cancer Res 2003;9(14):5078-5084.

301. Sömjen D, Binderman I, Weisman Y. The effects of 24R,25-dihydroxycholecalciferol and of 1α,25-dihydroxycholecalciferol on ornithine decarboxylase activity and on DNA synthesis in the epiphysis and diaphysis of rat bone and in the duodenum. Biochem J 1983;214(2):293-298.

302. Pedram A, Razandi M, Lewis M, Hammes S, Levin ER. Membrane-localized estrogen receptor α is required for normal organ development and function. Dev Cell 2014;29(4):482-490.

303. Boyan BD, Sylvia VL, Dean DD, Del Toro F, Schwartz Z. Differential regulation of growth plate chondrocytes by 1alpha,25-(OH)$_2$D$_3$ and 24R,25-(OH)$_2$D$_3$ involves cell-maturation-specific membrane-receptor-activated phospholipid metabolism.

Crit Rev Oral Biol Med 2002;13(2):143-154.

304. Swami S, Krishnan A V, Feldman D. 1α,25-dihydroxyvitamin D3 down-regulates receptor abundance and suppresses estrogen actions in MCF-7 human breast cancer cells abundance and suppresses estrogen actions in MCF-7. Clin Cancer Res 2000;6:3371-3379.
305. Rochefort H. Oestrogen- and anti-oestrogen-regulated genes in human breast cancer. Ciba Found Symp 1995;191:254-265; discussion 265-8.
306. Wang Z-Y, Yin L. Estrogen receptor α 36 (ERα36): A new player in human breast cancer. Mol Cell Endocrinol 2015;418 Pt 3:193-206.
307. Freedman DM, Dosemeci M, McGlynn K. Sunlight and mortality from breast, ovarian, colon, prostate, and non-melanoma skin cancer: A composite death certificate based case-control study. Occup Environ Med 2002;59(4):257-262.
308. Abbas S, Linseisen J, Slanger T, et al. Serum 25-hydroxyvitamin D and risk of post-menopausal breast cancer--results of a large case-control study. Carcinogenesis 2008;29(1):93-99.
309. Kim HJ, Lee YM, Ko BS, et al. Vitamin D deficiency is correlated with poor outcomes in patients with luminal-type breast cancer. Ann Surg Oncol 2011;18(7):1830-1836.
310. McCullough ML, Rodriguez C, Diver WR, et al. Dairy, calcium, and vitamin D intake and postmenopausal breast cancer risk in the cancer prevention study II nutrition cohort. Cancer Epidemiol Biomarkers Prev 2005;14(12):2898-2904.
311. Kim HJ, Koh BS, Yu JH, et al. Changes in serum hydroxyvitamin D levels of breast cancer patients during tamoxifen treatment or chemotherapy in premenopausal breast cancer patients. Eur J Cancer 2014;50(8):1403-1411.

312. Boyan BD, Hyzy SL, Pan Q, et al. 24R,25-dihydroxyvitamin D3 protects against articular cartilage damage following anterior cruciate ligament transection in male rats. PLoS One 2016;11(8):e0161782.

313. Verma A, Cohen DJ, Schwartz N, et al. 24R,25-Dihydroxyvitamin D3 regulates breast cancer cells in vitro and in vivo. Biochim Biophys Acta - Gen Subj 2019.

314. Doroudi M, Schwartz Z, Boyan BD. Phospholipase A2 activating protein is required for 1α,25-dihydroxyvitamin D3 dependent rapid activation of protein kinase C via Pdia3. J Steroid Biochem Mol Biol 2012;132(1-2):48-56.

315. Han X, Aenlle KK, Bean LA, et al. Role of estrogen receptor and in preserving hippocampal function during aging. J Neurosci 2013;33(6):2671-2683.

316. Yang T, Zhang H, Qiu H, et al. EFEMP1 is repressed by estrogen and inhibits the epithelial-mesenchymal transition via Wnt/beta-catenin signaling in endometrial carcinoma. Oncotarget 2016;7(18).

317. Lotz EM, Berger MB, Schwartz Z, Boyan BD. Regulation of osteoclasts by osteoblast lineage cells depends on titanium implant surface properties. Acta Biomater 2018;68(10):296-307.

318. Bessler H, Djaldetti M. 1α,25-dihydroxyvitamin D3 modulates the interaction between immune and colon cancer cells. Biomed Pharmacother 2012;66(6):428-432.

319. Tanaka Y, Castillo L, DeLuca HF, Ikekawa N. The 24 hydroxylation of 1,25 dihydroxyvitamin D3. J Biol Chem 1977;252(4):1421-1424.

320. Lechner D, Kállay E, Cross HS. 1α,25-Dihydroxyvitamin D3 downregulates CYP27B1 and induces CYP24A1 in colon cells. Mol Cell Endocrinol 2007;263(1-

2):55-64.

321. Matilainen JM, Malinen M, Turunen MM, Carlberg C, Väisänen S. The number of vitamin D receptor binding sites defines the different vitamin D responsiveness of the CYP24 gene in malignant and normal mammary cells. J Biol Chem 2010;285(31):24174-24183.
322. Haznadar M, Krausz KW, Margono E, et al. Inverse association of vitamin D3 levels with lung cancer mediated by genetic variation. Cancer Med 2018;7(6):2764-2775.
323. Levin ER. Extranuclear steroid receptors are essential for steroid hormone actions. Annu Rev Med 2015;66:271-280.
324. Elbaradie KBY, Wang Y, Boyan BD, Schwartz Z. Sex-specific response of rat costochondral cartilage growth plate chondrocytes to 17β-estradiol involves differential regulation of plasma membrane associated estrogen receptors. Biochim Biophys Acta - Mol Cell Res 2013;1833(5):1165-1172.
325. Kocanova S, Mazaheri M, Caze-Subra S, Bystricky K. Ligands specify estrogen receptor alpha nuclear localization and degradation. BMC Cell Biol 2010;11(1):98.

Vita

Anjali Verma received a Bachelor's of Science in Biomedical Engineering from Case Western Reserve University in 2013. She joined the Boyan-Schwartz Laboratory in 2014 as a research technician, and joined the Biomedical Engineering graduate program at VCU in August 2015. Anjali will graduate with a Doctorate of Philosophy in Biomedical Engineering program in August 2019. Anjali has authored five articles in *Steroids*, *BBA-MR.*, and *BBA-General Subjects*. Upon completion of her Ph.D., Anjali will begin a position as a postdoctoral research associate at the Eshelman School of Pharmacy at the University of North Carolina-Chapel Hill under Dr. Juliane Nguyen.